CRCLEME
Cooperative Research Centre for
Landscape Evolution & Mineral Exploration

CSIRO
EXPLORATION
AND MINING

AMIRA
Australian Mineral Industries Research Association Limited ACN 004 448 266

OPEN FILE
REPORT
SERIES

LATERITE GEOCHEMISTRY IN THE CSIRO-AGE DATABASE FOR THE CENTRAL YILGARN REGION

(Barlee, Bencubbin, Corrigin, Hyden, Jackson, Kalgoorlie, Kelleberrin, Southern Cross sheets)

Volume 1

E.C. Grunsky

CRC LEME OPEN FILE REPORT 22

September 1998

(CSIRO Division of Exploration Geoscience Report 121R, 1990.
Second impression 1998)

CRC LEME is an unincorporated joint venture between The Australian National University, University of Canberra, Australian Geological Survey Organisation and CSIRO Exploration and Mining, established and supported under the Australian Government's Cooperative Research Centres Program.

CRC

AMIRA
Australian Mineral Industries Research Association Limited ACN 004 448 266

CRCLEME
Cooperative Research Centre for
Landscape Evolution & Mineral Exploration

CSIRO
EXPLORATION
AND MINING

LATERITE GEOCHEMISTRY IN THE CSIRO-AGE DATABASE FOR THE CENTRAL YILGARN REGION

(Barlee, Bencubbin, Corrigin, Hyden, Jackson, Kalgoorlie, Kelleberrin, Southern Cross sheets)

Volume 1

E.C. Grunsky

CRC LEME OPEN FILE REPORT 22

September 1998

(CSIRO Division of Exploration Geoscience Report 121R, 1990.
Second impression 1998)

CRC LEME is an unincorporated joint venture between The Australian National University, University of Canberra, Australian Geological Survey Organisation and CSIRO Exploration and Mining
Headquarters: CRC LEME c/o CSIRO Exploration and Mining, Private Bag, PO Wembley, Western Australia, 6014

RESEARCH ARISING FROM CSIRO/AMIRA REGOLITH GEOCHEMISTRY PROJECTS 1987-1993

In 1987, CSIRO commenced a series of multi-client research projects in regolith geology and geochemistry which were sponsored by companies in the Australian mining industry, through the Australian Mineral Industries Research Association Limited (AMIRA). The initial research program, "Exploration for concealed gold deposits, Yilgarn Block, Western Australia" (1987-1993) had the aim of developing improved geological, geochemical and geophysical methods for mineral exploration that would facilitate the location of blind, buried or deeply weathered gold deposits. The program included the following projects:

P240: Laterite geochemistry for detecting concealed mineral deposits (1987-1991). Leader: Dr R.E. Smith.
Its scope was development of methods for sampling and interpretation of multi-element laterite geochemistry data and application of multi-element techniques to gold and polymetallic mineral exploration in weathered terrain. The project emphasised viewing laterite geochemical dispersion patterns in their regolith-landform context at local and district scales. It was supported by 30 companies.

P241: Gold and associated elements in the regolith - dispersion processes and implications for exploration (1987-1991). Leader: Dr C.R.M. Butt.
The project investigated the distribution of ore and indicator elements in the regolith. It included studies of the mineralogical and geochemical characteristics of weathered ore deposits and wall rocks, and the chemical controls on element dispersion and concentration during regolith evolution. This was to increase the effectiveness of geochemical exploration in weathered terrain through improved understanding of weathering processes. It was supported by 26 companies.

These projects represented "an opportunity for the mineral industry to participate in a multi-disciplinary program of geoscience research aimed at developing new geological, geochemical and geophysical methods for exploration in deeply weathered Archaean terrains". This initiative recognised the unique opportunities, created by exploration and open-cut mining, to conduct detailed studies of the weathered zone, with particular emphasis on the near-surface expression of gold mineralisation. The skills of existing and specially recruited research staff from the Floreat Park and North Ryde laboratories (of the then Divisions of Minerals and Geochemistry, and Mineral Physics and Mineralogy, subsequently Exploration Geoscience and later Exploration and Mining) were integrated to form a task force with expertise in geology, mineralogy, geochemistry and geophysics. Several staff participated in more than one project. Following completion of the original projects, two continuation projects were developed.

P240A: Geochemical exploration in complex lateritic environments of the Yilgarn Craton, Western Australia (1991-1993). Leaders: Drs R.E. Smith and R.R. Anand.
The approach of viewing geochemical dispersion within a well-controlled and well-understood regolith-landform and bedrock framework at detailed and district scales continued. In this extension, focus was particularly on areas of transported cover and on more complex lateritic environments typified by the Kalgoorlie regional study. This was supported by 17 companies.

P241A: Gold and associated elements in the regolith - dispersion processes and implications for exploration. Leader: Dr. C.R.M. Butt.
The significance of gold mobilisation under present-day conditions, particularly the important relationship with pedogenic carbonate, was investigated further. In addition, attention was focussed on the recognition of primary lithologies from their weathered equivalents. This project was supported by 14 companies.

Although the confidentiality periods of the research reports have expired, the last in December 1994, they have not been made public until now. Publishing the reports through the CRC LEME Report Series is seen as an appropriate means of doing this. By making available the results of the research and the authors' interpretations, it is hoped that the reports will provide source data for future research and be useful for teaching. CRC LEME acknowledges the Australian Mineral Industries Research Association and CSIRO Division of Exploration and Mining for authorisation to publish these reports. It is intended that publication of the reports will be a substantial additional factor in transferring technology to aid the Australian Mineral Industry.

This report (CRC LEME Open File Report 22) is a Second impression (second printing) of CSIRO, Division of Exploration Geoscience Restricted Report 121R, first issued in 1990, which formed part of the CSIRO/AMIRA Project P240.

Copies of this publication can be obtained from:
The Publication Officer, c/- CRC LEME, CSIRO Exploration and Mining, PMB, Wembley, WA 6014, Australia. Information on other publications in this series may be obtained from the above or from http://leme.anu.edu.au/
Cataloguing-in-Publication:
Grunksy, E.C.
Laterite geochemistry in the CSIRO-AGE Database for the Central Yilgarn Region (Barlee, Bencubbin, Corrigin, Hyden, Jackson, Kalgoorlie, Kellerberrin, Southern Cross sheets)
ISBN v1: 0 642 28201 3 v2: 0 642 28202 1 set: 0 642 28203 X
1. Geochemistry 2. Laterite - Western Australia - Yilgarn Region.
I. Title
CRC LEME Open File Report 22.
ISSN 1329-4768

ABSTRACT

A multi-element geochemical study has been carried out based upon laterite samples that cover parts of the main greenstone belts and portions of the granitoid/gneiss terrain of the BARLEE, JACKSON, KALGOORLIE, BENCUBBIN, KELLERBERRIN, SOUTHERN CROSS, CORRIGIN, and HYDEN 1:250 000 map sheets. This report presents a summary of the data and a provisional interpretation of selected parts of the data. The data used in the study are contained in the accompanying diskette (in the back pocket).

The sampling arose as part of a combined research programme between CSIRO and an experimental exploration programme (the AGE Joint Venture Programme) during the period 1983 to 1986. The study provides geochemical knowledge of the element abundance levels and shows variations in the geochemistry of lateritic and associated ferruginous materials, geochemistry that complement more specific information arising from orientation studies about mineral deposits.

The database which was used for the study is dominated by two major lithological groups: greenstone and granitoid rocks. The two lithologies have different geochemical characteristics, and thus have been, for the most part, treated separately. The database consists of both regional and follow-up samples. Most of the investigation for this report has emphasized the results from the regional samples as this will provide information for additional regional sampling programmes for the sponsors.

Laterite is by far the dominant material sampled in the area. The ferricretes, which are second priority in sampling, are represented by 184 samples, while the laterites are represented by 1815 samples.

In the region covered by the present report, a total of 2102 samples were analyzed for 30 elements. Summary statistics, histograms, and maps of the percentile classes are presented for selected elements in laterites. Several numerically-based procedures were applied for the purposes of outlining regional trends and detecting areas of relatively-high abundances of selected elements (anomalies). Numerical techniques included the use of ranking of individual elements, principal components analysis, CHI-6*X, PEG-4, and NUMCHI indices, and multivariate ranking of the chalcophile elements(χ^2 plots).

The resulting scores of these techniques have been ranked and plotted on maps and scatter plots. The most anomalous samples tend to occur as outliers when these methods are applied. The results of these applications confirm the presence of some broad regional geochemical trends that are related to bedrock lithologies and possible regional alteration processes.

The dominant geochemical features are:

- Several multi-element associations occur with Au, primarily in the greenstone belts, and a few in the granitoid/gneiss terrain. The characteristic elements are, Sb, Se, Ag, W, As, and Sn.

- Several Au anomalies occur in the Diemals, Marda, and Southern Cross greenstone belts.

- Regional, geochemical features that are characteristic of the greenstone belts are defined by higher relative abundances of Cr, Mn, V, Zn, Ni, Co, and Fe_2O_3.

- A chalcophile trend may be present striking parallel to the Southern Cross belt, parallel to the Johnston Range in the Diemals area, and parallel to the stratigraphy in the Marda complex.

- Additional elevated abundances of Sn, W, Mo, and P occur throughout the felsic and greenstone terrains and may be the result of mineralization, alteration, or fractionation. These anomalous areas should be followed up with several models in mind.

- Broad, regional, geochemical features, characteristic of the granitoid/gneiss terrain, are defined by higher relative abundances of Nb, Ga, Mo, and Pb.

- Elevated Au and chalcophile abundances occur within the gneiss terrain in the Kellerberrin area. These areas may be previously-unrecognized greenstone enclaves and may warrant further investigation.

The use of ranked data, empirical indices, principal components, and chi-square plots is discussed as a means of determining anomalies as target sites for mineral exploration.

PROJECT LEADER'S PREFACE

R. E. Smith, 5 July 1990

During the period 1980 to mid-1986 phases of testing the use of relatively wide-spaced sampling for laterite geochemistry in mineral exploration of the Yilgarn Block were carried out. These followed on from the CSIRO orientation studies on the Golden Grove (volcanogenic base metal sulphide) and Greenbushes (rare metal pegmatite) deposits. Sample coverage of the Yilgarn Block in these trials largely followed the strategy and tactics of the companies in the AGE joint venture with regard to ground availability, exploration potential, and the feasibility of follow up exploration. The CSIRO Laterite Geochemistry Group provided a research component for these trials, by guiding the scientific parameters including the fundamentals of sampling, data presentation, and data interpretation.

The priorities for sampling are shown in the figure below. These priorities initially were the most important factors in choosing terrain for sampling.

CSIRO/AGE 1983-1986

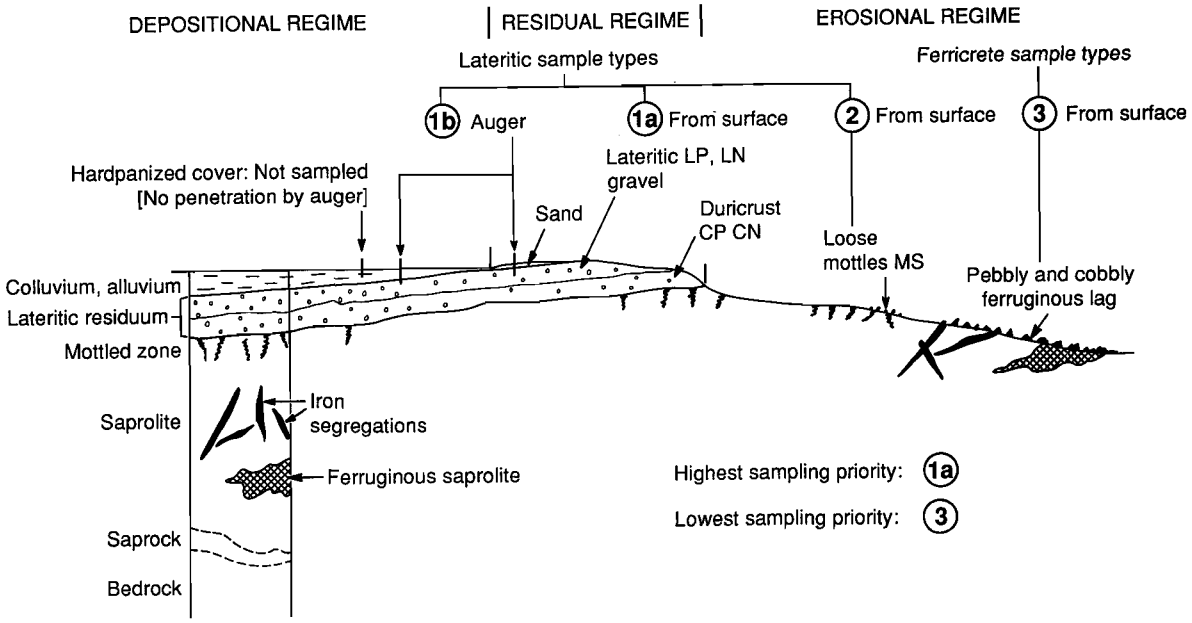

Terminology CSIRO/AGE 1983-1986 Sample type	Code	Equivalent Classification CSIRO/AMIRA 1989 Codes
Lateritic Types		
Loose Pisoliths	LP	LT102
Loose Nodules	LN	LT104
Cemented Pisoliths	CP	LT202, LT212
Cemented Nodules	CN	LT204, LT214
Vermiform Laterite	VL	LT231
Plinthite	PN	
Mottled Zone Scree	MS	LG105
Ferricrete Types		
Massive Ferricrete	MF	IS101, IS102, IS103 IS201, IS301, Some LT229
Ferricrete Fragments	FF	LG201, LG203, LG206
Cemented Pebbly Ferricrete	PF	Some LT228
Ferricrete Pellets	PE	LG201
Re-cemented Fe-rich Colluvium	RC	
Miscellaneous Types		
Ooliths Loose	OL	
Lateritized Rock	LR	
Gossan	GS	
Calareous Nodules	CC	
Other	OT	

It should be noted, that in the AGE reconnaissance stage it was not generally feasible to sample through areas of hardpanized colluvium to reach buried laterite profiles. Hand augering was not successful in such areas, nor was drilling using a light trailer-mounted auger rig where access allowed. Thus there are large gaps within the AGE sampling that can now be effectively explored using to advantage the findings of the current Laterite Geochemistry Project.

Besides generating numerous geochemical anomalies, the testing of which will continue for years to come, the CSIRO/AGE database provides knowledge of backgrounds, regional variation, and element levels in laterite tied, where feasible, to gross bedrock type. Such information thus complements that arising from the Laterite Geochemistry Project's orientation areas and is of relevance both to research and exploration.

TABLE OF CONTENTS

1.0 INTRODUCTION

The report summarizes the results of the progress of an on-going project to assess the geochemistry of laterites and associated ferruginous materials for the purposes of developing and improving exploration concepts, sampling strategies, and isolation of potentially-mineralized areas. The report presents the results of reconnaissance-scale laterite geochemistry on the BARLEE, JACKSON, KALGOORLIE, BENCUBBIN, KELLERBERRIN, SOUTHERN CROSS, CORRIGIN, and HYDEN 1:250,000 map sheets. The sampling was carried out in the 1983-1986 period as part of an application feasibility test of laterite geochemistry for mineral exploration. This work was collaborative between the AGE Joint Venture (Greenbushes Ltd., St. Joe Minerals, and later Sons of Gwalia, NL) and the Multi-element Geochemistry Group, CSIRO.

This report is produced in a format similar to that of the previous Exploration Geoscience Reports 2R, Southern Murchison region; and 68R, Northern Murchison region (Grunsky *et al.*, 1988, 1989).

Regional geochemical databases have been developed for a variety of uses in several countries. One of their ultimate aims has been to define geochemical provinces in which the bedrock sequences contain anomalous populations of specific elements that can be related to zones of mineralization.

The results of this report are part of a reconnaissance-scale survey that resulted in a geochemical database. The database contains samples that cover wide areas of the Yilgarn Block of Western Australia, and forms part of the foundations for on-going research into the use of laterite geochemistry in mineral exploration. The project has focused on the sampling and analysis of the laterite cover and other residual materials that are extensively, but variably, developed throughout the Yilgarn Block. Sampling within this area covers some migmatitic and granitoid terrain. The strategy was to provide multi-element information within felsic and gneissic terrains. This information provides a set of reference groups with which unknown samples may be compared.

1.1 CONCEPT AND SCOPE

The research objectives of establishing a regional geochemical database were:

- to provide knowledge of regional variations in laterite geochemistry which may be due to regional changes in climate or landform characteristics;
- to establish the types of variation in laterite composition encountered in areas away from orientation studies about specific ore deposits;
- to relate laterite composition to both regional and local geological variation;
- to test and further develop the most efficient sampling strategies that will allow cost-effective exploration.

Further discussions on the philosophy and strategy of developing a multi-element geochemical database for the Yilgarn block have been discussed by Smith (1987).

1.2 BACKGROUND TO THE STUDY

Primary and secondary haloes can develop, persist, or be greatly enhanced in size through the development of laterite profiles as documented by Smith *et al.* (1979) who found kilometre-scale chalcophile element haloes in the pisolitic laterite cover associated with the Golden Grove Cu-Zn orebodies. These haloes can occur locally, as well as occurring in a consistent and contiguous manner within greenstone areas. Smith *et al.* (1989) have outlined a number of "chalcophile corridors" within the Yilgarn block and propose that these areas have significantly-higher economic potential.

These observations, together with those of Mazzuchelli and James (1966) and Zeegers *et al.* (1981), provided the rationale for sampling various laterite materials and analyzing a suite of chalcophile and associated elements as well as additional indicator elements. By concisely defining the geochemical characteristics of the various laterite materials, it is expected that better control can be established on classifying the characteristics of unknown suites of samples with the ability to recognize geochemical anomalies that may be associated with mineralization.

Figure 1 shows the plan of the area. Some of the more significant localities are shown for reference purposes with the subsequent maps of this report.

The area forms part of the Archaean Yilgarn Block which is composed of synformal arcuate sequences of metamorphosed supracrustal volcanic and sedimentary assemblages intruded by felsic plutons. Most of the area is dominated by large expanses of gneissic terrain which represent assimilated plutonic and supracrustal rocks.

The region was sampled using a 3-km triangular grid with selected follow-up sampling at a spacing of 1 km and 300 m. A variety of laterite materials was sampled and classified as to the type of sample. Most samples belong to one of two groups consisting of either laterite or ferricrete materials. The most common forms of the laterites are nodular or pisolitic. The ferricrete material is typically Fe-rich, rubbly, or pebbly lag from partly truncated profiles. The sampling media are discussed below.

The geological map of Figure 1 is split into 3 sub-areas. Figure 1a shows the geology of the BARLEE-JACKSON-KALGOORLIE (1:250 000) sheets, where most of the sampling occurs in the Diemals, Marda, and Hunt Range greenstone belts. Figure 1b shows the geology of the BENCUBBIN-KELLERBERRIN-SOUTHERN CROSS (1:250 000) sheets where sampling has been carried out in the gneissic and plutonic terrain and in the Westonia, Holliston, and Southern Cross greenstone belts. Extensive regional sampling was carried out in the gneissic-plutonic domain of the CORRIGIN-HYDEN (1:250 000) map area (Figure 1c). Subsequent geochemical maps in this report are subdivided into these three areas. Extensive follow-up sampling was also carried out in the Diemals and Marda areas. These samples have been treated separately from the regional samples.

2.0 CLIMATE AND PHYSIOGRAPHY

The area falls within a semi-desert Mediterranean climatic regime with mild winters and hot summers with most rain falling in the cooler months of April-September although cyclonic systems can cause heavy falls in the summer months. Rainfall is variable but averages between 200-550 mm per year and decreases northeasterly. Temperature ranges from a winter period mean of 16° C to a summer period mean of 28° C in the general area although summer maxima in excess of 40° C are common.

The area shows only slight topographic variation, with the exception of the resistant bedrock that forms prominent hills. Areas of extensive sandplain, colluvium, and alluvium overlie a Tertiary laterite plateau that has been eroded to form an etchplain (Finkl and Churchward, 1973). This plateau consists of a partly- to completely-stripped laterite duricrust profile (Walker and Blight, 1983; Chin and Smith, 1983; Gee, 1982; Chin, 1986a; Blight, Chin, and Smith, 1984; Chin, 1986b; Chin, Hickman, and Thom, 1984). The laterite duricrust has been eroded in much of the area, resulting in broad alluvial valleys. The surface of the eroded laterite is commonly veneered with yellow sand and scattered pisoliths. Breakaways are common between the old erosional surface and valley floors.

Physiographically, the area is comprised of saline/playa lakes, lake deposits, calcretes, breakaways, bedrock outcrops, and surficial deposits. There are several drainage divides within the area. A substantial portion of the northern part of region drains into Lake Barlee, while much of the southern part of the region drains into the Avon River system.

2.1 SURFICIAL GEOLOGY

Erosion of the greenstone belts has resulted in elongate hills with laterite capping near the tops. Their height is dependent upon the nature of the underlying bedrock. Banded iron formation (BIF) resists weathering and often underlies the larger hills. The granitic/gneissic terrain is characterized by bold monoliths and a flat pavement type of physiography.

The distribution of the laterite materials changes from the south-west to north-east direction. Walker and Blight (1983) have noted that the laterite duricrust is more common in the north and north-east while it tends to be more eroded in the south and south-east. Yellow sand is commonly intermixed with the laterite and is probably locally derived.

In the HYDEN area, the laterite is chiefly composed of nodular duricrust that grades downward into a saprolitic horizon (Chin *et al.*, 1984). Chin *et al.* (1984) also noted that in areas of amphibolite and BIF, the laterite duricrust grades almost directly into fresh rock, with a very narrow zone of saprolite. This is in contrast to the areas that are underlain by felsic intrusions and gneisses, in which the saprolite zone is much thicker. The laterite profile over the ultramafic rocks tends to have a characteristic siliceous (chalcedony) caprock. Silcrete is more common in the laterite profile overlying granitic rocks.

Examination of Figures 2-4 shows a distinct difference in the nature of the laterite materials. Figure 2a shows that most of the laterite is composed of loose nodules (LN) and loose pisoliths (LP). Figures 3a and 4 show an increase in the amount of plinthite (PN) which partly reflects the nature of the underlying felsic intrusive/gneissic material. Its presence may also be due to an increase in the amount of the erosion caused by an increasing rainfall gradient.

3.0 GEOLOGICAL SETTING AND MINERALIZATION

3.1 REGIONAL GEOLOGY

Much of the discussion on the regional geology and mineralization has been synthesized from reports of the Geological Survey of Western Australia by Chin (1986a,b), Blight *et al.* (1984), Chin *et al.* (1984), Chin and Smith (1983), Gee (1982), Kriewaldt (1969), and Walker and Blight (1983).

The area is underlain by early supracrustal rocks, "greenstones", and surrounding felsic intrusive stocks and batholiths with enclaves of gneissic material, all of Archaean age. The supracrustal areas are comprised of predominantly mafic volcanics overlain by later felsic volcanic and sedimentary sequences that have been deformed, metamorphosed, and intruded by later post-kinematic plutons. Late stage faulting has occurred throughout the preserved greenstone belts. Many Au deposits have a proximity to these large scale fault systems. The felsic plutonic rocks are chiefly composed of orthoclase-bearing tonalite that has been commonly referred to as adamellite. The IUGS subcommission on the Systematics of Igneous Rocks recommends that this term be avoided and the term "monzogranite" be substituted (LeMaitre, 1989:40)

Two large arcuate greenstone belts occur within the area, plus a number of smaller "detached" more highly metamorphosed sequences that occur within the monzogranite-tonalite and gneiss terrain. The most northerly greenstone belt occurs in the BARLEE-JACKSON-KALGOORLIE sheets and trends north-westerly to north-easterly from the southwest part of the KALGOORLIE sheet through the Hunt Range, Marda, Diemals, Mt. Elvira, and Marmion areas. To the south, in the SOUTHERN CROSS, and HYDEN areas, the Southern Cross greenstone belts trends north-north-westerly for a distance of approximately 300 km. A U-Pb zircon age of 3340 Ma for the Southern Cross greenstone belt has been determined by Nieuwland and Compston (1981).

Hunt Range - Marda - Diemals Greenstone Belt

Two major volcanic cycles have been recognized within this greenstone belt. Walker and Blight (1983) describe the lower stratigraphy as being comprised of ultramafic and mafic metavolcanic rocks with numerous ultramafic and mafic intrusions and/or sills. The mafic volcanics within this lower sequence are chiefly tholeiitic volcanics with minor amounts of interbedded pelitic and clastic metasediments. The tholeiitic volcanics are primarily basalt in composition and form a monotonous sequence of thick flows. Occasional bed markers consisting of pillow breccias, flow top breccias, and intercalated metasediments have been noted (Chin and Smith, 1983). Banded iron-rich sediments are present in the greenstone enclave west of Johnson Rocks, and in the Diemals formation.

The Diemals formation unconformably overlays the lower sequence and is composed of silty argillite and conglomerate. Rythmically-layered argillites are common and may indicate a submarine fan type of environment. The metasediments are progressively finer-grained towards the top of the sequence indicating a lower energy depositional environment. Coeval with the development of the Diemals sequence is the Marda complex (Chin and Smith, 1983). The Diemals formation may be a distal facies equivalent of the Marda complex.

The Marda complex represents a volcanic complex comprised chiefly of intermediate to felsic pyroclastic volcanics associated with a large volcanic edifice. The volcanic rocks are a sequence of interfingering sub-aerial lavas, pyroclastics, and minor interbedded metasediments (Chin and Smith, 1983). Hallberg (1976:9) has classified the complex as calc-alkaline.

The metamorphic grade varies from prehnite-pumpellyite in the Diemals Formation (Walker and Blight, 1983:6) to upper amphibolite facies in the surrounding gneissic terrain. Greenschist to low-amphibolite metamorphism occurs throughout much of the greenstone belt. Metamorphic grade increases near the greenstone-felsic plutonic boundary.

The ultramafic metavolcanics are composed of three main mineral assemblages:

a) tremolite/actinolite-hornblende-oligoclase/andesine-chlorite-biotite-epidote,
b) talc-tremolite,
c) serpentine-tremolite-chlorite.

Mafic volcanic rocks are typically actinolite-plagioclase-epidote schists in the areas of lower grade metamorphism. Hornblende replaces the actinolite in the areas of higher grade metamorphism. The metamorphic mineralogy of the metasediments is dependent on the initial composition of the sediment. Within the Diemals Formation, andalusite-muscovite is the stable mineral assemblage of the predominantly-pelitic rocks, while muscovite - chlorite - quartz is the stable mineral assemblage of the wackes and arenites.

Southern Cross Greenstone Belt

The Southern Cross Greenstone belt is an accumulation of volcanics and sediments from a single volcanic cycle. The doming of Ghooli and Parker intrusions has exposed the lower stratigraphic units in the Southern Cross sequence (Gee, 1982:12). These lowermost units are quartz-muscovite schist and quartzite that are overlain by ultramafic and mafic metavolcanic rocks. Upwards, the sequence is predominantly ultramafic komatiites and tholeiitic basalts. Pillow structures have been observed in the Bullfinch area of the belt. The uppermost portion of the succession is composed chiefly of pelitic metasediments. The sequence extends northward in the JACKSON area, forming the Bullfinch part of the greenstone belt (Chin and Smith, 1983). Southward, the succession extends into the HYDEN area (Chin *et al.*, 1984) where it is known as the Forrestania belt. Both northward and southward extensions of the Southern Cross belt contain the same stratigraphic assemblages.

The lower quartzite-arenite units may be associated with platform-type volcanism as described by Thurston and Chivers (1990). Chin and Smith, (1983) describe a similar succession in the tectonically-dislocated extension (the Koolynobbing belt) of the Southern Cross belt. This area contains a similar lower sequence of quartz-rich rocks overlain by tholeiitic basalts and lacking significant amounts of ultramafic metavolcanics. In the Forrestania area, quartz-rich schists predominate in the upper part of the metasedimentary sequence. This may reflect distal facies felsic tuffaceous rocks that accumulated near the end of the volcanic cycle.

The pelitic metasediments are the uppermost units in the supracrustal sequence and due to the doming nature of the Ghooli and Parker intrusions, these units face away from the centre of the belt. Andalusite, cordierite, and staurolite have been reported from several assemblages (Gee, 1982) and indicate a high degree of metamorphism.

Banded Fe-rich metasediments occur throughout the sequence, and are more abundant near the top. Gee (1982) describes much of the Fe-rich metasediments as being poor in Fe-oxide and that most of the Fe occurs as Fe-silicates. It is not clear as to the nature of the Fe-rich units. They could be metamorphosed Fe-oxide-chert units or they could have been a mixture of mafic tuffs mixed with Fe-oxide-chert units being deposited simultaneously.

Greenstone Enclaves

Several smaller greenstone sequences occur west of the Southern Cross greenstone belt. These sequences extend from Holleton in the southern part of the SOUTHERN CROSS area, northward to Westonia, and westward to Bencubbin. These belts are more highly metamorphosed than the Marda-Diemals and Southern Cross belts (Gee, 1982; Blight *et al.*, 1984). Mafic to ultramafic metavolcanics with minor amounts of interbedded BIF have been observed in the Holleton, Westonia, and Bencubbin belts. Much of the Westonia belt is composed of a supracrustal derived biotite gneiss some of which is derived from felsic pyroclastic rocks (Gee, 1982:10). In the

HYDEN area, several small isolated greenstone enclaves have been reported by Chin *et al.* (1984). They also report a progressive change in the metamorphic grade from southwest to northeast. Greenstone enclaves are metamorphosed to granulite facies in the southwest, while the enclaves in the northeast are metamorphosed to upper amphibolite facies.

Remnant amphibolite, BIF, and quartzitic units occur as discontinuous lenses and rafts throughout the granitoid gneiss in the KELLERBERRIN and CORRIGIN areas. Relict bedding and cross-bedding in the quartzites have been noted in some of the outcrops (Chin, 1986a, 1986b).

Granitoid Rocks

Most of the area is underlain by felsic plutonic and gneissic rocks. The gneiss is derived from the deformation of felsic intrusions and from the assimilation of supracrustal material. In the BARLEE, JACKSON, SOUTHERN CROSS areas, the granitoid rocks can been subdivided into syn- and post-tectonic types (Gee, 1982). Syntectonic granitoids have tectonic fabrics and occur in elongate zones peripheral to, and enclosing the greenstone sequences. Post-tectonic granitoids have discordant boundaries and intrude the older granitoids and greenstone. The BENCUBBIN, KELLERBERRIN, and CORRIGIN areas are part of the Western Gneiss Terrain (Gee *et al.*, 1981).

BARLEE, JACKSON, SOUTHERN CROSS

Syntectonic granitoids are typically banded quartz-feldspar-biotite gneiss. These rocks are compositionally banded, complexly folded, with varying proportions of quartzo-feldspathic neosome. Gneissosity varies from well-developed compositional-banding to mineral segregation at the granular scale. The syntectonic gneisses are transitional between a foliated granoblastic granitoid to the well-developed compositionally-banded gneisses (Gee, 1982). Agmatitic orthogneiss has been observed in the western part of the Southern Cross greenstone belt.

Post tectonic granitoids are comprised of massive to foliated, biotite-bearing, variably-grained monzogranite, granite, and related rocks. Microcline porphyritic varieties are common. Magmatic layering can be observed in the larger exposures in some areas.

In the BARLEE area, the gneiss is composed of layered feldspar-quartz-biotite trending in a northerly direction (Walker and Blight, 1983). Narrow enclaves of meta-quartzite, BIF, and amphibolite are common and indicate assimilation of the supracrustal sequences. Banded quartzo-feldspathic ortho-gneiss is observed within and around the para-gneiss assemblages.

Layered, lineated, tonalite-monzogranite-granodiorite gneiss border the greenstone sequences. These gneissic rocks are composed of alternating layers of medium-grained, cystalloblastic plagioclase-microcline-biotite-quartz. The layering is continuous over considerable distances. Deformed pegmatite and aplite dykes intrude the sequence. The gneiss lacks enclaves of supracrustal material and is believed to be an orthogneiss derived from igneous granitoids. The gneiss is continuous throughout the BARLEE, JACKSON, and SOUTHERN CROSS areas. Orthogneiss is the dominant rock that separates the Southern Cross and the Marda-Diemals-Hunt Range greenstone sequences.

BENCUBBIN, KELLERBERRIN, CORRIGIN

The BENCUBBIN area is composed mainly of porphyritic to seriate monzogranite that is considered to be post-tectonic. A sequence of intrusions has been outlined by Blight *et al.* (1984). An early, foliated, fine- to medium-grained monzogranite-granite has been intruded by a homogeneous medium- to coarse-grained granite and monzogranite. This in turn, was intruded by a seriate monzogranite.

The most abundant rock type is a seriate, medium- to coarse-grained biotite-granite-monzogranite that occurs throughout most of the Yilgarn block (Blight *et al.*, 1984).

The KELLERBERRIN area is comprised mostly of the large Kellerberrin batholith which is seriate and porphyritic granite and monzogranite.

The CORRIGIN area is composed of seriate and porphyritic granite and monzogranite, deformed and recrystallized granite and monzogranite, and a recrystallized, foliated, and banded gneiss intruded by leucocratic monzogranite.

3.2 MINERALIZATION

Gold

The nature and distribution of Au deposits have been summarized by a number of researchers and agencies (Groves, 1988; Hickman and Watkins, 1988).

Gold is the most significant commodity in the area. In the BARLEE sheet, the most significant area of production was in the Evanston group (>1200 kg). Gold was mined from quartz-carbonate veins in an ultramafic schist. Figure 2e shows the locations of the Johnston Range Au deposits.

In the JACKSON area, several Au mining centres occur in a variety of geological settings. Most of the Au production (>20,932 kg Au) comes from the Bullfinch area. In addition, Ag was mined as a by-product in this area (>3949 kg Ag). The mineralization is associated with quartz stringers crosscutting mafic schist and jaspilite.

Gold production has been greatest in the Southern Cross greenstone belt. More than 46,696 kg of Au have been produced from this area. The largest producers have been in the Westonia, Marvel Loch, Mount Palmer, Southern Cross, Corinthia, Greenmount, and Parkers Range camps. A major feature of almost all of the deposits is the structural control that permitted the deposition of Au (Colvine *et al.*, 1988).

Gold has also been mined from the Forrestania area and more recently the Bounty Mine has been operating in the Mt. Holland area.

Silver has been recovered along with Au in some of the deposits.

Iron

Iron ore occurs within the Koolyanobbing Range. Iron ore reserves of up to 40 million tonnes occur at the Dowd Hill and 'A' orebodies. The grade averages 61.4% Fe with .13% P. Additional deposits include, Bungalbin Hill (61 million tonnes, 58% Fe), Koolyanobbing (54 million tonnes, 62% Fe), Mount Jackson (30.5 million tonnes, 62% Fe), and Windarling Peak (25.4 million tonnes, 65% Fe). The Fe occurs as:

- limonite-hematite,
- enriched Fe-oxide facies,
- massive goethite, specular hematite, limonite,
- minor magnetite.

Base Metals

Nickel reserves of 20,000 tonnes of 2.5% Ni within the basal part of an ultramafic sequence have been outlined in the Trough Well area (JACKSON). The Koolyanobbing area contains several Ni gossans within ultramafic schists.

Nickel deposits have been outlined in the southern part of the Forrestania greenstone belt in the Hatters Hill area. The ore appears to be at the base of an ultramafic succession of flows. A total of 11 million tonnes with a weighted average of 2.31% Ni has been outlined over 6 deposits (Chin *et al.*, 1984).

Copper has been mined (0.82 tonnes Cu) at Mount Jackson (JACKSON) from Cu-bearing carbonate fracture fills. No stratiform Cu-Zn deposits have been discovered to date.

Other Commodities

Arsenic (arsenopyrite) has been recovered from the Jupiter Mine where assay values have been recorded up to 18% As (Gee, 1982). The ore occurs in pelitic rocks and has been investigated for other metals.

Chromium has been reported at West Bendering (CORRIGIN) with concentrations up to 10% Cr.

Uranium occurs east of Brookton and Wogerlin Hill (CORRIGIN). No further developments have been made at these occurrences.

4.0 THE SAMPLING PROGRAMME

4.0.1 SAMPLING

A 3-km spaced triangular sampling grid was used over most of the sampled area, with limitations caused by the distribution of access roads, the extent of erosional dissection of the laterite cover, the extent of cover by younger alluvium/colluvium, and the extent of mining and other land tenements. Various follow-up and fill-in samples were also taken, usually closing the sample spacing to 1 km, in some cases to 330 m; the locations of follow-up sampling being obvious in the plots showing sample sites, for example at 1:250,000 scale or more detailed. Figures 2, 3, and 4 show the distribution of the samples collected throughout the area according to the two major sample groups, the laterite and the ferricrete materials. In addition, the maps of each of the three areas are subdivided into "Regional (R)" samples and "Follow-up (F2/F3)" samples. Follow-up samples were not collected in the Bencubbin-Kellerberrin-Southern Cross and Corrigin-Hyden areas.

The database is composed of samples collected from all three phases of the study. Samples that are labelled "R" in the description field (see Appendix 1) are those initially collected at the 3-km spacing regional scale. Samples labelled "F2" are those collected during follow-up work at the 1-km spacing interval, and samples labelled "F3" are those samples collected at less than 1-km spacing from additional follow-up work after the F2 samples were collected. The number of samples for each type is:

R	Regional Samples	1579
F2	Follow-up Phase 2	199
F3	Follow-up Phase 3	324
Total		2102

Not all of the greenstone areas have been sampled. Areas that were not included in the sampling programme are the: Koolyanobbing, Bullfinch (northern Southern Cross), northern Hunt Range, Mt. Manning Range, Mt. Elvire, Mt. Marmion, Yerilgee-Dodanea (Kalgoorlie) greenstone belts.

The strategy was to sample the cemented pisolitic laterite blanket and/or the loose laterite pisoliths which had been released from the duricrust by natural disaggregation. Laterite nodules and pisoliths in the range of 1-cm to 2-cm diameter were sought in order to avoid the possibility of skewing the sample characteristics if very coarse material were collected and to aid sample preparation by providing suitable feed for the disk grinding stage (avoiding coarse crushing). Sampling was typically carried out over a 10 metre radius in order to suppress any unforeseen local variation. A 1-kg sample was collected for crushing, grinding and analysis of an aliquot. A separate 1-kg sample was collected for permanent reference. Other sample types were collected where the prime media were not available. A breakdown of the number of samples collected is given in Table 1. Where available, 1:50,000 photomosaics were used in selecting sample sites and for recording the locations. Each sample was assigned AMG coordinates.

The classification used in this report is the scheme adopted during the AGE study of 1983-1986. A more comprehensive and, in due course, genetic classification scheme is currently under development within the CSIRO/AMIRA Laterite Geochemistry Project. The most recent terminology and classification can be found in Anand *et al.* (1989) in which the terminology and classification of laterite and ferruginous materials has been expanded. The terms used in this report follow the older terms that are general enough to be considered useful for the purposes of a regional study. Correlation between the older and current schemes is given in Table 1.

4.0.2 SAMPLE TYPES

I LATERITE SAMPLE TYPES

Samples belonging to the laterite family often occurring geomorphically above breakaways (i.e. a relatively complete laterite profile):

Loose Pisoliths (LP) and Cemented Pisoliths (CP) - Ferruginous particles with high sphericity, 2 mm - 3 cm in diameter, and a concretionary Fe-rich or Fe-bearing coating. Internal concentric banding is common. This sample type commonly forms a blanket deposit, whether loose or cemented, up to a few metres in thickness. Also forms redistributed colluvium.

Loose Nodular Laterite (LN) Cemented Nodular Laterite (CN) - Ferruginous particles with low sphericity but rounded. Commonly 1 - 4 cm across and a goethitic cutan (skin). Lateritic nodules and pisoliths form a continuous series and commonly occur together.

Vermiform or Vermicular Laterite (VL) - Iron-rich cemented mottled zone saprolite containing sinuous worm-like tunnels, holes or clay zones. May contain spaced pisoliths, nodules, or sporadic rock fragments.

Plinthite (PN) - Grit cemented by goethite, with visible quartz grains. Plinthite fragments do not have a concretionary goethite cutan.

Mottled Zone Scree (MS) - Loose, locally-derived scree or float derived from Fe-rich mottles within the lateritic weathering profile.

II FERRICRETE SAMPLE TYPES

Samples belonging to the ferricrete family typically occurring in situations where the nodular/pisolitic laterite has been removed by erosion, but stripping has not cut deeply into saprolite. These include:

Massive Ferricrete (MF) - Iron rich material lacking pisolith- nodule texture, commonly has a botryoidal texture.

Ferricrete Fragments (FF) - Rounded fragments of Fe-rich material often showing relict internal structure but have no Fe-rich concretionary skin.

Cemented Pebbly Ferricrete (PF) - Dense black Fe-rich material with pebbly texture and irregular shape. This type normally occurs at the top of a full laterite profile.

Ferricrete Pellets (PE) - Particles of Fe-rich material with moderate to high sphericity, up to 1.5 cm across and no Fe-rich concretionary skin.

Recemented Fe-rich Colluvium (RC) - Fe-rich angular to sub-rounded rock fragments in a fine Fe-rich matrix.

III OTHER CATEGORIES

Loose Ooliths (OL) - Ferruginous particles with high sphericity <2 mm in size with a definite concretionary Fe-rich coating. Commonly they are black or very dark brown. These may occur in soil, as surface lag or may be cemented. They do not form blanket deposits.

Lateritized Rock (LR) - Saprolite that is enriched in Fe-bearing weathering minerals; goethite and hematite.

Figure 2 shows the distribution of the laterite sample materials (LN, LP, CN, CP, MS, PN) and Figure 3 shows the distribution of the ferricrete materials (FF, MF, PF, RC, PE). Sampling of ferricretes is more widespread in the northern part of the area, whilst sampling of loose nodules dominates the southern part of the area.

Table 1. Sample Type, Abbreviation, and Number of Samples.

Sample type	Code	Number of Samples	Equivalent Classification CSIRO/AMIRA 1989 Codes
Lateritic Types			
Loose Pisoliths	LP	428	LT102
Cemented Pisoliths	CP	20	LT202, LT212
Loose Nodules	LN	1083	LT104
Cemented Nodules	CN	12	LT204, LT214
Vermiform Laterite	VL	3	LT231
Plinthite	PN	156	
Mottled Zone Scree	MS	113	LG105
Total		1815	
Ferricrete Types			
Massive Ferricrete	MF	48	IS101, IS102, IS103, IS201, IS301, Some LT229
Ferricrete Fragments	FF	97	LG201, LG203, LG206
Cemented Pebbly Ferricrete	PF	10	Some LG228
Ferricrete Pellets	PE	11	LG201
Re-cemented Fe-rich Colluvium	RC	18	
Total		184	
Miscellaneous Types			
Ooliths Loose	OL	20	
Lateritized Rock	LR	83	
Total		103	
GRAND TOTAL		2102	

4.0.3 SAMPLE PREPARATION

The samples were prepared using non-metallic sample preparation methods described by Smith *et al.* (1987). Oversized material from 1 kg samples is reduced to minus 8 mm by crushing between zirconia plates in an automated hydraulic press. The crushed oversized material, together with the direct feed material, is then fed to an epoxy-resin lined disc grinder with alumina plates and further reduced to minus 1 mm. Final milling is done in an agate or alumina mill. Cleaning of the equipment is performed by a combination of air- and sand-blasting and the passage of a quartz blank.

4.1.0 ANALYTICAL METHODS

A total 2102 samples were analyzed by Amdel Ltd. (Adelaide) for 24 elements. An additional 7 elements were analyzed by the CSIRO analytical facilities on 40% of the samples. Gold was analyzed by Analabs (Perth) on 1152 of the samples. The methods of analysis are outlined in Table 2. Tin and Bi were analyzed by two methods because of their perceived importance in laterite geochemistry and to provide a consistent gauge of confidence in the results. At this point, the following elements have been analyzed by the methods outlined in Table 2: SiO_2, Fe_2O_3, MgO, CaO, TiO_2, Au, Mn, Cr, V, Cu, Pb, Zn, Ni, Co, As, Sb, Bi1, Bi2, Mo, Ag, Sn1, Sn2, Ge, Ga, W, Ba, Zr, Nb, Ta, Se, and, Be. Additional elements may be analyzed later on. Only Bi2 and Sn2 have been used in this report. *All references to these two elements have been made with respect to Bi2 and Sn2.* The data on the accompanying diskette contain Bi1, Bi2, Sn1, and Sn2. Appendix 1 indicates the format of the data.

TABLE 2

ANALYTICAL METHODS AND LOWER LIMITS OF DETECTION

Element	Reported as	Detection Limit	Laboratory	Analysis	Digestion Method
SiO2	WT%	0.5	CSIRO	ICP FS	
Al2O3	WT%	0.5	CSIRO	ICP FS	
Fe2O3	WT%	0.1	AMDEL	AAS	HF
MgO	WT%	0.05	CSIRO	ICP FS	
CaO	WT%	0.05	CSIRO	ICP FS	
TiO2	WT%	0.003	CSIRO	ICP FS	
Mn	PPM	5	AMDEL	AAS	HF
Cr	PPM	5	AMDEL	XRF	
V	PPM	10	AMDEL	XRF	
Cu	PPM	2	AMDEL	AAS	HF
Pb	PPM	4	AMDEL	XRF	
Zn	PPM	2	AMDEL	AAS	HF
Ni	PPM	5	AMDEL	AAS	HF
Co	PPM	5	AMDEL	AAS	HF
As	PPM	2	AMDEL	XRF	
Sb	PPM	2	AMDEL	XRF	
Bi1	PPM	1	AMDEL	OES	
Bi2	PPM	1	AMDEL	XRF	
Mo	PPM	2	AMDEL	XRF	
Ag	PPM	0.1	AMDEL	OES	
Sn1	PPM	1	AMDEL	OES	
Sn2	PPM	1	AMDEL	XRF	
Ge	PPM	1	AMDEL	OES	
Ga	PPM	1	AMDEL	OES	
W	PPM	10	AMDEL	XRF	
Ba	PPM	100	CSIRO	ICP FS	
Zr	PPM	50	CSIRO	ICP FS	
Nb	PPM	3	AMDEL	XRF	
Ta	PPM	3	AMDEL	XRF	
Se	PPM	1	AMDEL	XRF	
Be	PPM	1	AMDEL	OES	
Au	PPB	1	ANALABS	Carbon Rod	Aqua Regia

Legend: AAS Atomic Absorption Spectroscopy
XRF X-ray Flouresence
ICP FS Inductively Coupled Plasma Fusion
OES Optical Emmission Spectroscopy

Samples analyzed by CSIRO were carried out on an Inductively Coupled Plasma Spectrometer (ICP) using a lithium metaborate fusion dissolved in nitric acid. Gold was analyzed by Analabs Laboratories using Atomic Absorption Spectroscopy (Graphite Furnace) after aqua-regia dissolution of 50 g of sample pulp.

4.1.1 ANALYTICAL QUALITY CONTROL

Each batch of samples submitted for analysis contained three control samples that represent a spectrum of multi-element values. These control samples were submitted in a scrambled numerical sequence. The samples were also subjected to replicate analysis both by the CSIRO analytical facilities and by an independent laboratory. Problems of between-batch variation could usually be detected by examination of maps of the plotted data. If any clustering or unusual patterns were noted, the duplicated samples were submitted for assay.

5.0 DATA PRESENTATION AND ANALYSIS

The geochemical data that accompany this report are contained on a 5.25" floppy diskette which can be found in the back pocket of the report. Appendix 1 provides the details regarding the format of the data.

A summary of the multi-element geochemical data is listed in Tables 3-8. The Tables list the number of samples analyzed for each element, the 1, 5, 10, 25, 50, 75, 90, 95, and 99th percentiles, minimum, maximum, mode, mean values, and the standard deviation.

Table 3 provides summary statistics for the entire dataset of laterite materials and Table 4 lists the summary statistics of the entire suite of ferricrete materials. However, because the distribution of samples covers both greenstone and felsic plutonic/gneissic domains, the data were split into sub-groups for additional statistical summaries. The Tables list the summary statistics for the following groups of data:

Table 3: Summary Statistics for Barlee-Jackson-Kalgoorlie-Bencubbin-Kellerberrin-Southern Cross-Corrigin-Hyden sheets, all Regional (R), and Follow-up (F2/F3) samples for **Lateritic** materials (LN, LP, CN, CP, PN, VL, MS).

Table 4: Summary Statistics for Barlee-Jackson-Kalgoorlie-Bencubbin-Kellerberrin-Southern Cross-Corrigin-Hyden sheets, all Regional (R), and Follow-up (F2/F3) samples for **Ferricrete** materials (MF, FF, PF, PE ,RC).

Table 5a: Summary Statistics for Barlee-Jackson-Kalgoorlie sheets, all Regional (R) samples for **Lateritic** materials (LN, LP, CN, CP, PN, VL, MS).

Table 5b: Summary Statistics for Barlee-Jackson-Kalgoorlie sheets, all Follow-up (F2/F3) samples for **Lateritic** materials (LN, LP, CN, CP, PN, VL, MS).

Table 6a: Summary Statistics for Barlee-Jackson-Kalgoorlie sheets, all Regional (R) samples for **Ferricrete** materials (MF, FF, PF, PE ,RC).

Table 6b: Summary Statistics for Barlee-Jackson-Kalgoorlie sheets, all Follow-up (F2/F3) samples for **Ferricrete** materials (MF, FF, PF, PE ,RC).

Table 7: Summary Statistics for Bencubbin-Kellerberrin-Southern Cross-Corrigin-Hyden sheets, all Regional (R) samples for **Lateritic** materials (LN, LP, CN, CP, PN, VL, MS).

Table 8: Summary Statistics for Bencubbin-Kellerberrin-Southern Cross-Corrigin-Hyden sheets, all Regional (R) samples for **Ferricrete** materials (MF, FF, PF, PE ,RC).

Materials which were classified as loose nodules (LN), loose pisoliths (LP), cemented nodules (CN), cemented pisoliths (CP), plinthite (PN), vermicular laterite (VL), and mottled zone scree (MS) are generally known to be compatible sample media and were therefore grouped together. These samples, placed in the laterite family, total 1815, and their statistics are shown in Tables 3, 5, and 7. Similarly, samples of the ferricrete categories, ferricrete fragments (FF), massive ferricrete (MF), cemented pebbly ferricrete (PF), and re-cemented Fe-rich colluvium (RC) were grouped together, totalling 184 samples, and their statistics are listed in Table 4, 6, and 8. This region is far more abundant in lateritic material than the area to the north (northern Murchison area, Grunsky *et al.*, 1989) and more similar to the distribution of sample types as seen in the southern Murchison area (Grunsky *et al.*, 1988).

Many samples were analyzed for elements whose values were below the detection limit. In these cases, the value of the variable was set to one third of the detection limit as the default minimum value. Subsequent statistical and numerical procedures used this minimum value. As mentioned above, not all samples have been analysed for the full set of elements, at this stage. In such cases, for calculations of statistics the number of samples used to compute the statistic was reduced. The number of samples used for the calculations of the statistics of each element is indicated in the Tables.

Examination of the Tables is useful in making preliminary assessments about the data. The first part of each table provides insight as to how the values of data are distributed over the range of the data. By scanning the values over the range of percentiles, the nature of the distribution of the data can be quickly observed. Elements with highly skewed distribution (e.g. Au) tend to have similar concentrations over the range of percentiles, increasing rapidly at the 90, 95, and 99 percentile rankings. More normally-distributed elements (e.g. V) show a more uniform change in abundance with increasing percentile levels. Samples that occur in the upper percentile range (>95th percentile) are usually of interest in an exploration programme. It is these "high" or "anomalous" values that may be indicative of a mineralized zone whose chemistry is unlike that of the regional geochemical patterns.

The 50th percentile gives the abundance value of the midpoint of the distribution of samples and can be quite different from the arithmetic mean of the sample population. This 50th percentile value is recommended for estimating the central value of a distribution. The Tables also list minimum, maximum, median, mode, mean, and standard deviation for each element. Normally-distributed populations tend to have similar values for the median, mode, and mean. The standard deviation gives an estimate of the range of the data around the arithmetic mean.

Comparison of Tables 3 and 4 clearly show significant differences of chemistry between the two populations of laterites and ferricretes over the entire area. Examination of Tables 5a and 5b show that the chemistry between the regional samples ("R") and the follow-up samples ("F2/F3") is similar in range with the exception of Cu, As, Sb, Sn. These differences are to be expected since the F2/F3 samples were following up anomalies or possible anomalies in the reconnaissance sampling.

Statistical tests involving the t-test (testing the similarities of the means) and the F-test (testing the similarities of variances) have not been carried out because many of the frequency distributions are non-normal and any statistical inferences may be misleading. Procedures exist for transforming the data into more normal-like distributions for subsequent statistical inferences (e.g., power transformations, see Smith *et al.*, 1984); however, such a task is beyond the scope of this report.

Tables 6a and 6b list the summary statistics of ferricretes for the regional samples ("R") and the follow-up samples ("F2/F3") for the Barlee-Jackson-Kalgoorlie areas only. In these Tables, there appears to be some significant differences between the regional and follow-up sampling for SiO_2, MgO, TiO_2, Cr, V, Ni, Co, As, Sb, Bi, and Nb. The higher levels of As, Sb, and Bi in the F2/F3 sampling are to be expected in the follow-up of chalcophile anomalies. Statistical testing of these observations has not been carried out and would require transformation procedures.

Table 7 lists the summary statistics for laterites collected over the Bencubbin-Kellerberrin-Southern Cross-Corrigin-Hyden sheets and Table 8 lists the summary statistics for ferricrete materials over the same area.

Barium must be interpreted with caution as the method of sample preparation (from alumina disks) adds an average of about 100 ppm of Ba, because of an impurity in the alumina, depending on the hardness of the sample.

Bismuth and Sn include two methods of analysis one by OES and the other by XRF. Both methods confirm consistency of the results.

In conjunction with the summary tables, Table 9 provides a list of the samples that are in the plus 99th percentile ranking of the **Lateritic** (LN, LP, CN, CP, PN, VL, MS) samples for each element/oxide. The Table includes the sample number, regional/follow-up sample, easting, northing and the corresponding element/oxide value. As a single element tool, these ranked sample lists can assist in exploration programmes.

5.1 HISTOGRAMS

Histograms of the data were plotted for selected elements of specific sample types. These plots are shown in Figures 5 - 34. The histograms were computed using 40 class divisions based on the minimum and maximum values of the variables. For presentation purposes, the minimum and maximum values were truncated at the mean ± three standard deviations. Above each histogram is a box and

truncated at the mean ± three standard deviations. Above each histogram is a box and whisker plot that shows the median (50th percentile), left hinge (25th percentile), right hinge (75th percentile) and range (minimum and maximum values) of the data. Each histogram also lists these values in a numerical form at the right-hand side of the figure.

The presentation of the data is different from previous reports (Grunsky *et al.*, 1988, 1989). Previous reports provided comparative histograms of the laterites and ferricretes; however in this area the ferricrete samples represent only 10% of the sample population. Therefore, comparative histograms are shown between two compositionally- and lithologically-distinct areas. Thus the first histogram is composed of laterite samples from the BARLEE-JACKSON-KALGOORLIE laterites and the second histogram is composed of laterite samples from the BENCUBBIN-KELLERBERRIN-SOUTHERN CROSS-CORRIGIN-HYDEN areas. Sampling covers a greater area of gneisses, migmatites, and granitoids in the latter region.

A visual comparison of the histograms yields the following observations:

- The abundances of SiO_2 in the BARLEE-JACKSON-KALGOORLIE area are distinctly less than SiO_2 abundances in the BENCUBBIN-KELLERBERRIN-SOUTHERN CROSS-CORRIGIN-HYDEN area (Figures 5a,b). The underlying lithologies are generally reflected by SiO_2 abundance.

- There is no distinct difference in the abundances and ranges of values for Al_2O_3, MgO, and CaO between the BARLEE-JACKSON-KALGOORLIE and BENCUBBIN-KELLERBERRIN-SOUTHERN CROSS-CORRIGIN-HYDEN terrains (Figures 6a,b, 8a,b, 9a,b).

- The abundances of Fe_2O_3 in the BARLEE-JACKSON-KALGOORLIE area are distinctly greater than Fe_2O_3 abundances in the BENCUBBIN-KELLERBERRIN-SOUTHERN CROSS-CORRIGIN-HYDEN area (Figures 7a,b). Lithological variation and the effects of weathering processes can be reflected by the abundances of Fe_2O_3.

- The range of TiO_2 abundances in the BARLEE-JACKSON-KALGOORLIE area is greater than the range of TiO_2 in the BENCUBBIN-KELLERBERRIN-SOUTHERN CROSS-CORRIGIN-HYDEN area (Figures 10a,b). The median values are similar. The nature of the underlying lithologies are usually indicated by TiO_2 abundances.

- The range of Ag abundances in the BARLEE-JACKSON-KALGOORLIE area is greater than the Ag range in the BENCUBBIN-KELLERBERRIN-SOUTHERN CROSS-CORRIGIN-HYDEN area (Figures 11a,b). Both areas show similar background values.

- The range and median values of Mn, Cr, V, Ni and Co abundances in the BARLEE-JACKSON-KALGOORLIE area are greater than the Mn, Cr, V, Ni, and Co range of abundances and median values in the BENCUBBIN-KELLERBERRIN-SOUTHERN CROSS-CORRIGIN-HYDEN area (Figures 12a,b, 13a,b, 14a,b, 18a,b, 19a,b). These elements tend to show variation in the underlying lithologies, but can also reflect weathering and mineralization processes.

- The ranges of abundances and median values of Cu, and Zn in the BARLEE-JACKSON-KALGOORLIE area are greater than those in the BENCUBBIN-KELLERBERRIN-SOUTHERN CROSS-CORRIGIN-HYDEN area (Figures 15a,b, 17a,b). These elements tend to show variation in the underlying lithologies and mineralization processes.

- The range of abundances and median value of Pb in the BARLEE-JACKSON-KALGOORLIE area are less than the range of abundances and median value of Pb in the BENCUBBIN-KELLERBERRIN-SOUTHERN CROSS-CORRIGIN-HYDEN area (Figures 16a,b). The background abundance of Pb is generally higher in felsic plutonic and gneissic terrains relative to supracrustal rocks. Elevated values of Pb can also reflect mineralization processes.

• The ranges of As and Sb values in the BARLEE-JACKSON-KALGOORLIE area are greater than the As and Sb ranges of values in the BENCUBBIN-KELLERBERRIN-SOUTHERN CROSS-CORRIGIN-HYDEN area (Figures 20a,b, 21a,b). These elements can reflect the presence of alteration zones and mineralizing events. The background values between the two terrains are similar.

• The ranges of abundances and distributions of Bi, Sn, Ge, Ga, and W (Figures 22a,b, 24a,b, 25a,b, 26a,b) are similar between the BARLEE-JACKSON-KALGOORLIE and BENCUBBIN-KELLERBERRIN-SOUTHERN CROSS-CORRIGIN-HYDEN areas. For these elements, background values are similar and, when present in significant amounts, they reflect alteration/mineralization processes.

• Molybdenum (Figures 23a,b) shows a slightly greater mean value and range of abundances in the BENCUBBIN-KELLERBERRIN-SOUTHERN CROSS-CORRIGIN-HYDEN area relative to the BARLEE-JACKSON-KALGOORLIE area. The presence of differentiated felsic intrusive rocks and mineralizing processes can be reflected by the relative range of Mo abundances.

• Tungsen (Figures 27a,b) shows a greater range of values in the BARLEE-JACKSON-KALGOORLIE area relative to the BENCUBBIN-KELLERBERRIN-SOUTHERN CROSS-CORRIGIN-HYDEN area. Significant amounts of W reflects alteration/mineralization processes.

• Barium (Figures 28a,b) shows a greater mean value and range of abundances in the supracrustal rocks of the BARLEE-JACKSON-KALGOORLIE area relative to the BENCUBBIN-KELLERBERRIN-SOUTHERN CROSS-CORRIGIN-HYDEN area.

• Zirconium (Figures 29a,b) shows a greater mean value and range of abundances in the felsic domain of the BENCUBBIN-KELLERBERRIN-SOUTHERN CROSS-CORRIGIN-HYDEN area relative to the supracrustal rocks of the BENCUBBIN-KELLERBERRIN-SOUTHERN CROSS-CORRIGIN-HYDEN area. Zirconium generally reflects the composition of the underlying lithologies.

• Niobium (Figures 30a,b) shows a greater median and range of values in the felsic granitoids of the BENCUBBIN-KELLERBERRIN-SOUTHERN CROSS-CORRIGIN-HYDEN area relative to the supracrustal rocks of the BENCUBBIN-KELLERBERRIN-SOUTHERN CROSS-CORRIGIN-HYDEN area. It can reflect the presence of underlying felsic granitoid terrains.

• Tantalum and Beryllium (Figures 31a,b, 33a,b) display little variation in abundances and are of limited use. Almost all of the values are less than detection limit; however, where they are elevated they may reflect alteration/mineralization events.

• Selenium (Figures 32a,b) shows a similar median and range values for both supracrustal and felsic granitoid terrains. Its presence may relate more to the nature of the weathering than to the underlying lithologies or alteration/mineralization processes.

• The range of Au abundances is greater in the BARLEE-JACKSON-KALGOORLIE area relative to the BENCUBBIN-KELLERBERRIN-SOUTHERN CROSS-CORRIGIN-HYDEN area. However, the median value of Au in the BENCUBBIN-KELLERBERRIN-SOUTHERN CROSS-CORRIGIN-HYDEN area is greater. This difference may reflect the presence of some elevated Au samples in the Southern Cross belt that have been included in the samples of the BENCUBBIN-KELLERBERRIN-SOUTHERN CROSS-CORRIGIN-HYDEN area.

Some elements exhibit bi-modal or poly-modal distributions. This usually occurs with elements that reflect underlying lithologies and alteration/mineralizing events. Elements that exhibit these characteristics are SiO_2, Al_2O_3, Fe_2O_3, TiO_2, Ag, Cr, V, Cu, Zn, Ni, As, Sb, Bi, Mo, Sn, W, Zr, and Au.

Elements that also show bi-modal characteristics related to greenstone lithologies include SiO_2, Al_2O_3, Fe_2O_3, TiO_2, Cr, V, and Zr. The bi-modal characteristics occur in the BARLEE-JACKSON-KALGOORLIE area where there is a greater diversity of lithologies (basalts vs. rhyolites, etc.). These same elements display a more uni-modal distribution in the BENCUBBIN-KELLERBERRIN-SOUTHERN CROSS-CORRIGIN-HYDEN area where the compositional range of the underlying lithologies (granitoid rocks) is not as diverse. Elements such as Ag, Cu, Zn, As, Sb, Bi, Mo, Sn, W, and Au tend to show similar distribution shapes for both of the areas. However, the BARLEE-JACKSON-KALGOORLIE area tends to have more outliers and a higher median value for the chalcophile elements since most of the mineralized and altered zones occur within the greenstone areas.

Most of the elements have non-normal frequency distributions and for many of the histograms of these elements positively skewed values can represent fractionated igneous environments or anomalous values that are potentially associated with various types of mineralization. Some elements, in particular the chalcophile suite (As, Sb, Bi, Se, Pb, Ge, Zn, Cu, Ag) are known to be good pathfinders for both base-metal sulphide mineralization and precious metal mineralization. These elements form the basis for the empirical chalcophile and pegmatophile functions as well as for use in multivariate statistical analysis that have been developed by Smith and Perdrix (1983) and Smith *et al.* (1984).

An analysis of the nature of the causes of the frequency distributions of the elements is beyond the scope of this report. The non-normal nature of the distributions may be due to a mixture of samples from different geological environments, some of which may represent rare occurrences due to mineralization (e.g. As, Sb, Bi, Ag, Au).

5.2 ELEMENT MAPS

Maps of the the ranked abundances of most of the elements listed in Table 2 are shown in Figures 35a,b,c - 57a,b,c. Only the values for the lateritic materials are shown. A large number of follow-up samples were collected in the Johnston Range area of the BARLEE sheet, leading to the discovery of a cluster of new Au deposits. Resolution at the scale of presentation is difficult. To assist in the spatial interpretation of the data, enlargements of the Johnston Range area have been made for a selected group of elements namely, Fe_2O_3, Ag, Cu, Zn, As, Sb, Bi, Mo, Sn, Ga, W, Nb, Se, and Au (Figures 35d, 37d, 41d, 43d, 46d, 47d, 48d, 49d, 50d, 51d, 52d 55d, 56d, and 57d).

Since the sample sites are not distributed uniformly over the map area, methods of data presentation such as contour maps are not appropriate for describing the spatial variation of the data at the scale presented. However, the data can be conveniently presented by using symbols whose sizes are based upon the percentile ranking of the data relative to the *maximum* and *minimum* values of the data. A commonly-used method of expressing concentrations over irregularly-sampled areas is expression of each concentration by a symbol whose size is proportional to its magnitude (Howarth, 1983:124). The use of such symbols can be employed to indicate areas that are enriched or depleted. However, caution is advised in the interpretation of these proportionally-sized symbols. Symbol size does not necessarily reflect anomalously low or high values, rather it reflects the maximum and minimum values of the data which may or may not be "anomalous" with respect to zones of mineralization.

The size of the symbols is not a linear function of concentration of the elements. For visual ease and assistance in the recognition of outlier data, the symbol sizes are defined as:

$$\text{Map Symbol Size} = \text{Minimum Symbol Size for Map} + \text{Constant Symbol Size} * (\text{Percentile}/100)^4,$$

where the percentile is the percentile ranking of the sample for the particular element being considered. This quartic function enhances the size of the symbols for the high end outliers of the data whilst making the samples that fit in the rankings of less than 75 percentile range more equal in size. This non-linear distribution of symbol sizes assists in a faster visual assessment of anomalous values.

5.3 INTERPRETATION OF THE GEOCHEMICAL DISTRIBUTIONS

Interpretation of the geochemical maps requires some knowledge of the geological processes that have acted upon, or are still acting within an area. Inference about the geological environment can

be made from many of the geochemical maps and can assist in refining geological models. Hallberg (1984) has shown that within the saprolitic laterite profile, ratios of TiO_2, Cr, and Zr retain characteristics of the original lithologies. Titanium and Cr ratios commonly outline the mafic volcanic or mafic volcanic derived sedimentary assemblages, whilst Zr is useful in outlining the Zr-enriched felsic volcanics. Maps of these elements must be interpreted with caution as the abundances may have been modified by several processes, particularly during weathering. Fractionated igneous rocks tend to show enrichment in Mo, Be, W, Ga, and Sn and laterite geochemistry on a regional scale could be expected to reflect such effects. Birrell and Smith (1984) have previously reviewed chalcophile distributions for selected portions of the Yilgarn block. They recommended that for selected chalcophile elements, samples which rank above the 90th percentile are significant and that the areas from which these samples were taken be considered for follow-up sampling.

The salient features of the elements are:

- Iron ,Fe_2O_3, (Figure 35), TiO_2 (Figure 36), Mn, Cr, V, Cu, Zn, Ni, Co tend to show elevated abundances in the Diemals and Marda areas, but less significant abundances in the Southern Cross area. The differences between the geochemical characteristics of the two areas may be related to the location of the sampling relative to major structural features and influence of granitoid rocks. In the Barlee-Jackson area, Fe_2O_3 (Figures 35a,d) shows elevated abundances in the Diemals and Marda areas. Many of the Fe_2O_3 abundances are related to the presence of ironstones and other Fe-silicate bearing sediments. The abundances of Fe_2O_3 in the northern part of the area may be related to the increase in ferricrete materials that exist further northward. Thus the Fe_2O_3 abundances may reflect this pattern.

- Elevated Mn (Figure 38) abundances are generally higher in the materials associated with supracrustal materials as shown in Figures 38a-c. Elevated Mn values in the granitoid terrains may be of significance and two were noted in the KELLERBERRIN sheet. Elevated levels of Pb, Mo, Sn, and Nb occur with elevated levels of Mn in the northeast part of the KELLERBERRIN sheet (Anomaly KE01). Elevated abundances of Mn, associated with increased abundances of Pb, Co, Mo, W, Nb, and Se, also occur in the Danberrin Hill area of the KELLERBERRIN sheet (Anomaly KE07).

- Chromium distribution is shown in Figures 39a,b,c. Elevated values of Cr occur throughout the Diemals and Marda greenstone belt areas. Increased abundances also occur in the Marvel Loch and Bullfinch areas of the Southern Cross belt and the Westonia belt. In this area, Cr mostly reflects the presence of ultramafic flows and sills. Nickel (Figures 44a,b,c) and Co (Figures 45a,b,c) mimic the distribution of Cr and suggest that these three elements have a common association and source, namely the ultramafic flows and intrusions. A few very high values of Cr occur in the Marda and Diemals area (see Table 9). These high values may possibly relate to ultramafic intrusions. Vanadium (V) (Figure 40) abundances are often correlated with Cr, Ni, and Co. This can be observed when comparing the figures.

- Elevated Co values (Figure 45a) also occur in the northeast part of the KELLERBERRIN (anomaly KE07) and the northwest arm of the Diemals greenstone belt (BARLEE). Silver (Figure 37a), Mn (Figure 38a), Zn (Figure 43a), Bi (Figure 48a), Mo (Figure 49a), W (Figure 52a), Nb (Figure 55a), and Au (Figure 57a) show elevated abundances in Diemals area.

- Copper (Figures 41a,b,c,d) and Zn (Figures 43a,b,c,d) values are noticeably elevated in the greenstone areas, relative to the granitoid areas. The Diemals and Marda areas have significant levels of Cu and Zn. Comparison of the abundances between the Diemals-Marda area with the Southern Cross area shows a substantial difference between the two areas. Some slightly-elevated Zn values occur in the northern parts of the CORRIGIN and HYDEN sheets (Figure 43c). Examination of the Cu and Zn levels in Figures 41d and 43d shows that increased levels occur in the Yarbu, Deception Hill, and Broadbents area (Johnston Range). Copper and Zn anomalies are difficult to assess since their abundance levels are also a function of lithology.

Besides being economic commodities, they are also ubiquitously associated with alteration zones within bedrock. Thus elevated values must be interpreted cautiously. Methods of anomaly detection for these elements can be assisted by using methods such as those advocated by Smith *et al.* (1984), Stanley and Sinclair (1987), and Garrett (1989).

• Lead (Figures 42a,b,c) shows elevated abundances across both the supracrustal and granitoid/gneissic terrains. Elevated abundances of Pb in the supracrustal rocks in the Diemals, Marda, Bullfinch, and Marvel Loch areas are possibly associated with alteration processes and/or shear zones and thus may be a useful pathfinder for precious metal mineralization. Its presence as an economic quantity in itself is unlikely within the Archaean supracrustal sequences. In the granitoid gneiss terrains, elevated values are found throughout the BENCUBBIN, KELLERBERRIN, CORRIGIN, and HYDEN sheets. The highest abundances are associated with the Kellerberrin batholith and some gneissic enclaves (Figure 42b). Levels of 25 to 50 ppm can exist within feldspars in some of the felsic plutonic rocks (R.E. Smith, personal communication, 1990). The distribution of Mo abundances (Figure 49c) is similar to that for Pb. These areas of increased Pb and Mo may indicate underlying zones of more fractionated felsic plutonic material.

Elements that are related to mineralization and alteration processes show elevated abundances primarily in the greenstone belts and outlying greenstone/gneiss enclaves. Silver (Figure 37) shows significant abundances in the Johnston Range, Mt. Jackson, Bungalbin, and Marvel Loch areas. In the Johnston Range area, elevated Ag values occur in the Yarbu, Deception Hill, and southwest of Broadbents. In the Jackson area, elevated abundances of Ag (>2ppm) occur in the laterite northwest and southeast of Bungalbin Hill.

• Arsenic and Sb abundances and distribution are shown in Figures 46a,b,c,d and 47a,b,c,d. Both elements show elevated abundances in the supracrustal rocks of the Diemals-Marda and the Southern Cross greenstone belts. Figures 46d and 47d show the distribution of the two elements in the Diemals area. Elevated values occur in the Yarbu, Deception Hill, and Broadbents areas. In the Southern Cross belt, elevated abundances occur in the Marvel Loch area.

• Elevated abundances of Bi (Figures 48a,b,c,d) occur in the Diemal-Marda and Southern Cross greenstone belts. This supracrustal association is most likely related to zones of alteration and shearing. Elevated values occur in the Deception Hill, Broadbents, and Evanston areas of the Diemals greenstone belt (BARLEE), the Bungalbin-Mt. Jackson area in the Marda belt (JACKSON), and in the Bullfinch and Marvel Loch areas of the Southern Cross belt (SOUTHERN CROSS). Additionally, significant Bi abundances occur south of the Parker Range (SOUTHERN CROSS) and north of the Mt. Holland (HYDEN) areas and in the Forrestania area (HYDEN). The Bounty Mine is associated with this elevated signature of Bi. Increased abundances of Bi occur in the SOUTHERN CROSS sheet within granitoid rocks between Mt. Cramphorne and Noombenberry Rock and the Mt. Hampton to Holleton area. Felsic/sedimentary supracrustal enclaves occur within this granitoid terrain and may be, in part, the source for the increased Bi. Bismuth is significant as a pathfinder for precious, base-metal, polymetallic, and rare metal deposits.

• Molybdenum (Figures 49a,b,c,d) is associated with several elements as noted above. In addition, increased levels of Mo occur in the area east of Broadbents (BARLEE) and northeast of Evanston (Figure 49d) and indicate the presence of the granitoid rocks that intrude the supracrustal assemblage. There is a suggestion of some association with the elevated Bi abundances in the JACKSON and SOUTHERN CROSS sheets (Figure 49a,b). Increased values of Mo occur in the Bungalbin area of the Marda belt and elevated Mo values occur in the Southern Cross belt at Bullfinch, Mt. Holland, and Forrestania. Isolated increased levels occur in the CORRIGN sheet, primarily associated with the gneiss terrains.

• Tin (Figures 50a,b,c,d) occurs in elevated abundances in both the supracrustal and granitoid/gneiss terrains. Elevated Sn values occur south of Yarbu, the Broadbents, and south of Deception Hill areas of the BARLEE sheet. Increased values also occur east of Mount Jackson and around the Bungalbin area. Significant Sn values occur in the Westonia, Bullfinch, and

Marvel Loch areas. Within the granitoid gneiss terrains, elevated Sn values occur in the eastern part of KELLERBERRIN sheet. Isolated values of increased Sn occur throughout the CORRIGIN and HYDEN sheets. These elevated values may reflect various degrees of fractionation within the felsic plutonic/gneissic environment.

- Gallium abundances are shown in Figures 51a,b,c,d. Increased Ga abundances occur almost exclusively with the supracrustal rocks. Elevated values occur in the Deception Hill and Broadbents area of the Diemals belt; the Bungalbin Hill area of the Marda belt; the Westonia belt, Bullfinch, Marvel Loch, and Forrestania areas of the Southern Cross belt.

- Figures 52a,b,c,d show abundances of W throughout the region. Increased W levels occur in the Diemals belt, around the Deception Hill and Broadbents areas. In the Marda belt increased levels of W occur in the Mt. Jackson and Bungalbin Hill area as well as southeastward into the KALGOORLIE sheet. Increased levels occur in the Bullfinch, Marvel Loch and Forrestania areas of the Southern Cross greenstone belt, and in the Westonia belt. Isolated increased levels of W occur within the granitoid/gneiss terrains of the KELLERBERRIN, CORRIGIN and HYDEN sheets.

- Barium (Figures 53a,b,c) shows increased abundances associated with the supracrustal rocks in the Diemals and Marda greenstone belts. In the granitoid/gneiss terrain, the levels of Ba are less than those values in the greenstone belts and show less variation.

- Zirconium (Figures 54a,b,c) displays elevated abundances throughout the granitoid/gneiss terrain reflecting the fractionated nature of the felsic plutonic and gneissic rocks.

- The distribution of Nb in Figures 55a,b,c,d shows elevated values associated with areas within the greenstone belts and in the granitoid/gneiss terrain. The presence of Nb suggests that it is associated with fractionated intrusive rocks. Its increased abundances near multi-element chalcophile anomalies suggest that it might possibly be associated with alteration zones within the supracrustal rocks. Elevated Nb values occur in the Broadbents area of the Johnston Range, the Mt. Jackson and Bungalbin Hill areas of the Marda greenstone belt, and the Westonia belt. Elevated Nb values occur scattered throughout the granitoid/gneiss terrain.

- The distribution of Se is shown in Figures 56a,b,c,d. Values of Se below 10 ppm need to be interpreted with caution. Elevated values of Se in the supracrustal rocks occur in the Yarbu, Johnston Range, and Bungalbin Hill areas of the Diemals-Marda greenstone belts. Increased Se values occur in the Bullfinch, and Marvel Loch areas of the Southern Cross belt; and in the Westonia belt. Increased abundances also occur in the Holleton belt in the northern part of the HYDEN sheet. Scattered elevated abundances also occur throughout the granitoid/gneiss terrain in the KELLERBERRIN, SOUTHERN CROSS, and CORRIGIN sheets. Selenium can be associated with altered supracrustal rocks and fractionated felsic plutonic/gneissic rocks.

- Gold distribution is shown in Figures 57a,b,c,d. Elevated Au values occur in the Deception Hill area, south of Broadbents in the vicinity of the Johnston Range (Diemals belt), the Bungalbin Hill areas of the Marda belt, and the Bullfinch and Marvel Loch areas of the Southern Cross belt. Elevated Au values also occur in the Watt Hills area in the southeast part of the Marda belt (KALGOORLIE).

A synthesis of the patterns of the elements throughout the area suggests that there are some common features in the geochemistry. As suggested above, the abundances of many of the elements reflects the compositions of the underlying lithologies. The elements that most commonly reflect the underlying supracrustal rocks of the greenstone belts include: Fe_2O_3, TiO_2, SiO_2, Cr, Mn, V, Ni, Co, Zr, Cu, Zn, Ga, and Nb. Elements such as SiO_2, Mo, Sn, Pb, Nb, and Se tend to reflect underlying lithologies associated with the felsic granitoid/gneissic terrains which are largely fractionated environments. The effects of weathering processes can be reflected by the abundances of Fe_2O_3, TiO_2, Cr, Mn, V, Ni, and Zr. These elements tend to be residual even after the lateritic material weathers. Thus, the interpretation of some of these elements must be cautiously applied. Other elements such as Cu, Zn, Ga, and Nb can also reflect secondary processes, for example alteration, that are commonly associated with

mineralization. Elements such as Ag, As, Sb, Bi, Mo, Sn, W, Se, Ga, and Nb can also reflect environments that are associated with alteration and mineralization. Any one element in itself is not necessarily a good pathfinder associated with an altered/mineralized zone. However, a combination of a selected group of elements may be a suitable means of isolating areas with more mineral potential.

5.4 MULTIVARIATE DATA ANALYSIS

The usefulness of multivariate data analysis methods applied to geochemical data has been well documented (Howarth and Sinding-Larsen, 1983, Chapter 6). The most commonly used multivariate methods include, principal components, cluster, factor, regression, and canonical analyses. Multivariate techniques have been specifically applied to Archaean volcanic terrains from which a number of geological processes can be inferred, ranging from primary compositional variation to alteration and associated mineralization (Grunsky, 1986). Multivariate techniques also include empirical techniques such as the chalcophile and pegmatophile indices developed by Smith and Perdrix (1983). Multivariate techniques were applied in previous studies (Grunsky *et al.*, 1988, 1989) and quite clearly outlined multi-element geochemical signatures that could warrant further investigation.

There are some fundamental problems that commonly occur in geochemical databases such as the regional geochemical database that is being compiled for the Yilgarn block.

1) Most elements have a "censored" distribution, meaning that values at less than the detection limit can only be reported as being less than that limit.

2) The data do not occur as normally-distributed abundances.

3) The data have missing values. That is, not every sample has been analysed for the same number of elements.

4) Not every element has been analysed by the same method or the limits of detection of the method have changed over time.

These problems create difficulties when applying mathematical or statistical procedures to the data. Statistical procedures have been devised to deal with all except the last problem. To overcome the problems of censored distributions, procedures have been developed by applying transformations to estimate replacement values for the purposes of statistical calculations by the CSIRO Division of Mathematics and Statistics. Non-normally distributed data can be transformed using standard procedures as outlined by Smith *et al.* (1984). When the data have missing values, several procedures can be applied to estimate replacement values. Most procedures use a multiple regression procedure which estimates the replacement value based on a regression with samples that have complete analyses.

It is beyond the scope of this study to apply and report on all of these procedures. However, one of the more basic procedures can be applied to the data in order to enhance zones of increased abundances, or anomalies. This involves the use of robust estimates of means, correlations and covariances of the data. Because the nature of most of the element distributions is non-normal and positively skewed, the arithmetic means of these distributions tend to be higher than the medians or "true" means of the populations (cf. Histograms, Figures 5-34). Robust statistical procedures determine mean values and subsequent correlations and covariances between the elements based on finding a value of the mean closer to the median of the sample population. Robust procedures were subsequently applied to two procedures used in this report. Principal components analysis has been carried out using robust estimates of the means and correlations for the multivariate populations examined. The use of the Mahalanobis distance as an estimate of whether an unknown sample is anomalous or not is based on a robust estimate of the mean. These procedures are discussed below.

5.5 GEOCHEMICAL ANOMALIES

Geochemical anomalies can be defined by a number of techniques. Simple ranking and examination of the extremes of pathfinder and target elements are an effective means of defining anomalies.

Previous work by the Laterite Geochemistry Group of the Division of Exploration Geoscience, CSIRO outlined a number of anomalies associated with element enrichments determined by a number of methods. These methods detected anomalies through:

a) element abundances above known background thresholds,

b) samples in which several elements had elevated abundances above specified percentile levels after the data were ranked,

c) the use of empirical indices, developed from orientation studies, such as the chalcophile index, CHI-6*X, the pegmatophile index, PEG-4, and the NUMCHI index.

Figures 58a,b and Table 10 show the anomalies that were noted from the initial regional sampling programme. Samples that are associated with these anomalies are noted in the database file that accompanies this report. These anomalies were outlined by a number of empirical procedures including selection by abundances greater than the 95th percentile, ranking of chalcophile elements, CHI-6*X, and PEG-4 indices.

5.6 PRINCIPAL COMPONENTS ANALYSIS

Many of geochemical patterns that were described above can be determined by the use of systematic and statistical means of data analysis. One such commonly used technique is principal components analysis which is now discussed.

A fundamental objective in the analysis of data is the extraction of meaningful information from which a reasonable interpretation can be made. As the number of variables increase, the more detail is provided; however, this is at the expense of simplicity of interpretation. There are several good reviews that discuss the basics of multivariate data analysis techniques (e.g. Jöreskog *et al.*, 1976; Davis, 1986; Howarth and Sinding-Larsen, 1983).

In geological applications, and particularly within the study of igneous rocks, the foundation of petrology is based upon the systematic variation of the elements involved in magmatic fractionation. It is already known that the lithogeochemistry of igneous rocks contains a number of chemical variables that will correlate with one another. Because of this, it would be easier to examine just a few critical elements to extract a meaningful interpretation. However, it is not always known which elements are involved in the magmatic process during fractionation of igneous rocks nor is it always known what subsequent alteration or metamorphism has occurred. Thus, there is uncertainty in choosing, a priori, which variables to include in a subsequent data analysis. A way to overcome this uncertainty is to apply some technique of data analysis that will assist in reducing the number of variables based on correlations or covariances of the variables. Techniques such as factor analysis, principal components analysis, and cluster analysis, have been developed in response to these problems.

The objective of principal components analysis is to reduce the number of variables necessary to describe the observed variation within a set of data. This is done by forming linear combinations of the variables (components) that describe the distribution of the data. Ideally, to the geologist, each component might be interpreted as describing a geological process such as differentiation (partial melting, crystal fractionation, etc.), alteration/mineralization (carbonatization, silicification, alkali depletion, metal associations and enrichments, etc.), and weathering processes (bedrock-saprolite-laterite).

A method of principal components analysis known as Simultaneous RQ-Mode Principal Components Analysis (Zhou *et al.*, 1983) was carried out on the correlation matrix of the regional ("R") laterite and ("F2/F3") laterite data groups separately. The two groups were kept separate since the follow-up samples tend to be biased towards areas that suggest alteration and/or mineralization. The "R" samples represent the regional sampling strategy and thus suggest the patterns that might be indicated from a regional sampling programme. The technique of RQ-mode principal components analysis presented here is different from the methods presented in earlier reports (Grunsky *et al.*, 1988, 1989) in

that the correlation matrix used to compute the principal components has been derived by robust estimation methods. Robust estimation gives a better estimate of the means and correlations of the variables by down-weighting the influence of anomalous samples.

The complete set of oxides/elements were not used in the analysis. A subset of 19 oxides/elements was chosen as listed in Tables 11 and 12. Two reasons influence the choice of a subset of variables. Firstly, not all of the samples were analyzed for all of the elements (e.g. SiO_2, Al_2O_3, TiO_2, MgO, CaO, Ba, Zr, etc.) or the elements were of such low abundance levels that it was not considered useful to include them in the analysis (e.g. Bi, Ge, Ta, Be). Secondly, only those samples with non-zero values for all elements were included in the analysis. The "R" (regional) samples were calculated separately from the "F2/F3" (follow-up) samples.

Tables 11 and 12 show the results of the principal components analysis using "R" and "F2/F3" samples respectively. Tables 11a, 12a give the element correlations; Tables 11b, 12b list the eigenvalues and corresponding variance for which each components accounts. Tables 11c, 12c list the component loadings of the elements, and Tables 11d, 12d list the contribution (relative significance) that each element makes to each component of the reduced variable space.

The correlation coefficients can be useful in assessing pairs of significant relationships between elements. Correlation coefficients can be tested for their significance by statistical procedures (Student's t-test). In the case of the "R" laterites and the "F2/F3" laterites of 488 and 379 samples respectively, significant correlation coefficients are defined by absolute correlation coefficient values greater than 0.1053 and 0.1195 at the 99% confidence level respectively. A description of the correlations between the elements would be awkward. The relationships can be expressed best by the examination of the principal component scores in Tables 11c,d and 12c,d. As well, the relationships can be visually assessed by the projecting the principal component scores of the elements and samples on to the principal component axes.

5.6.1 PRINCIPAL COMPONENTS ANALYSIS: "R" LATERITE SAMPLES

A general rule is that eigenvalues (see Table 11b) which are greater than 1.0 are considered to be significant components. Thus in Table 11b, the first 7 components would be considered worth examining. The cumulative contribution of the eigenvalues accounts for 69.4% of the data variation.

The relationships between the elements are expressed in Tables 11c,d. Table 11c shows the principal component scores for the elements. The positive and negative associations between the three groups of variables can be observed in the first two columns of Table 11c. Table 11d shows how much the variation of sample is accounted for by that particular component. This assists in determining which component is the most significant for each element. For example, most of the Fe_2O_3 variation is accounted for in the first component (>76%) while the variation of Au is distributed over three components (F6, F7, and F9). A discussion of all of the principal components is not practical for the purpose of this report. Only those components which are considered to be useful for assistance in exploration are discussed here.

Tables 11c,d show that two groups of elements contribute to the first principal component. The first group consists of positively correlated Fe_2O_3, Mn, Cr, V, Cu, Zn, Ni, and Co and the second group consists of positively associated Pb, Mo, Ga, and Nb. The two groups, however, are inversely associated. These two groups most likely represent the differences between the samples collected over the greenstone terrains (the first group) from the samples collected over the granitoid/gneiss terrains (the second group). This component accounts for 29% of the total variation of the data. Figure 59a shows the samples and elements plotted on to the first two principal component axes. The strong inverse relationships between the two groups can be clearly seen in the diagram. *Each sample is plotted as a small cross and each element is also projected onto the F1-F2 plane. In this way the relationship between the samples and the elements can be graphically displayed.* Figures 60a,b,c,d show maps of the first principal component score. Large negative scores (asterisks) are associated with Mo, Ga, Nb and Pb enriched areas while large positive scores (circles) are associated with the mafic rocks in the greenstone belts in the Diemals, Marda, Westonia, Bullfinch, Marvel Loch, and Forrestania areas. It is important to

note that some of the Mo, Pb, Ga, Nb enrichment also occurs in the greenstone belt areas and may be related to hydrothermal systems associated with some of the known mineralization. Examination of Figure 59a shows that Fe_2O_3, Co, Cu, Cr, Mn, Ni, and V are closely associated together along the positive side of the F1 axis. Thus samples that plot towards these elements tend to be enriched in these elements relative to other elements on the diagram. Similarly, Ga, Mo, Pb, and Nb cluster together at the negative end of the F1 axis, and samples that plot towards these elements tend to be enriched in these elements relative to the other elements on the diagram. The cloud of points at the centre of the plot shows a bi-modal nature. The cloud of points on the negative side of the F1 axis is associated with the felsic rocks while the cloud of points on the positive side of the F1 axis is associated with the greenstones.

The second principal component, which accounts for 8.7% of the data variation, is dominated As, Sb, Se, and Ag. Figure 59a shows a plot of the elements and samples projected onto the F1-F2 plane. This figure shows the relationships of the elements and the samples with respect to the first two principal components. The sum of the variance of these two components account for 37.9% of the variation of the data. Thus the plot exhibits the relative relationships of the elements and the samples for about 37% of the observed variation. The principal component scores of the samples are listed in Table 11c. Along the negative end of the F2 axis the association of As, Sb, and Se show a distinct trend that is different from the other two groups of elements. Samples with elevated abundances of Ag plot on the positive side of the F2 axis and are thus inversely related to the abundances of As, Se, and Sb. The samples that are associated with these elements are quite distinct from the main cloud of points that occurs near the origin of the diagram. These samples are most probably related to alteration/mineralization processes and are possibly good exploration targets. Figures 61a,b,c,d show the maps of the scores of the second principal component. The large negative scores are associated with As, Sb, Se enrichment and may be potential sites for follow-up exploration. Figure 61a shows large postive and negative F2 scores in the Johnston Range area, the Bungalbin Hill area of the Marda belt, and the Marvel Loch area. These large negative F2 scores are associated with the greenstone belts and may represent alteration associated with mineralized systems. The positive scores represent an enrichment of Ag while the negative scores indicate an increased abundance of As, Sb, and Se.

The fourth principal component accounts for 7.3% of the data variation and is dominated primarily by Sn (see Tables 11c,d). Positive F4 scores show an affinity for Sn enrichment, while negative F4 scores show a possible enrichment of Au in the granitoid rocks (Figure 59b). Figure 62 shows the maps of the F4 scores of the samples. Large positive scores (Sn affinity) occur in the Johnston Range, Mt. Jackson, Marvel Loch, and northeast Kellerberrin areas. Large negative scores associated with Au, occur in the Johnston Range, Deception Hill, Marvel Loch, Westonia, southeast Kellerberrin, and the Forrestania areas.

The fifth principal component accounts for 6% of the variation and shows significant contributions by Pb, Mo, Se, and W. Figure 59c shows the relationships of the samples and elements on the F1-F5 axes. From the diagram and Table 11c, it can be seen that Se, Sb, and Ag have a positive association, while Mo, Pb, and W are inversely associated. Figures 63a,b,c,d show the maps of the F5 scores. Large F5 scores associated with Ag, Se, and Sb enrichment occur in the Diemals, Marda, Watt Hills, and Marvel Loch areas. Large negative F6 scores associated with W occur in the Evanston, Bungalbin Hill, Marvel Loch, and Forrestania areas. Both the negative and positive scores often occur in proximity to each other. This suggests that although the presence of the suites of elements are mutually exclusive, they may be associated with the same geological process.

The sixth principal component accounts for 5.4% of the variation and 16.7% of the variation of Au is accounted for by this component. Figure 59d shows that Au, Se, Pb, and Ag are associated with negative F6 scores, while W and Sb are associated with positive F6 scores. Figures 64a,b,c,d shows large positive (W, Sb) scores in the Johnston Range, Deception Hill, Bungalbin Hill, Marvel Loch, Forrestania, and southeast Kellerberrin areas. Large negative F6 scores (Au associated) occur in the Johnston Range, Deception Hill, Bungalbin Hill, Bullfinch, Marvel Loch, and eastern Kellerberrin areas.

The seventh principal component accounts for 5.3% of the variation of the data. Over 32% of the Au variation is accounted for by this component. This suggests that Au associations for this component are significant. Figure 59e shows that Au and W are associated with large positive F7 scores. Negative F7 scores tend to show a small degree of Sb and Ag enrichment. Figures 65a,b,c,d show large

positive scores with Au-W associations in the Johnston Range, Deception Hill, Watt Hills, Bullfinch, Marvel Loch, and southeast Kellerberrin areas. Negative Ag-Sb associated scores occur in the Mt. Jackson, Bungalbin Hill, Watt Hills, Forrestania, and northeast Kellerberrin areas.

The eighth principal component accounts for 38% of the variation of Ag although the eighth component itself only accounts for 4.6% of the overall variation of the data. Figure 59f shows the scores of the first and eighth components plotted onto the F1-F8 plane. Silver and W show a close association as large positive F8 scores. Large positive F8 scores occur in the Johnston Range, Bungalbin Hill, Watt Hills, Marvel Loch, and Forrestania areas.

The ninth principal component accounts for over 33% of the Au variation and thus can be considered to represent a significant amount of Au variation in the area. Figure 59g and Table 11c show that Au has a strong positive association with Sb. Figures 67a,b,c,d show that the strong Au-Sb association occurs in the Johnston Range, Deception Hill, Mt. Jackson, Bungalbin Hill, and Marvel Loch areas.

It is of interest to note that the samples that are related to alteration/mineralization as shown for the second, fifth, sixth, eighth and ninth components, are all associated with the positive side of the F1 axis. The samples associated with Cr, Ni, Co, Mn, V, Fe_2O_3, Cu, and Zn are located on this side of the axis and represent samples from the greenstone areas. Exceptions to this are the fourth and seventh components in which there is a tendency for Au to be associated with more felsic rocks. Thus, the association of Au and related alteration assemblages in lateritic materials can be related to the underlying lithologies.

5.6.2 PRINCIPAL COMPONENTS ANALYSIS: "F2/F3" LATERITE SAMPLES

The results of the principal components analysis applied to the follow-up samples is shown in Table 12. Figures 68a,b,c,d,e shows the plots of the samples and elements on the component axes, and Figures 68-75 show the maps of the component scores for F1, F4, F5, F6, F7, F8, and F9 respectively. Note, that "F2/F3" were collected only within the BARLEE, JACKSON and KALGOORLIE sheets.

Figure 68a shows the relationships between the samples and elements for the first two principal components. Table 12 shows that the first two components account for 18.5% and 10.8% of the data variation respectively. Tables 12c,d show that Co, Cu, Ni, Mo, and Nb account for most of the variation within the first component and Fe_2O_3, V, Sb, As, and Sn account for most of the variation in the second component. Copper, Co, and Ni are positively associated with the greenstone samples on the positive side of the F1 axis, while Mo, Nb, and Ga are positively associated with the materials that may be fractionated materials (incompatible elements) associated with mineralization or some granitoid rocks. The second component shows an association of As and Sb with V, Fe_2O_3, Zn, Mn, Sn, and Pb. The samples that are associated with these element lie along the positive side of the F2 axis and represent altered supracrustal materials.

These relationships are strikingly different from what was observed for the "R" samples. This is due primarily to the nature of the samples. Most of the "F2/F3" samples were collected over the greenstone areas. Thus the multi-element relationships will be those associated with supracrustal rocks. Thus, the bimodal nature of the materials due to the presence of supracrustal and granitoid materials that was suggested in Figure 59 is not present in this group of samples. Figures 69a,b show the maps of the first component. Both large positive and negative scores occur within the Diemals and Marda areas. Since the sampling is largely within the greenstone belts, the negative scores are most likely related to alteration processes that occur within the supracrustal sequences.

Figure 68a shows that a small number of Au associations occur with Cu, Ni, Co enriched rocks near the origin of the plot. The contribution of Au to the second component (2.4%, Table 12d) is not very significant and thus does not represent a significant number of samples with this type of association. Nonetheless, samples with large positive F1 scores and large negative F2 scores (4 or 5 samples) will have this relationship of increased Au. No map is shown for this component.

Figure 68b shows a plot of the samples and elements plotted onto the F1-F4 plane. The fourth component accounts for 8.3% of the variation of the data. The association of Au with Fe_2O_3 and W is indicated for a few samples that plot along the negative side of the F4 axis and the postive side of the F1

It is important to note that within a mineralized zone, several types of elemental associations can exist such that Au can occur without As, Sb or other chalcophile elements in one part of an alteration/mineralized zone, while it may have a strong positive correlation with these elements just a few metres away. Principal components analysis does not take into account the spatial relationships of the data. The distinction between elemental associations within the different components is due to the nature of the method and does not necessarily reflect different geological processes.

The fifth component (7.5% of the data variation) is dominated by the variation of Nb, Ga, Sn, As, Sb, Se, and Au (Tables 12c,d). Figure 68c shows that large negative F5 scores are associated with Se, Au, As, and Sb. Large positive F5 scores are associated primarily with Nb, Ga, and Sn enrichment. The figure also shows Ag enrichment (4 samples) associated with Mn and Cr combined with positive F5 and F1 scores. This component shows that Au is clearly related to increases in As and Sb. Figures 71a,b show that the large negative scores occur mostly in the Johnston Range area.

The sixth component (6.4% of the data variation) shows positive F6 scores associated with As and W in the felsic rocks (negative side of the F1 axis) and Au-Mn-Zn associations with the more mafic rocks (positive side of the F1 axis) in Figure 68d. Figures 72a,b show the Au-Mn-Zn association in the Johnston Range area.

The seventh component (Figures 68e, 73a,b) shows a strong association of W, Sb, and As with negative F7 scores. Figures 73a,b, show large negative scores in the Johnston Range and Yarbu areas.

The eighth component (4.7% of the data variation) shows a strong positive association of Au with W, Se, Ag, and Sn. Figure 68f shows this association for positive F8 scores. Figures 74a,b show the locations of large F8 scores occur primarily in the Yarbu and Johnston Range areas.

The ninth component (4.5% of the data variation) shows increased Au abundances without any other elemental associations. This is reflected in Figure 68g where large positive F9 scores are associated only with Au. Tables 12c,d also show that Au is not closely associated with other elements. Figures 75a,b show large positive F9 scores in the Johnston Range and Bungalbin Hill areas.

The application of principal components analysis has shown that there are several multi-element associations with Au. Although these associations occur as distinct principal components, these relationships all occur within the same altered/mineralized areas and thus the components do not necessarily reflect different geological processes, but rather variations in the style of one or two processes.

5.7 ANOMALY RECOGNITION BY THE CHI-6*X, PEG-4, and NUMCHI INDICES

The initial regional samples of **laterites** were selected from the database and were used to calculate the CHI-6*X, PEG-4, and NUMCHI indices as outlined by Smith and Perdrix (1983). These indices are based on the empirical selection of pathfinder elements, from orientation studies, that are combined to produce a "score". The magnitude of the score is directly proportional to the significance of the exploration target. The indices are calculated according to the following formulae:

$$\text{CHI-6*X} = \text{As} + 3.56\times\text{Sb} + 10\times\text{Bi} + 3\times\text{Mo} + 30\times\text{Ag} + 30\times\text{Sn} + 10\times\text{W} + 3.5\times\text{Se}$$

$$\text{PEG-4} = .09\times\text{As} + 1.33\times\text{Sb} + \text{Sn} + .14\times\text{Ga} + .4\times\text{W} + .6\times\text{Nb} + \text{Ta}$$

CHI-6*X and PEG-4 indices must be interpreted cautiously as these indices can be very large, but the value can be the result of only one anomalous element. A useful adjunct to these indices is the NUMCHI index.

The NUMCHI index is based on an integer accumulation of the presence of a number of elements that exceed a given threshold. The following elements and thresholds were used for the NUMCHI index:

	1	2	3	4	5	6	7	8	9	10	11
Element:	Cu	Pb	Zn	As	Sb	Bi	Mo	Ag	Sn	W	Se
Threshold: (ppm)	242.0	53.0	48.0	99.0	7.0	3.0	7.0	0.4	4.0	15.0	6.0

For a given sample, a cumulative score is obtained by adding 1 for each element that exceeds the threshold. Thus, for this NUMCHI index, a maximum possible score would be 11. The threshold values were chosen as the 90 percentile value for the distributions of the elements. These values were taken from Table 5a which provides background values for the "R" (regional) samples that were collected over the Diemals-Marda-Southern Cross greenstone belts. Thus this index would not be suitable for the granitoid/gneissic areas. The NUMCHI index provides a measure of the *number* of anomalous elements that are present.

These indices are subject to modification which is largely dependent upon the regional background values for which the indices are calculated. These formulae should not be applied without careful consideration of the materials being used, preferably from an orientation study, over the area. Depending on the commodities being sought, the NUMCHI index can be varied by adding or deleting elements and varying the threshold coefficients.

Samples that rank in the upper percentile range of any individual index are the most worthy of further follow-up, provided that the index is above the regional background total for the index used. Tables 13a,b list the CHI-6*X and PEG-4 indices for the samples that scored greater than the 90 percentile level for the "R" regional laterite samples. Table 13c lists the samples for which NUMCHI is greater than 3 (more than 3 anomalous elements).

Figures 76, 77, and 78 show the maps of the CHI-6*X, PEG-4, and NUMCHI indices over the areas. Large CHI-6*X and PEG-4 indices occur in the Evanstan and Deception Hill areas of the BARLEE sheet, the Bungalbin Hill, and Mt. Jackson areas, Bullfinch, Westonia, Marvel Loch, Forrestania, and the eastern part of the KELLERBERRIN sheet. Large NUMCHI values occur in the Deception Hill, Johnston Range, Bungalbin Hill, Bullfinch, Marvel Loch, and Forrestania areas. Based on the combined presence of elevated CHI-6*X, PEG-4, and NUMCHI indices, further follow-up investigation might be warranted for these areas.

5.8 ANOMALY RECOGNITION BY PRINCIPAL COMPONENTS ANALYSIS

The results of the principal components analysis, discussed above, can be used as a means for ranking anomalies. Because the method determines factors based on the variance of the data, extreme values of the factors represent samples that are enriched in the linear combinations of elements that comprise that factor.

Tables 14a,b,c,d list the ranked scores for a selected number of components (see Table 11) that suggest alteration and Au association. These are the components computed for the "R" regional samples over the entire area. Only positive scores are ranked for F2 and F4, while both positive and negative scores are ranked for F6 and F8. Ranked scores were not prepared for the follow-up samples. Many of these scores are coincident with high ranking (>90 percentile) abundances of individual elements and the CHI-6*X, PEG-4, and NUMCHI indices. Robust principal component scores assist in verifying the atypical nature of some of these "outlier" samples. The areas of highest score ranking have already been discussed in the section on "Principal Components Analysis".

5.9 ANOMALY RECOGNITION BY THE USE OF χ^2[CHI-SQUARE] PLOTS

Most anomaly recognition procedures are based upon determining the threshold that distinguishes background from anomalous values. However, the use of multivariate procedures can be useful in determining background from anomalous samples for a set of desired elements.

Garrett (1989, in press) describes the use of the covariance matrix as a tool for distinguishing background from anomalous sample populations. The covariance matrix contains information on the variability of the elements as well as their inter-relationships. The multi-element data define a hyper-ellipsoid in multi-dimensional space. In a multivariate normal sample population, most samples fall within a close distance of each other and by definition are part of the background group of samples. However, if outliers are included in the data, the shape of the hyper-ellipsoid that is defined by the covariance matrix changes. The distance of each sample to the centroid of the cloud of points is the Mahalanobis distance.

Outliers can be distinguished from the main background population by determining the Mahalanobis distance of each sample to the group centroid. The distances can be compared to the "expected" distances of a multivariate normal population (cumulative probability with the number of degrees of freedom defined as the number of variables) by the use of chi-square (χ^2) values. This procedure *should not be confused* with the CHI-6*X index which uses a suite of chalcophile elements for the calculation of a chalcophile index.

A graphical procedure of plotting the Mahalanobis distances of the observed from the expected allows for the detection of outliers. If the sample population is multivariate normal, then the chi-square plot is a straight line. If the population contains outliers, then the observed Mahalanobis distances are greater than the expected chi-square values and the plot becomes non-linear.

The procedure was carried out on a selected group of elements of chalcophile affinity, namely: Cu, Zn, Pb, As, Sb, Bi, Mo, Ag, Sn, W, Se, Ga, Nb, and Ta. Table 15 and Figures 79a,b, 80a,b,c show the results of the Chi-square/Mahalanobis Distance procedure. Figure 79a shows a plot of the Mahalanobis distances vs. theoretical Chi-square distances for 1400 regional "R" samples. The samples that have high Mahalanobis distances depart significantly from the expected Chi-square values. This results in upper samples breaking away from the trend of the main group of data. One hundred (100) samples with the highest Mahalanobis distances were removed from the data and the values were recalculated. Figure 79b shows the plot for 1300 samples. The curve appears to be more continuous and it is likely that most of these samples form part of one continuous multivariate population. Ideally, in a multivaraite normal population, the line should be straight with a slope of 1. However, because the distributions are skewed and non-normal, the line tends to be curved.

The 100 samples that were removed are shown in Table 15. For each sample, the Table lists the sample type, easting and northing coordinates, the Mahalanobis distance and the expected chi-square value. These ranked samples are plotted on the maps in Figures 80a,b,c. All of these samples should be considered anomalous. The symbol size reflects the degree of abnormality. Not surprisingly, most of the anomalies occur in the Diemals and Marda greenstone belt areas. Additional anomalies occur in the Marvel Loch, Bullfinch, Forrestania, and Kellerberrin areas.

It is important to keep in mind that these anomalies are based on a selected suite of elements (Cu, Zn, Pb, As, Sb, Bi, Mo, Ag, Sn, W, Se, Ga, Nb, Ta) that best reflect chalcophile enrichment and thus, may not reflect other processes that might be investigated. This analysis naturally is biased towards anomalous groups of elements that are likely to be associated within the greenstone sequences. Thus, the granitoid areas would not show many significant anomalies with this suite of elements.

6.0 DISCUSSION AND CONCLUSIONS

Gold mineralization is commonly associated with an increase in the abundance of a variety of elements, most commonly, As, Sb, W, Mo, B, Ag, Li, Ba, Rb, and Cr in the unweathered profile. As well, Cu, Pb, and Zn can be present in some Au deposits (Groves, 1988; Colvine *et al.*, 1988). However, not all of these elements are present for all types of deposits. Pegmatite associated rare metal deposits can be indicated by enrichment of Bi, As, Sb, Mo, Sn, Ge, W, Nb, and Au. Any one or combination of these elements can be considered as possible pathfinders to a variety of ore deposits.

The tables of summary statistics and histograms are a useful means of determining the range and distribution of elemental abundances within the area being investigated. In this particular study, the histograms clearly reflect the bimodal nature of the materials associated with the greenstone and the granitoid areas. The histograms in this study may assist as a basis of comparison between terrains in which the underlying lithologies are uncertain. Statistical procedures, such as those outlined by Smith *et al.* (1984), could be applied to unknown samples which could characterize the affinity with either greenstone or granitoid lithologies. This approach is currently being investigated.

The maps of the elements can be useful for isolating elevated abundances for further follow-up. In particular, Au (Figure 59) abundances are useful for isolating the more obvious areas of potential economic Au. Figure 59 shows that Au values increase primarily in the Diemals, Marda, and Marvel Loch areas. Isolated elevated abundances of Au also occur in the Kellerberrin area.

Other elements are difficult to assess individually. Since most economic commodities being sought have multi-element geochemical signatures, it makes sense to employ methods that make use of these multi-element characteristics. The results of the principal components analysis, the CHI-6*X, PEG-4, and NUMCHI indices, and Mahalanobis distance methods all show zones that have multi-element enrichment and suggest additional follow-up investigation. Exploration for Au and associated precious metal deposits may be assisted by the use of several of these multi-element methods.

The search for rare metal deposits associated with the granitoid/gneiss terrain may also be carried out using a multi-element approach. In this case, the granitoid/gneissic areas must be evaluated using data from that terrain only. The CHI-6*X, PEG-4, and NUMCHI indices must be reset, and an appropriate selection of elements must be made for the Chi-square/Mahalanobis distance procedure. Similarly, the use of principal components analysis should be applied to the granitoid/gneiss areas only.

Previous reports (Grunsky *et al.*, 1988, 1989) suggested the presence of chalcophile corridors with the Murchison belt, and other areas in the Yilgarn block (Smith *et al.*, 1989) that define zones of economic mineral potential. The east-west trend of the Diemals and Marda belts suggests this trend exists. Additionally, a chalcophile trend most probably exists in the northerly direction defined by the boundary of the Southern Cross belt. However, sampling over these greenstone belts lacks the continuiuty to state that such corridors exist with certainty.

The existence of numerous supracrustal enclaves in the KELLERBERRIN sheet area suggests that other previously-unrecognized enclaves might be discovered. In view of the fact that areas such as the Westonia belt have significant amounts of precious metal mineralization, a re-evaluation of the gneiss terrain might be warranted.

The data and results presented in this report, plus additional geophysical, lithological, lithogeochemical, and structural data, may provide sufficient information for a selective and cost efficient exploration programme.

7.0 REFERENCES

Anand, R.R., Smith, R.E., Innes, J., Churchward, H.M., Perdrix, J.L. and Grunsky, E.C., 1989. Laterite Types and Associated Ferruginous Materials, Yilgarn Block WA, Terminology, Classification, and Atlas; Chapter 3, *CSIRO Exploration Geoscience Restricted Report 60R.*

Birrell, R.D. and Smith, R.E., 1984. Project C Report, Review of Anomalies, Geochemical Assessment, CSIRO, September 1984, 12pp.

Blight, D.F., Chin, R.J. and Smith, R.A. 1984. BENCUBBIN, 1:250 000 *Geological Series-Explanatory Notes*, Sheet SH/50-11, Geological Survey of Western Australia, 11pp., accompanied by 1:250 000 Geological Map.

Chin, R.J., 1986a. KELLERBERRIN, 1:250 000 *Geological Series-Explanatory Notes*, Sheet SH/50-15, Geological Survey of Western Australia, 25pp., accompanied by 1:250 000 Geological Map.

Chin, R.J., 1986b. CORRIGIN, 1:250 000 *Geological Series-Explanatory Notes*, Sheet SI/50-3, Geological Survey of Western Australia, 22pp., accompanied by 1:250 000 Geological Map.

Chin, R.J. and Smith, R.A., 1983. JACKSON, 1:250 000 *Geological Series-Explanatory Notes*, Sheet SH/50-12, Geological Survey of Western Australia, 30pp., accompanied by 1:250 000 Geological Map.

Chin, R.J., Hickman, A.H. and Thom, R., 1984. HYDEN, 1:250 000 *Geological Series-Explanatory Notes*, SI/50-4, 21pp., accompanied by 1:250 000 Geological Map.

Colvine, A.C. *et al.*, 1988. Archaean Lode Gold Deposits in Ontario; *Ontario Geological Survey Miscellaneous Paper 139*, 136pp.

Davis, J.C., 1986. *Statistics and Data Analysis in Geology*, John Wiley & Sons Inc., second edition, 646pp.

Finkl, C.W. and Churchward, H.M., 1973. The etched land surfaces of Southwestern Australia; *Geol. Soc. Australia Jour.*, **20**(3):295-307

Garrett, R.G., 1989. The chi-square plot: a tool for multivariate outlier detection, *J. Geochem. Explor.*, **32**:319-41.

Garrett, R.G., in press. A Robust Multivariate Procedure with Applications to Geochemical Data, in Proceedings of the Colloquium on "*Statistical Applications in the Earth Sciences*"

Gee, R.D, 1982. SOUTHERN CROSS, 1:250 000 *Geological Series-Explanatory Notes*, Sheet SH/50-16, Geological Survey of Western Australia, 25pp, accompanied by 1:250 000 Geological Map.

Gee, R.D., Baxter, J.L., Wilde, S.A. and Williams, I.R., 1981. Crustal development in the Archaean Yilgarn Block, Western Australia: *Geol. Soc. Australia Spec. Pub. 7*, 43-56.

Groves, D.I. 1988. Gold Mineralization in the Yilgarn Block, Western Australia, *Bicentennial Gold 88, Extended Abstracts, Oral Programme*, Geological Society of Australia Inc., Abstracts No. 22, 13-23.

Grunsky, E.C., 1986. Recognition of Alteration in Volcanic Rocks Using Statistical Analysis of Lithogeochemical Data, *J. Geochem. Explor.*, **25**:157-83.

Grunsky, E.C., Innes, J., Smith, R.E. and Perdrix, J.L., 1988. Report on Laterite Geochemistry in the CSIRO-AGE Database for the Southern Murchison Region, *Exploration Geoscience Restricted Report, 2R*, 92pp., 1 5.25" diskette.

Grunsky, E.C., Innes, J., Smith, R.E. and Perdrix, J.L., 1989. Report on Laterite Geochemistry in the CSIRO-AGE Database for the Norhern Murchison Region, *Exploration Geoscience Restricted Report, 68R*, 148pp., 1 5.25" diskette.

Hallberg, J.A., 1976. A petrochemical study of a portion of the western Yilgarn Block. *CSIRO Div. of Mineralogy Rept. FP 13, 38pp.*

Hallberg, J.A., 1984. A Geochemical Aid to Igneous Rock Type Identification in Deeply Weathered Terrain, *J. Geochem. Explor.*, **20**:1-8.

Hickman, A.H. and Watkins, K.P., 1988. Gold Mineralization in the Murchison Province, Western Australia, in *Bicentennial Gold 88, Extended Abstract, Poster Programme*, Vol. 1, Geological Society of Australia Inc., Abstracts No. 23, 23-25.

Howarth, R.J., 1983. Statistics and Data Analysis in Geochemical Prospecting, edited by R.J. Howarth, Vol. 2, in *Handbook of Exploration Geochemistry*, edited by G.J.S. Govett, Elsevier, 437pp.

Howarth, R.J. and Sinding-Larsen, 1983. Multivariate Data Analysis, Chapter 6; Statistics and Data Analysis in Geochemical Prospecting, edited by R.J. Howarth, Vol. 2, in *Handbook of Exploration Geochemistry*, edited by G.J.S. Govett, Elsevier, 437pp.

Jöreskog, K.G., Klovan, J.E. and Reyment, R.A., 1976. *Geological Factor Analysis*. Elsevier Scientific Publishing Company, New York, 178pp.

Kriewaldt, M.J.B., 1969. KALGOORLIE, 1:250 000 *Geological Series-Explanatory Notes*, Sheet SH/51-9, Geological Survey of Western Australia, 18pp., accompanied by 1:250 000 Geological Map.

LeMaitre, R.W., 1989. *A Classification of Igneous Rocks and Glossary of Terms*, Recommendations of the International Union of Geological Sciences Subcommission on the Systematics of Igneous Rocks, R.W. LeMaitre, editor, Blackwell Scientific Publications, Melbourne, 193pp.

Mazzuchelli, R.H. and James, C.H., 1966. Arsenic as a guide to gold mineralization in laterite-covered areas of Western Australia., *Trans. Inst. Min. Metall.* Sect, B, **75**:285-94.

Nieuwland, D.A. and Compston, W., 1981. Crustal evolution in the Yilgarn Block near Perth, Western Australia, *Geol. Soc. Australia Spec. Pub. No. 7*, 159-71.

Smith, R.E., 1987. Current Research at CSIRO Australia on Multi-element Laterite Geochemistry for Detecting Concealed Mineral Deposits, *Chemical Geology*, **60**:205-11.

Smith, R.E., Moeskops, P.G. and Nickel, E.H., 1979. Multi-element geochemistry at the Golden Grove Cu-Zn-Ag deposit. In: J.E. Glover, D.I. Groves, and R.E. Smith (Editors), *Pathfinder and Multi-element Geochemistry in Mineral Exploration*. Univ. W.Australia, Geol. Dept. Extension Service, Publ. 4, 30-41.

Smith, R.E. and Perdrix, J.L. 1983. Pisolitic laterite geochemistry in the Golden Grove massive sulphide district, Western Australia, *J. Geochem. Explor.*, **18**:131-64.

Smith, R.E., Campbell, N.A. and Litchfield, R. 1984. Multivariate Statistical Techniques Applied To Pisolitic Laterite Geochemistry At Golden Grove, Western Australia, *J. Geochem. Explor.*, **22**:193-216.

Smith, R.E., Perdrix, J.L. and Davis, J.M. 1987. Dispersion into Pisolitic Laterite from the Greenbushes Mineralized Sn-Ta Pegmatite System, Western Australia, *J. Geochem. Explor.*, **28**:251-65.

Smith, R.E., Birrell, R.D. and Brigden, J.F.. 1989. The implications to exploration of chalcophile corridors in the Archaean Yilgarn Block, Western Australia, as revealed by laterite geochemistry, *J. Geochem. Explor.*, **32**:169-84.

Stanley, C.R. and Sinclair, A.J., 1987. Anomaly recognition for multi-element geochemical data- A background characterization approach. *J. Geochem. Explor.*, **29**:333-53.

Thurston, P.C. and Chivers, K.M., 1990. Secular Variation in Greenstone Sequence Development Emphasizing Superior Province, Canada, *Precambrian Research*, **46**:21-58.

Walker, I.W. and Blight, D.F., 1983. BARLEE, 1:250 000 *Geological Series-Explanatory Notes*, Sheet SH/50-8, Geological Survey of Western Australia, 22pp., accompanied by 1:250 000 Geological Map

Zeegers, H., Goni, J. and Wilhem, E., 1981. Geochemistry of lateritic profiles over a disseminated Cu-Mo mineralization in Upper Volta (West Africa) - preliminary results. In M.K. Roychowdhury, B.P. Radhakrishna, R. Vaidyanadhan, P.K. Banerjee and K. Ranganathan (Editors), *Lateritization Processes*. Balkema Publishers, Rotterdam, pp. 359-368.

Zhou, D., Chang, T. and Davis, J.C., 1983. Dual Extraction of R-Mode and Q-Mode Factor Solutions, *Mathematical Geology*, **15**(5):581-606.

APPENDIX 1

Data Format of the Central Yilgarn Database

The data is contained on a double sided high density (1.2Mb)
5.25" floppy diskette formatted for an IBM PC or compatible computer running under DOS.

The name of the file that contains the data is: BJKBKSCH.SDF

Refer to Table 2 for the meaning of the various element codes.
The data is recorded in ASCII format and each record of the file has the following attributes:

Field	Name	Type	Width	Dec	Field	Name	Type	Width	Dec
1	SAMPLE	Character	7		21	ZN	Numeric	7	0
2	SAMPLETYPE	Character	5		22	NI	Numeric	7	0
3	GEOLOGY	Character	5		23	CO	Numeric	7	0
4	MAPREF	Character	8		24	AS	Numeric	7	0
5	EASTING	Numeric	6	0	25	SB	Numeric	7	0
6	NORTHING	Numeric	7	0	26	BI1	Numeric	7	0
7	DESCRIPT	Character	3		27	BI2	Numeric	7	0
8	ANOMALY	Character	5		28	MO	Numeric	7	0
9	SIO2	Numeric	7	2	29	SN1	Numeric	7	0
10	AL2O3	Numeric	7	2	30	SN2	Numeric	7	0
11	FE2O3	Numeric	7	2	31	GE	Numeric	7	0
12	MGO	Numeric	7	3	32	GA	Numeric	7	0
13	CAO	Numeric	7	3	33	W	Numeric	7	0
14	TIO2	Numeric	7	3	34	BA	Numeric	7	0
15	AG	Numeric	7	1	35	ZR	Numeric	7	0
16	MN	Numeric	7	0	36	NB	Numeric	7	0
17	CR	Numeric	7	0	37	TA	Numeric	7	0
18	V	Numeric	7	0	38	SE	Numeric	7	0
19	CU	Numeric	7	0	39	BE	Numeric	7	0
20	PB	Numeric	7	0	40	AU	Numeric	7	0

For the variable, GEOLOGY, the following codes are used to define the geology of the areas where the samples were collected:

AVR - Acid Volcanic Rocks
BIF - Banded Iron Formation
FGM - Foliated Granite and Migmatite
GIR - Granitic Intrusions
LBU - Layered Basic and Ultrabasic Intrusions
MBU - Metabasic and Ultrabasic Rocks
MSR - Metasedimentary Rocks
UMG - Undifferentiated Massive Granitic Rocks

The codes were derived from the geological maps of the Western Australia Geological Survey.

A FORTRAN 77 format statement would read in the data in the following manner

```
      CHARACTER*3 ANOMALY
      CHARACTER*5 SAMTYP,GEOL,DESCRIPT
      CHARACTER*7 SAMPLE
      CHARACTER*8 MAPREF
      REAL*4  EAST,NORTH,
     $        SIO2,AL2O3,FE2O3,MGO,CAO,TIO2,AG,MN,CR,V,CU,PB,
     $        ZN,NI,CO,AS,SB,BI1,BI2,MO,SN1,SN2,GE,GA,W,BA,ZR,
     $        NB,TA,SE,BE,AU
      READ(5,10) SAMPLE,SAMTYP,GEOL,MAPREF,DESCRIPT,ANOMALY,
     $        EAST,NORTH,
     $        SIO2,AL2O3,FE2O3,MGO,CAO,TIO2,AG,MN,CR,V,CU,PB,
     $        ZN,NI,CO,AS,SB,BI1,BI2,MO,SN1,SN2,GE,GA,W,BA,ZR,
     $        NB,TA,SE,BE,AU
 10   FORMAT(A7,2A5,A8,A5,A3,F6.0,F7.0,3F6.2,3F6.3,F6.1,25F6.0)
```

Negative values indicate less than detection limit. The detection limit is defined as the absolute value of the quoted value.

Zero values indicate that no analysis was performed for that element.

Table 3
Summary statistics for Barlee-Jackson-Kalgoorlie-Bencubbin-Kellerberrin-Southern Cross-Corrigin-Hyden
Laterites "R/F2/F3" Samples
Sample types:
LP CP LN CN PN VL MS
No. of Samples in Group: 1815

Element		Lab	Method	L.L.D.	#Samples	Percentiles								
						1%	5%	10%	25%	50%	75%	90%	95%	99%
SiO2	Wt%	Csiro	ICP-FS	0.5	642	3.49	6.94	12.34	20.35	36.83	49.99	58.81	63.14	70.84
Al2O3	Wt%	Csiro	ICP-FS	0.5	642	4.61	10.35	12.48	16.08	19.42	22.58	25.37	27.43	34.69
Fe2O3	Wt%	Amdel	AAS-HF	0.1	1780	5.70	8.83	10.54	13.96	23.22	41.45	56.69	65.38	76.06
MgO	Wt%	Csrio	ICP-FS	0.05	642	0.02	0.02	0.04	0.05	0.07	0.09	0.13	0.17	0.41
CaO	Wt%	Csiro	ICP-FS	0.05	642	0.02	0.02	0.02	0.04	0.05	0.07	0.10	0.14	0.38
TiO2	Wt%	Csiro	ICP-FS	0.003	642	0.20	0.35	0.42	0.54	0.68	0.95	1.44	1.93	3.43
Ag	ppm	Amdel	OES	0.1	1781	0.03	0.03	0.03	0.03	0.03	0.03	0.20	0.40	0.80
Mn	ppm	Amdel	AAS	5.0	1780	5.00	10.00	10.00	20.00	40.00	100.00	185.00	294.00	805.00
Cr	ppm	Amdel	XRF	5.0	1780	85.00	126.00	151.00	211.00	402.00	1179.00	3603.00	6386.00	9999.00
V	ppm	Amdel	XRF	10.0	1780	22.00	108.00	150.00	233.00	388.00	756.00	1161.00	1425.00	1892.00
Cu	ppm	Amdel	AA-HF	2.0	1780	0.67	2.00	2.00	6.00	14.00	61.00	163.00	230.00	388.00
Pb	ppm	Amdel	XRF	4.0	1780	0.67	5.00	8.00	16.00	29.00	43.00	58.00	69.00	103.00
Zn	ppm	Amdel	AA-HF	2.0	1780	4.00	6.00	7.00	10.00	15.00	26.00	42.00	56.00	103.00
Ni	ppm	Amdel	AA-HF	5.0	1780	1.67	7.00	10.00	20.00	35.00	79.00	185.00	317.00	739.00
Co	ppm	Amdel	AA-HF	5.0	1779	1.67	1.67	1.67	5.00	6.00	12.00	20.00	27.00	57.00
As	ppm	Analb	XRF	2.0	1780	5.00	9.00	12.00	17.00	26.00	41.00	82.00	167.00	599.00
Sb	ppm	Amdel	XRF	2.0	1780	0.67	0.67	0.67	0.67	0.67	3.00	6.00	10.00	49.00
Bi	ppm	Amdel	XRF	1.0	1779	0.33	0.33	0.33	0.33	0.33	1.00	2.00	3.00	6.00
Cd	ppm	Amdel	AAS	1.0	1781	0.33	0.33	0.33	0.33	0.33	0.33	0.33	0.33	0.33
Mo	ppm	Amdel	XRF	2.0	1781	0.67	0.67	0.67	0.67	3.00	5.00	7.00	8.00	15.00
Sn	ppm	Amdel	XRF	1.0	1781	0.33	0.33	0.33	0.33	2.00	4.00	6.00	7.00	10.00
Ge	ppm	Amdel	OES	1.0	1781	0.33	0.33	0.33	0.33	0.33	0.33	0.33	1.00	1.00
Ga	ppm	Amdel	OES	1.0	1781	3.00	6.00	10.00	15.00	20.00	25.00	30.00	30.00	50.00
W	ppm	Amdel	XRF	10.0	1781	3.33	3.33	3.33	3.33	3.33	3.33	12.00	16.00	31.00
Ba	ppm	Csiro	ICP	100.0	642	27.00	33.33	33.33	33.33	79.00	131.00	180.00	262.00	505.00
Zr	ppm	Csiro	ICP-FS	50.0	642	141.00	168.00	190.00	231.00	301.00	380.00	502.00	609.00	834.00
Nb	ppm	Amdel	XRF	3.0	1781	1.33	1.33	1.33	4.00	9.00	13.00	19.00	23.00	36.00
Ta	ppm	Amdel	XRF	3.0	1781	1.00	1.00	1.00	1.00	1.00	1.00	1.00	1.00	7.00
Se	ppm	Amdel	XRF	1.0	1781	0.33	0.33	0.33	0.67	3.00	4.00	6.00	7.00	9.00
Be	ppm	Amdel	OES	1.0	1781	0.33	0.33	0.33	0.33	0.33	0.33	0.33	1.00	1.00
Au	ppb	Amdel	234	1.0	902	0.33	0.33	0.33	1.00	4.00	10.00	30.00	108.00	880.00

Table 3 (cont'd)
Summary statistics for Barlee-Jackson-Kalgoorlie-Bencubbin-Kellerberrin-Southern Cross-Corrigin-Hyden Laterites "R/F2/F3" Samples
Sample types:
LP CP LN CN PN VL MS

Element		Lab	Method	L.L.D.	#Samples	Minimum	Maximum	Median	Mode	Mean	Std. Dev.
SiO2	Wt%	Csiro	ICP-FS	0.5	642	2.18	91.11	36.68	23.82	35.30	17.96
Al2O3	Wt%	Csiro	ICP-FS	0.5	642	0.80	44.49	19.41	19.04	19.30	5.61
Fe2O3	Wt%	Amdel	AAS-HF	0.1	1780	1.57	85.75	23.22	13.37	29.15	18.20
MgO	Wt%	Csrio	ICP-FS	0.05	642	0.02	7.06	0.07	0.02	0.10	0.33
CaO	Wt%	Csiro	ICP-FS	0.05	642	0.02	26.16	0.05	0.02	0.14	1.33
TiO2	Wt%	Csiro	ICP-FS	0.003	642	0.06	7.12	0.68	0.65	0.86	0.64
Ag	ppm	Amdel	OES	0.1	1781	0.03	3.00	0.03	0.04	0.10	0.20
Mn	ppm	Amdel	AAS	5.0	1780	1.67	7200.00	40.00	14.82	96.17	282.22
Cr	ppm	Amdel	XRF	5.0	1780	44.00	12237.00	402.00	202.55	1268.52	2045.62
V	ppm	Amdel	XRF	10.0	1780	3.33	2759.00	388.00	237.91	542.15	423.69
Cu	ppm	Amdel	AA-HF	2.0	1780	0.67	802.00	14.00	4.11	52.85	85.65
Pb	ppm	Amdel	XRF	4.0	1780	0.67	235.00	29.00	1.01	32.27	21.80
Zn	ppm	Amdel	AA-HF	2.0	1780	0.67	324.00	15.00	9.80	21.51	21.33
Ni	ppm	Amdel	AA-HF	5.0	1780	1.67	2611.00	35.00	19.01	81.12	153.50
Co	ppm	Amdel	AA-HF	5.0	1779	1.67	150.00	6.00	5.09	10.01	11.54
As	ppm	Analb	XRF	2.0	1780	0.67	2172.00	26.00	14.81	50.92	115.26
Sb	ppm	Amdel	XRF	2.0	1780	0.33	385.00	0.67	0.67	3.40	12.00
Bi	ppm	Amdel	XRF	1.0	1779	0.33	51.00	0.33	0.35	1.04	1.96
Cd	ppm	Amdel	AAS	1.0	1781	0.33	8.00	0.33	0.00	0.34	0.18
Mo	ppm	Amdel	XRF	2.0	1781	0.67	48.00	3.00	0.70	3.62	3.47
Sn	ppm	Amdel	XRF	1.0	1781	0.33	23.00	2.00	0.37	2.52	2.43
Ge	ppm	Amdel	OES	1.0	1781	0.33	6.00	0.33	0.34	0.39	0.27
Ga	ppm	Amdel	OES	1.0	1781	0.33	80.00	20.00	20.06	20.36	8.15
W	ppm	Amdel	XRF	10.0	1781	3.33	205.00	3.33	3.40	5.52	8.26
Ba	ppm	Csiro	ICP	100.0	642	19.00	1625.00	78.00	32.37	101.07	104.92
Zr	ppm	Csiro	ICP-FS	50.0	642	44.00	1057.00	301.00	210.68	326.99	138.97
Nb	ppm	Amdel	XRF	3.0	1781	1.33	62.00	9.00	1.44	9.94	7.58
Ta	ppm	Amdel	XRF	3.0	1781	1.00	18.00	1.00	0.00	1.23	1.20
Se	ppm	Amdel	XRF	1.0	1781	0.33	16.00	3.00	0.37	2.91	2.32
Be	ppm	Amdel	OES	1.0	1781	0.33	4.00	0.33	0.34	0.38	0.21
Au	ppb	Amdel	234	1.0	902	0.33	3260.00	4.00	0.87	42.22	241.02

NOTE: Mode estimated by binning of data: # of bins= 100.
Bin width=(95%ile-minimum value)/100.0

Table 4
Summary statistics for Barlee-Jackson-Kalgoorlie-Bencubbin-Kellerberrin-Southern Cross-Corrigin-Hyden
Ferricretes "R/F2/F3" Samples
Sample types:
MF FF PF PE RC
No. of Samples in Group: 184

Element		Lab	Method	L.L.D.	#Samples	Percentiles								
						1%	5%	10%	25%	50%	75%	90%	95%	99%
SiO2	Wt%	Csiro	ICP-FS	0.5	91	2.18	3.60	4.73	7.82	11.10	24.22	45.54	67.67	95.95
Al2O3	Wt%	Csiro	ICP-FS	0.5	91	0.67	2.27	3.74	6.11	8.88	11.82	19.39	22.53	38.96
Fe2O3	Wt%	Amdel	AAS-HF	0.1	177	2.71	9.12	16.52	43.16	63.81	75.07	83.47	86.60	95.15
MgO	Wt%	Csrio	ICP-FS	0.05	91	0.02	0.05	0.05	0.06	0.08	0.10	0.22	0.67	8.67
CaO	Wt%	Csiro	ICP-FS	0.05	91	0.02	0.05	0.06	0.08	0.09	0.13	0.24	0.40	1.59
TiO2	Wt%	Csiro	ICP-FS	0.003	91	0.03	0.10	0.21	0.56	0.87	1.34	1.82	2.91	4.06
Ag	ppm	Amdel	OES	0.1	177	0.03	0.03	0.03	0.03	0.03	0.10	0.20	0.30	0.80
Mn	ppm	Amdel	AAS	5.0	177	10.00	30.00	60.00	158.00	280.00	496.00	890.00	1453.00	5020.00
Cr	ppm	Amdel	XRF	5.0	177	38.00	93.00	154.00	425.00	1185.00	3662.00	6166.00	7892.00	11095.00
V	ppm	Amdel	XRF	10.0	177	13.00	76.00	132.00	384.00	841.00	1324.00	1624.00	2075.00	2622.00
Cu	ppm	Amdel	AA-HF	2.0	177	2.00	6.00	10.00	23.00	47.00	80.00	175.00	218.00	310.00
Pb	ppm	Amdel	XRF	4.0	177	0.67	4.00	6.00	15.00	30.00	44.00	64.00	76.00	154.00
Zn	ppm	Amdel	AA-HF	2.0	177	0.67	4.00	10.00	21.00	33.00	46.00	73.00	110.00	206.00
Ni	ppm	Amdel	AA-HF	5.0	177	1.67	5.00	15.00	34.00	81.00	144.00	270.00	402.00	1704.00
Co	ppm	Amdel	AA-HF	5.0	177	1.67	1.67	1.67	7.00	12.00	19.00	28.00	44.00	128.00
As	ppm	Analb	XRF	2.0	177	0.67	6.00	8.00	18.00	37.00	96.00	216.00	358.00	1161.00
Sb	ppm	Amdel	XRF	2.0	177	0.67	0.67	0.67	0.67	3.00	7.00	13.00	23.00	71.00
Bi	ppm	Amdel	XRF	1.0	176	0.33	0.33	0.33	0.33	0.33	1.00	2.00	4.00	6.00
Cd	ppm	Amdel	AAS	1.0	177	0.33	0.33	0.33	0.33	0.33	0.33	0.33	0.33	0.33
Mo	ppm	Amdel	XRF	2.0	177	0.67	0.67	0.67	0.67	3.00	4.00	6.00	8.00	38.00
Sn	ppm	Amdel	XRF	1.0	177	0.33	0.33	0.33	0.33	2.00	4.00	6.00	8.00	12.00
Ge	ppm	Amdel	OES	1.0	177	0.33	0.33	0.33	0.33	0.33	0.33	0.33	1.00	2.00
Ga	ppm	Amdel	OES	1.0	177	0.33	1.00	3.00	6.00	15.00	20.00	25.00	30.00	40.00
W	ppm	Amdel	XRF	10.0	177	3.33	3.33	3.33	3.33	3.33	10.00	19.00	26.00	35.00
Ba	ppm	Csiro	ICP	100.0	91	33.33	33.33	99.00	141.00	155.00	191.00	219.00	249.00	381.00
Zr	ppm	Csiro	ICP-FS	50.0	91	47.00	136.00	196.00	244.00	292.00	346.00	391.00	420.00	546.00
Nb	ppm	Amdel	XRF	3.0	177	1.33	1.33	1.33	1.33	4.00	8.00	14.00	16.00	51.00
Ta	ppm	Amdel	XRF	3.0	177	1.00	1.00	1.00	1.00	1.00	1.00	5.00	7.00	12.00
Se	ppm	Amdel	XRF	1.0	177	0.33	0.33	0.33	0.33	2.00	4.00	6.00	8.00	11.00
Be	ppm	Amdel	OES	1.0	177	0.33	0.33	0.33	0.33	0.33	0.33	0.33	0.33	1.00
Au	ppb	Amdel	234	1.0	149	0.33	0.33	0.33	1.00	3.00	7.00	17.00	40.00	120.00

Table 4 (cont'd)
Summary statistics for Barlee-Jackson-Kalgoorlie-Bencubbin-Kellerberrin-Southern Cross-Corrigin-Hyden Ferricretes "R/F2/F3" Samples
Sample types:
MF FF PF PE RC

Element		Lab	Method	L.L.D.	#Samples	Minimum	Maximum	Median	Mode	Mean	Std. Dev.
SiO2	Wt%	Csiro	ICP-FS	0.5	91	2.18	95.95	11.09	9.06	19.00	19.67
Al2O3	Wt%	Csiro	ICP-FS	0.5	91	0.67	38.96	8.74	7.34	9.86	6.17
Fe2O3	Wt%	Amdel	AAS-HF	0.1	177	1.57	95.15	63.67	72.57	57.36	23.75
MgO	Wt%	Csrio	ICP-FS	0.05	91	0.02	8.67	0.08	0.05	0.26	1.01
CaO	Wt%	Csiro	ICP-FS	0.05	91	0.02	1.59	0.09	0.08	0.15	0.23
TiO2	Wt%	Csiro	ICP-FS	0.003	91	0.03	4.06	0.87	0.88	1.03	0.79
Ag	ppm	Amdel	OES	0.1	177	0.03	0.80	0.03	0.03	0.08	0.13
Mn	ppm	Amdel	AAS	5.0	177	5.00	9999.00	280.00	243.92	482.39	911.69
Cr	ppm	Amdel	XRF	5.0	177	19.00	11896.00	1180.00	58.37	2301.24	2509.05
V	ppm	Amdel	XRF	10.0	177	3.33	2766.00	837.00	75.84	893.58	599.94
Cu	ppm	Amdel	AA-HF	2.0	177	2.00	357.00	46.00	3.08	67.73	68.19
Pb	ppm	Amdel	XRF	4.0	177	0.67	344.00	30.00	18.37	35.14	34.22
Zn	ppm	Amdel	AA-HF	2.0	177	0.67	247.00	33.00	1.21	40.96	38.74
Ni	ppm	Amdel	AA-HF	5.0	177	1.67	1817.00	81.00	3.67	138.21	232.88
Co	ppm	Amdel	AA-HF	5.0	177	1.67	213.00	12.00	4.84	16.36	21.53
As	ppm	Analb	XRF	2.0	177	0.67	3036.00	36.00	27.47	106.65	274.13
Sb	ppm	Amdel	XRF	2.0	177	0.33	156.00	3.00	0.67	6.31	14.31
Bi	ppm	Amdel	XRF	1.0	176	0.33	8.00	0.33	0.35	0.91	1.22
Cd	ppm	Amdel	AAS	1.0	177	0.33	0.33	0.33	0.00	0.33	0.00
Mo	ppm	Amdel	XRF	2.0	177	0.67	153.00	3.00	0.70	4.05	11.95
Sn	ppm	Amdel	XRF	1.0	177	0.33	12.00	2.00	0.37	2.48	2.57
Ge	ppm	Amdel	OES	1.0	177	0.33	4.00	0.33	0.34	0.43	0.39
Ga	ppm	Amdel	OES	1.0	177	0.33	40.00	15.00	20.06	13.97	8.30
W	ppm	Amdel	XRF	10.0	177	3.33	66.00	3.33	3.45	7.39	8.53
Ba	ppm	Csiro	ICP	100.0	91	33.33	381.00	155.00	34.41	161.28	59.38
Zr	ppm	Csiro	ICP-FS	50.0	91	47.00	546.00	289.00	265.21	291.27	86.46
Nb	ppm	Amdel	XRF	3.0	177	1.33	53.00	4.00	1.41	5.75	7.06
Ta	ppm	Amdel	XRF	3.0	177	1.00	14.00	1.00	1.03	1.84	2.19
Se	ppm	Amdel	XRF	1.0	177	0.33	11.00	2.00	0.37	2.64	2.55
Be	ppm	Amdel	OES	1.0	177	0.33	3.00	0.33	0.00	0.36	0.21
Au	ppb	Amdel	234	1.0	149	0.33	248.00	3.00	0.93	9.47	26.24

NOTE: Mode estimated by binning of data: # of bins= 100.
Bin width=(95%ile-minimum value)/100.0

Table 5a
Summary statistics for Barlee-Jackson-Kalgoorlie
Laterites "R" Samples
Sample types:
LP CP LN CN PN VL MS
No. of Samples in Group: 379

Element		Lab	Method	L.L.D.	#Samples	Percentiles								
						1%	5%	10%	25%	50%	75%	90%	95%	99%
SiO2	Wt%	Csiro	ICP-FS	0.5	40	4.33	5.67	9.82	14.50	21.74	49.45	65.67	87.01	91.11
Al2O3	Wt%	Csiro	ICP-FS	0.5	40	0.80	1.10	4.61	14.68	16.72	19.75	23.71	24.63	38.03
Fe2O3	Wt%	Amdel	AAS-HF	0.1	345	8.69	17.09	20.08	28.92	42.73	56.26	67.80	73.50	79.48
MgO	Wt%	Csrio	ICP-FS	0.05	40	0.03	0.03	0.04	0.05	0.07	0.12	0.36	4.48	7.06
CaO	Wt%	Csiro	ICP-FS	0.05	40	0.03	0.04	0.05	0.06	0.07	0.11	0.27	21.24	26.16
TiO2	Wt%	Csiro	ICP-FS	0.003	40	0.06	0.12	0.35	0.60	0.83	1.00	1.43	1.73	2.98
Ag	ppm	Amdel	OES	0.1	345	0.03	0.03	0.03	0.03	0.03	0.20	0.40	0.60	2.00
Mn	ppm	Amdel	AAS	5.0	345	15.00	20.00	25.00	43.00	90.00	182.00	352.00	610.00	1274.00
Cr	ppm	Amdel	XRF	5.0	345	209.00	365.00	488.00	718.00	1196.00	3025.00	7367.00	9088.00	9999.00
V	ppm	Amdel	XRF	10.0	345	26.00	282.00	370.00	556.00	827.00	1157.00	1549.00	1749.00	2189.00
Cu	ppm	Amdel	AA-HF	2.0	345	12.00	16.00	19.00	30.00	69.00	145.00	242.00	309.00	443.00
Pb	ppm	Amdel	XRF	4.0	345	0.67	6.00	9.00	16.00	27.00	39.00	53.00	59.00	91.00
Zn	ppm	Amdel	AA-HF	2.0	345	7.00	10.00	12.00	18.00	27.00	37.00	48.00	60.00	90.00
Ni	ppm	Amdel	AA-HF	5.0	345	19.00	30.00	34.00	50.00	88.00	160.00	359.00	612.00	1236.00
Co	ppm	Amdel	AA-HF	5.0	345	1.67	1.67	6.00	9.00	13.00	20.00	32.00	47.00	85.00
As	ppm	Analb	XRF	2.0	345	4.00	7.00	10.00	16.00	30.00	52.00	99.00	175.00	514.00
Sb	ppm	Amdel	XRF	2.0	345	0.67	0.67	0.67	0.67	0.67	4.00	7.00	10.00	29.00
Bi	ppm	Amdel	XRF	1.0	345	0.33	0.33	0.33	0.33	0.33	2.00	3.00	4.00	6.00
Mo	ppm	Amdel	XRF	2.0	345	0.67	0.67	0.67	0.67	3.00	5.00	7.00	9.00	12.00
Sn	ppm	Amdel	XRF	1.0	345	0.33	0.33	0.33	0.33	0.33	2.00	4.00	6.00	10.00
Ge	ppm	Amdel	OES	1.0	345	0.33	0.33	0.33	0.33	0.33	0.33	1.00	1.00	1.00
Ga	ppm	Amdel	OES	1.0	345	1.00	6.00	10.00	15.00	20.00	20.00	25.00	30.00	30.00
W	ppm	Amdel	XRF	10.0	345	3.33	3.33	3.33	3.33	3.33	3.33	15.00	18.00	31.00
Ba	ppm	Csiro	ICP	100.0	40	26.00	43.00	50.00	94.00	120.00	171.00	200.00	527.00	530.00
Zr	ppm	Csiro	ICP-FS	50.0	40	44.00	51.00	196.00	229.00	257.00	331.00	394.00	404.00	551.00
Nb	ppm	Amdel	XRF	3.0	345	1.33	1.33	1.33	1.33	4.00	8.00	14.00	18.00	37.00
Ta	ppm	Amdel	XRF	3.0	345	1.00	1.00	1.00	1.00	1.00	1.00	1.00	4.00	7.00
Se	ppm	Amdel	XRF	1.0	345	0.33	0.33	0.33	2.00	3.00	5.00	6.00	8.00	10.00
Be	ppm	Amdel	OES	1.0	345	0.33	0.33	0.33	0.33	0.33	0.33	0.33	0.33	0.33
Au	ppb	Amdel	234	1.0	358	0.33	0.33	0.33	1.00	3.00	7.00	25.00	240.00	1880.00

Table 5a (cont'd)
Summary statistics for Barlee-Jackson-Kalgoorlie
Laterites "R" Samples
Sample types:
LP CP LN CN PN VL MS

Element		Lab	Method	L.L.D.	#Samples	Minimum	Maximum	Median	Mode	Mean	Std. Dev.
SiO2	Wt%	Csiro	ICP-FS	0.5	40	4.33	91.11	20.73	5.50	31.15	23.27
Al2O3	Wt%	Csiro	ICP-FS	0.5	40	.80	38.03	16.38	14.90	16.10	7.33
Fe2O3	Wt%	Amdel	AAS-HF	0.1	345	2.28	85.75	42.30	38.96	43.03	17.84
MgO	Wt%	Csrio	ICP-FS	0.05	40	.03	7.06	.07	.06	.39	1.29
CaO	Wt%	Csiro	ICP-FS	0.05	40	.03	26.16	.07	.05	1.27	5.24
TiO2	Wt%	Csiro	ICP-FS	0.003	40	.06	2.98	.82	.84	.84	.50
Ag	ppm	Amdel	OES	0.1	345	.03	3.00	.03	.04	.16	.30
Mn	ppm	Amdel	AAS	5.0	345	11.00	7200.00	89.00	37.95	183.37	436.97
Cr	ppm	Amdel	XRF	5.0	345	151.00	9999.00	1179.00	642.54	2459.86	2683.11
V	ppm	Amdel	XRF	10.0	345	3.33	2358.00	824.00	884.90	888.54	456.11
Cu	ppm	Amdel	AA-HF	2.0	345	9.00	802.00	69.00	28.50	104.73	104.54
Pb	ppm	Amdel	XRF	4.0	345	.67	147.00	27.00	17.29	29.30	18.69
Zn	ppm	Amdel	AA-HF	2.0	345	4.00	324.00	27.00	27.80	30.24	22.46
Ni	ppm	Amdel	AA-HF	5.0	345	1.67	2016.00	87.00	47.44	162.67	227.83
Co	ppm	Amdel	AA-HF	5.0	345	1.67	136.00	13.00	10.05	17.33	15.31
As	ppm	Analb	XRF	2.0	345	.67	2172.00	29.00	13.74	56.53	136.60
Sb	ppm	Amdel	XRF	2.0	345	.67	84.00	.67	.71	3.43	7.52
Bi	ppm	Amdel	XRF	1.0	345	.33	17.00	.33	.35	1.23	1.55
Mo	ppm	Amdel	XRF	2.0	345	.67	45.00	3.00	.71	3.56	3.58
Sn	ppm	Amdel	XRF	1.0	345	.33	14.00	.33	.36	1.56	2.13
Ge	ppm	Amdel	OES	1.0	345	.33	2.00	.33	.34	.41	.22
Ga	ppm	Amdel	OES	1.0	345	.33	80.00	20.00	20.06	18.61	7.27
W	ppm	Amdel	XRF	10.0	345	3.33	35.00	3.33	3.41	6.18	5.90
Ba	ppm	Csiro	ICP	100.0	40	26.00	530.00	119.00	93.28	144.32	105.66
Zr	ppm	Csiro	ICP-FS	50.0	40	44.00	551.00	256.00	245.71	272.80	98.93
Nb	ppm	Amdel	XRF	3.0	345	1.33	60.00	4.00	1.42	6.08	7.12
Ta	ppm	Amdel	XRF	3.0	345	1.00	7.00	1.00	1.01	1.27	1.07
Se	ppm	Amdel	XRF	1.0	345	.33	12.00	3.00	2.98	3.38	2.36
Be	ppm	Amdel	OES	1.0	345	.33	1.00	.33	.00	.34	.06
Au	ppb	Amdel	234	1.0	358	.33	3260.00	3.00	1.53	61.10	317.10

NOTE: Mode estimated by binning of data: # of bins= 100.
Bin width=(95%ile-minimum value)/100.0

Table 5b
Summary statistics for Barlee-Jackson-Kalgoorlie
Laterites "F2/F3" Samples
Sample types:
LP CP LN CN PN VL MS
No. of Samples in Group: 380

Element		Lab	Method	L.L.D.	#Samples	Percentiles								
						1%	5%	10%	25%	50%	75%	90%	95%	99%
SiO2	Wt%	Csiro	ICP-FS	0.5	263	2.42	4.11	6.48	13.63	20.76	26.90	41.54	48.23	59.37
Al2O3	Wt%	Csiro	ICP-FS	0.5	263	4.79	8.41	10.35	13.08	17.05	20.89	24.68	28.42	35.24
Fe2O3	Wt%	Amdel	AAS-HF	0.1	379	15.67	20.51	23.22	32.19	42.02	56.12	65.81	72.64	81.05
MgO	Wt%	Csrio	ICP-FS	0.05	263	.02	.02	.04	.05	.06	.09	.15	.20	.41
CaO	Wt%	Csiro	ICP-FS	0.05	263	.02	.02	.04	.05	.06	.09	.13	.19	.41
TiO2	Wt%	Csiro	ICP-FS	0.003	263	.20	.31	.41	.55	.75	1.16	1.98	2.45	4.97
Ag	ppm	Amdel	OES	0.1	380	.03	.03	.03	.03	.10	.30	.60	.60	1.00
Mn	ppm	Amdel	AAS	5.0	379	13.00	19.00	24.00	40.00	90.00	144.00	250.00	361.00	968.00
Cr	ppm	Amdel	XRF	5.0	379	151.00	255.00	377.00	669.00	1552.00	3497.00	6388.00	8211.00	9999.00
V	ppm	Amdel	XRF	10.0	379	65.00	243.00	344.00	532.00	747.00	1077.00	1484.00	1639.00	2108.00
Cu	ppm	Amdel	AA-HF	2.0	379	9.00	14.00	20.00	39.00	90.00	174.00	251.00	340.00	536.00
Pb	ppm	Amdel	XRF	4.0	379	.67	1.33	5.00	9.00	17.00	29.00	41.00	47.00	63.00
Zn	ppm	Amdel	AA-HF	2.0	379	7.00	9.00	11.00	17.00	27.00	44.00	80.00	101.00	159.00
Ni	ppm	Amdel	AA-HF	5.0	379	1.67	19.00	28.00	48.00	96.00	174.00	330.00	421.00	676.00
Co	ppm	Amdel	AA-HF	5.0	379	1.67	1.67	1.67	8.00	12.00	17.00	26.00	34.00	69.00
As	ppm	Analb	XRF	2.0	379	5.00	10.00	14.00	24.00	47.00	100.00	230.00	374.00	982.00
Sb	ppm	Amdel	XRF	2.0	379	.67	.67	.67	.67	3.00	7.00	21.00	37.00	80.00
Bi	ppm	Amdel	XRF	1.0	378	.33	.33	.33	.33	.33	1.00	3.00	4.00	6.00
Mo	ppm	Amdel	XRF	2.0	380	.67	.67	.67	.67	2.00	4.00	6.00	7.00	12.00
Sn	ppm	Amdel	XRF	1.0	380	.33	.33	.33	.33	3.00	5.00	7.00	9.00	11.00
Ge	ppm	Amdel	OES	1.0	380	.33	.33	.33	.33	.33	.33	1.00	1.00	2.00
Ga	ppm	Amdel	OES	1.0	380	1.00	3.00	6.00	10.00	15.00	20.00	30.00	40.00	50.00
W	ppm	Amdel	XRF	10.0	380	3.33	3.33	3.33	3.33	3.33	11.00	18.00	25.00	43.00
Ba	ppm	Csiro	ICP	100.0	263	33.33	33.33	54.00	89.00	123.00	163.00	249.00	346.00	554.00
Zr	ppm	Csiro	ICP-FS	50.0	263	141.00	154.00	167.00	199.00	236.00	300.00	357.00	399.00	462.00
Nb	ppm	Amdel	XRF	3.0	380	1.33	1.33	1.33	1.33	1.33	6.00	10.00	12.00	26.00
Ta	ppm	Amdel	XRF	3.0	380	1.00	1.00	1.00	1.00	1.00	1.00	1.00	6.00	12.00
Se	ppm	Amdel	XRF	1.0	380	.33	.33	.33	1.00	3.00	5.00	7.00	8.00	9.00
Be	ppm	Amdel	OES	1.0	380	.33	.33	.33	.33	.33	.33	.33	.33	.33
Au	ppb	Amdel	234	1.0	380	.33	.33	.33	1.00	4.00	14.00	40.00	83.00	600.00

Table 5b (cont'd)

Summary statistics for Barlee-Jackson-Kalgoorlie
Laterites "F2/F3" Samples
Sample types:
LP CP LN CN PN VL MS

Element		Lab	Method	L.L.D.	#Samples	Minimum	Maximum	Median	Mode	Mean	Std. Dev.
SiO2	Wt%	Csiro	ICP-FS	0.5	263	2.18	64.82	20.70	20.83	22.09	12.81
Al2O3	Wt%	Csiro	ICP-FS	0.5	263	2.58	44.49	17.02	16.92	17.44	6.08
Fe2O3	Wt%	Amdel	AAS-HF	0.1	379	11.11	84.89	42.02	37.88	44.16	15.78
MgO	Wt%	Csrio	ICP-FS	0.05	263	.02	.56	.06	.02	.09	.07
CaO	Wt%	Csiro	ICP-FS	0.05	263	.02	1.37	.06	.02	.08	.10
TiO2	Wt%	Csiro	ICP-FS	0.003	263	.06	7.12	.75	.65	1.03	.87
Ag	ppm	Amdel	OES	0.1	380	.03	3.00	.10	.04	.21	.26
Mn	ppm	Amdel	AAS	5.0	379	10.00	2579.00	90.00	22.28	126.49	185.27
Cr	ppm	Amdel	XRF	5.0	379	84.00	12237.00	1548.00	368.44	2553.53	2513.24
V	ppm	Amdel	XRF	10.0	379	3.33	2759.00	745.00	534.92	835.97	432.14
Cu	ppm	Amdel	AA-HF	2.0	379	8.00	799.00	90.00	19.62	119.83	108.21
Pb	ppm	Amdel	XRF	4.0	379	.67	68.00	16.00	1.36	20.30	14.29
Zn	ppm	Amdel	AA-HF	2.0	379	.67	297.00	27.00	23.24	36.83	31.50
Ni	ppm	Amdel	AA-HF	5.0	379	1.67	956.00	95.00	45.70	139.62	135.71
Co	ppm	Amdel	AA-HF	5.0	379	1.67	96.00	12.00	1.83	14.18	11.66
As	ppm	Analb	XRF	2.0	379	.67	1304.00	47.00	24.93	100.32	166.16
Sb	ppm	Amdel	XRF	2.0	379	.33	385.00	3.00	.52	8.93	24.05
Bi	ppm	Amdel	XRF	1.0	378	.33	36.00	.33	.35	1.00	2.16
Mo	ppm	Amdel	XRF	2.0	380	.67	25.00	2.00	.70	2.62	2.76
Sn	ppm	Amdel	XRF	1.0	380	.33	23.00	3.00	.38	3.48	2.99
Ge	ppm	Amdel	OES	1.0	380	.33	6.00	.33	.34	.45	.39
Ga	ppm	Amdel	OES	1.0	380	.33	60.00	15.00	10.05	17.15	10.79
W	ppm	Amdel	XRF	10.0	380	3.33	171.00	3.33	3.44	8.14	11.80
Ba	ppm	Csiro	ICP	100.0	263	33.33	1625.00	123.00	34.90	147.18	130.80
Zr	ppm	Csiro	ICP-FS	50.0	263	114.00	499.00	234.00	212.32	251.86	74.92
Nb	ppm	Amdel	XRF	3.0	380	1.33	49.00	1.33	1.39	4.29	5.09
Ta	ppm	Amdel	XRF	3.0	380	1.00	18.00	1.00	1.02	1.57	2.12
Se	ppm	Amdel	XRF	1.0	380	.33	10.00	3.00	.37	3.48	2.43
Be	ppm	Amdel	OES	1.0	380	.33	1.00	.33	.00	.34	.05
Au	ppb	Amdel	234	1.0	380	.33	3000.00	4.00	.75	30.89	171.02

NOTE: Mode estimated by binning of data: # of bins= 100.
Bin width=(95%ile-minimum value)/100.0

Table 6a
Summary statistics for Barlee-Jackson-Kalgoorlie
Ferricretes "R" Samples
Sample types:
MF FF PF PE RC
No. of Samples in Group: 55

Element		Lab	Method	L.L.D.	#Samples	Percentiles								
						1%	5%	10%	25%	50%	75%	90%	95%	99%
SiO2	Wt%	Csiro	ICP-FS	0.5	12	7.43	7.43	7.78	23.44	30.46	82.31	89.75	95.95	95.95
Al2O3	Wt%	Csiro	ICP-FS	0.5	12	.67	.67	.86	3.99	12.97	20.34	22.68	22.96	22.96
Fe2O3	Wt%	Amdel	AAS-HF	0.1	48	8.55	10.68	28.63	44.44	59.68	69.80	77.06	83.47	95.15
MgO	Wt%	Csrio	ICP-FS	0.05	12	.03	.03	.05	.09	.36	.72	4.42	8.67	8.67
CaO	Wt%	Csiro	ICP-FS	0.05	12	.05	.05	.05	.06	.24	.50	1.58	1.59	1.59
TiO2	Wt%	Csiro	ICP-FS	0.003	12	.03	.03	.09	.13	.87	1.53	1.54	1.54	1.54
Ag	ppm	Amdel	OES	0.1	48	.03	.03	.03	.03	.03	.10	.20	.60	.80
Mn	ppm	Amdel	AAS	5.0	48	16.00	50.00	61.00	172.00	280.00	514.00	1126.00	1616.00	2398.00
Cr	ppm	Amdel	XRF	5.0	48	142.00	262.00	414.00	710.00	1150.00	3332.00	7823.00	9202.00	11896.00
V	ppm	Amdel	XRF	10.0	48	31.00	85.00	110.00	352.00	722.00	1045.00	1624.00	2033.00	2442.00
Cu	ppm	Amdel	AA-HF	2.0	48	8.00	11.00	25.00	59.00	101.00	200.00	251.00	272.00	357.00
Pb	ppm	Amdel	XRF	4.0	48	.67	3.00	4.00	8.00	15.00	36.00	71.00	101.00	344.00
Zn	ppm	Amdel	AA-HF	2.0	48	16.00	20.00	21.00	28.00	37.00	60.00	157.00	185.00	247.00
Ni	ppm	Amdel	AA-HF	5.0	48	28.00	35.00	38.00	66.00	135.00	241.00	847.00	904.00	1817.00
Co	ppm	Amdel	AA-HF	5.0	48	1.67	1.67	6.00	12.00	19.00	26.00	61.00	84.00	128.00
As	ppm	Analb	XRF	2.0	48	3.00	4.00	6.00	13.00	21.00	44.00	83.00	184.00	941.00
Sb	ppm	Amdel	XRF	2.0	48	.33	.67	.67	.67	.67	5.00	9.00	10.00	15.00
Bi	ppm	Amdel	XRF	1.0	47	.33	.33	.33	.33	.33	1.00	2.00	3.00	5.00
Mo	ppm	Amdel	XRF	2.0	48	.67	.67	.67	.67	2.00	4.00	7.00	9.00	153.00
Sn	ppm	Amdel	XRF	1.0	48	.33	.33	.33	.33	.33	3.00	4.00	4.00	7.00
Ge	ppm	Amdel	OES	1.0	48	.33	.33	.33	.33	.33	.33	.33	1.00	2.00
Ga	ppm	Amdel	OES	1.0	48	.33	.33	1.00	6.00	10.00	20.00	25.00	25.00	25.00
W	ppm	Amdel	XRF	10.0	48	3.33	3.33	3.33	3.33	3.33	3.33	18.00	21.00	29.00
Ba	ppm	Csiro	ICP	100.0	12	41.00	41.00	48.00	99.00	147.00	219.00	249.00	337.00	337.00
Zr	ppm	Csiro	ICP-FS	50.0	12	47.00	47.00	67.00	96.00	237.00	305.00	369.00	378.00	378.00
Nb	ppm	Amdel	XRF	3.0	48	1.33	1.33	1.33	1.33	1.33	4.00	6.00	12.00	19.00
Ta	ppm	Amdel	XRF	3.0	48	1.00	1.00	1.00	1.00	1.00	3.00	6.00	7.00	9.00
Se	ppm	Amdel	XRF	1.0	48	.33	.33	.33	.33	1.00	4.00	5.00	6.00	7.00
Be	ppm	Amdel	OES	1.0	48	.33	.33	.33	.33	.33	.33	.33	.33	.33
Au	ppb	Amdel	234	1.0	53	.33	.33	.33	1.00	4.00	6.67	25.00	60.00	120.00

Table 6a (cont'd)
Summary statistics for Barlee-Jackson-Kalgoorlie
Ferricretes "R" Samples
Sample types:
MF FF PF PE RC

Element		Lab	Method	L.L.D.	#Samples	Minimum	Maximum	Median	Mode	Mean	Std. Dev.
SiO2	Wt%	Csiro	ICP-FS	0.5	12	7.43	95.95	29.18	7.87	43.55	32.49
Al2O3	Wt%	Csiro	ICP-FS	0.5	12	.67	22.96	11.73	.78	11.01	8.57
Fe2O3	Wt%	Amdel	AAS-HF	0.1	48	8.55	95.15	59.11	46.38	55.08	20.42
MgO	Wt%	Csrio	ICP-FS	0.05	12	.03	8.67	.19	.07	1.29	2.62
CaO	Wt%	Csiro	ICP-FS	0.05	12	.05	1.59	.14	.06	.42	.56
TiO2	Wt%	Csiro	ICP-FS	0.003	12	.03	1.54	.79	.04	.79	.64
Ag	ppm	Amdel	OES	0.1	48	.03	.80	.03	.04	.10	.16
Mn	ppm	Amdel	AAS	5.0	48	16.00	2398.00	275.00	56.00	468.17	518.65
Cr	ppm	Amdel	XRF	5.0	48	142.00	11896.00	1126.00	730.90	2430.90	2815.36
V	ppm	Amdel	XRF	10.0	48	31.00	2442.00	712.00	101.07	790.40	568.71
Cu	ppm	Amdel	AA-HF	2.0	48	8.00	357.00	95.00	11.96	122.92	88.14
Pb	ppm	Amdel	XRF	4.0	48	.67	344.00	14.00	4.18	31.09	52.52
Zn	ppm	Amdel	AA-HF	2.0	48	16.00	247.00	37.00	33.74	59.17	54.09
Ni	ppm	Amdel	AA-HF	5.0	48	28.00	1817.00	120.00	102.46	244.63	337.04
Co	ppm	Amdel	AA-HF	5.0	48	1.67	128.00	19.00	22.66	24.79	24.39
As	ppm	Analb	XRF	2.0	48	3.00	941.00	20.00	14.76	62.06	157.99
Sb	ppm	Amdel	XRF	2.0	48	.33	15.00	.67	.67	3.13	3.47
Bi	ppm	Amdel	XRF	1.0	47	.33	5.00	.33	.35	.94	1.16
Mo	ppm	Amdel	XRF	2.0	48	.67	153.00	2.00	.71	5.71	21.89
Sn	ppm	Amdel	XRF	1.0	48	.33	7.00	.33	.35	1.40	1.70
Ge	ppm	Amdel	OES	1.0	48	.33	2.00	.33	.34	.40	.27
Ga	ppm	Amdel	OES	1.0	48	.33	25.00	10.00	10.08	11.69	8.00
W	ppm	Amdel	XRF	10.0	48	3.33	29.00	3.33	3.42	6.59	6.72
Ba	ppm	Csiro	ICP	100.0	12	41.00	337.00	134.00	42.48	154.83	87.15
Zr	ppm	Csiro	ICP-FS	50.0	12	47.00	378.00	236.00	237.32	214.58	117.70
Nb	ppm	Amdel	XRF	3.0	48	1.33	19.00	1.33	1.39	2.95	3.64
Ta	ppm	Amdel	XRF	3.0	48	1.00	9.00	1.00	1.03	2.15	2.10
Se	ppm	Amdel	XRF	1.0	48	.33	7.00	1.00	.36	2.13	2.05
Be	ppm	Amdel	OES	1.0	48	.33	.33	.33	.00	.33	.00
Au	ppb	Amdel	234	1.0	53	.33	120.00	3.00	1.23	10.15	22.20

NOTE: Mode estimated by binning of data: # of bins= 100.
Bin width=(95%ile-minimum value)/100.0

Table 6b
Summary statistics for Barlee-Jackson-Kalgoorlie
Ferricretes "F2/F3" Samples
Sample types:
MF FF PF PE RC
No. of Samples in Group: 89

Element		Lab	Method	L.L.D.	#Samples	Percentiles								
						1%	5%	10%	25%	50%	75%	90%	95%	99%
SiO2	Wt%	Csiro	ICP-FS	0.5	67	2.18	3.26	4.39	6.30	9.18	12.61	17.41	26.88	49.04
Al2O3	Wt%	Csiro	ICP-FS	0.5	67	1.96	2.63	3.74	6.09	7.90	10.08	11.76	12.03	13.41
Fe2O3	Wt%	Amdel	AAS-HF	0.1	89	20.80	39.03	53.27	64.38	72.93	79.62	86.03	88.31	95.15
MgO	Wt%	Csrio	ICP-FS	0.05	67	.02	.05	.05	.06	.08	.08	.10	.11	.67
CaO	Wt%	Csiro	ICP-FS	0.05	67	.02	.06	.07	.08	.09	.12	.15	.18	.44
TiO2	Wt%	Csiro	ICP-FS	0.003	67	.06	.10	.32	.63	.93	1.45	2.28	3.00	4.06
Ag	ppm	Amdel	OES	0.1	89	.03	.03	.03	.03	.03	.10	.20	.30	.60
Mn	ppm	Amdel	AAS	5.0	89	76.00	126.00	169.00	237.00	325.00	510.00	747.00	950.00	5020.00
Cr	ppm	Amdel	XRF	5.0	89	201.00	286.00	404.00	1064.00	2350.00	4572.00	7245.00	7964.00	11095.00
V	ppm	Amdel	XRF	10.0	89	198.00	310.00	472.00	841.00	1191.00	1465.00	1811.00	2155.00	2766.00
Cu	ppm	Amdel	AA-HF	2.0	89	13.00	19.00	21.00	32.00	45.00	57.00	85.00	104.00	308.00
Pb	ppm	Amdel	XRF	4.0	89	.67	6.00	10.00	18.00	34.00	45.00	56.00	69.00	122.00
Zn	ppm	Amdel	AA-HF	2.0	89	.67	.67	5.00	25.00	34.00	46.00	57.00	77.00	110.00
Ni	ppm	Amdel	AA-HF	5.0	89	17.00	24.00	26.00	47.00	104.00	135.00	192.00	246.00	448.00
Co	ppm	Amdel	AA-HF	5.0	89	1.67	5.00	7.00	9.00	12.00	14.00	22.00	24.00	39.00
As	ppm	Analb	XRF	2.0	89	7.00	16.00	20.00	35.00	82.00	136.00	274.00	479.00	1161.00
Sb	ppm	Amdel	XRF	2.0	89	.67	.67	.67	.67	5.00	11.00	23.00	32.00	156.00
Bi	ppm	Amdel	XRF	1.0	89	.33	.33	.33	.33	.33	1.00	3.00	4.00	8.00
Mo	ppm	Amdel	XRF	2.0	89	.67	.67	.67	.67	3.00	4.00	5.00	6.00	38.00
Sn	ppm	Amdel	XRF	1.0	89	.33	.33	.33	.33	3.00	5.00	8.00	8.00	12.00
Ge	ppm	Amdel	OES	1.0	89	.33	.33	.33	.33	.33	.33	.33	1.00	2.00
Ga	ppm	Amdel	OES	1.0	89	.33	3.00	3.00	6.00	15.00	20.00	20.00	30.00	40.00
W	ppm	Amdel	XRF	10.0	89	3.33	3.33	3.33	3.33	3.33	11.00	19.00	26.00	66.00
Ba	ppm	Csiro	ICP	100.0	67	122.00	128.00	136.00	147.00	156.00	191.00	210.00	224.00	381.00
Zr	ppm	Csiro	ICP-FS	50.0	67	174.00	193.00	199.00	261.00	298.00	346.00	412.00	420.00	466.00
Nb	ppm	Amdel	XRF	3.0	89	1.33	1.33	1.33	1.33	1.33	7.00	10.00	13.00	51.00
Ta	ppm	Amdel	XRF	3.0	89	1.00	1.00	1.00	1.00	1.00	1.00	5.00	9.00	14.00
Se	ppm	Amdel	XRF	1.0	89	.33	.33	.33	.33	2.00	4.00	7.00	8.00	11.00
Be	ppm	Amdel	OES	1.0	89	.33	.33	.33	.33	.33	.33	.33	.33	.33
Au	ppb	Amdel	234	1.0	88	.33	.33	.33	1.00	3.00	8.00	17.00	21.00	248.00

Table 6b (cont'd)
Summary statistics for Barlee-Jackson-Kalgoorlie
Ferricretes "F2/F3" Samples
Sample types:
MF FF PF PE RC

Element		Lab	Method	L.L.D.	#Samples	Minimum	Maximum	Median	Mode	Mean	Std. Dev.
SiO2	Wt%	Csiro	ICP-FS	0.5	67	2.18	49.04	9.09	11.20	10.75	7.26
Al2O3	Wt%	Csiro	ICP-FS	0.5	67	1.96	13.41	7.79	7.35	7.83	2.78
Fe2O3	Wt%	Amdel	AAS-HF	0.1	89	20.80	95.15	72.93	71.77	71.07	14.20
MgO	Wt%	Csrio	ICP-FS	0.05	67	.02	.67	.07	.06	.08	.08
CaO	Wt%	Csiro	ICP-FS	0.05	67	.02	.44	.09	.08	.11	.06
TiO2	Wt%	Csiro	ICP-FS	0.003	67	.06	4.06	.92	.72	1.15	.85
Ag	ppm	Amdel	OES	0.1	89	.03	.60	.03	.03	.08	.10
Mn	ppm	Amdel	AAS	5.0	89	76.00	5020.00	317.00	237.69	466.09	595.04
Cr	ppm	Amdel	XRF	5.0	89	201.00	11095.00	2349.00	395.07	3057.48	2444.79
V	ppm	Amdel	XRF	10.0	89	198.00	2766.00	1188.00	1303.70	1172.49	540.70
Cu	ppm	Amdel	AA-HF	2.0	89	13.00	308.00	44.00	36.21	50.91	36.29
Pb	ppm	Amdel	XRF	4.0	89	.67	122.00	33.00	18.09	34.57	20.93
Zn	ppm	Amdel	AA-HF	2.0	89	.67	110.00	34.00	1.05	36.63	21.64
Ni	ppm	Amdel	AA-HF	5.0	89	17.00	448.00	102.00	25.01	108.04	79.10
Co	ppm	Amdel	AA-HF	5.0	89	1.67	39.00	12.00	14.06	12.94	6.41
As	ppm	Analb	XRF	2.0	89	7.00	1161.00	79.00	23.52	131.75	185.34
Sb	ppm	Amdel	XRF	2.0	89	.67	156.00	5.00	.82	9.96	19.33
Bi	ppm	Amdel	XRF	1.0	89	.33	8.00	.33	.35	1.02	1.40
Mo	ppm	Amdel	XRF	2.0	89	.67	38.00	3.00	.69	3.24	4.21
Sn	ppm	Amdel	XRF	1.0	89	.33	12.00	3.00	.37	3.23	2.85
Ge	ppm	Amdel	OES	1.0	89	.33	2.00	.33	.34	.39	.23
Ga	ppm	Amdel	OES	1.0	89	.33	40.00	15.00	20.06	13.79	8.14
W	ppm	Amdel	XRF	10.0	89	3.33	66.00	3.33	3.45	8.27	9.69
Ba	ppm	Csiro	ICP	100.0	67	122.00	381.00	156.00	150.05	169.34	38.40
Zr	ppm	Csiro	ICP-FS	50.0	67	174.00	466.00	296.00	263.79	302.46	69.28
Nb	ppm	Amdel	XRF	3.0	89	1.33	51.00	1.33	1.39	4.90	6.28
Ta	ppm	Amdel	XRF	3.0	89	1.00	14.00	1.00	1.04	2.00	2.62
Se	ppm	Amdel	XRF	1.0	89	.33	11.00	2.00	.37	2.86	2.72
Be	ppm	Amdel	OES	1.0	89	.33	.33	.33	.00	.33	.00
Au	ppb	Amdel	234	1.0	88	.33	248.00	2.00	1.06	9.58	29.54

NOTE: Mode estimated by binning of data: # of bins= 100.
Bin width=(95%ile-minimum value)/100.0

Table 7
Summary statistics for Bencubbin-Kellerberrin-Southern Cross-Corrigin-Hyden
Laterites "R" Samples
Sample types:
LP CP LN CN PN VL MS
No. of Samples in Group: 1056

Element		Lab	Method	L.L.D.	#Samples	Percentiles								
						1%	5%	10%	25%	50%	75%	90%	95%	99%
SiO2	Wt%	Csiro	ICP-FS	0.5	339	11.23	22.17	27.97	38.19	46.72	54.90	62.26	65.98	70.84
Al2O3	Wt%	Csiro	ICP-FS	0.5	339	12.23	14.63	16.10	18.23	21.03	23.74	25.97	27.43	33.88
Fe2O3	Wt%	Amdel	AAS-HF	0.1	1056	5.27	7.83	9.26	11.82	15.53	23.08	35.61	43.87	54.55
MgO	Wt%	Csrio	ICP-FS	0.05	339	0.02	0.04	0.05	0.06	0.07	0.09	0.12	0.13	0.20
CaO	Wt%	Csiro	ICP-FS	0.05	339	0.02	0.02	0.02	0.02	0.05	0.06	0.08	0.10	0.13
TiO2	Wt%	Csiro	ICP-FS	0.003	339	0.31	0.40	0.44	0.52	0.64	0.83	1.14	1.35	2.05
Ag	ppm	Amdel	OES	0.1	1056	0.03	0.03	0.03	0.03	0.03	0.03	0.03	0.03	0.40
Mn	ppm	Amdel	AAS	5.0	1056	5.00	5.00	10.00	15.00	25.00	55.00	110.00	150.00	280.00
Cr	ppm	Amdel	XRF	5.0	1056	69.00	112.00	132.00	175.00	238.00	368.00	730.00	1104.00	2999.00
V	ppm	Amdel	XRF	10.0	1056	16.00	85.00	122.00	185.00	269.00	385.00	597.00	789.00	1203.00
Cu	ppm	Amdel	AA-HF	2.0	1056	0.67	2.00	2.00	4.00	6.00	10.00	24.00	44.00	120.00
Pb	ppm	Amdel	XRF	4.0	1056	0.67	8.00	13.00	23.00	35.00	49.00	63.00	76.00	116.00
Zn	ppm	Amdel	AA-HF	2.0	1056	4.00	6.00	6.00	8.00	10.00	16.00	22.00	28.00	48.00
Ni	ppm	Amdel	AA-HF	5.0	1056	1.67	5.00	10.00	15.00	20.00	35.00	50.00	60.00	200.00
Co	ppm	Amdel	AA-HF	5.0	1055	1.67	1.67	1.67	5.00	5.00	5.00	10.00	13.00	23.00
As	ppm	Analb	XRF	2.0	1056	6.00	10.00	12.00	17.00	24.00	32.00	42.00	53.00	206.00
Sb	ppm	Amdel	XRF	2.0	1056	0.67	0.67	0.67	0.67	0.67	2.00	4.00	4.00	6.00
Bi	ppm	Amdel	XRF	1.0	1056	0.33	0.33	0.33	0.33	0.33	1.00	2.00	3.00	6.00
Cd	ppm	Amdel	AAS	1.0	1056	0.33	0.33	0.33	0.33	0.33	0.33	0.33	0.33	0.33
Mo	ppm	Amdel	XRF	2.0	1056	0.67	0.67	0.67	2.00	4.00	5.00	7.00	9.00	17.00
Sn	ppm	Amdel	XRF	1.0	1056	0.33	0.33	0.33	0.33	2.00	4.00	5.00	6.00	9.00
Ge	ppm	Amdel	OES	1.0	1056	0.33	0.33	0.33	0.33	0.33	0.33	0.33	0.33	1.00
Ga	ppm	Amdel	OES	1.0	1056	10.00	10.00	15.00	20.00	20.00	25.00	30.00	30.00	50.00
W	ppm	Amdel	XRF	10.0	1056	3.33	3.33	3.33	3.33	3.33	3.33	3.33	12.00	18.00
Ba	ppm	Csiro	ICP	100.0	339	24.00	32.00	33.33	33.33	33.33	63.00	125.00	150.00	268.00
Zr	ppm	Csiro	ICP-FS	50.0	339	186.00	220.00	251.00	296.00	353.00	450.00	607.00	684.00	941.00
Nb	ppm	Amdel	XRF	3.0	1056	1.33	5.00	7.00	9.00	12.00	16.00	21.00	26.00	36.00
Ta	ppm	Amdel	XRF	3.0	1056	1.00	1.00	1.00	1.00	1.00	1.00	1.00	1.00	4.00
Se	ppm	Amdel	XRF	1.0	1056	0.33	0.33	0.33	0.33	2.00	4.00	5.00	7.00	9.00
Be	ppm	Amdel	OES	1.0	1056	0.33	0.33	0.33	0.33	0.33	0.33	0.33	1.00	1.00
Au	ppb	Amdel	234	1.0	164	0.33	1.00	1.00	2.00	4.00	7.00	21.00	27.00	590.00

Table 7 (cont'd)
Summary statistics for Bencubbin-Kellerberrin-Southern Cross-Corrigin-Hyden
Laterites "R" Samples
Sample types:
LP CP LN CN PN VL MS

Element		Lab	Method	L.L.D.	#Samples	Minimum	Maximum	Median	Mode	Mean	Std. Dev.
SiO2	Wt%	Csiro	ICP-FS	0.5	339	5.79	74.14	46.63	37.99	46.05	12.98
Al2O3	Wt%	Csiro	ICP-FS	0.5	339	10.37	39.86	20.95	18.99	21.12	4.20
Fe2O3	Wt%	Amdel	AAS-HF	0.1	1056	1.57	73.64	15.53	12.78	19.23	11.11
MgO	Wt%	Csrio	ICP-FS	0.05	339	0.02	0.91	0.07	0.07	0.08	0.06
CaO	Wt%	Csiro	ICP-FS	0.05	339	0.02	1.46	0.05	0.02	0.05	0.08
TiO2	Wt%	Csiro	ICP-FS	0.003	339	0.19	3.20	0.64	0.64	0.73	0.34
Ag	ppm	Amdel	OES	0.1	1056	0.03	1.00	0.03	0.00	0.04	0.06
Mn	ppm	Amdel	AAS	5.0	1056	1.67	6037.00	25.00	14.27	56.80	235.34
Cr	ppm	Amdel	XRF	5.0	1056	44.00	9999.00	237.00	187.10	418.12	815.19
V	ppm	Amdel	XRF	10.0	1056	3.33	1641.00	269.00	235.11	323.54	223.32
Cu	ppm	Amdel	AA-HF	2.0	1056	0.67	230.00	6.00	3.92	11.86	20.94
Pb	ppm	Amdel	XRF	4.0	1056	0.67	235.00	35.00	26.66	37.54	23.07
Zn	ppm	Amdel	AA-HF	2.0	1056	2.00	80.00	10.00	9.93	13.17	8.28
Ni	ppm	Amdel	AA-HF	5.0	1056	1.67	2611.00	20.00	20.04	33.49	102.63
Co	ppm	Amdel	AA-HF	5.0	1055	1.67	150.00	5.00	5.01	6.12	7.78
As	ppm	Analb	XRF	2.0	1056	0.67	1916.00	24.00	19.24	31.37	71.80
Sb	ppm	Amdel	XRF	2.0	1056	0.67	11.00	0.67	0.68	1.40	1.42
Bi	ppm	Amdel	XRF	1.0	1056	0.33	51.00	0.33	0.35	0.99	2.01
Cd	ppm	Amdel	AAS	1.0	1056	0.33	8.00	0.33	0.00	0.34	0.24
Mo	ppm	Amdel	XRF	2.0	1056	0.67	48.00	4.00	0.71	3.99	3.59
Sn	ppm	Amdel	XRF	1.0	1056	0.33	11.00	2.00	0.36	2.49	2.15
Ge	ppm	Amdel	OES	1.0	1056	0.33	4.00	0.33	0.00	0.36	0.22
Ga	ppm	Amdel	OES	1.0	1056	0.33	50.00	20.00	20.06	22.09	6.73
W	ppm	Amdel	XRF	10.0	1056	3.33	205.00	3.33	3.38	4.36	7.05
Ba	ppm	Csiro	ICP	100.0	339	19.00	505.00	33.33	32.75	60.19	52.66
Zr	ppm	Csiro	ICP-FS	50.0	339	164.00	1057.00	351.00	348.60	391.68	149.02
Nb	ppm	Amdel	XRF	3.0	1056	1.33	62.00	12.00	11.08	13.23	6.63
Ta	ppm	Amdel	XRF	3.0	1056	1.00	9.00	1.00	0.00	1.09	0.61
Se	ppm	Amdel	XRF	1.0	1056	0.33	16.00	2.00	0.37	2.55	2.19
Be	ppm	Amdel	OES	1.0	1056	0.33	4.00	0.33	0.34	0.40	0.27
Au	ppb	Amdel	234	1.0	164	0.33	2180.00	4.00	2.07	27.25	177.67

NOTE: Mode estimated by binning of data: # of bins= 100.
Bin width=(95%ile-minimum value)/100.0

Table 8
Summary statistics for Bencubbin-Kellerberrin-Southern Cross-Corrigin-Hyden Ferricretes "R" Samples
Sample types:
MF FF PF PE RC
No. of Samples in Group: 40

Element		Lab	Method	L.L.D.	#Samples	Percentiles								
						1%	5%	10%	25%	50%	75%	90%	95%	99%
SiO2	Wt%	Csiro	ICP-FS	0.5	12	20.58	20.58	24.22	30.46	44.25	55.86	56.47	67.67	67.67
Al2O3	Wt%	Csiro	ICP-FS	0.5	12	11.97	11.97	13.37	17.19	19.66	22.53	25.85	38.96	38.96
Fe2O3	Wt%	Amdel	AAS-HF	0.1	40	1.57	2.85	5.98	13.82	31.76	46.44	54.70	61.82	65.52
MgO	Wt%	Csrio	ICP-FS	0.05	12	0.05	0.05	0.05	0.09	0.13	0.22	0.24	1.18	1.18
CaO	Wt%	Csiro	ICP-FS	0.05	12	0.02	0.02	0.02	0.05	0.08	0.14	0.31	0.32	0.32
TiO2	Wt%	Csiro	ICP-FS	0.003	12	0.21	0.21	0.34	0.55	0.65	0.88	0.88	0.92	0.92
Ag	ppm	Amdel	OES	0.1	40	0.03	0.03	0.03	0.03	0.03	0.03	0.03	0.10	0.80
Mn	ppm	Amdel	AAS	5.0	40	5.00	20.00	25.00	35.00	90.00	280.00	1100.00	2644.00	9999.00
Cr	ppm	Amdel	XRF	5.0	40	19.00	45.00	63.00	108.00	186.00	556.00	1199.00	1440.00	4547.00
V	ppm	Amdel	XRF	10.0	40	3.33	25.00	68.00	113.00	300.00	551.00	1038.00	1324.00	1428.00
Cu	ppm	Amdel	AA-HF	2.0	40	2.00	2.00	2.00	6.00	16.00	40.00	145.00	200.00	230.00
Pb	ppm	Amdel	XRF	4.0	40	2.00	5.00	14.00	24.00	34.00	54.00	74.00	127.00	154.00
Zn	ppm	Amdel	AA-HF	2.0	40	4.00	6.00	8.00	10.00	16.00	28.00	60.00	160.00	204.00
Ni	ppm	Amdel	AA-HF	5.0	40	1.67	1.67	5.00	5.00	20.00	45.00	110.00	325.00	1704.00
Co	ppm	Amdel	AA-HF	5.0	40	1.67	1.67	1.67	1.67	5.00	10.00	35.00	50.00	213.00
As	ppm	Analb	XRF	2.0	40	0.67	0.67	0.67	10.00	21.00	34.00	94.00	233.00	3036.00
Sb	ppm	Amdel	XRF	2.0	40	0.67	0.67	0.67	0.67	0.67	3.00	5.00	7.00	8.00
Bi	ppm	Amdel	XRF	1.0	40	0.33	0.33	0.33	0.33	0.33	0.33	2.00	3.00	4.00
Cd	ppm	Amdel	AAS	1.0	40	0.33	0.33	0.33	0.33	0.33	0.33	0.33	0.33	0.33
Mo	ppm	Amdel	XRF	2.0	40	0.67	0.67	0.67	0.67	3.00	5.00	8.00	13.00	27.00
Sn	ppm	Amdel	XRF	1.0	40	0.33	0.33	0.33	0.33	1.00	3.00	6.00	6.00	11.00
Ge	ppm	Amdel	OES	1.0	40	0.33	0.33	0.33	0.33	0.33	0.33	1.00	2.00	4.00
Ga	ppm	Amdel	OES	1.0	40	2.00	6.00	6.00	10.00	20.00	25.00	25.00	30.00	40.00
W	ppm	Amdel	XRF	10.0	40	3.33	3.33	3.33	3.33	3.33	3.33	21.00	30.00	35.00
Ba	ppm	Csiro	ICP	100.0	12	33.33	33.33	33.33	33.33	103.00	215.00	259.00	321.00	321.00
Zr	ppm	Csiro	ICP-FS	50.0	12	136.00	136.00	206.00	254.00	312.00	358.00	393.00	546.00	546.00
Nb	ppm	Amdel	XRF	3.0	40	1.33	1.33	1.33	6.00	11.00	15.00	20.00	24.00	53.00
Ta	ppm	Amdel	XRF	3.0	40	1.00	1.00	1.00	1.00	1.00	1.00	1.00	3.00	3.00
Se	ppm	Amdel	XRF	1.0	40	0.33	0.33	0.33	0.33	2.00	4.00	6.00	10.00	11.00
Be	ppm	Amdel	OES	1.0	40	0.33	0.33	0.33	0.33	0.33	0.33	0.33	1.00	3.00
Au	ppb	Amdel	234	1.0	8	1.00	1.00	1.00	2.00	3.00	4.00	14.00	14.00	14.00

Table 8 (cont'd)
Summary statistics for Bencubbin-Kellerberrin-Southern Cross-Corrigin-Hyden
Ferricretes "R" Samples
Sample types:
MF FF PF PE RC

Element		Lab	Method	L.L.D.	#Samples	Minimum	Maximum	Median	Mode	Mean	Std. Dev.
SiO2	Wt%	Csiro	ICP-FS	0.5	12	20.58	67.67	34.66	20.82	40.50	14.67
Al2O3	Wt%	Csiro	ICP-FS	0.5	12	11.97	38.96	19.39	17.23	20.08	7.12
Fe2O3	Wt%	Amdel	AAS-HF	0.1	40	1.57	65.52	28.20	6.09	29.60	19.01
MgO	Wt%	Csrio	ICP-FS	0.05	12	0.05	1.18	0.12	0.05	0.22	0.31
CaO	Wt%	Csiro	ICP-FS	0.05	12	0.02	0.32	0.06	0.02	0.11	0.10
TiO2	Wt%	Csiro	ICP-FS	0.003	12	0.21	0.92	0.61	0.88	0.64	0.23
Ag	ppm	Amdel	OES	0.1	40	0.03	0.80	0.03	0.03	0.05	0.12
Mn	ppm	Amdel	AAS	5.0	40	5.00	9999.00	90.00	18.19	535.72	1619.89
Cr	ppm	Amdel	XRF	5.0	40	19.00	4547.00	183.00	68.74	463.00	761.17
V	ppm	Amdel	XRF	10.0	40	3.33	1428.00	284.00	9.94	396.81	362.08
Cu	ppm	Amdel	AA-HF	2.0	40	2.00	230.00	12.00	2.99	38.95	58.38
Pb	ppm	Amdel	XRF	4.0	40	2.00	154.00	33.00	20.12	41.28	30.21
Zn	ppm	Amdel	AA-HF	2.0	40	4.00	204.00	14.00	9.46	28.73	39.82
Ni	ppm	Amdel	AA-HF	5.0	40	1.67	1704.00	15.00	6.52	77.64	271.93
Co	ppm	Amdel	AA-HF	5.0	40	1.67	213.00	5.00	4.81	13.82	34.08
As	ppm	Analb	XRF	2.0	40	0.67	3036.00	20.00	11.12	104.31	477.12
Sb	ppm	Amdel	XRF	2.0	40	0.67	8.00	0.67	0.70	2.00	2.02
Bi	ppm	Amdel	XRF	1.0	40	0.33	4.00	0.33	0.35	0.64	0.79
Cd	ppm	Amdel	AAS	1.0	40	0.33	0.33	0.33	0.00	0.33	0.00
Mo	ppm	Amdel	XRF	2.0	40	0.67	27.00	3.00	0.73	3.87	4.70
Sn	ppm	Amdel	XRF	1.0	40	0.33	11.00	1.00	0.36	2.10	2.28
Ge	ppm	Amdel	OES	1.0	40	0.33	4.00	0.33	0.34	0.54	0.68
Ga	ppm	Amdel	OES	1.0	40	2.00	40.00	15.00	20.06	17.10	8.22
W	ppm	Amdel	XRF	10.0	40	3.33	35.00	3.33	3.47	6.40	7.63
Ba	ppm	Csiro	ICP	100.0	12	33.33	321.00	76.00	34.77	122.72	101.68
Zr	ppm	Csiro	ICP-FS	50.0	12	136.00	546.00	272.00	138.05	305.50	105.40
Nb	ppm	Amdel	XRF	3.0	40	1.33	53.00	11.00	1.45	11.00	8.99
Ta	ppm	Amdel	XRF	3.0	40	1.00	3.00	1.00	1.01	1.10	0.44
Se	ppm	Amdel	XRF	1.0	40	0.33	11.00	2.00	0.38	2.78	2.68
Be	ppm	Amdel	OES	1.0	40	0.33	3.00	0.33	0.34	0.43	0.44
Au	ppb	Amdel	234	1.0	8	1.00	14.00	2.00	1.07	3.75	4.27

NOTE: Mode estimated by binning of data: # of bins= 100.
Bin width=(95%ile-minimum value)/100.0

Table 9: Ranked Samples > 99th Percentile

Central Yilgarn "R/F2/F3" Samples
(Barlee, Bencubbin, Jackson, Kalgoorlie, Kellerberrin, Southern Cross, Corrigin, Hyden)
Laterites LP CP LN CN PN VL MS

Element	Lab	Method	L.L.D.	#Samples
SiO2 Wt%	Csiro	ICP-FS	0.5	1815

Sample	Type	Easting	Northing	Value
G08038	R	767950.	6633050.	91.1
G08039	R	767950.	6632050.	87.0
G08052	R	767950.	6631650.	82.0
G04627	R	541300.	6590900.	74.1
G02829	R	570800.	6416800.	72.4
G02784	R	689806.	6366573.	71.7
G02787	R	691898.	6367148.	70.8
G02785	R	689805.	6366573.	70.8
G02782	R	699853.	6368224.	69.9
G02915	R	572300.	6394900.	69.9
G02837	R	578400.	6416950.	68.9
G04539	R	602500.	6421000.	68.8
G02801	R	592950.	6429500.	67.8
G02795	R	701243.	6450930.	67.6
G04568	R	544300.	6418300.	67.3
G04855	R	767700.	6488250.	67.1
G04560	R	544350.	6443950.	67.1
G04849	R	769650.	6467200.	66.8
G04645	R	519000.	6610200.	66.4
G02892	R	566800.	6380700.	66.0

Element	Lab	Method	L.L.D.	#Samples
Al2O3 Wt%	Csiro	ICP-FS	0.5	1815

Sample	Type	Easting	Northing	Value
G05464	F3	731680.	6709570.	44.5
G04566	R	540900.	6428400.	39.9
G05498	F3	735530.	6710880.	39.1
G03319	R	746500.	6639300.	38.0
G06858	F2	739100.	6642150.	35.2
G02931	R	587900.	6410700.	35.1
G05470	F3	732350.	6710290.	34.7
G02896	R	588600.	6377700.	34.5
G05615	F3	746350.	6721720.	34.5
G02802	R	590600.	6430700.	33.9
G02909	R	569000.	6387600.	33.4
G02956	R	552400.	6412200.	32.8
G04482	R	622400.	6379000.	32.3
G06663	F3	739500.	6717450.	31.6
G06658	F3	740250.	6718400.	31.5
G04502	R	598500.	6453500.	30.7
G06659	F3	739700.	6718450.	30.1
G02803	R	586450.	6430850.	30.0
G05471	F3	732210.	6710660.	29.8
G06633	F3	739250.	6717150.	29.8

Element	Lab	Method	L.L.D.	#Samples
Fe2O3 Wt%	Amdel	AAS-HF	0.1	1815

Sample	Type	Easting	Northing	Value
G04965	R	798083.	6602730.	85.8
G03425	R	729800.	6641100.	85.8
G03643	F2	730680.	6707650.	84.9
G06631	F3	739800.	6716800.	84.5
G06900	F2	705650.	6689450.	84.3
G05595	F3	734430.	6712030.	81.1
G06685	F3	726250.	6701000.	80.1
G03370	R	743500.	6635400.	80.1
G03496	R	721250.	6694400.	79.5
G03639	F2	729786.	6707298.	79.5
G04984	R	791029.	6624439.	79.1
G03403	R	743600.	6642400.	78.9
G04995	R	711800.	6746800.	78.6
G06899	F2	705250.	6688400.	78.1
G04994	R	710400.	6744250.	77.6
G03515	R	729600.	6717000.	76.8
G05492	F3	735020.	6710060.	76.5
G03410	R	736100.	6641600.	76.1
G03405	R	742200.	6644700.	75.8
G05593	F3	734475.	6712130.	75.6

Element	Lab	Method	L.L.D.	#Samples
MgO Wt%	Csrio	ICP-FS	0.05	1815

Sample	Type	Easting	Northing	Value
G08035	R	767950.	6634550.	7.1
G08049	R	768450.	6633300.	4.5
G02905	R	579000.	6380900.	0.9
G06901	F2	705550.	6691000.	0.6
G06865	F2	739950.	6641750.	0.5
G06903	F2	707700.	6689400.	0.4
G06858	F2	739100.	6642150.	0.4
G08038	R	767950.	6633050.	0.4
G06872	F2	740950.	6642000.	0.4
G06900	F2	705650.	6689450.	0.4
G08039	R	767950.	6632050.	0.4
G03312	R	748900.	6633300.	0.3
G04864	R	761650.	6459850.	0.3
G03315	R	744300.	6633000.	0.3
G06870	F2	740850.	6641150.	0.3
G03803	R	756800.	6410000.	0.3
G08050	R	768450.	6632800.	0.3
G06864	F2	738650.	6642000.	0.3
G06863	F2	738700.	6642800.	0.2
G06861	F2	739650.	6642650.	0.2

Table 9: (Cont'd)

Element		Lab	Method	L.L.D.	#Samples
CaO	Wt%	Csiro	ICP-FS	0.05	1815

Sample	Type	Easting	Northing	Value
G08035	R	767950.	6634550.	26.2
G08049	R	768450.	6633300.	21.2
G02905	R	579000.	6380900.	1.5
G06903	F2	707700.	6689400.	1.4
G06861	F2	739650.	6642650.	0.6
G06865	F2	739950.	6641750.	0.4
G08050	R	768450.	6632800.	0.4
G06864	F2	738650.	6642000.	0.3
G06855	F2	739800.	6643650.	0.3
G06900	F2	705650.	6689450.	0.3
G06858	F2	739100.	6642150.	0.3
G05435	F3	731570.	6708040.	0.3
G06872	F2	740950.	6642000.	0.3
G03312	R	748900.	6633300.	0.3
G04499	R	599900.	6457000.	0.3
G06863	F2	738700.	6642800.	0.2
G06852	F2	752600.	6647050.	0.2
G05438	F3	730130.	6708980.	0.2
G05449	F3	732270.	6709040.	0.2
G06660	F3	739650.	6718150.	0.2

Element		Lab	Method	L.L.D.	#Samples
TiO2	Wt%	Csiro	ICP-FS	0.003	1815

Sample	Type	Easting	Northing	Value
G06640	F3	745700.	6721600.	7.1
G05441	F3	731000.	6708770.	5.8
G06670	F3	729800.	6706800.	5.0
G06651	F3	745600.	6722100.	4.5
G05456	F3	734980.	6710490.	4.0
G05442	F3	731300.	6709000.	3.6
G06677	F3	730200.	6706600.	3.4
G06675	F3	729550.	6705550.	3.3
G02841	R	589550.	6390900.	3.2
G06679	F3	726000.	6704800.	3.1
G03317	R	741200.	6635600.	3.0
G06867	F2	739800.	6642450.	3.0
G06676	F3	729350.	6707150.	2.9
G06632	F3	740000.	6716600.	2.7
G04563	R	541850.	6445850.	2.6
G05471	F3	732210.	6710660.	2.5
G06673	F3	727800.	6704350.	2.5
G06688	F3	724300.	6700750.	2.4
G05428	F3	730770.	6708110.	2.4
G06671	F3	730200.	6706000.	2.3

Element		Lab	Method	L.L.D.	#Samples
Ag	ppm	Amdel	OES	0.1	1815

Sample	Type	Easting	Northing	Value
G04975	R	791570.	6615798.	3.0
G03612	F2	756412.	6645861.	3.0
G04956	R	769900.	6639100.	2.0
G04949	R	773000.	6636600.	2.0
G03359	R	750900.	6636600.	2.0
G05453	F3	730700.	6709080.	1.0
G03626	F2	748533.	6644934.	1.0
G03763	R	735200.	6516500.	1.0
G03502	R	706400.	6694100.	1.0
G08017	R	769300.	6632950.	1.0
G04950	R	770200.	6638000.	1.0
G08128	F3	770350.	6636350.	1.0
G04951	R	766300.	6638000.	1.0
G08074	R	771490.	6636150.	1.0
G03680	F2	705215.	6694995.	1.0
G03663	F2	735860.	6711600.	0.8
G06853	F2	752050.	6646800.	0.8
G03402	R	741600.	6642100.	0.8
G05489	F3	736500.	6712280.	0.8
G03491	R	722100.	6697200.	0.8

Element		Lab	Method	L.L.D.	#Samples
Mn	ppm	Amdel	AAS	5.0	1815

Sample	Type	Easting	Northing	Value
G03319	R	746500.	6639300.	7200.0
G03781	R	744300.	6505500.	6037.0
G05273	R	589700.	6543700.	4200.0
G06900	F2	705650.	6689450.	2579.0
G04918	R	782200.	6631200.	1640.0
G08050	R	768450.	6632800.	1517.0
G08109	F3	728800.	6701700.	1353.0
G03399	R	749200.	6640100.	1274.0
G04981	R	791043.	6620933.	1264.0
G05236	R	636600.	6561500.	1200.0
G04972	R	794739.	6607617.	1076.0
G04924	R	782200.	6638200.	1076.0
G05487	F3	733690.	6712110.	1029.0
G03654	F2	733500.	6709320.	968.0
G08039	R	767950.	6632050.	942.0
G03425	R	729800.	6641100.	906.0
G05230	R	638450.	6550450.	820.0
G08074	R	771490.	6636150.	805.0
G03370	R	743500.	6635400.	760.0
G03446	R	746600.	6724200.	751.0

Element		Lab	Method	L.L.D.	#Samples
Cr	ppm	Amdel	XRF	5.0	1815

Sample	Type	Easting	Northing	Value
G08103	F3	731550.	6704200.	12237.0
G06674	F3	728250.	6706600.	12043.0
G03371	R	742900.	6634200.	9999.0
G05501	F3	736710.	6710740.	9999.0
G03642	F2	728787.	6707103.	9999.0
G03688	R	729458.	6695291.	9999.0
G06895	F2	738550.	6711700.	9999.0
G05878	F3	734340.	6709580.	9999.0
G05577	R	739370.	6705625.	9999.0
G03313	R	746300.	6631700.	9999.0
G04917	R	785350.	6621600.	9999.0
G03409	R	734100.	6649100.	9999.0
G03801	R	714000.	6550250.	9999.0
G03771	R	737100.	6516150.	9999.0
G06927	R	735700.	6696250.	9999.0
G03645	F2	730639.	6709591.	9999.0
G03901	R	718900.	6714600.	9999.0
G03767	R	734850.	6521000.	9999.0
G04951	R	766300.	6638000.	9999.0
G03762	R	736150.	6516500.	9933.0

Element		Lab	Method	L.L.D.	#Samples
V	ppm	Amdel	XRF	10.0	1815

Sample	Type	Easting	Northing	Value
G05442	F3	731300.	6709000.	2759.0
G03643	F2	730680.	6707650.	2454.0
G03425	R	729800.	6641100.	2358.0
G03368	R	738800.	6636800.	2356.0
G03370	R	743500.	6635400.	2254.0
G03617	F2	749641.	6646635.	2246.0
G03496	R	721250.	6694400.	2189.0
G03516	R	728500.	6720000.	2142.0
G08131	R	769450.	6638050.	2125.0
G06867	F2	739800.	6642450.	2108.0
G03519	R	715100.	6641900.	2030.0
G03441	R	719800.	6648700.	2016.0
G03632	F2	745114.	6643810.	1979.0
G04900	R	766800.	6632300.	1970.0
G05899	F3	732170.	6709900.	1932.0
G04930	R	777500.	6648300.	1914.0
G03923	R	711200.	6644500.	1898.0
G03433	R	724300.	6652900.	1892.0
G06853	F2	752050.	6646800.	1815.0
G03668	F2	705177.	6698753.	1807.0

Element		Lab	Method	L.L.D.	#Samples
Cu	ppm	Amdel	AA-HF	2.0	1815

Sample	Type	Easting	Northing	Value
G08145	R	767000.	6629900.	802.0
G06901	F2	705550.	6691000.	799.0
G08073	R	774000.	6637250.	675.0
G06910	F2	707400.	6692450.	631.0
G08128	F3	770350.	6636350.	554.0
G05382	F2	729621.	6712385.	536.0
G04938	R	752900.	6630200.	497.0
G05392	F2	732580.	6712200.	468.0
G06896	F2	738050.	6710500.	463.0
G06904	F2	708200.	6692000.	455.0
G04919	R	787000.	6631300.	443.0
G03470	R	738440.	6711370.	433.0
G04929	R	777600.	6645400.	412.0
G06880	F2	742900.	6711350.	407.0
G05395	F2	734230.	6712740.	403.0
G05397	F2	734790.	6712050.	393.0
G04933	R	755400.	6627300.	392.0
G03637	F2	742081.	6641998.	388.0
G06865	F2	739950.	6641750.	386.0
G03478	R	736140.	6712450.	384.0

Element		Lab	Method	L.L.D.	#Samples
Pb	ppm	Amdel	XRF	4.0	1815

Sample	Type	Easting	Northing	Value
G05320	R	528450.	6498000.	235.0
G05245	R	601900.	6538900.	171.0
G05163	R	634000.	6492000.	167.0
G05273	R	589700.	6543700.	152.0
G04842	R	760200.	6455700.	151.0
G04882	R	764400.	6627900.	147.0
G03208	R	705600.	6475700.	138.0
G04756	R	674000.	6485000.	130.0
G05271	R	590600.	6549000.	130.0
G03077	R	515250.	6617300.	123.0
G05244	R	599200.	6536000.	118.0
G05285	R	581050.	6476050.	116.0
G05248	R	595400.	6541200.	115.0
G05286	R	578550.	6474375.	112.0
G05313	R	571400.	6486600.	108.0
G03797	R	708100.	6555100.	108.0
G04957	R	768500.	6638900.	106.0
G05242	R	605950.	6536650.	103.0
G05311	R	573000.	6502000.	102.0
G03188	R	698800.	6475400.	102.0

Element		Lab	Method	L.L.D.	#Samples
Zn	ppm	Amdel	AA-HF	2.0	1815

Sample	Type	Easting	Northing	Value
G04918	R	782200.	6631200.	324.0
G06901	F2	705550.	6691000.	297.0
G06911	F2	705200.	6693500.	171.0
G03654	F2	733500.	6709320.	161.0
G05474	F3	731960.	6711080.	159.0
G06906	F2	708100.	6687450.	156.0
G06849	F2	752450.	6647350.	138.0
G05423	F3	730290.	6708050.	131.0
G05879	F3	734515.	6709470.	130.0
G05489	F3	736500.	6712280.	126.0
G05472	F3	731680.	6710800.	111.0
G05469	F3	731750.	6710390.	111.0
G08109	F3	728800.	6701700.	110.0
G06896	F2	738050.	6710500.	108.0
G05585	F3	734850.	6712900.	106.0
G03686	R	727922.	6698957.	106.0
G06634	F3	746000.	6722500.	105.0
G06870	F2	740850.	6641150.	103.0
G06880	F2	742900.	6711350.	103.0
G06835	F2	754328.	6647020.	102.0

Element		Lab	Method	L.L.D.	#Samples
Ni	ppm	Amdel	AA-HF	5.0	1815

Sample	Type	Easting	Northing	Value
G03803	R	756800.	6410000.	2611.0
G04968	R	797485.	6610274.	2016.0
G03315	R	744300.	6633000.	1600.0
G03762	R	736150.	6516500.	1364.0
G08135	R	767450.	6634800.	1243.0
G03459	R	736000.	6717100.	1236.0
G05575	R	738890.	6705340.	1046.0
G03477	R	732730.	6713110.	1015.0
G03317	R	741200.	6635600.	980.0
G03756	R	666450.	6533600.	956.0
G06674	F3	728250.	6706600.	956.0
G08049	R	768450.	6633300.	949.0
G03767	R	734850.	6521000.	862.0
G04917	R	785350.	6621600.	823.0
G08038	R	767950.	6633050.	818.0
G05395	F2	734230.	6712740.	778.0
G03470	R	738440.	6711370.	756.0
G04914	R	780800.	6628000.	739.0
G03471	R	737200.	6710300.	736.0
G08141	R	766000.	6637000.	695.0

Element		Lab	Method	L.L.D.	#Samples
Co	ppm	Amdel	AA-HF	5.0	1815

Sample	Type	Easting	Northing	Value
G05273	R	589700.	6543700.	150.0
G04968	R	797485.	6610274.	136.0
G03762	R	736150.	6516500.	118.0
G04918	R	782200.	6631200.	105.0
G03654	F2	733500.	6709320.	96.0
G03803	R	756800.	6410000.	86.0
G03756	R	666450.	6533600.	86.0
G04929	R	777600.	6645400.	85.0
G03315	R	744300.	6633000.	85.0
G05575	R	738890.	6705340.	83.0
G08013	F3	702090.	6736230.	78.0
G05395	F2	734230.	6712740.	75.0
G08141	R	766000.	6637000.	73.0
G03319	R	746500.	6639300.	70.0
G08109	F3	728800.	6701700.	69.0
G04947	R	777600.	6636600.	66.0
G05417	F3	729263.	6708018.	58.0
G08135	R	767450.	6634800.	57.0
G03637	F2	742081.	6641998.	53.0
G06988	F3	722550.	6696550.	53.0

Element		Lab	Method	L.L.D.	#Samples
As	ppm	Analb	XRF	2.0	1815

Sample	Type	Easting	Northing	Value
G03499	R	706300.	6686400.	2172.0
G03777	R	743350.	6507900.	1916.0
G08102	F3	732000.	6704600.	1304.0
G05485	F3	733540.	6711960.	1294.0
G06985	F3	722600.	6697000.	1008.0
G05423	F3	730290.	6708050.	982.0
G03782	R	743000.	6505550.	894.0
G06899	F2	705250.	6688400.	814.0
G05589	F3	734520.	6712360.	778.0
G06901	F2	705550.	6691000.	723.0
G06669	F3	730500.	6707650.	698.0
G05588	F3	734715.	6712350.	686.0
G03491	R	722100.	6697200.	668.0
G05550	F3	707497.	6695045.	660.0
G08103	F3	731550.	6704200.	635.0
G03763	R	735200.	6516500.	620.0
G03487	R	719800.	6700200.	603.0
G06634	F3	746000.	6722500.	599.0
G03639	F2	729786.	6707298.	598.0
G03364	R	753800.	6646500.	514.0

Table 9: (Cont'd)

Element		Lab	Method	L.L.D.	#Samples
Sb	ppm	Amdel	XRF	2.0	1815

Sample	Type	Easting	Northing	Value
G06901	F2	705550.	6691000.	385.0
G06911	F2	705200.	6693500.	93.0
G06853	F2	752050.	6646800.	93.0
G03502	R	706400.	6694100.	84.0
G06913	F2	705750.	6694300.	80.0
G06912	F2	706100.	6694550.	78.0
G06909	F2	705400.	6692500.	76.0
G03672	F2	706618.	6696817.	73.0
G03491	R	722100.	6697200.	70.0
G06985	F3	722600.	6697000.	69.0
G06905	F2	706700.	6686950.	66.0
G06904	F2	708200.	6692000.	64.0
G03623	F2	750946.	6645280.	61.0
G03499	R	706300.	6686400.	55.0
G03613	F2	752412.	6646263.	53.0
G06915	F2	707050.	6694550.	51.0
G06895	F2	738550.	6711700.	50.0
G06917	F2	707350.	6693550.	49.0
G06900	F2	705650.	6689450.	48.0
G05550	F3	707497.	6695045.	42.0

Element		Lab	Method	L.L.D.	#Samples
Bi	ppm	Amdel	XRF	1.0	1815

Sample	Type	Easting	Northing	Value
G03773	R	739300.	6514500.	51.0
G06885	F2	740650.	6711850.	36.0
G03809	R	749550.	6407600.	21.0
G05575	R	738890.	6705340.	17.0
G03203	R	715600.	6465300.	8.0
G03261	R	733000.	6505300.	8.0
G04995	R	711800.	6746800.	8.0
G04744	R	675500.	6499700.	7.0
G03271	R	696600.	6446700.	7.0
G03770	R	737050.	6520100.	7.0
G03789	R	744900.	6511150.	7.0
G04990	R	703000.	6742000.	7.0
G03810	R	748800.	6411650.	6.0
G06653	F3	745050.	6722700.	6.0
G08011	F3	725850.	6698700.	6.0
G05438	F3	730130.	6708980.	6.0
G04748	R	669000.	6493800.	6.0
G06658	F3	740250.	6718400.	6.0
G08104	F3	731750.	6703500.	6.0
G03368	R	738800.	6636800.	6.0

Element		Lab	Method	L.L.D.	#Samples
Mo	ppm	Amdel	XRF	2.0	1815

Sample	Type	Easting	Northing	Value
G03809	R	749550.	6407600.	48.0
G04995	R	711800.	6746800.	45.0
G04582	R	524000.	6472000.	44.0
G05346	R	597700.	6546900.	33.0
G08122	F3	705450.	6740110.	25.0
G05313	R	571400.	6486600.	24.0
G06874	F2	743850.	6711750.	21.0
G02791	R	699117.	6442807.	21.0
G05283	R	583700.	6473125.	19.0
G05311	R	573000.	6502000.	19.0
G04604	R	636800.	6565000.	19.0
G04614	R	636900.	6573400.	17.0
G05348	R	597725.	6546750.	17.0
G03797	R	708100.	6555100.	17.0
G05579	R	740050.	6707375.	16.0
G05227	R	629000.	6531900.	16.0
G05306	R	572850.	6491000.	16.0
G05340	R	518150.	6521750.	15.0
G04586	R	534400.	6478400.	15.0
G04583	R	525900.	6476700.	15.0

Element		Lab	Method	L.L.D.	#Samples
Sn	ppm	Amdel	XRF	1.0	1815

Sample	Type	Easting	Northing	Value
G08128	F3	770350.	6636350.	23.0
G06899	F2	705250.	6688400.	14.0
G06867	F2	739800.	6642450.	14.0
G06927	R	735700.	6696250.	14.0
G06654	F3	745150.	6722500.	11.0
G06900	F2	705650.	6689450.	11.0
G03752	R	669100.	6537150.	11.0
G04357	R	664900.	6413550.	11.0
G06890	F2	739350.	6709850.	11.0
G03696	R	734850.	6699950.	11.0
G05578	R	739950.	6707125.	11.0
G06894	F2	738550.	6710850.	11.0
G05173	R	630450.	6497400.	10.0
G02768	R	678500.	6389700.	10.0
G06898	F2	737450.	6708500.	10.0
G06924	R	734450.	6691950.	10.0
G06889	F2	739400.	6710600.	10.0
G04535	R	607100.	6427700.	10.0
G08131	R	769450.	6638050.	9.0
G04473	R	604000.	6362250.	9.0

Table 9: (Cont'd)

Element		Lab	Method	L.L.D.	#Samples
Ge	ppm	Amdel	OES	1.0	1815

Sample	Type	Easting	Northing	Value
G05896	F3	732085.	6710250.	6.0
G03783	R	743000.	6504500.	4.0
G03785	R	739900.	6511050.	4.0
G05348	R	597725.	6546750.	2.0
G04391	R	597300.	6403000.	2.0
G03296	R	756350.	6457200.	2.0
G05467	F3	732200.	6710070.	2.0
G05615	F3	746350.	6721720.	2.0
G03763	R	735200.	6516500.	2.0
G03651	F2	732421.	6707398.	2.0
G03760	R	735700.	6514000.	2.0
G04941	R	757900.	6633400.	2.0
G03611	F2	755007.	6646357.	2.0
G05495	F3	734690.	6709460.	1.0
G06653	F3	745050.	6722700.	1.0
G05599	F3	732540.	6710035.	1.0
G03669	F2	707056.	6698718.	1.0
G08030	R	771350.	6631850.	1.0
G04583	R	525900.	6476700.	1.0
G05881	F3	732085.	6709165.	1.0

Element		Lab	Method	L.L.D.	#Samples
Ga	ppm	Amdel	OES	1.0	1815

Sample	Type	Easting	Northing	Value
G08032	R	771400.	6633700.	80.0
G06681	F3	724650.	6703200.	60.0
G06881	F2	741850.	6710500.	60.0
G03757	R	730800.	6515800.	50.0
G03799	R	705500.	6554650.	50.0
G03802	R	717150.	6550900.	50.0
G03797	R	708100.	6555100.	50.0
G03790	R	712800.	6556400.	50.0
G03754	R	662400.	6534600.	50.0
G06638	F3	746300.	6722250.	50.0
G06874	F2	743850.	6711750.	50.0
G06673	F3	727800.	6704350.	50.0
G03768	R	739500.	6517700.	50.0
G03746	R	660000.	6532000.	50.0
G03798	R	705800.	6552950.	50.0
G03758	R	732900.	6512800.	50.0
G03786	R	739950.	6508150.	50.0
G06658	F3	740250.	6718400.	50.0
G03812	R	743950.	6405100.	50.0
G03773	R	739300.	6514500.	50.0

Element		Lab	Method	L.L.D.	#Samples
W	ppm	Amdel	XRF	10.0	1815

Sample	Type	Easting	Northing	Value
G03774	R	739750.	6512600.	205.0
G05462	F3	738720.	6711360.	171.0
G06687	F3	723100.	6701250.	61.0
G06651	F3	745600.	6722100.	55.0
G04513	R	613000.	6439600.	52.0
G06640	F3	745700.	6721600.	43.0
G06685	F3	726250.	6701000.	40.0
G06633	F3	739250.	6717150.	36.0
G03515	R	729600.	6717000.	35.0
G02791	R	699117.	6442807.	33.0
G03659	F2	736014.	6707014.	32.0
G06983	F3	723400.	6697200.	32.0
G05867	F3	707640.	6695000.	32.0
G02768	R	678500.	6389700.	32.0
G08074	R	771490.	6636150.	31.0
G06632	F3	740000.	6716600.	31.0
G06669	F3	730500.	6707650.	31.0
G04930	R	777500.	6648300.	31.0
G05575	R	738890.	6705340.	31.0
G03469	R	738300.	6715100.	30.0

Element		Lab	Method	L.L.D.	#Samples
Ba	ppm	Csiro	ICP	100.0	1815

Sample	Type	Easting	Northing	Value
G05469	F3	731750.	6710390.	1625.0
G06864	F2	738650.	6642000.	702.0
G06874	F2	743850.	6711750.	554.0
G08039	R	767950.	6632050.	530.0
G03687	R	727085.	6696110.	527.0
G02850	R	592350.	6364650.	505.0
G06852	F2	752600.	6647050.	505.0
G06657	F3	742000.	6720700.	459.0
G06853	F2	752050.	6646800.	426.0
G06845	F2	752800.	6647850.	419.0
G06855	F2	739800.	6643650.	417.0
G06851	F2	753000.	6646650.	406.0
G04569	R	545150.	6415400.	383.0
G06696	F3	723450.	6697650.	379.0
G05447	F3	732200.	6708650.	378.0
G05467	F3	732200.	6710070.	373.0
G06872	F2	740950.	6642000.	360.0
G05613	F3	747030.	6723320.	346.0
G06683	F3	726100.	6701800.	338.0
G05472	F3	731680.	6710800.	336.0

Table 9: (Cont'd)

Element		Lab	Method	L.L.D.	#Samples
Zr	ppm	Csiro	ICP-FS	50.0	1815

Sample	Type	Easting	Northing	Value
G02805	R	584500.	6440050.	1057.0
G04562	R	541400.	6439000.	960.0
G02820	R	576900.	6423750.	941.0
G02807	R	582850.	6442150.	941.0
G02825	R	556000.	6432300.	839.0
G02942	R	575600.	6417300.	839.0
G02906	R	575300.	6380800.	834.0
G04645	R	519000.	6610200.	830.0
G04646	R	517900.	6613000.	828.0
G02829	R	570800.	6416800.	827.0
G02790	R	705330.	6368882.	795.0
G02841	R	589550.	6390900.	767.0
G02850	R	592350.	6364650.	754.0
G02797	R	593200.	6421100.	737.0
G04632	R	536100.	6593200.	727.0
G02888	R	572000.	6372400.	696.0
G02875	R	588400.	6360800.	684.0
G02832	R	576900.	6410600.	678.0
G02893	R	567300.	6377300.	674.0
G02810	R	581600.	6451200.	666.0

Element		Lab	Method	L.L.D.	#Samples
Nb	ppm	Amdel	XRF	3.0	1815

Sample	Type	Easting	Northing	Value
G05236	R	636600.	6561500.	62.0
G05579	R	740050.	6707375.	60.0
G08126	F3	770300.	6634700.	49.0
G03752	R	669100.	6537150.	49.0
G03518	R	717800.	6641000.	48.0
G04756	R	674000.	6485000.	47.0
G03200	R	715100.	6470500.	44.0
G02849	R	589750.	6365750.	42.0
G08133	R	769350.	6635700.	41.0
G04605	R	641400.	6562650.	41.0
G05260	R	592000.	6560650.	40.0
G04336	R	682250.	6427050.	39.0
G02807	R	582850.	6442150.	37.0
G04611	R	632400.	6582300.	37.0
G08029	R	771300.	6630900.	37.0
G02906	R	575300.	6380800.	36.0
G04347	R	673200.	6426450.	36.0
G04387	R	609000.	6400250.	36.0
G03211	R	703800.	6482700.	36.0
G04562	R	541400.	6439000.	35.0

Element		Lab	Method	L.L.D.	#Samples
Ta	ppm	Amdel	XRF	3.0	1815

Sample	Type	Easting	Northing	Value
G06638	F3	746300.	6722250.	18.0
G06648	F3	745120.	6722200.	15.0
G06679	F3	726000.	6704800.	14.0
G08112	F3	706100.	6744720.	12.0
G06683	F3	726100.	6701800.	12.0
G06658	F3	740250.	6718400.	12.0
G06995	F3	721100.	6697400.	11.0
G06636	F3	746575.	6722500.	10.0
G03632	F2	745114.	6643810.	9.0
G06664	F3	740000.	6717000.	9.0
G04560	R	544350.	6443950.	9.0
G06640	F3	745700.	6721600.	8.0
G05615	F3	746350.	6721720.	8.0
G04483	R	625500.	6379000.	8.0
G08035	R	767950.	6634550.	7.0
G03910	R	704600.	6713900.	7.0
G06675	F3	729550.	6705550.	7.0
G06660	F3	739650.	6718150.	7.0
G06982	F3	723350.	6697400.	7.0
G04441	R	594500.	6390200.	7.0

Element		Lab	Method	L.L.D.	#Samples
Se	ppm	Amdel	XRF	1.0	1815

Sample	Type	Easting	Northing	Value
G03222	R	717300.	6498700.	16.0
G03406	R	742200.	6647500.	12.0
G04863	R	759650.	6459100.	12.0
G04876	R	760000.	6627300.	11.0
G05213	R	630000.	6526000.	11.0
G03188	R	698800.	6475400.	11.0
G03270	R	697800.	6448400.	11.0
G05245	R	601900.	6538900.	11.0
G05267	R	585250.	6553850.	11.0
G04547	R	605850.	6419700.	10.0
G03506	R	710600.	6697900.	10.0
G03688	R	729458.	6695291.	10.0
G03497	R	713300.	6689400.	10.0
G03446	R	746600.	6724200.	10.0
G03225	R	723000.	6497800.	10.0
G05885	F3	734950.	6711500.	10.0
G03384	R	746600.	6646700.	10.0
G03041	R	617200.	6499300.	9.0
G03485	R	722000.	6703800.	9.0
G06686	F3	724000.	6701800.	9.0

Table 9 (cont'd)

Element	Lab	Method	L.L.D.	#Samples
Be ppm	Amdel	OES	1.0	1815

Sample	Type	Easting	Northing	Value
G02811	R	581350.	6453200.	4.0
G05320	R	528450.	6498000.	3.0
G05271	R	590600.	6549000.	3.0
G02957	R	549100.	6408600.	2.0
G05248	R	595400.	6541200.	2.0
G05244	R	599200.	6536000.	2.0
G04352	R	670450.	6406400.	2.0
G02827	R	557800.	6425700.	2.0
G02829	R	570800.	6416800.	2.0
G02977	R	561300.	6435900.	1.0
G02893	R	567300.	6377300.	1.0
G05242	R	605950.	6536650.	1.0
G04600	R	626800.	6562350.	1.0
G02910	R	573900.	6387200.	1.0
G03927	R	684300.	6646000.	1.0
G05158	R	629000.	6489800.	1.0
G02760	R	675400.	6399900.	1.0
G05253	R	594250.	6546600.	1.0
G04397	R	617800.	6378300.	1.0
G02953	R	554700.	6418200.	1.0

Element	Lab	Method	L.L.D.	#Samples
Au ppb	Amdel	234	1.0	1815

Sample	Type	Easting	Northing	Value
G05546	R	734200.	6712520.	3260.0
G03469	R	738300.	6715100.	3100.0
G05498	F3	735530.	6710880.	3000.0
G05539	R	733540.	6712030.	2500.0
G03789	R	744900.	6511150.	2180.0
G05541	R	733780.	6712230.	1880.0
G05515	R	735520.	6710960.	1600.0
G03475	R	732280.	6710720.	1110.0
G05531	R	732180.	6710300.	1060.0
G05542	R	733830.	6712310.	880.0
G05597	F3	734325.	6712000.	690.0
G03647	F2	732310.	6710630.	600.0
G05523	R	735830.	6711870.	600.0
G05487	F3	733690.	6712110.	600.0
G03763	R	735200.	6516500.	590.0
G05601	F3	740076.	6717249.	519.0
G05886	F3	734200.	6710820.	515.0
G05485	F3	733540.	6711960.	420.0
G05524	R	735950.	6711770.	400.0
G06669	F3	730500.	6707650.	365.0

Table 10: Regional Anomalies of the Central Yilgarn Area

Sample	Type	Easting	Northing	Anomaly #
G06905	LN	706700	6686950	BA 01
G03496	LP	721250	6694400	BA 02
G03487	LN	719800	6700200	BA 03
G03513	LN	713000	6708600	BA 04
G03488	LN	721600	6700600	BA 05
G03447	FF	746200	6722910	BA 06
G05356	LN	520050	6502800	DU 01
G04943	LN	766400	6635300	JA 01
G03405	LP	742200	6644700	JA 02
G03402	LN	741600	6642100	JA 03
G05236	LP	636600	6561500	KE 01
G05209	RC	638550	6525850	KE 02
G05204	LP	634850	6518200	KE 03
G05163	LP	634000	6492000	KE 04
G05149	LN	633600	6480600	KE 05
G05245	LP	601900	6538900	KE 06
G05259	LN	589850	6558900	KE 07
G03052	LN	624300	6476700	KE 09
G04983	LP	793267	6623218	KL
G03793	LN	708350	6561150	SX
G04795	LN	645100	6512500	SX 01
G03262	LN	732400	6502700	SX 02
G04830	LN	738000	6457300	SX 03

Area Codes:
BA: Barlee
JA: Jackson
DU: Kellerberrin
KE: Kellerberrin
KL: Kalgoorlie
SX: Southern Cross

Table 11: Robust Principal Components: Central Yilgarn Area
Observations: 488 Variables: 19

Robust Means

Fe203	29.78	As	34.15
Ag	.12	Sb	2.56
Mn	60.34	Mo	4.66
Cr	888.58	Sn	2.22
V	634.44	Ga	23.47
Cu	47.27	W	10.15
Pb	34.24	Nb	9.07
Zn	19.06	Se	3.47
Ni	60.34	Au	4.65
Co	9.44		

Table 11a: Robust Correlation Matrix

	Fe203	Ag	Mn	Cr	V	Cu	Pb	Zn	Ni	Co
Fe203	1.0000	.1172	.6976	.4576	.7841	.4592	-.2039	.7217	.2940	.5043
Ag	.1172	1.0000	.1058	.1357	.1136	.3924	-.1440	.1397	.2673	.2444
Mn	.6976	.1058	1.0000	.3122	.5751	.3353	-.1639	.5797	.2592	.4607
Cr	.4576	.1357	.3122	1.0000	.4744	.4446	-.1806	.3688	.6775	.4404
V	.7841	.1136	.5751	.4744	1.0000	.5190	-.1357	.5409	.2859	.5290
Cu	.4592	.3924	.3353	.4446	.5190	1.0000	-.3121	.5532	.5271	.6238
Pb	-.2039	-.1440	-.1639	-.1806	-.1357	-.3121	1.0000	-.2044	-.2133	-.2535
Zn	.7217	.1397	.5797	.3688	.5409	.5532	-.2044	1.0000	.3231	.5117
Ni	.2940	.2673	.2592	.6775	.2859	.5271	-.2133	.3231	1.0000	.5951
Co	.5043	.2444	.4607	.4404	.5290	.6238	-.2535	.5117	.5951	1.0000
As	-.1992	-.1699	-.2655	-.0241	-.1128	-.2416	.2305	-.1270	-.1168	-.2443
Sb	.0474	-.0410	.0593	.0425	.0703	.0327	.0054	.1051	.0714	.0271
Mo	-.3683	-.1900	-.3629	-.1215	-.2289	-.3941	.3836	-.3292	-.1765	-.2797
Sn	-.0963	.1193	-.0570	-.0250	-.0918	-.1372	.0280	-.1628	-.1454	-.1238
Ga	-.4203	-.1172	-.2706	-.1823	-.2743	-.3399	.0967	-.3722	-.1589	-.2952
W	.1110	-.0026	.0522	.0993	.1055	.0118	-.0407	.0324	.0389	.0409
Nb	-.4059	-.1664	-.2127	-.3546	-.3787	-.4344	.2971	-.4061	-.3568	-.3954
Se	.0245	-.0549	-.0323	.0423	.0822	-.0623	.0741	.0198	-.1121	-.1695
Au	-.1799	-.0252	-.1512	-.1091	-.1382	-.1546	.0576	-.2179	-.0673	-.1588

	As	Sb	Mo	Sn	Ga	W	Nb	Se	Au
Fe203	-.1992	.0474	-.3683	-.0963	-.4203	.1110	-.4059	.0245	-.1799
Ag	-.1699	-.0410	-.1900	.1193	-.1172	-.0026	-.1664	-.0549	-.0252
Mn	-.2655	.0593	-.3629	-.0570	-.2706	.0522	-.2127	-.0323	-.1512
Cr	-.0241	.0425	-.1215	-.0250	-.1823	.0993	-.3546	.0423	-.1091
V	-.1128	.0703	-.2289	-.0918	-.2743	.1055	-.3787	.0822	-.1382
Cu	-.2416	.0327	-.3941	-.1372	-.3399	.0118	-.4344	-.0623	-.1546
Pb	.2305	.0054	.3836	.0280	.0967	-.0407	.2971	.0741	.0576
Zn	-.1270	.1051	-.3292	-.1628	-.3722	.0324	-.4061	.0198	-.2179
Ni	-.1168	.0714	-.1765	-.1454	-.1589	.0389	-.3568	-.1121	-.0673
Co	-.2443	.0271	-.2797	-.1238	-.2952	.0409	-.3954	-.1695	-.1588
As	1.0000	.1595	.3670	-.0081	.1829	.0083	-.0065	.2520	.0437
Sb	.1595	1.0000	-.0270	-.1153	-.0632	-.0056	-.0282	.1262	-.1118
Mo	.3670	-.0270	1.0000	.0412	.1622	-.0495	.2994	.0564	.0866
Sn	-.0081	-.1153	.0412	1.0000	.4718	.0664	.2205	.0561	-.0334
Ga	.1829	-.0632	.1622	.4718	1.0000	.0056	.2498	.0721	.0754
W	.0083	-.0056	-.0495	.0664	.0056	1.0000	-.0442	-.0984	-.0514
Nb	-.0065	-.0282	.2994	.2205	.2498	-.0442	1.0000	-.0450	.0685
Se	.2520	.1262	.0564	.0561	.0721	-.0984	-.0450	1.0000	-.0285
Au	.0437	-.1118	.0866	-.0334	.0754	-.0514	.0685	-.0285	1.0000

Table 11b:

	Eigenvalues	% Trace	Cumulative Trace
1	5.5401	29.1582	29.1582
2	1.6544	8.7071	37.8654
3	1.4254	7.5020	45.3673
4	1.3840	7.2842	52.6515
5	1.1413	6.0069	58.6585
6	1.0382	5.4642	64.1227
7	1.0057	5.2934	69.4160
8	.8705	4.5817	73.9977
9	.8444	4.4444	78.4420
10	.6907	3.6352	82.0772
11	.5877	3.0933	85.1705
12	.5142	2.7063	87.8768
13	.4881	2.5687	90.4455
14	.4530	2.3841	92.8296
15	.4204	2.2125	95.0422
16	.3772	1.9854	97.0276
17	.2586	1.3612	98.3888
18	.1939	1.0205	99.4093
19	.1122	.5907	100.0000

Table 11c: Principal Component R-Scores

	1	2	3	4	5	6	7	8	9	10
Fe2O3	.8161	-.2208	-.1806	.3068	-.1042	-.1005	.0968	.0192	.0253	-.0432
Ag	.3175	.4062	.2918	-.0822	.2033	-.2071	-.2452	.5924	.2233	-.0551
Mn	.6807	-.0876	-.2389	.3836	-.1160	-.1159	-.0444	-.1456	.1600	-.0263
Cr	.6262	-.1503	.4904	-.0935	-.1952	-.0088	.0545	-.1964	-.0476	.2855
V	.7454	-.2802	-.0023	.2620	-.1378	-.1459	.0956	.0226	.0472	-.0524
Cu	.7734	.1521	.1486	-.1614	.1132	-.0578	-.1019	.1391	-.0135	-.0350
Pb	-.3914	-.3860	-.0068	.0447	-.4209	-.2813	-.3129	.2241	.1273	-.0059
Zn	.7670	-.2069	-.1463	.1388	.0323	-.0493	-.0386	.0345	-.0304	-.1858
Ni	.6189	.0886	.4864	-.3558	-.1490	.0428	-.1073	-.2176	.0443	.1707
Co	.7683	.1061	.1378	-.1074	-.1538	-.0201	-.1465	-.1053	-.0072	-.1224
As	-.3113	-.6216	.3574	-.1294	.0536	.0674	.1518	.1308	-.0559	-.3766
Sb	.0806	-.4295	.0129	-.0885	.3458	.4208	-.3366	-.1534	.5756	-.0485
Mo	-.5052	-.3656	.2352	-.1655	-.4022	-.1432	-.1666	.0612	-.1090	-.0448
Sn	-.2129	.2713	.4695	.6679	.0433	-.1031	-.0659	-.0066	.0613	-.1007
Ga	-.4861	.1445	.4951	.3780	.0866	.0303	.0769	-.2922	.0217	-.2086
W	.0928	.0282	.1166	.2419	-.3959	.6446	.3456	.3982	.1366	.1675
Nb	-.5855	.0970	-.1207	.2481	-.2320	-.0674	-.3629	-.1102	.2140	.2835
Se	-.0690	-.5211	.1841	.1973	.5096	-.2554	.1715	.1471	-.0583	.4592
Au	-.2293	.1305	-.0032	-.2704	-.1337	-.4054	.5697	-.0873	.5711	-.0425

Table 11d: Relative Contributions: Variables

	1	2	3	4	5	6	7	8	9	10
Fe2O3	76.1425	5.5710	3.7295	10.7613	1.2410	1.1541	1.0721	.0424	.0732	.2129
Ag	11.1276	18.2161	9.4019	.7461	4.5604	4.7338	6.6377	38.7355	5.5059	.3351
Mn	61.6469	1.0202	7.5944	19.5816	1.7890	1.7877	.2617	2.8218	3.4044	.0923
Cr	47.3904	2.7294	29.0624	1.0557	4.6056	.0094	.3590	4.6624	.2735	9.8522
V	73.3312	10.3604	.0007	9.0621	2.5065	2.8092	1.2055	.0676	.2946	.3622
Cu	83.4580	3.2291	3.0812	3.6336	1.7890	.4656	1.4492	2.6986	.0254	.1704
Pb	21.1318	20.5538	.0064	.2755	24.4412	10.9161	13.5049	6.9290	2.2366	.0048
Zn	82.4646	6.0019	3.0010	2.7020	.1459	.3402	.2084	.1672	.1294	4.8394
Ni	44.1306	.9044	27.2500	14.5809	2.5582	.2108	1.3263	5.4546	.2261	3.3580
Co	83.8827	1.5987	2.6983	1.6405	3.3622	.0575	3.0492	1.5761	.0073	2.1273
As	11.8154	47.0972	15.5744	2.0400	.3500	.5543	2.8074	2.0862	.3810	17.2939
Sb	.6727	19.0960	.0173	.8100	12.3766	18.3274	11.7260	2.4356	34.2951	.2433
Mo	36.5041	19.1095	7.9107	3.9175	23.1362	2.9312	3.9686	.5348	1.6999	.2874
Sn	5.5539	9.0177	27.0060	54.6503	.2298	1.3020	.5323	.0054	.4609	1.2417
Ga	29.9494	2.6478	31.0751	18.1134	.9496	.1166	.7501	10.8224	.0595	5.5160
W	.8792	.0812	1.3892	5.9817	16.0188	42.4674	12.2071	16.2034	1.9058	2.8663
Nb	45.3049	1.2446	1.9241	8.1328	7.1131	.5996	17.4052	1.6037	6.0516	10.6205
Se	.5068	28.9129	3.6085	4.1442	27.6412	6.9439	3.1321	2.3039	.3613	22.4453
Au	5.3353	1.7301	.0010	7.4208	1.8159	16.6850	32.9461	.7736	33.1088	.1833

Table 12: Robust Principal Components: Central Yilgarn Area
Observations: 379 Variables: 19

Robust Means

Fe2O3	42.95	As	53.42
Ag	.22	Sb	5.13
Mn	102.00	Mo	2.97
Cr	2531.57	Sn	3.47
V	838.09	Ga	17.56
Cu	112.00	W	11.81
Pb	19.59	Nb	5.39
Zn	32.74	Se	3.61
Ni	131.74	Au	10.54
Co	12.77		

Table 12a: Robust Correlation Matrix

	Fe2O3	Ag	Mn	Cr	V	Cu	Pb	Zn	Ni	Co
Fe2O3	1.0000	-.1330	.4543	.1561	.4045	-.0453	.0146	.1919	-.0768	.0713
Ag	-.1330	1.0000	-.0973	.0631	.0662	.2172	.0250	.0257	.1585	.0815
Mn	.4543	-.0973	1.0000	.0880	.1769	.1238	-.1323	.3008	.0734	.3365
Cr	.1561	.0631	.0880	1.0000	.1282	.0261	.0203	-.0313	.6940	.3297
V	.4045	.0662	.1769	.1282	1.0000	.0060	.1304	.0540	-.0840	-.0974
Cu	-.0453	.2172	.1238	.0261	.0060	1.0000	-.2860	.4899	.3738	.4864
Pb	.0146	.0250	-.1323	.0203	.1304	-.2860	1.0000	-.0878	-.1352	-.2180
Zn	.1919	.0257	.3008	-.0313	.0540	.4899	-.0878	1.0000	.1301	.1914
Ni	-.0768	.1585	.0734	.6940	-.0840	.3738	-.1352	.1301	1.0000	.6407
Co	.0713	.0815	.3365	.3297	-.0974	.4864	-.2180	.1914	.6407	1.0000
As	-.0066	-.0520	-.0311	.0771	.0796	-.0720	.3215	.1392	-.0038	-.1447
Sb	.1151	.0079	-.0174	.0358	.2289	-.0304	.2431	.1793	-.0912	-.1455
Mo	-.2515	-.1656	-.2014	-.0425	-.0808	-.3995	.3773	-.1516	-.2463	-.2835
Sn	-.0041	.1157	-.0225	-.0668	.1107	-.1691	.1616	.0522	-.2086	-.2123
Ga	-.2130	.1187	-.1068	-.1064	-.0085	-.2268	.1231	-.0274	-.1859	-.2344
W	.2112	-.1140	.0345	-.0427	-.0952	-.1473	.0810	-.0971	-.0694	-.0428
Nb	-.1247	-.0904	-.0078	-.0678	-.0361	-.3807	.1662	-.1409	-.2272	-.2207
Se	.0338	-.0658	.0018	-.0404	.0607	-.0169	-.0063	.0643	-.0375	-.1284
Au	.0025	-.0859	-.0442	.2193	-.1154	.1560	-.1665	-.0579	.2910	.1813

	As	Sb	Mo	Sn	Ga	W	Nb	Se	Au
Fe2O3	-.0066	.1151	-.2515	-.0041	-.2130	.2112	-.1247	.0338	.0025
Ag	-.0520	.0079	-.1656	.1157	.1187	-.1140	-.0904	-.0658	-.0859
Mn	-.0311	-.0174	-.2014	-.0225	-.1068	.0345	-.0078	.0018	-.0442
Cr	.0771	.0358	-.0425	-.0668	-.1064	-.0427	-.0678	-.0404	.2193
V	.0796	.2289	-.0808	.1107	-.0085	-.0952	-.0361	.0607	-.1154
Cu	-.0720	-.0304	-.3995	-.1691	-.2268	-.1473	-.3807	-.0169	.1560
Pb	.3215	.2431	.3773	.1616	.1231	.0810	.1662	-.0063	-.1665
Zn	.1392	.1793	-.1516	.0522	-.0274	-.0971	-.1409	.0643	-.0579
Ni	-.0038	-.0912	-.2463	-.2086	-.1859	-.0694	-.2272	-.0375	.2910
Co	-.1447	-.1455	-.2835	-.2123	-.2344	-.0428	-.2207	-.1284	.1813
As	1.0000	.5171	.1907	.0890	.0715	.0163	.1010	.0060	.1302
Sb	.5171	1.0000	.1390	.0693	.1046	-.0545	.0107	.0261	-.1024
Mo	.1907	.1390	1.0000	.2110	.2799	.0366	.3978	.1020	-.1487
Sn	.0890	.0693	.2110	1.0000	.2326	.0242	.3362	-.0168	-.1760
Ga	.0715	.1046	.2799	.2326	1.0000	.0554	.3670	-.0618	-.2150
W	.0163	-.0545	.0366	.0242	.0554	1.0000	.1460	-.0763	.0042
Nb	.1010	.0107	.3978	.3362	.3670	.1460	1.0000	-.0560	-.1549
Se	.0060	.0261	.1020	-.0168	-.0618	-.0763	-.0560	1.0000	.0644
Au	.1302	-.1024	-.1487	-.1760	-.2150	.0042	-.1549	.0644	1.0000

Table 12b:

	Eigenvalues	% Trace	Cumulative Trace
1	3.5231	18.5426	18.5426
2	2.0615	10.8498	29.3924
3	1.7743	9.3383	38.7308
4	1.5699	8.2627	46.9935
5	1.4247	7.4982	54.4916
6	1.2126	6.3819	60.8735
7	1.0723	5.6438	66.5173
8	.9062	4.7697	71.2869
9	.8581	4.5164	75.8033
10	.7751	4.0794	79.8827
11	.6388	3.3621	83.2449
12	.6017	3.1671	86.4120
13	.5475	2.8815	89.2935
14	.4777	2.5145	91.8079
15	.4544	2.3913	94.1993
16	.4054	2.1339	96.3332
17	.3088	1.6252	97.9584
18	.2511	1.3214	99.2798
19	.1368	.7202	100.0000

Table 12c: Principal Component R-Scores

	1	2	3	4	5	6	7	8	9	10
Fe203	.1973	.6476	-.4148	-.3812	.0692	-.1281	-.0609	.1006	.0330	.0064
Ag	.1309	-.0492	.2170	.5109	.3018	-.4521	-.1610	.2961	.2057	.0524
Mn	.3315	.4778	-.3448	-.1655	.3273	.2538	.1763	-.1561	-.0729	.0316
Cr	.3934	.1836	.5804	-.4054	.2330	-.2409	.1728	-.0258	-.0300	.0776
V	-.0145	.6202	-.1345	-.0027	.0403	-.5335	.1046	.0245	-.1506	.0713
Cu	.6870	.0451	.0148	.4887	-.0318	.1867	-.0522	.0859	.0950	-.0705
Pb	-.4634	.3129	.3461	-.0833	-.0417	-.1320	-.1446	-.1905	.4240	-.2921
Zn	.3274	.4579	-.0819	.4642	.0332	.4579	.1107	.0257	.1054	-.0531
Ni	.6890	-.0453	.5737	-.1409	.2012	-.0185	.1009	-.0178	.0974	.0564
Co	.7357	-.0066	.1894	-.0623	.3056	.1936	.0250	-.1836	.0950	-.0547
As	-.2252	.4879	.4985	.0382	-.3204	.2638	-.1996	.1147	-.1449	-.0184
Sb	-.2130	.6122	.3107	.2094	-.2831	.0551	-.1921	-.0795	-.0953	.2165
Mo	-.6408	-.0258	.3209	-.1046	.0031	.1961	.2759	-.2182	.1614	-.0872
Sn	-.4110	.1969	.0372	.1989	.4139	-.0126	.1878	.3914	-.1162	-.4878
Ga	-.4884	-.0312	.1629	.2501	.3996	.1072	.0375	.0891	-.0976	.5480
W	-.1421	.0357	-.1478	-.4509	.2002	.2759	-.4396	.3906	.4415	.1518
Nb	-.5710	-.0097	.1108	-.1442	.4426	.2595	.1854	.0738	-.1882	.0075
Se	-.0377	.0840	-.0754	.0048	-.4014	-.0194	.7115	.2809	.3968	.1947
Au	.3616	-.1401	.2716	-.3231	-.3421	.1355	.0264	.4893	-.3170	-.0825

Table 12: Relative Contributions: Variables

	1	2	3	4	5	6	7	8	9	10
Fe203	4.7959	51.6571	21.1970	17.8962	.5895	2.0224	.4571	1.2455	.1343	.0050
Ag	2.1930	.3096	6.0221	33.3850	11.6535	26.1439	3.3159	11.2148	5.4111	.3511
Mn	15.3154	31.8045	16.5635	3.8159	14.9228	8.9718	4.3313	3.3943	.7409	.1395
Cr	18.4355	4.0159	40.1307	19.5795	6.4680	6.9097	3.5569	.0792	.1069	.7177
V	.0290	52.7978	2.4835	.0010	.2226	39.0704	1.5030	.0825	3.1132	.6968
Cu	61.0579	.2630	.0284	30.8944	.1307	4.5087	.3526	.9542	1.1675	.6426
Pb	27.5018	12.5399	15.3442	.8890	.2228	2.2304	2.6761	4.6465	23.0243	10.9252
Zn	13.7972	27.0003	.8634	27.7445	.1421	26.9975	1.5772	.0849	1.4301	.3630
Ni	53.3544	.2306	36.9919	2.2323	4.5482	.0383	1.1438	.0358	1.0671	.3576
Co	71.3786	.0058	4.7296	.5117	12.3193	4.9416	.0827	4.4447	1.1907	.3953
As	6.4567	30.3123	31.6497	.1854	13.0729	8.8605	5.0707	1.6754	2.6731	.0433
Sb	6.1072	50.4479	12.9952	5.9013	10.7906	.4088	4.9659	.8501	1.2234	6.3096
Mo	56.9425	.0925	14.2822	1.5162	.0013	5.3335	10.5568	6.6058	3.6139	1.0552
Sn	19.6400	4.5071	.1606	4.6014	19.9235	.0185	4.1003	17.8097	1.5703	27.6687
Ga	29.1237	.1186	3.2385	7.6376	19.4983	1.4046	.1718	.9691	1.1621	36.6756
W	2.1792	.1377	2.3569	21.9438	4.3267	8.2177	20.8579	16.4619	21.0320	2.4861
Nb	46.7241	.0136	1.7597	2.9807	28.0808	9.6507	4.9277	.7807	5.0741	.0080
Se	.1484	.7383	.5945	.0024	16.8506	.0393	52.9451	8.2493	16.4659	3.9662
Au	16.1136	2.4199	9.0902	12.8688	14.4227	2.2636	.0856	29.5088	12.3875	.8394

Table 13a: Central Yilgarn Laterites
"R" Samples

CHI-6*X Indices > 90th percentile rankings

G03774	LN	R	739750.	6512600.	2509.9
G03499	LN	R	706300.	6686400.	2422.5
G03777	LN	R	743350.	6507900.	2372.0
G03782	MS	R	743000.	6505550.	1069.1
G03491	MS	R	722100.	6697200.	994.9
G03809	LN	R	749550.	6407600.	891.9
G03763	LN	R	735200.	6516500.	888.6
G03773	LP	R	739300.	6514500.	880.5
G05578	LN	R	739950.	6707125.	859.2
G03487	LN	R	719800.	6700200.	803.3
G04921	LN	R	779500.	6636400.	773.9
G03761	LN	R	734150.	6515750.	728.2
G03364	LN	R	753800.	6646500.	691.4
G05575	LN	R	738890.	6705340.	666.7
G03759	LN	R	736700.	6513300.	636.2
G03696	MS	R	734850.	6699950.	632.6
G03771	LN	R	737100.	6516150.	613.8
G03783	LP	R	743000.	6504500.	590.2
G05579	LN	R	740050.	6707375.	562.2
G03752	LN	R	669100.	6537150.	549.8
G03502	LN	R	706400.	6694100.	538.7
G03760	LN	R	735700.	6514000.	527.7
G05574	MS	R	739050.	6705800.	508.1
G06927	LP	R	735700.	6696250.	507.2
G03799	LN	R	705500.	6554650.	494.7
G03515	LN	R	729600.	6717000.	492.1
G03762	LN	R	736150.	6516500.	489.0
G05154	LP	R	633950.	6485000.	474.7
G03473	LN	R	730770.	6708580.	463.4
G08137	LN	R	768450.	6637600.	456.3
G03797	LP	R	708100.	6555100.	455.2
G04941	CN	R	757900.	6633400.	449.1
G05577	LN	R	739370.	6705625.	448.9
G08133	PN	R	769350.	6635700.	448.7
G05149	LN	R	633600.	6480600.	446.2
G03789	LN	R	744900.	6511150.	431.0
G08074	LN	R	771490.	6636150.	430.6
G03770	LN	R	737050.	6520100.	427.7
G03448	LP	R	745680.	6722040.	422.9
G05571	LP	R	739850.	6706900.	422.3
G03689	LN	R	728007.	6692610.	420.0
G03907	LP	R	710000.	6710500.	417.0
G03383	LN	R	745800.	6650000.	416.9
G03469	LN	R	738300.	6715100.	414.7
G08143	LN	R	765400.	6636050.	411.7
G08030	LN	R	771350.	6631850.	409.7
G08027	LN	R	770100.	6629650.	407.2
G08141	LN	R	766000.	6637000.	405.0
G04969	LP	R	797713.	6612666.	403.4
G03510	LN	R	708000.	6702300.	401.4

Table 13b: Central Yilgarn Laterites
"R" Samples

PEG-4 Indices > 90th percentile rankings

G03499	LN	R	706300.	6686400.	274.7
G03777	LN	R	743350.	6507900.	204.6
G03491	MS	R	722100.	6697200.	159.3
G03502	LN	R	706400.	6694100.	130.8
G03774	LN	R	739750.	6512600.	119.9
G03782	MS	R	743000.	6505550.	103.5
G03487	LN	R	719800.	6700200.	98.2
G03364	LN	R	753800.	6646500.	90.9
G03763	LN	R	735200.	6516500.	75.7
G05579	LN	R	740050.	6707375.	63.2
G04921	LN	R	779500.	6636400.	62.4
G03752	LN	R	669100.	6537150.	60.7
G03448	LP	R	745680.	6722040.	60.0
G05236	LP	R	636600.	6561500.	57.3
G03522	LN	R	715700.	6649900.	56.3
G03501	LN	R	706100.	6696900.	56.3
G05578	LN	R	739950.	6707125.	53.2
G08133	PN	R	769350.	6635700.	51.0
G03761	LN	R	734150.	6515750.	50.8
G04971	LN	R	796233.	6609340.	50.4
G08137	LN	R	768450.	6637600.	50.1
G03783	LP	R	743000.	6504500.	49.1
G03917	LN	R	710800.	6651300.	47.1
G03518	LN	R	717800.	6641000.	46.1
G03771	LN	R	737100.	6516150.	44.5
G04941	CN	R	757900.	6633400.	43.6
G04951	LN	R	766300.	6638000.	42.8
G05571	LP	R	739850.	6706900.	41.8
G03402	LN	R	741600.	6642100.	41.4
G08141	LN	R	766000.	6637000.	40.3
G03759	LN	R	736700.	6513300.	40.2
G04965	LN	R	798083.	6602730.	39.5
G03799	LN	R	705500.	6554650.	39.0
G03419	MS	R	731100.	6642600.	39.0
G03383	LN	R	745800.	6650000.	38.1
G03760	LN	R	735700.	6514000.	37.1
G05154	LP	R	633950.	6485000.	37.0
G03463	LP	R	735000.	6720100.	36.7
G03473	LN	R	730770.	6708580.	36.2
G03809	LN	R	749550.	6407600.	36.0
G03773	LP	R	739300.	6514500.	34.8
G03510	LN	R	708000.	6702300.	34.6
G03696	MS	R	734850.	6699950.	34.4
G03907	LP	R	710000.	6710500.	34.0
G03689	LN	R	728007.	6692610.	33.9
G04967	CN	R	796642.	6607615.	33.6
G03762	LN	R	736150.	6516500.	33.0
G03909	LP	R	711100.	6712600.	32.6
G08029	PN	R	771300.	6630900.	32.5
G03380	LN	R	753500.	6644600.	32.5

Table 13c: Central Yilgarn Laterites
"R" Samples

NUMCHI Indices > 3 Anomalous Elements

G04951	LN	R	766300.	6638000.	5.0
G03777	LN	R	743350.	6507900.	5.0
G05578	LN	R	739950.	6707125.	5.0
G03809	LN	R	749550.	6407600.	5.0
G08022	LN	R	769000.	6629400.	4.0
G08027	LN	R	770100.	6629650.	4.0
G03491	MS	R	722100.	6697200.	4.0
G03470	LN	R	738440.	6711370.	4.0
G03759	LN	R	736700.	6513300.	4.0
G03771	LN	R	737100.	6516150.	4.0
G03797	LP	R	708100.	6555100.	4.0
G03513	LN	R	713000.	6708600.	3.0
G04950	LN	R	770200.	6638000.	3.0
G04969	LP	R	797713.	6612666.	3.0
G04975	LN	R	791570.	6615798.	3.0
G03696	MS	R	734850.	6699950.	3.0
G03487	LN	R	719800.	6700200.	3.0
G08028	LN	R	771250.	6629850.	3.0
G08039	PN	R	767950.	6632050.	3.0
G03364	LN	R	753800.	6646500.	3.0
G08133	PN	R	769350.	6635700.	3.0
G08141	LN	R	766000.	6637000.	3.0
G08145	LN	R	767000.	6629900.	3.0
G03448	LP	R	745680.	6722040.	3.0
G03402	LN	R	741600.	6642100.	3.0
G05236	LP	R	636600.	6561500.	3.0
G03300	LN	R	741350.	6471150.	3.0
G03746	LN	R	660000.	6532000.	3.0
G03752	LN	R	669100.	6537150.	3.0
G03762	LN	R	736150.	6516500.	3.0
G03764	LN	R	734100.	6518800.	3.0
G03770	LN	R	737050.	6520100.	3.0
G03774	LN	R	739750.	6512600.	3.0
G03502	LN	R	706400.	6694100.	3.0
G03789	LN	R	744900.	6511150.	3.0
G05571	LP	R	739850.	6706900.	3.0
G03794	LN	R	716050.	6554650.	3.0
G05575	LN	R	738890.	6705340.	3.0
G03473	LN	R	730770.	6708580.	3.0
G03927	LN	R	684300.	6646000.	3.0
G04905	LN	R	773900.	6634300.	3.0
G04906	LN	R	775200.	6632300.	3.0

Table 14a: Central Yilgarn Laterites

"R" Regional Samples

Component 4

Ordered Principal Component Scores
< 5 percentile & >95 percentile ranking

G03469	LN	738300.	6715100.	-6.0220
G03789	LN	744900.	6511150.	-4.4388
G03475	LP	732280.	6710720.	-2.4904
G03763	LN	735200.	6516500.	-1.4125
G03491	MS	722100.	6697200.	-1.1578
G03803	LN	756800.	6410000.	-.9883
G04968	LN	797485.	6610274.	-.8713
G03499	LN	706300.	6686400.	-.8110
G03315	LN	744300.	6633000.	-.5991
G03046	LN	625400.	6489700.	-.5516
G03459	LN	736000.	6717100.	-.4849
G03364	LN	753800.	6646500.	-.4584
G03470	LN	738440.	6711370.	-.4447
G03762	LN	736150.	6516500.	-.4446
G03502	LN	706400.	6694100.	-.4002
G04901	LN	768000.	6634600.	-.4002
G08135	MS	767450.	6634800.	-.3873
G03477	LN	732730.	6713110.	-.3852
G04988	LN	703300.	6739100.	-.3661
G08049	VL	768450.	6633300.	-.3657
G03487	LN	719800.	6700200.	-.3645
G04951	LN	766300.	6638000.	-.3598
G03756	LN	666450.	6533600.	-.3559
G03777	LN	743350.	6507900.	-.3414
G03383	LN	745800.	6650000.	.1914
G03463	LP	735000.	6720100.	.2053
G03518	LN	717800.	6641000.	.2077
G04981	LN	791043.	6620933.	.2119
G05574	MS	739050.	6705800.	.2155
G04941	CN	757900.	6633400.	.2195
G03794	LN	716050.	6554650.	.2248
G03446	LP	746600.	6724200.	.2313
G03370	LN	743500.	6635400.	.2443
G08133	PN	769350.	6635700.	.2496
G03696	MS	734850.	6699950.	.2633
G08039	PN	767950.	6632050.	.2718
G04970	LP	796414.	6612735.	.2854
G05154	LP	633950.	6485000.	.3158
G08050	PN	768450.	6632800.	.3168
G03809	LN	749550.	6407600.	.3210
G03425	LN	729800.	6641100.	.3501
G03752	LN	669100.	6537150.	.3520
G08074	LN	771490.	6636150.	.4797
G03515	LN	729600.	6717000.	.5557
G05236	LP	636600.	6561500.	.5666
G03781	MS	744300.	6505500.	.9044
G03319	LN	746500.	6639300.	1.7410
G03774	LN	739750.	6512600.	3.2384

Table 14b: Central Yilgarn Laterites

"R" Regional Samples

Component 6

Ordered Principal Component Scores
< 5 percentile & >95 percentile ranking

G03469	LN	738300.	6715100.	-9.9713
G03789	LN	744900.	6511150.	-7.8225
G03475	LP	732280.	6710720.	-3.8900
G03763	LN	735200.	6516500.	-2.0434
G03781	MS	744300.	6505500.	-1.3995
G03046	LN	625400.	6489700.	-.9064
G04901	LN	768000.	6634600.	-.6554
G04975	LN	791570.	6615798.	-.5287
G04988	LN	703300.	6739100.	-.4332
G03779	MS	744250.	6506500.	-.3566
G03448	LP	745680.	6722040.	-.3562
G04956	LN	769900.	6639100.	-.3143
G04949	LN	773000.	6636600.	-.2955
G03319	LN	746500.	6639300.	-.2823
G03359	LN	750900.	6636600.	-.2576
G03792	LP	717650.	6558800.	-.2423
G03764	LN	734100.	6518800.	-.2302
G08017	LN	769300.	6632950.	-.2258
G05236	LP	636600.	6561500.	-.2123
G03470	LN	738440.	6711370.	-.1769
G03790	PN	712800.	6556400.	-.1672
G04995	LN	711800.	6746800.	-.1664
G04902	LN	769000.	6632000.	-.1527
G04906	LN	775200.	6632300.	-.1488
G04953	LN	761800.	6637200.	.4491
G08028	LN	771250.	6629850.	.4571
G08133	PN	769350.	6635700.	.4697
G08020	LN	769250.	6630750.	.4704
G03487	LN	719800.	6700200.	.4747
G03777	LN	743350.	6507900.	.4768
G04921	LN	779500.	6636400.	.4872
G08141	LN	766000.	6637000.	.5335
G08039	PN	767950.	6632050.	.5362
G03696	MS	734850.	6699950.	.6093
G03761	LN	734150.	6515750.	.6311
G03522	LN	715700.	6649900.	.6605
G08143	LN	765400.	6636050.	.7185
G05574	MS	739050.	6705800.	.7450
G04970	LP	796414.	6612735.	.7626
G03809	LN	749550.	6407600.	.8297
G03771	LN	737100.	6516150.	.8391
G08074	LN	771490.	6636150.	.9220
G05154	LP	633950.	6485000.	.9688
G05575	LN	738890.	6705340.	1.1494
G03502	LN	706400.	6694100.	1.1684
G03499	LN	706300.	6686400.	1.2040
G03515	LN	729600.	6717000.	1.3123
G03774	LN	739750.	6512600.	10.1453

Table 14c: Central Yilgarn Laterites

"R" Regional Samples

Component 7

Ordered Principal Component Scores
< 5 percentile & >95 percentile ranking

G03502	LN	706400.	6694100.	-1.1610
G04975	LN	791570.	6615798.	-.6043
G04968	LN	797485.	6610274.	-.5709
G04949	LN	773000.	6636600.	-.3575
G03803	LN	756800.	6410000.	-.3541
G04956	LN	769900.	6639100.	-.3491
G03359	LN	750900.	6636600.	-.3307
G03402	LN	741600.	6642100.	-.3109
G04951	LN	766300.	6638000.	-.2889
G03501	LN	706100.	6696900.	-.2872
G04950	LN	770200.	6638000.	-.2725
G03315	LN	744300.	6633000.	-.2693
G05236	LP	636600.	6561500.	-.2275
G03917	LN	710800.	6651300.	-.2234
G04965	LN	798083.	6602730.	-.2109
G03493	LN	723900.	6693300.	.2606
G03452	LN	743800.	6722800.	.2758
G03782	MS	743000.	6505550.	.2811
G03771	LN	737100.	6516150.	.2869
G03809	LN	749550.	6407600.	.2975
G05578	LN	739950.	6707125.	.3086
G03696	MS	734850.	6699950.	.3118
G03764	LN	734100.	6518800.	.3332
G03792	LP	717650.	6558800.	.3377
G03364	LN	753800.	6646500.	.3817
G04970	LP	796414.	6612735.	.4053
G04921	LN	779500.	6636400.	.4077
G05575	LN	738890.	6705340.	.4116
G05574	MS	739050.	6705800.	.4138
G08074	LN	771490.	6636150.	.4164
G08143	LN	765400.	6636050.	.4299
G03761	LN	734150.	6515750.	.5069
G04988	LN	703300.	6739100.	.5582
G03777	LN	743350.	6507900.	.5822
G05154	LP	633950.	6485000.	.5970
G03779	MS	744250.	6506500.	.6018
G03448	LP	745680.	6722040.	.6092
G03515	LN	729600.	6717000.	.6551
G03491	MS	722100.	6697200.	.6926
G04901	LN	768000.	6634600.	.8160
G03781	MS	744300.	6505500.	1.1087
G03046	LN	625400.	6489700.	1.2608
G03473	LN	730770.	6708580.	1.2670
G03763	LN	735200.	6516500.	3.0280
G03774	LN	739750.	6512600.	5.6825
G03475	LP	732280.	6710720.	5.6918
G03789	LN	744900.	6511150.	10.9728
G03469	LN	738300.	6715100.	16.2751

Table 14d: Central Yilgarn Laterites

"R" Regional Samples

Component 8

Ordered Principal Component Scores
>90 percentile ranking

G08145	LN	767000.	6629900.	.2092
G03493	LN	723900.	6693300.	.2098
G03782	MS	743000.	6505550.	.2180
G03383	LN	745800.	6650000.	.2190
G03262	LN	732400.	6502700.	.2200
G05578	LN	739950.	6707125.	.2226
G08030	LN	771350.	6631850.	.2357
G04861	LN	765350.	6461050.	.2365
G03422	LN	730000.	6648200.	.2367
G04969	LP	797713.	6612666.	.2389
G03436	MS	725500.	6645000.	.2515
G03367	LP	739400.	6640000.	.2729
G08133	PN	769350.	6635700.	.2745
G03424	LN	729800.	6643600.	.2769
G03760	LN	735700.	6514000.	.2821
G04872	LN	752100.	6628300.	.2881
G08020	LN	769250.	6630750.	.2903
G04951	LN	766300.	6638000.	.2953
G08028	LN	771250.	6629850.	.3114
G03521	LN	715300.	6646300.	.3135
G04943	LN	766400.	6635300.	.3155
G04906	LN	775200.	6632300.	.3219
G08039	PN	767950.	6632050.	.3269
G05575	LN	738890.	6705340.	.3358
G08072	LN	772950.	6636650.	.3486
G08143	LN	765400.	6636050.	.3507
G08027	LN	770100.	6629650.	.3511
G03696	MS	734850.	6699950.	.3589
G04950	LN	770200.	6638000.	.3768
G08017	LN	769300.	6632950.	.3904
G04921	LN	779500.	6636400.	.3904
G05574	MS	739050.	6705800.	.4999
G04905	LN	773900.	6634300.	.5112
G04970	LP	796414.	6612735.	.5218
G04953	LN	761800.	6637200.	.5667
G03759	LN	736700.	6513300.	.5695
G03473	LN	730770.	6708580.	.5794
G05154	LP	633950.	6485000.	.6370
G03761	LN	734150.	6515750.	.6455
G03777	LN	743350.	6507900.	.6536
G03515	LN	729600.	6717000.	.7637
G03809	LN	749550.	6407600.	.8293
G03359	LN	750900.	6636600.	.8688
G04949	LN	773000.	6636600.	.8920
G04956	LN	769900.	6639100.	.9027
G08074	LN	771490.	6636150.	1.0852
G04975	LN	791570.	6615798.	1.2572
G03774	LN	739750.	6512600.	7.0258

Table 14e: Central Yilgarn Laterites

"R" Regional Samples

Component 9

Ordered Principal Component Scores
>90 percentile ranking

G08032	LN	771400.	6633700.	.2489
G08050	PN	768450.	6632800.	.2584
G04951	LN	766300.	6638000.	.2599
G08020	LN	769250.	6630750.	.2673
G04980	LN	790201.	6620177.	.2688
G03809	LN	749550.	6407600.	.2689
G08137	LN	768450.	6637600.	.2699
G05575	LN	738890.	6705340.	.2721
G04950	LN	770200.	6638000.	.2792
G03764	LN	734100.	6518800.	.2852
G03792	LP	717650.	6558800.	.2857
G03359	LN	750900.	6636600.	.2899
G03771	LN	737100.	6516150.	.2936
G03761	LN	734150.	6515750.	.3070
G03470	LN	738440.	6711370.	.3083
G04949	LN	773000.	6636600.	.3133
G05154	LP	633950.	6485000.	.3201
G08039	PN	767950.	6632050.	.3266
G04956	LN	769900.	6639100.	.3277
G04965	LN	798083.	6602730.	.3810
G03402	LN	741600.	6642100.	.3956
G03515	LN	729600.	6717000.	.3982
G04968	LN	797485.	6610274.	.3983
G08141	LN	766000.	6637000.	.4517
G03917	LN	710800.	6651300.	.4629
G04967	CN	796642.	6607615.	.4740
G03487	LN	719800.	6700200.	.5183
G04975	LN	791570.	6615798.	.5365
G08074	LN	771490.	6636150.	.5665
G03501	LN	706100.	6696900.	.5719
G04988	LN	703300.	6739100.	.6376
G03522	LN	715700.	6649900.	.7047
G03779	MS	744250.	6506500.	.7412
G03448	LP	745680.	6722040.	.9023
G04901	LN	768000.	6634600.	.9365
G03499	LN	706300.	6686400.	.9486
G03319	LN	746500.	6639300.	1.0514
G03364	LN	753800.	6646500.	1.1318
G03473	LN	730770.	6708580.	1.2361
G03046	LN	625400.	6489700.	1.3640
G03781	MS	744300.	6505500.	2.1347
G03502	LN	706400.	6694100.	2.1555
G03774	LN	739750.	6512600.	2.4815
G03491	MS	722100.	6697200.	3.3423
G03763	LN	735200.	6516500.	3.3847
G03475	LP	732280.	6710720.	6.0869
G03789	LN	744900.	6511150.	12.1718
G03469	LN	738300.	6715100.	17.4644

Table 15: χ^2 Anomalous Samples for the Multi-element Group Cu Zn Pb As Sb Bi Mo Ag Sn W Se Ga Nb Ta "R" Samples Laterites

Sample/Type		Easting	Northing	Expected χ^2	Observed χ^2 (Mahalanobis Distance)
G04929 LN	R	777600.	6645400.	22.38	103.98
G04967 CN	R	796642.	6607615.	22.42	105.58
G04968 LN	R	797485.	6610274.	22.46	105.67
G05245 LP	R	601900.	6538900.	22.50	106.86
G04933 LN	R	755400.	6627300.	22.54	108.02
G02887 LP	R	576100.	6369400.	22.58	108.41
G02890 PN	R	570000.	6368300.	22.62	108.74
G02880 LP	R	573800.	6365900.	22.66	109.37
G04564 LN	R	539300.	6430850.	22.70	109.87
G04566 LN	R	540900.	6428400.	22.74	111.59
G04971 LN	R	796233.	6609340.	22.78	111.78
G03449 LN	R	745500.	6720100.	22.82	114.04
G02895 LN	R	584400.	6375800.	22.87	114.09
G03789 LN	R	744900.	6511150.	22.91	117.25
G03759 LN	R	736700.	6513300.	22.95	119.01
G03473 LN	R	730770.	6708580.	22.99	119.83
G04562 LN	R	541400.	6439000.	23.04	120.55
G03470 LN	R	738440.	6711370.	23.08	122.71
G04547 LN	R	605850.	6419700.	23.13	123.53
G04480 LN	R	627300.	6402200.	23.17	132.20
G05154 LP	R	633950.	6485000.	23.22	132.62
G08022 LN	R	769000.	6629400.	23.27	132.74
G04909 LN	R	780200.	6632000.	23.31	137.80
G03463 LP	R	735000.	6720100.	23.36	138.31
G03448 LP	R	745680.	6722040.	23.41	143.21
G05579 LN	R	740050.	6707375.	23.46	146.28
G03761 LN	R	734150.	6515750.	23.51	146.32
G04919 LN	R	787000.	6631300.	23.56	149.96
G05320 LP	R	528450.	6498000.	23.61	150.44
G08137 LN	R	768450.	6637600.	23.66	153.58
G08032 LN	R	771400.	6633700.	23.71	156.46
G04906 LN	R	775200.	6632300.	23.76	157.76
G08072 LN	R	772950.	6636650.	23.82	159.22
G08039 PN	R	767950.	6632050.	23.87	159.84
G05578 LN	R	739950.	6707125.	23.93	161.89
G08141 LN	R	766000.	6637000.	23.98	167.16
G04938 LN	R	752900.	6630200.	24.04	173.13
G04926 LN	R	776800.	6643100.	24.09	176.77
G04930 LN	R	777500.	6648300.	24.15	179.03
G02768 LP	R	678500.	6389700.	24.21	195.00
G05346 LP	R	597700.	6546900.	24.27	195.86
G03783 LP	R	743000.	6504500.	24.33	197.46
G03696 MS	R	734850.	6699950.	24.39	200.70
G03469 LN	R	738300.	6715100.	24.45	225.85
G03515 LN	R	729600.	6717000.	24.52	234.41
G04950 LN	R	770200.	6638000.	24.58	238.83
G03402 LN	R	741600.	6642100.	24.65	246.81
G08017 LN	R	769300.	6632950.	24.71	257.44
G03917 LN	R	710800.	6651300.	24.78	258.80
G04958 LN	R	766300.	6638600.	24.85	262.43
G04951 LN	R	766300.	6638000.	24.92	298.08
G02791 LP	R	699117.	6442807.	24.99	298.73
G04921 LN	R	779500.	6636400.	25.07	311.43
G08073 LN	R	774000.	6637250.	25.14	331.51
G08074 LN	R	771490.	6636150.	25.22	352.62
G04582 LP	R	524000.	6472000.	25.29	375.59
G03501 LN	R	706100.	6696900.	25.37	380.31
G05575 LN	R	738890.	6705340.	25.45	420.00
G03522 LN	R	715700.	6649900.	25.53	426.79
G04524 LN	R	595800.	6434500.	25.62	428.91
G02876 LP	R	592400.	6360900.	25.70	429.69
G04530 LN	R	622150.	6429300.	25.79	439.46
G03489 LN	R	720400.	6698500.	25.88	448.11
G03453 LN	R	742000.	6724200.	25.98	451.96
G08145 LN	R	767000.	6629900.	26.07	452.25
G08021 LN	R	769250.	6629850.	26.17	458.24
G05571 LP	R	739850.	6706900.	26.27	462.92
G04995 LN	R	711800.	6746800.	26.37	463.62
G03422 LN	R	730000.	6648200.	26.48	593.33
G03364 LN	R	753800.	6646500.	26.59	617.79
G03763 LN	R	735200.	6516500.	26.70	627.15
G04513 LN	R	613000.	6439600.	26.81	654.47
G03487 LN	R	719800.	6700200.	26.93	681.30
G04563 LP	R	541850.	6445850.	27.06	965.64

Table 15: (cont'd)
χ^2 Anomalous Samples for the Multi-element
Group Cu Zn Pb As Sb Bi Mo Ag Sn W Se Ga Nb Ta
"R" Samples Laterites

Sample/Type		Easting	Northing	Expected χ^2	Observed χ^2 (Mahalanobis Distance)
G04956 LN	R	769900.	6639100.	28.24	1079.47
G03493 LN	R	723900.	6693300.	27.19	969.03
G04548 LP	R	609800.	6421000.	27.32	974.97
G03482 LN	R	729600.	6710300.	27.46	979.07
G03809 LN	R	749550.	6407600.	27.60	984.59
G04949 LN	R	773000.	6636600.	27.75	1038.60
G03782 MS	R	743000.	6505550.	27.91	1042.31
G03359 LN	R	750900.	6636600.	28.07	1046.14
G04918 CN	R	782200.	6631200.	28.42	1197.76
G02881 LP	R	575300.	6361700.	28.61	1740.23
G03910 PN	R	704600.	6713900.	28.81	1743.00
G03446 LP	R	746600.	6724200.	29.03	1745.42
G04945 LN	R	760500.	6635300.	29.26	1747.51
G08035 VL	R	767950.	6634550.	29.50	1748.97
G04441 LP	R	594500.	6390200.	29.77	1758.97
G03317 LP	R	741200.	6635600.	30.06	1783.21
G04943 LN	R	766400.	6635300.	30.37	1924.09
G04975 LN	R	791570.	6615798.	30.72	2555.27
G04483 LN	R	625500.	6379000.	31.11	2748.65
G03491 MS	R	722100.	6697200.	31.55	3053.68
G03773 LP	R	739300.	6514500.	32.06	3142.69
G04560 PN	R	544350.	6443950.	32.67	3931.55
G03502 LN	R	706400.	6694100.	33.43	4538.51
G03777 LN	R	743350.	6507900.	34.43	4995.76
G03499 LN	R	706300.	6686400.	35.93	6952.51
G03774 LN	R	739750.	6512600.	39.06	13874.75

Figure 1 in back pocket.

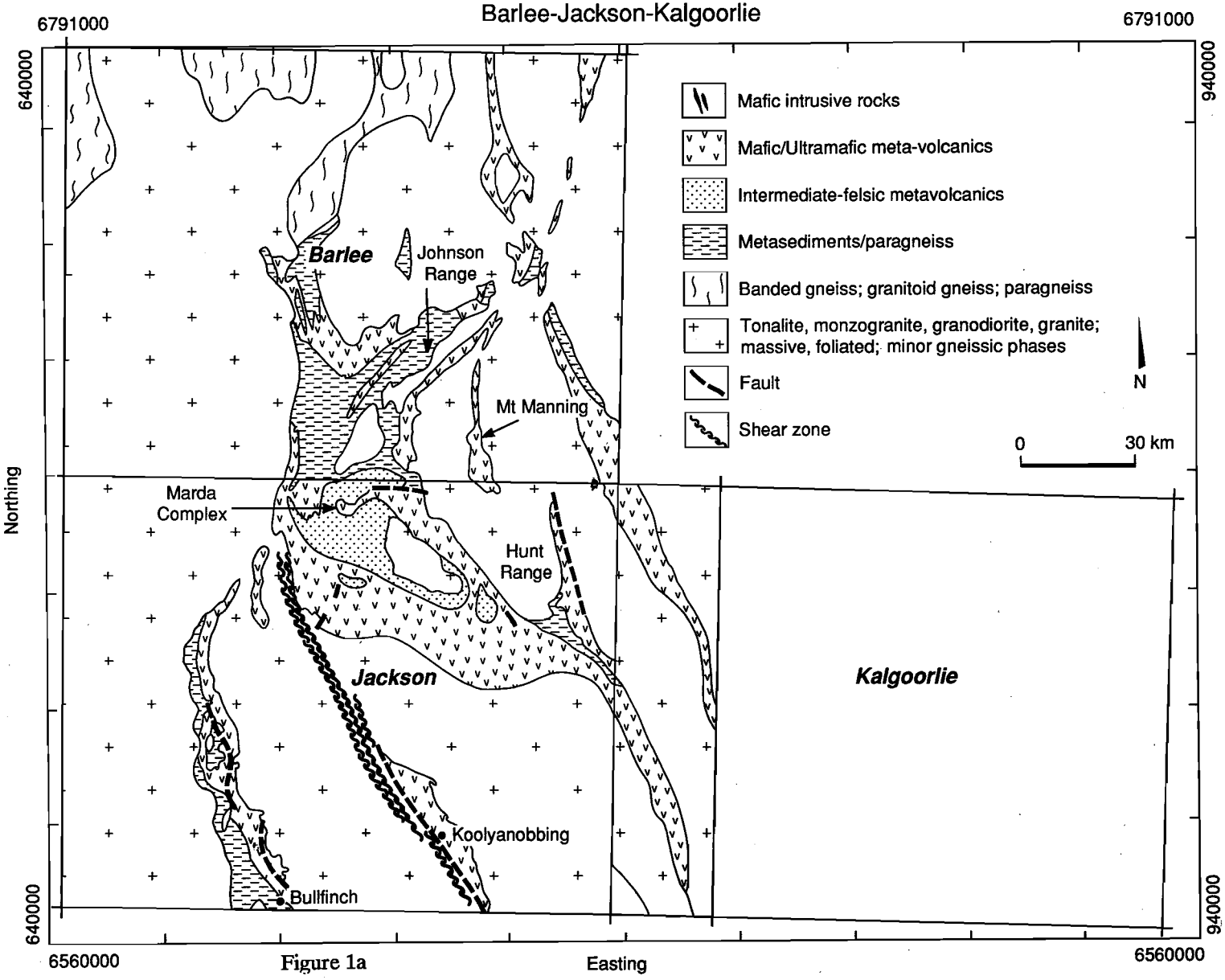
Barlee-Jackson-Kalgoorlie
6791000
6791000
640000
940000
Northing
Barlee
Johnson Range
Mt Manning
Marda Complex
Hunt Range
Jackson
Kalgoorlie
Koolyanobbing
Bullfinch
Mafic intrusive rocks
Mafic/Ultramafic meta-volcanics
Intermediate-felsic metavolcanics
Metasediments/paragneiss
Banded gneiss; granitoid gneiss; paragneiss
Tonalite, monzogranite, granodiorite, granite; massive, foliated; minor gneissic phases
Fault
Shear zone
N
0
30 km
6560000
Easting
6560000

Figure 1a

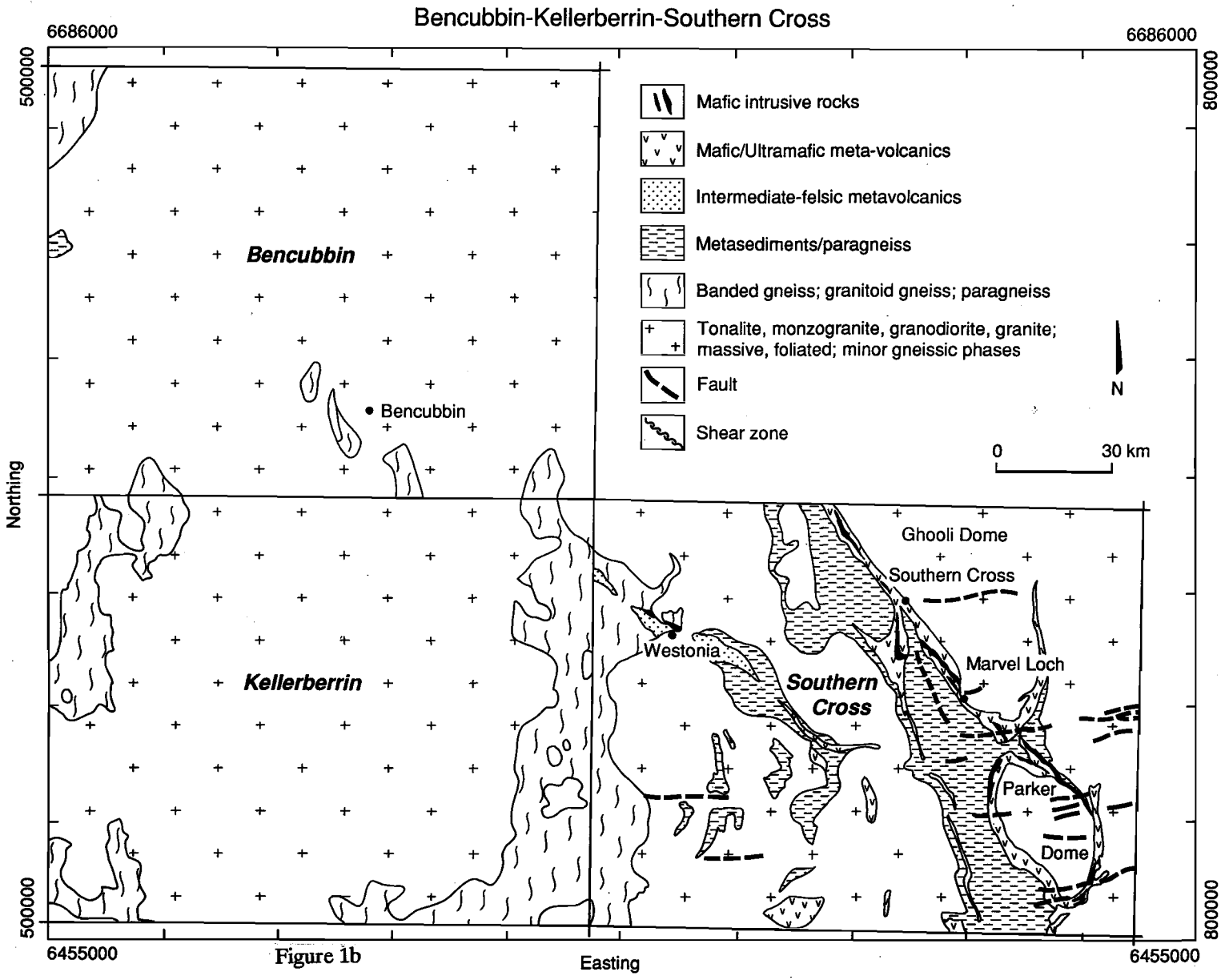
Bencubbin-Kellerberrin-Southern Cross
6686000
6686000
500000
800000
Mafic intrusive rocks
Mafic/Ultramafic meta-volcanics
Intermediate-felsic metavolcanics
Metasediments/paragneiss
Banded gneiss; granitoid gneiss; paragneiss
Tonalite, monzogranite, granodiorite, granite; massive, foliated; minor gneissic phases
Fault
Shear zone
N
0
30 km
Bencubbin
Bencubbin
Kellerberrin
Ghooli Dome
Southern Cross
Westonia
Marvel Loch
Southern Cross
Parker
Dome
Northing
Easting
6455000
6455000

Figure 1b

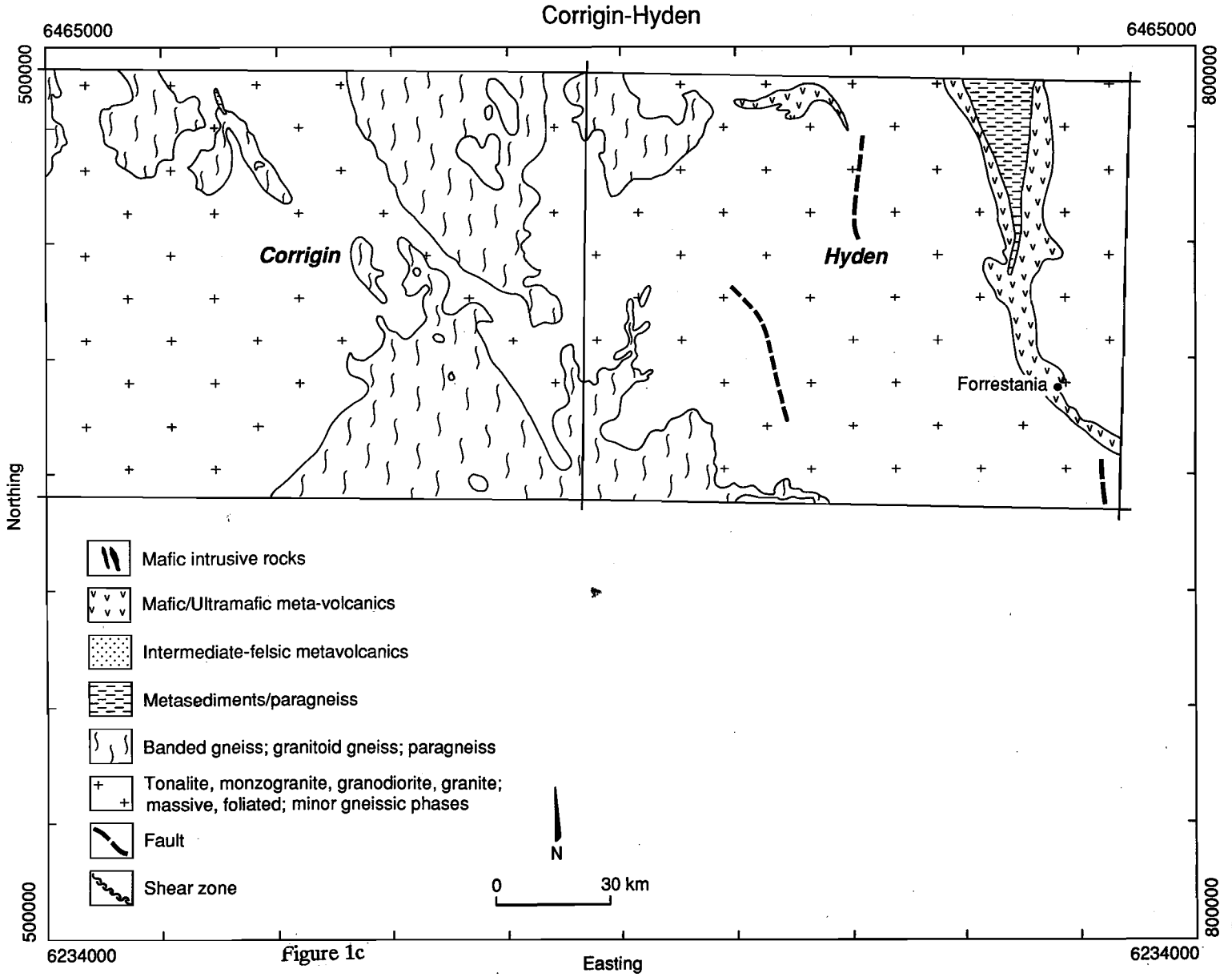
Corrigin-Hyden
6465000
6465000
500000
800000
Corrigin
Hyden
Forrestania
Northing
Mafic intrusive rocks
Mafic/Ultramafic meta-volcanics
Intermediate-felsic metavolcanics
Metasediments/paragneiss
Banded gneiss; granitoid gneiss; paragneiss
Tonalite, monzogranite, granodiorite, granite; massive, foliated; minor gneissic phases
Fault
Shear zone
N
0
30 km
500000
800000
6234000
6234000
Easting

Figure 1c

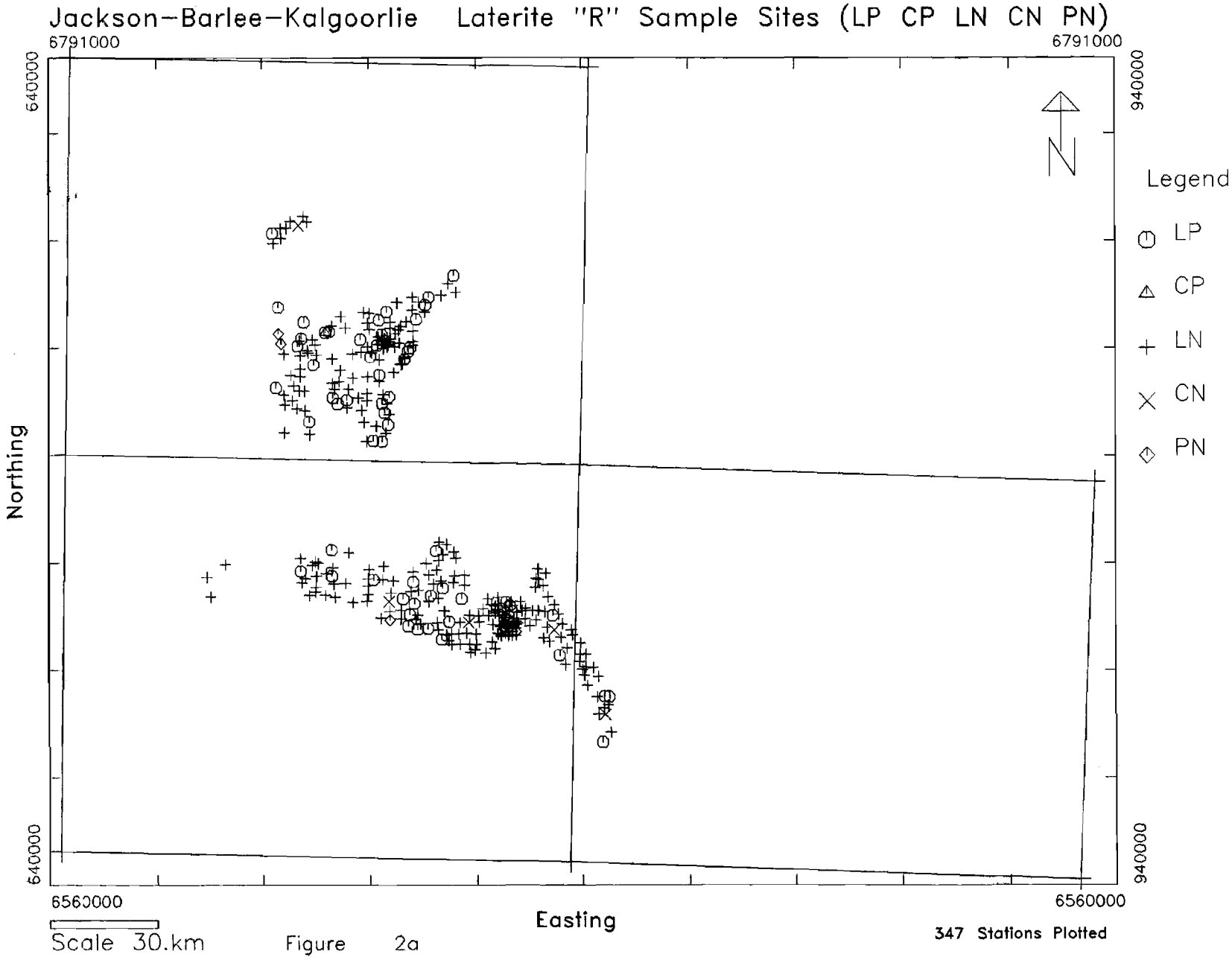
Jackson–Barlee–Kalgoorlie Laterite "R" Sample Sites (LP CP LN CN PN)
6791000
6791000
640000
940000
Northing
Legend
LP
CP
LN
CN
PN
640000
940000
6560000
6560000
Easting
Scale 30.km
347 Stations Plotted

Figure 2a

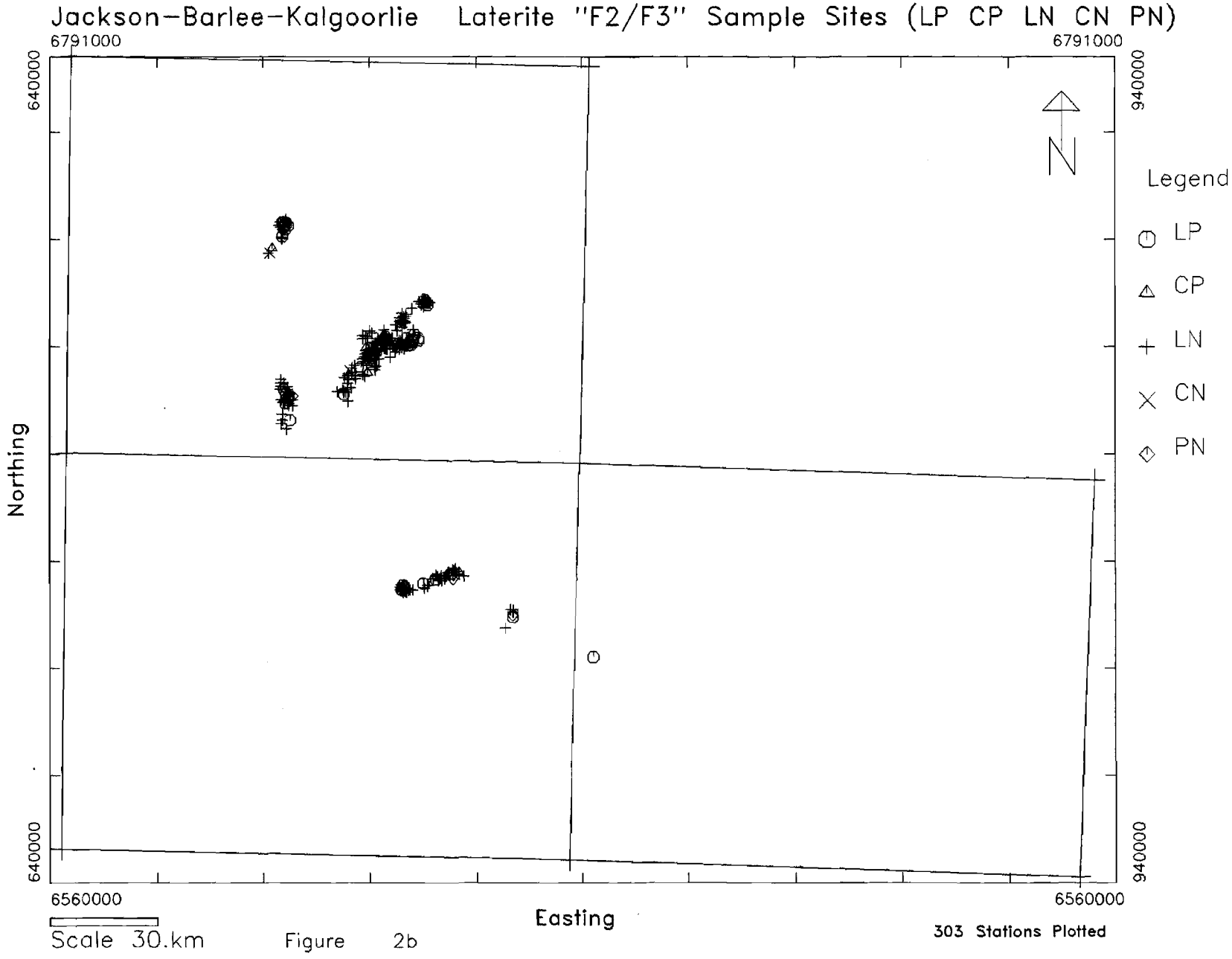
Jackson–Barlee–Kalgoorlie Laterite "F2/F3" Sample Sites (LP CP LN CN PN)
6791000
6791000
640000
940000
N
Legend
LP
CP
LN
CN
PN
Northing
640000
940000
6560000
6560000
Easting
Scale 30.km
303 Stations Plotted

Figure 2b

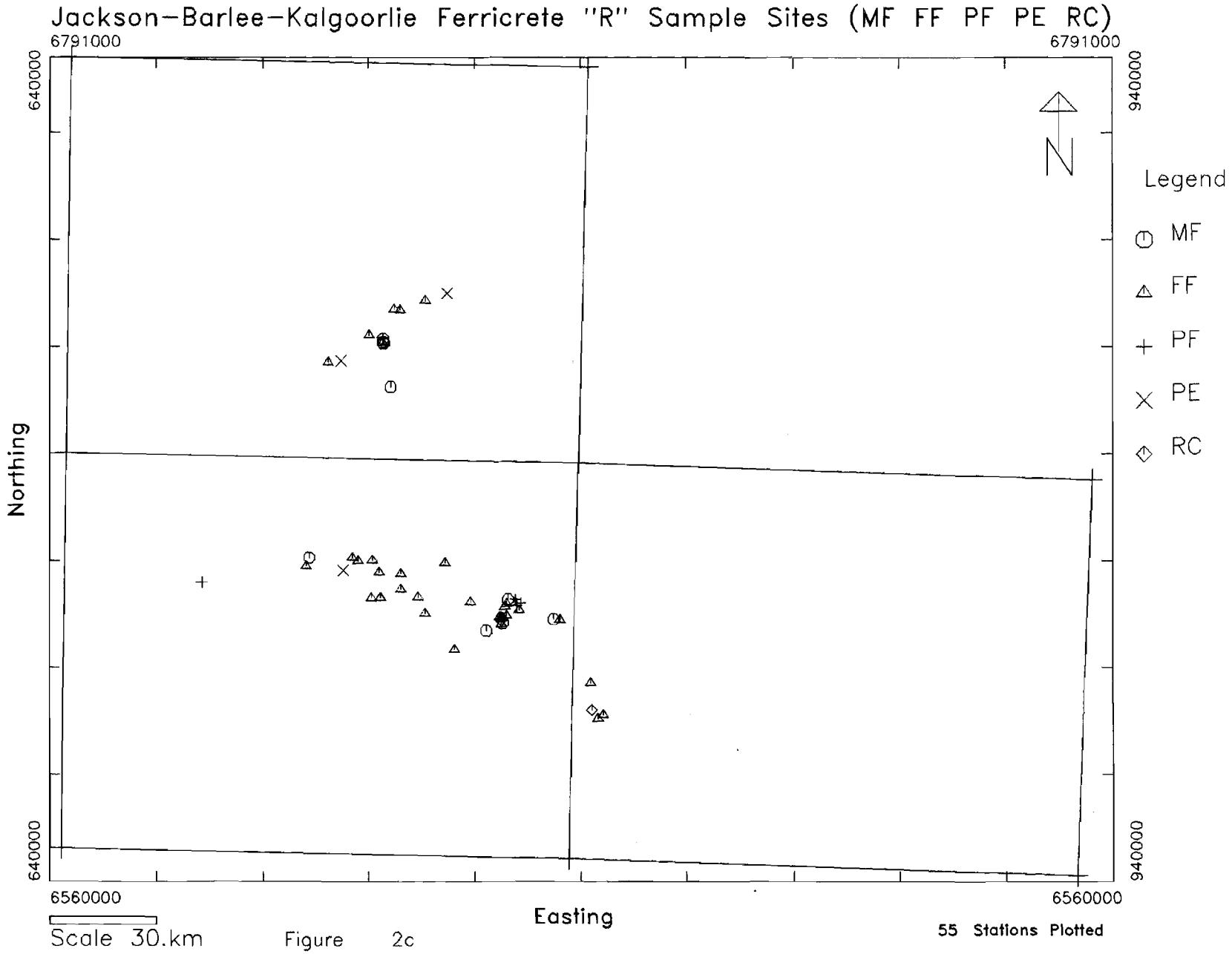
Jackson–Barlee–Kalgoorlie Ferricrete "R" Sample Sites (MF FF PF PE RC)
6791000
6791000
640000
940000
N
Legend
MF
FF
PF
PE
RC
Northing
640000
940000
6560000
6560000
Easting
Scale 30.km
55 Stations Plotted

Figure 2c

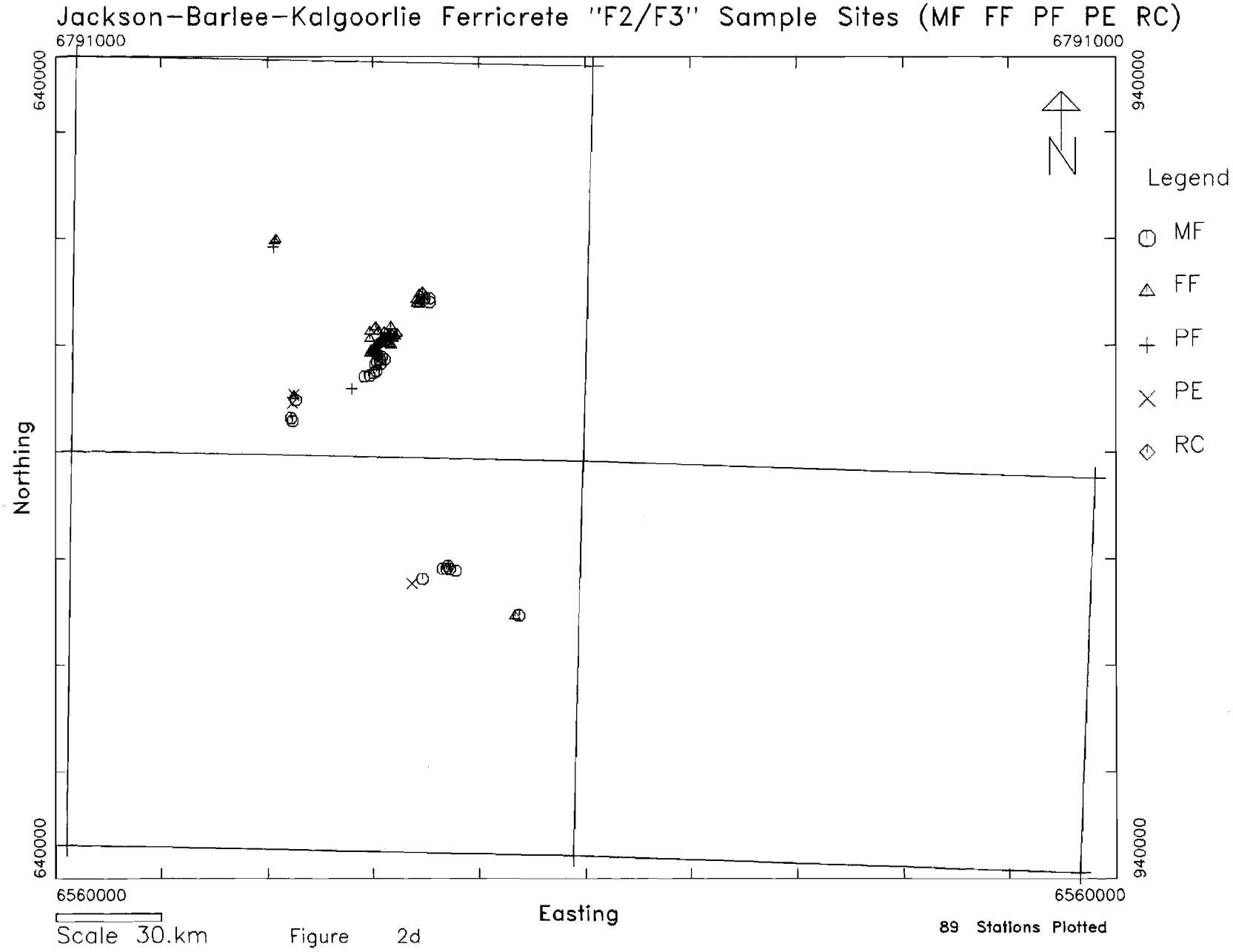
Jackson–Barlee–Kalgoorlie Ferricrete "F2/F3" Sample Sites (MF FF PF PE RC)
6791000
6791000
640000
940000
N
Legend
MF
FF
PF
PE
RC
Northing
640000
940000
6560000
6560000
Easting
Scale 30.km
89 Stations Plotted

Figure 2d

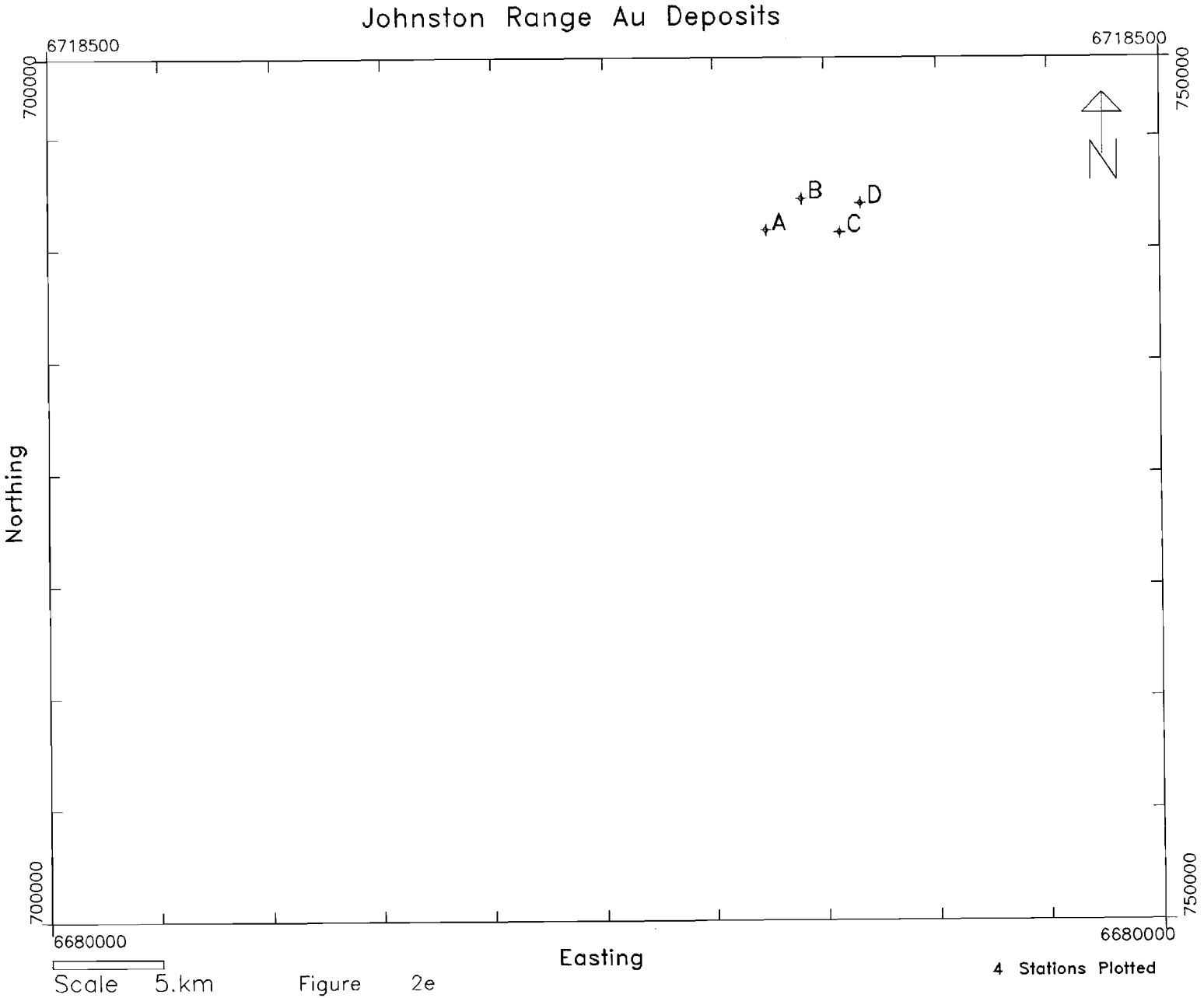
Johnston Range Au Deposits
6718500
6718500
700000
750000
N
B
D
A
C
Northing
700000
750000
6680000
6680000
Easting
Scale 5.km
4 Stations Plotted

Figure 2e

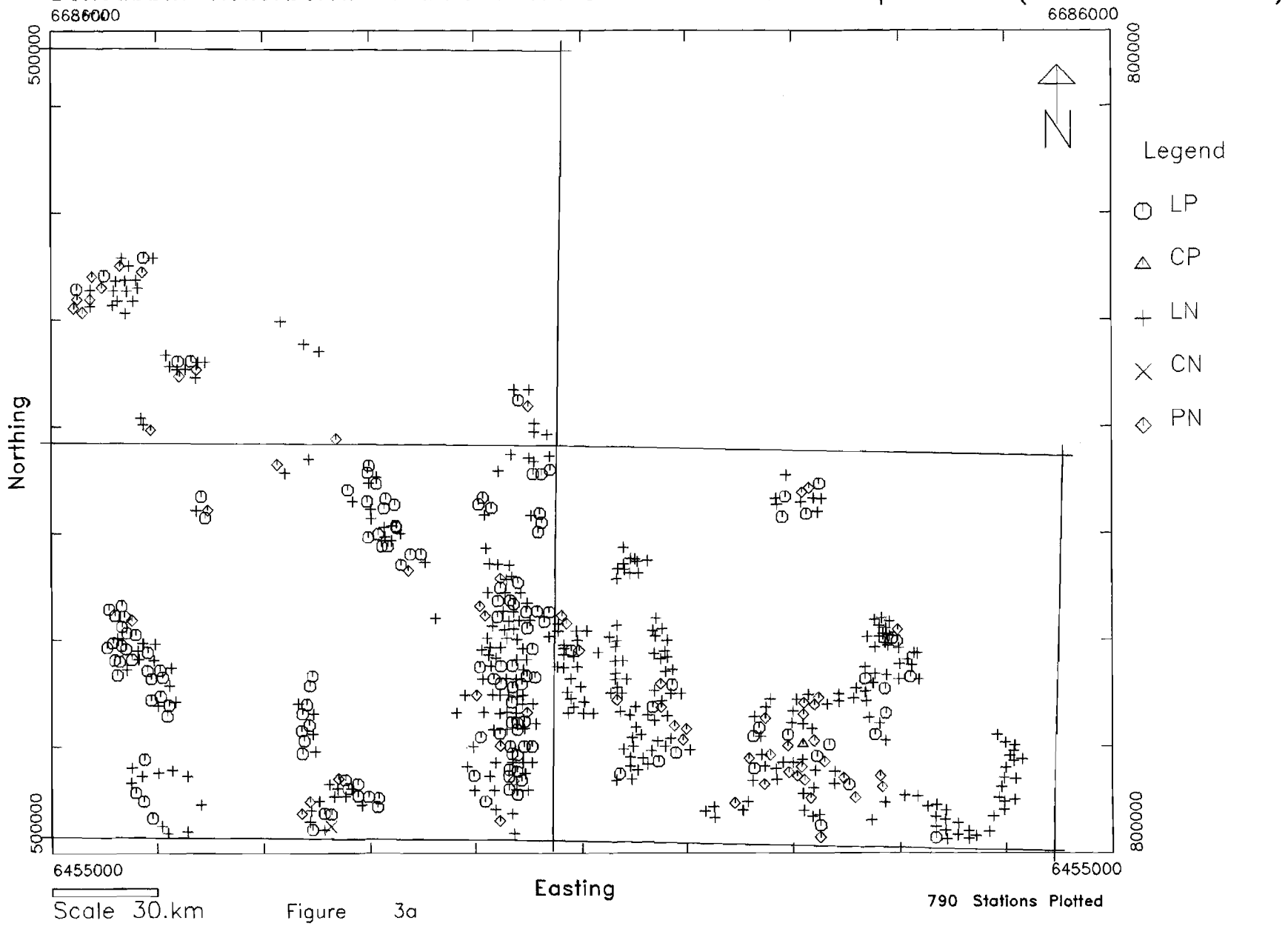
Bencubbin–Kellerberrin–Southern Cross Laterite "R" Sample Sites (LP CP LN CN PN)
6686000
6686000
500000
800000
N
Legend
LP
CP
LN
CN
PN
Northing
500000
800000
6455000
6455000
Easting
Scale 30.km
790 Stations Plotted

Figure 3a

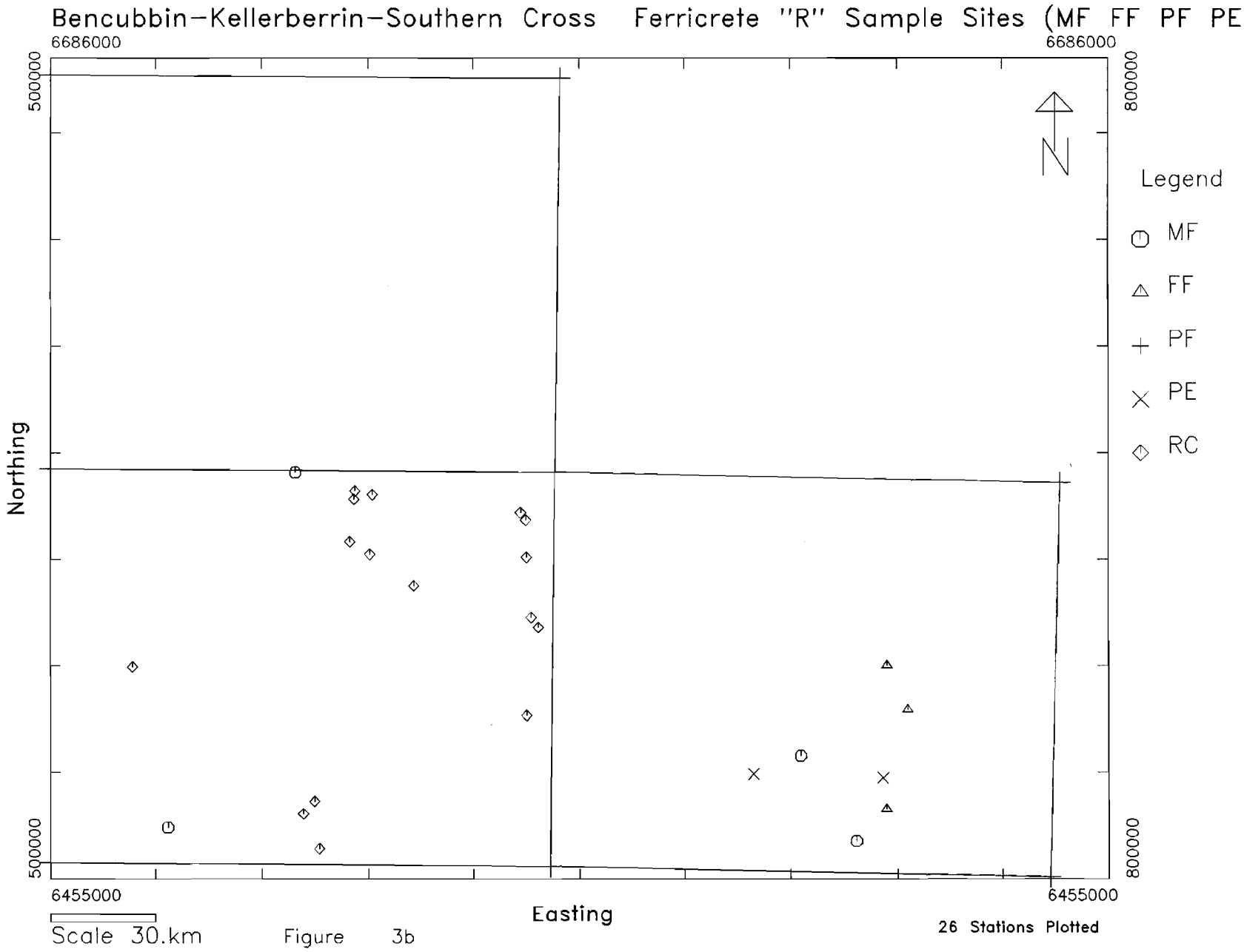
Bencubbin–Kellerberrin–Southern Cross Ferricrete "R" Sample Sites (MF FF PF PE RC)
6686000
6686000
500000
800000
N
Legend
MF
FF
PF
PE
RC
Northing
500000
800000
6455000
6455000
Easting
Scale 30.km
Figure 3b
26 Stations Plotted

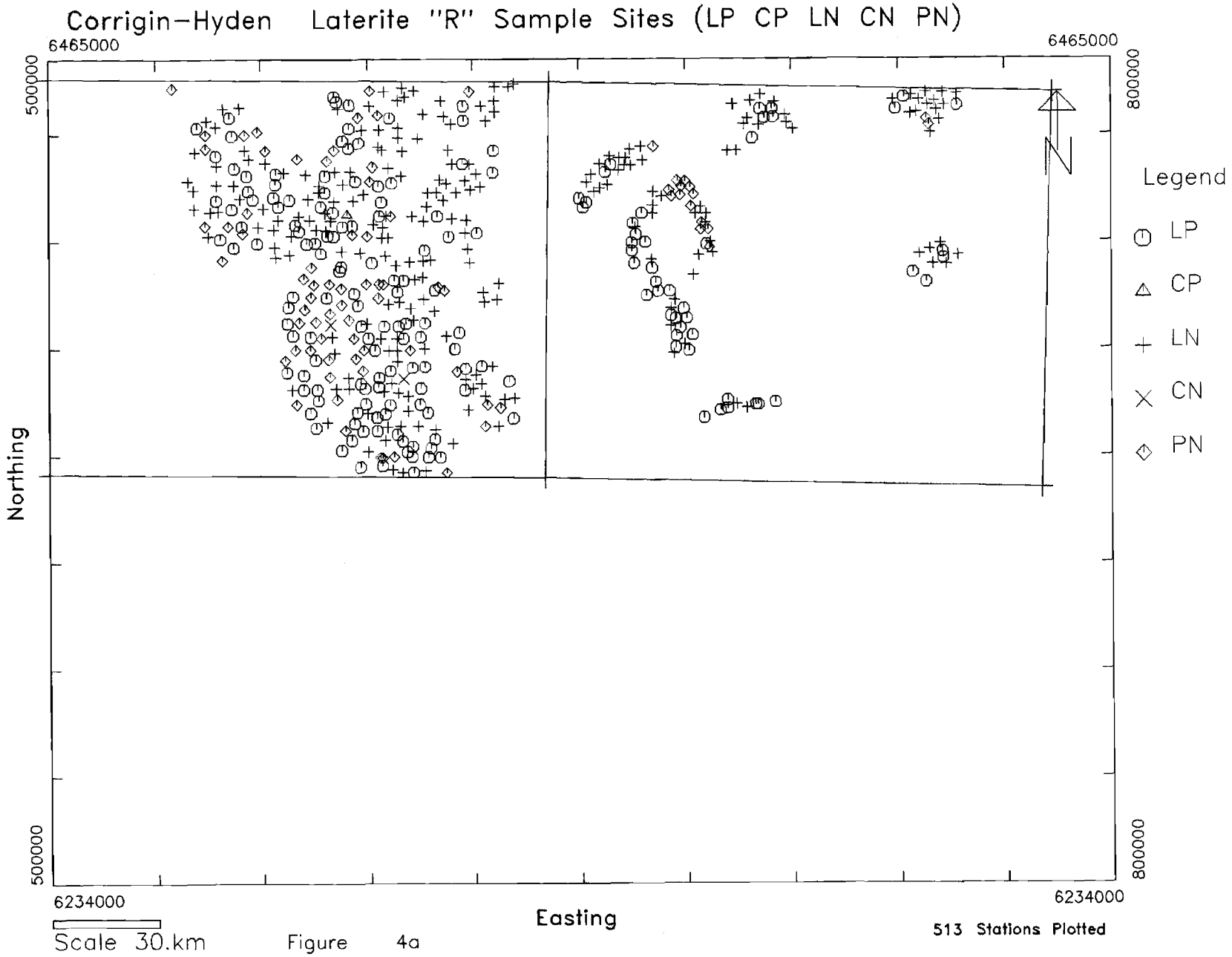
Corrigin–Hyden Laterite "R" Sample Sites (LP CP LN CN PN)
6465000
6465000
500000
800000
Legend
LP
CP
LN
CN
PN
Northing
500000
800000
6234000
6234000
Easting
Scale 30.km
513 Stations Plotted

Figure 4a

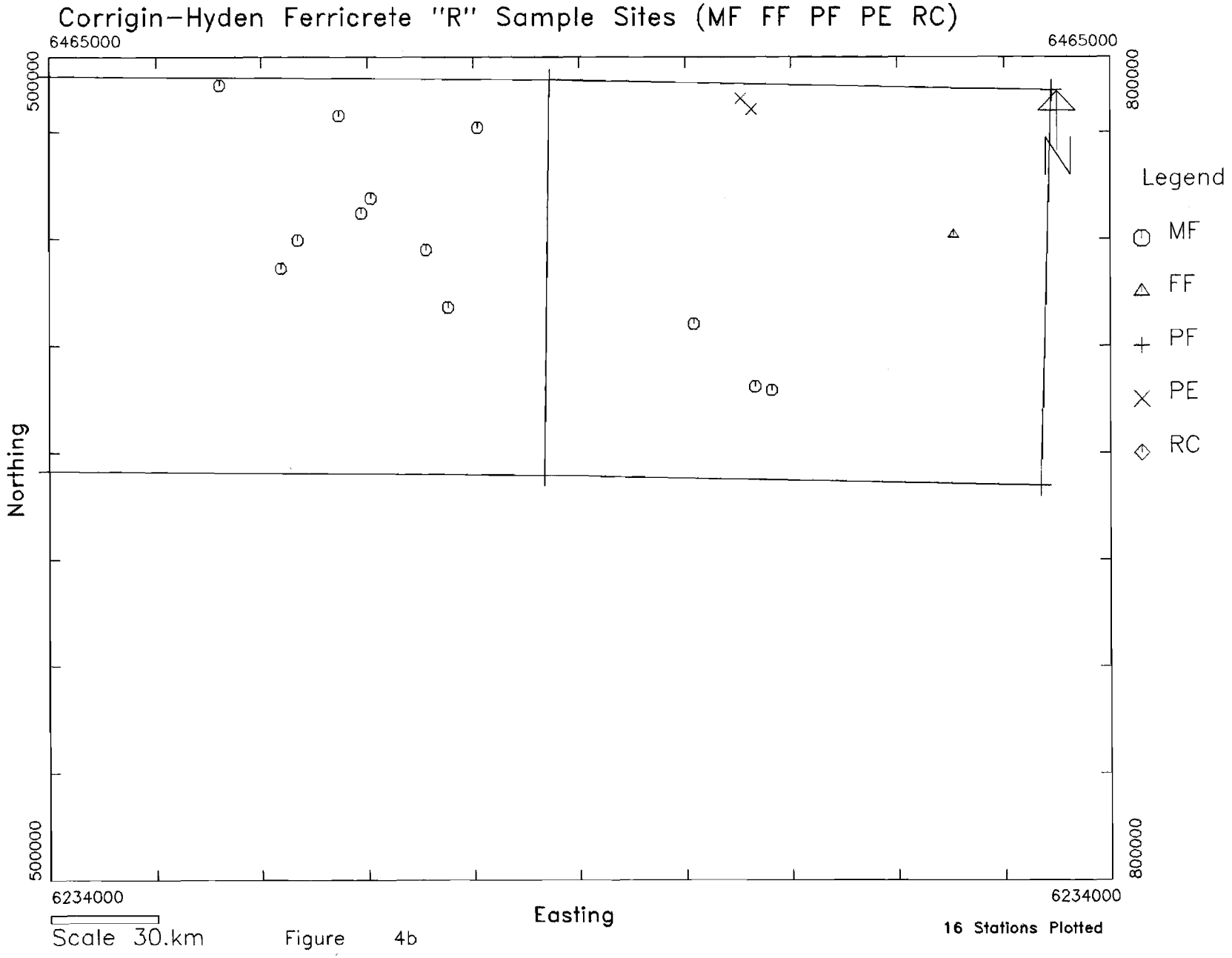
Corrigin–Hyden Ferricrete "R" Sample Sites (MF FF PF PE RC)
6465000
6465000
500000
800000
Legend
MF
FF
PF
PE
RC
Northing
500000
800000
6234000
6234000
Easting
Scale 30.km
16 Stations Plotted

Figure 4b

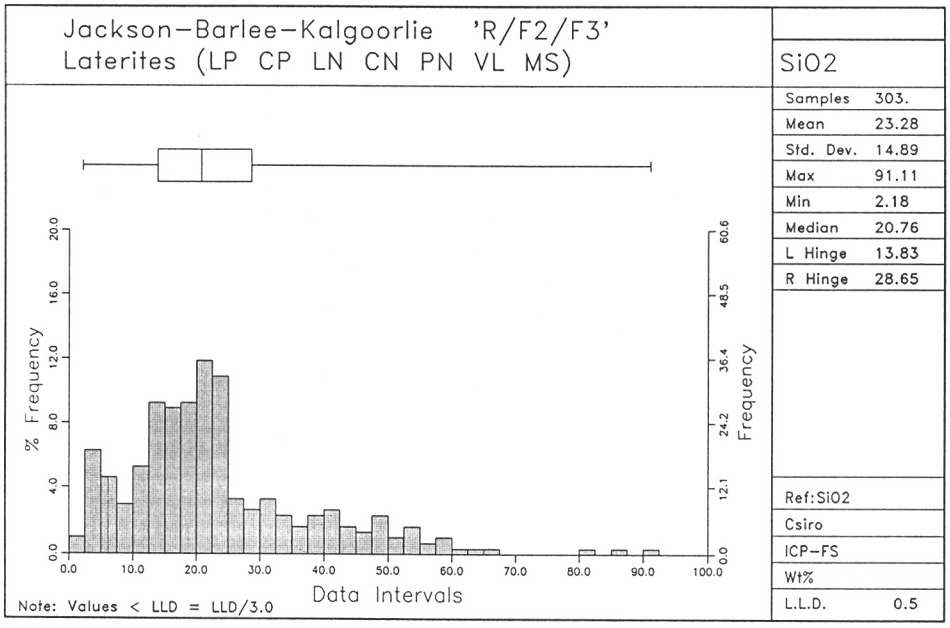

Figure 5a

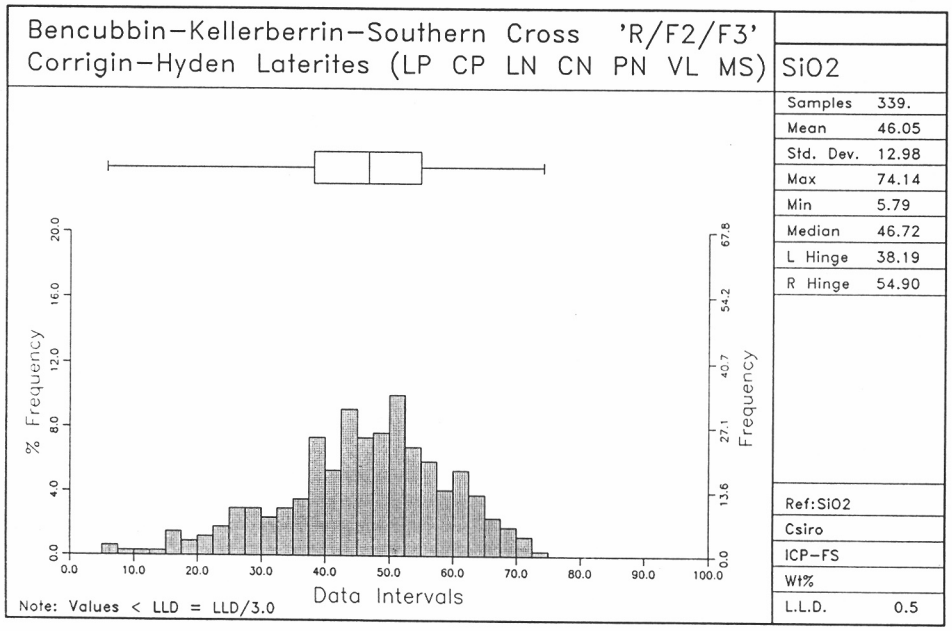

Figure 5b

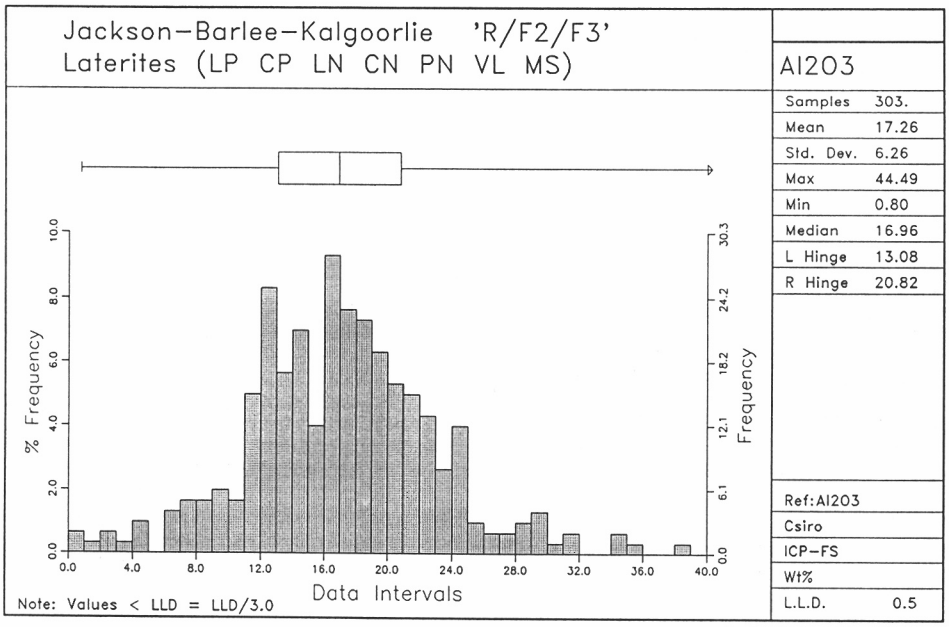

Figure 6a

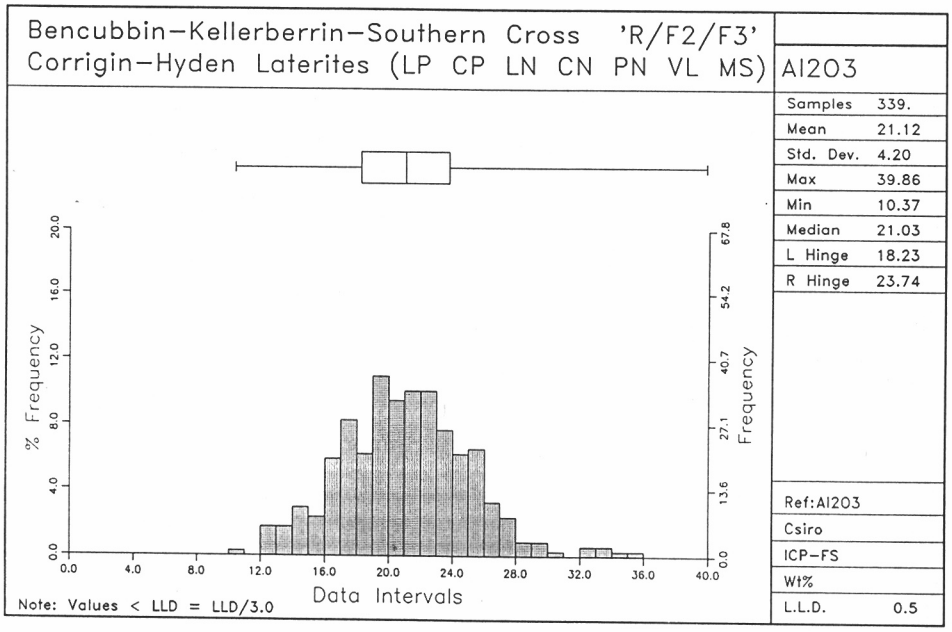

Figure 6b

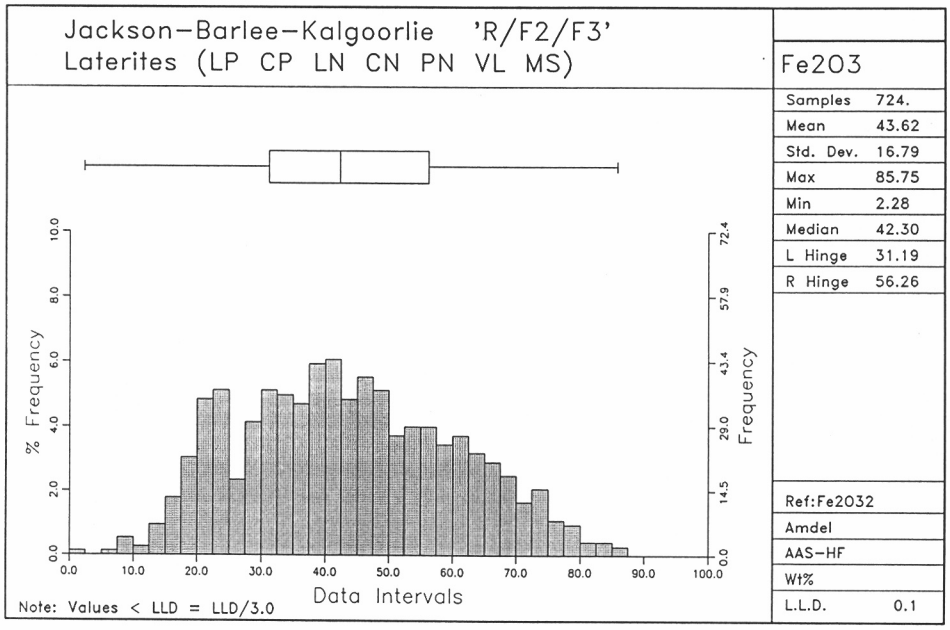

Figure 7a

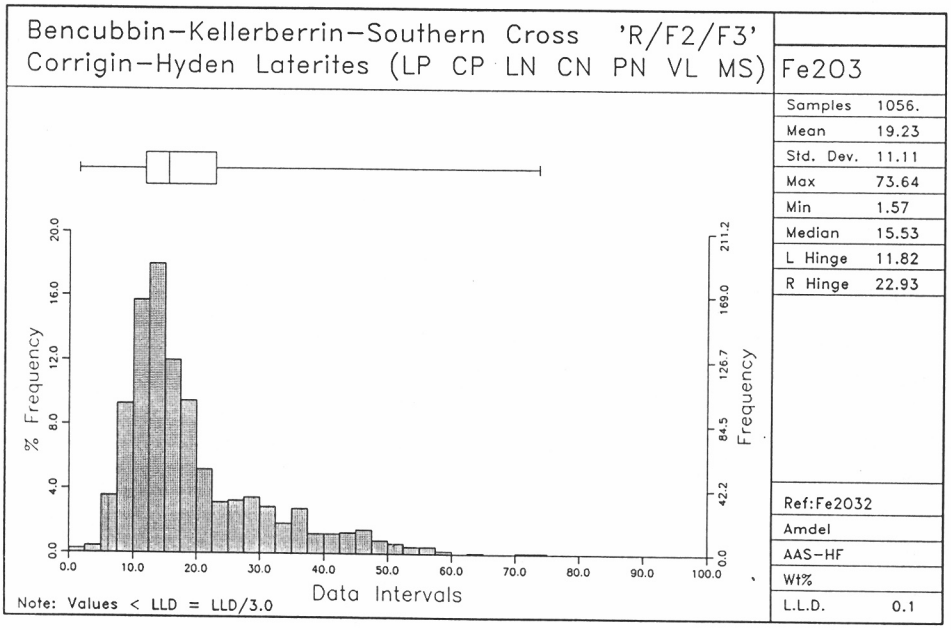

Figure 7b

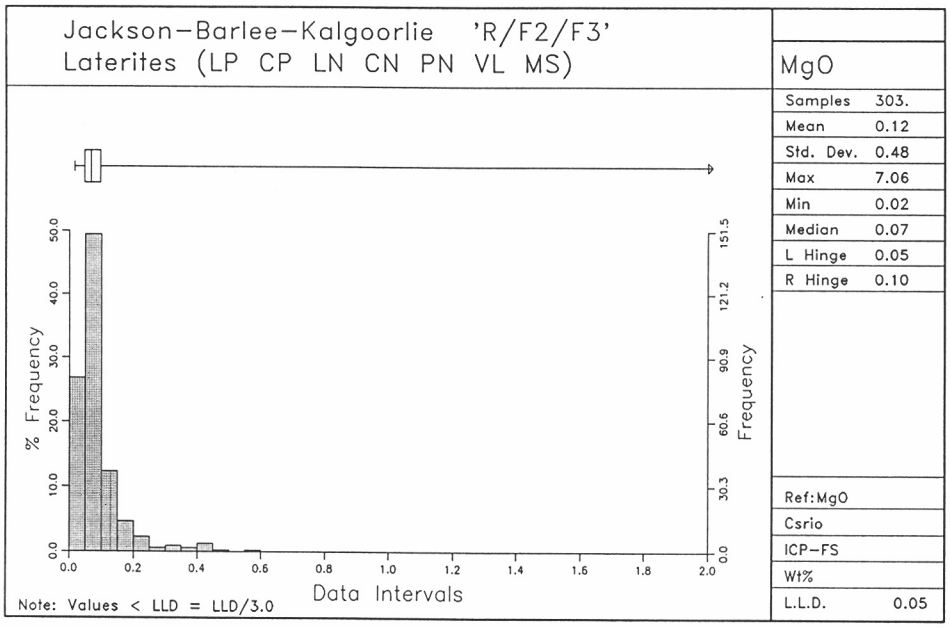

Figure 8a

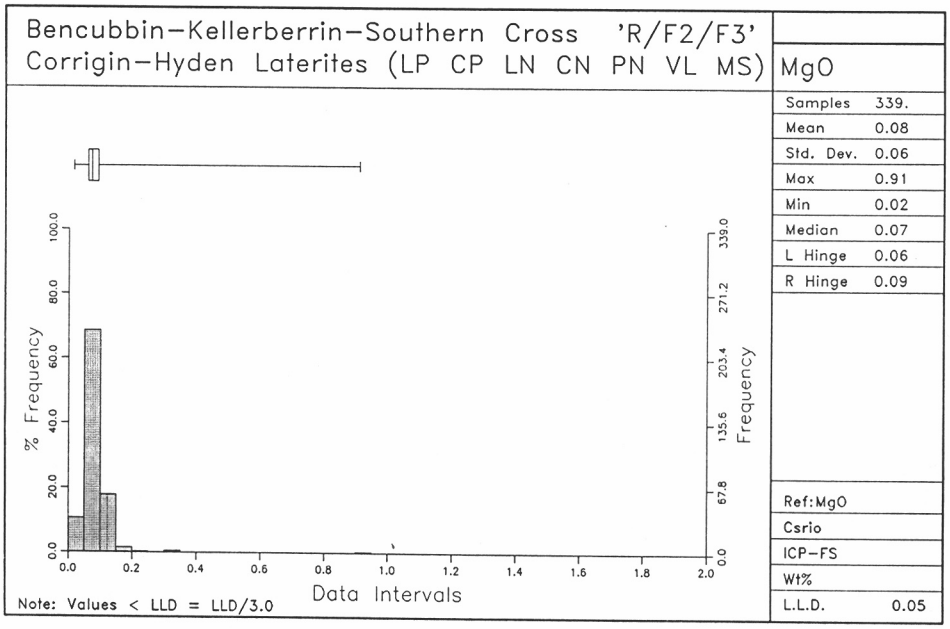

Figure 8b

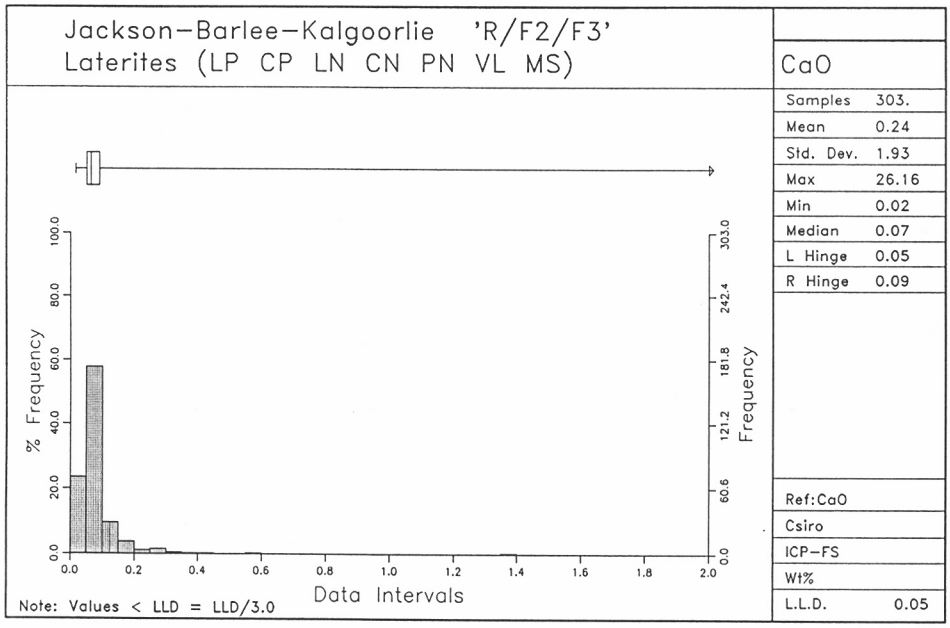

Figure 9a

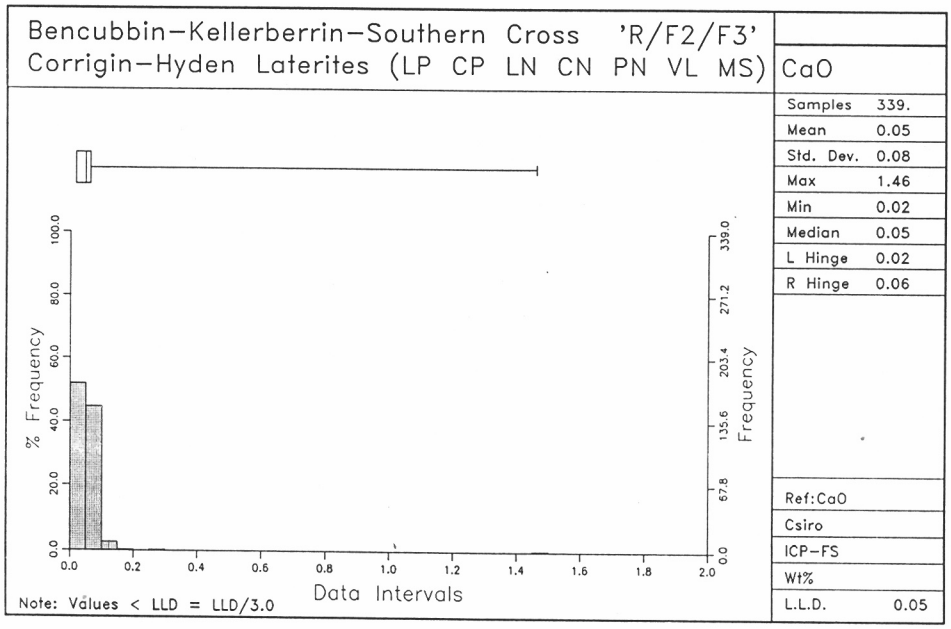

Figure 9b

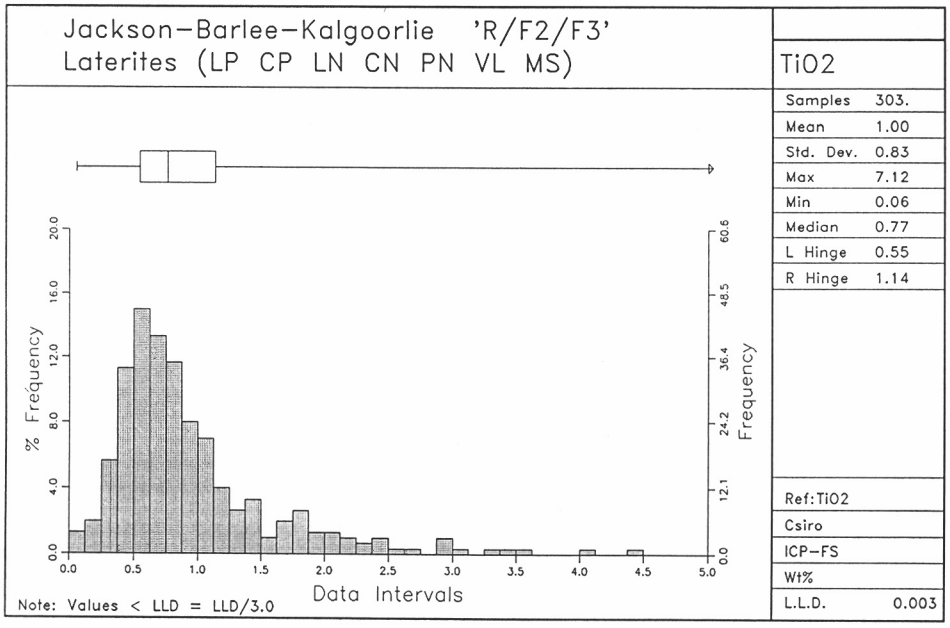

Figure 10a

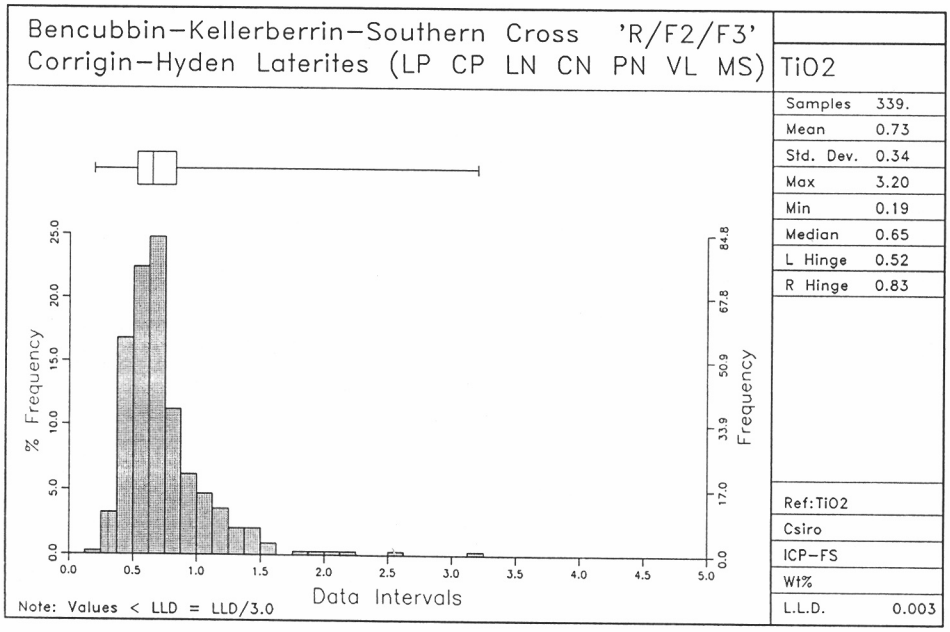

Figure 10b

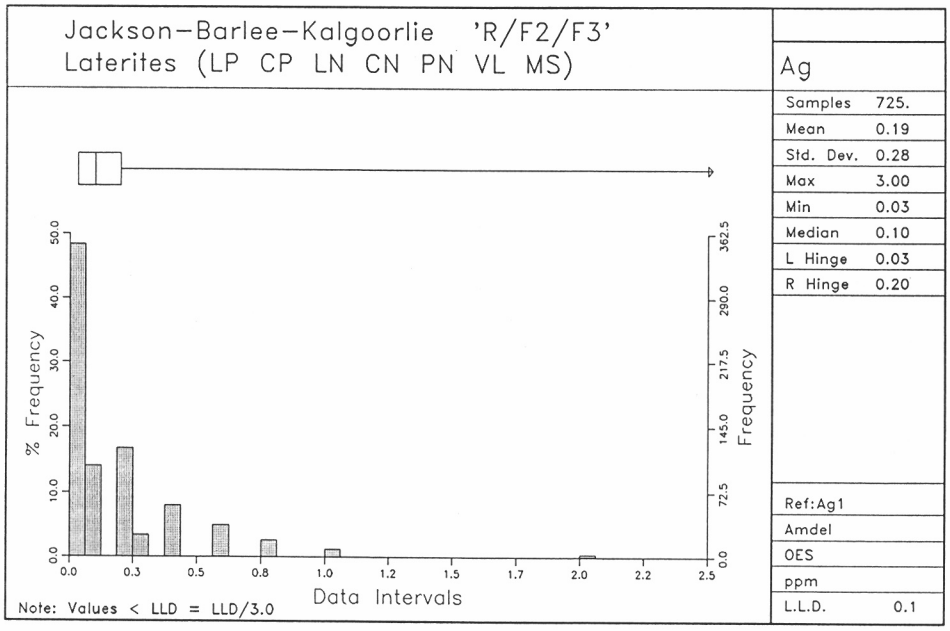

Figure 11a

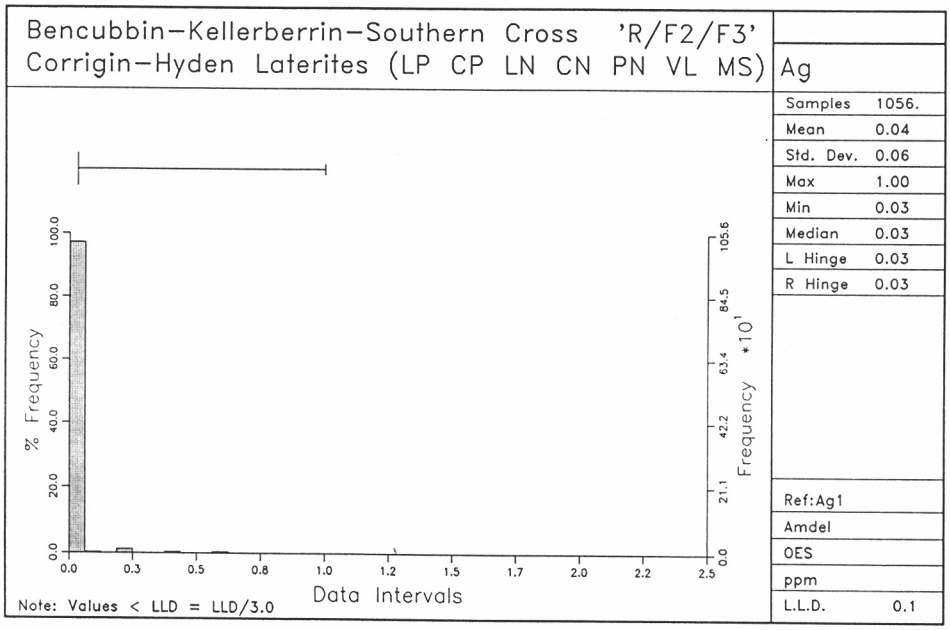

Figure 11b

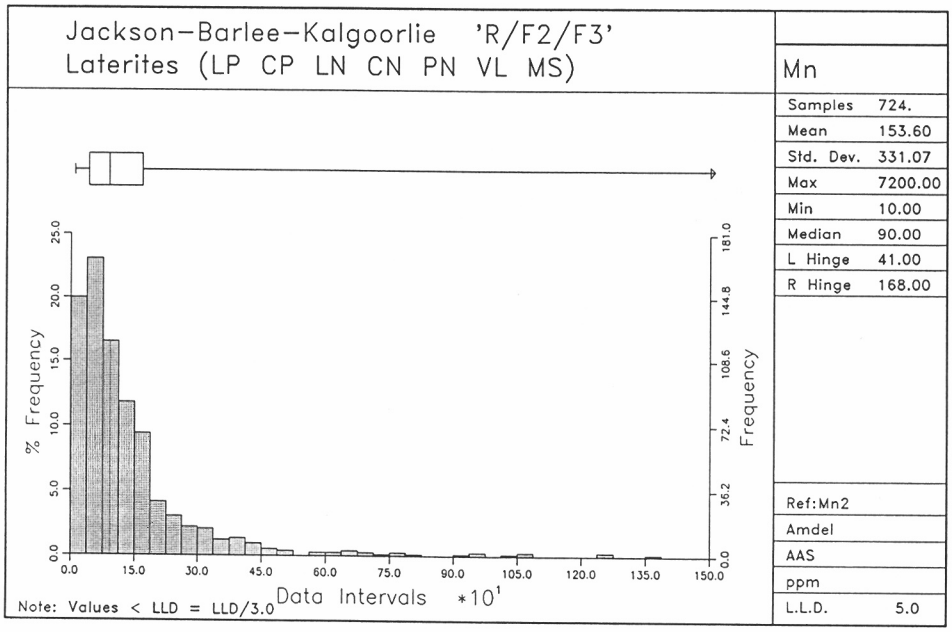

Figure 12a

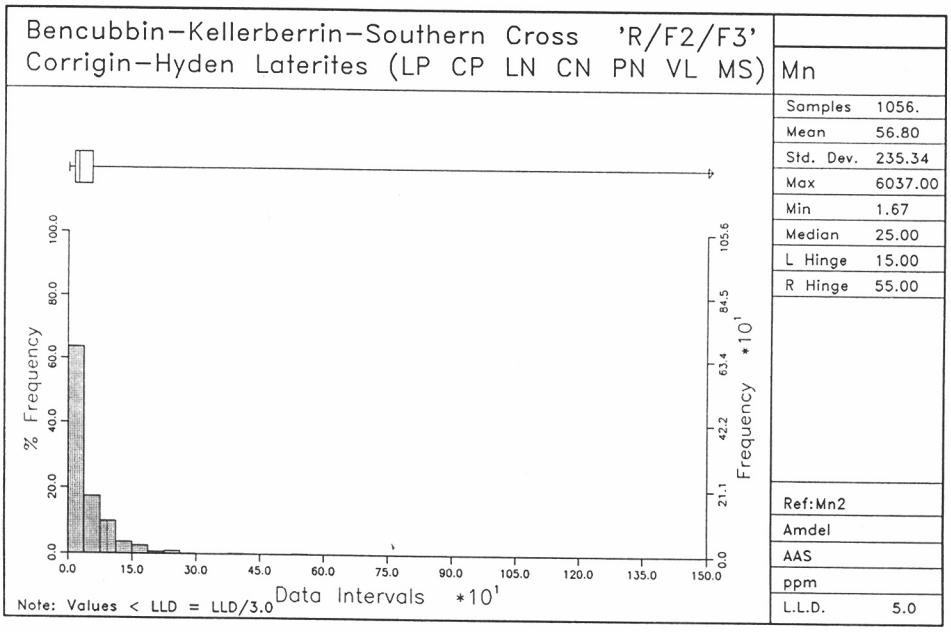

Figure 12b

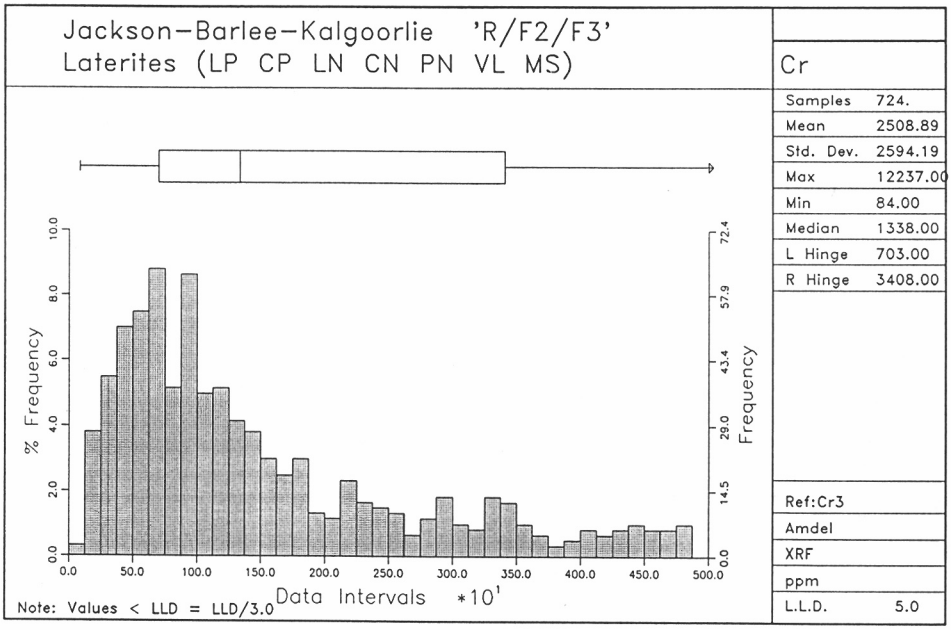

Figure 13a

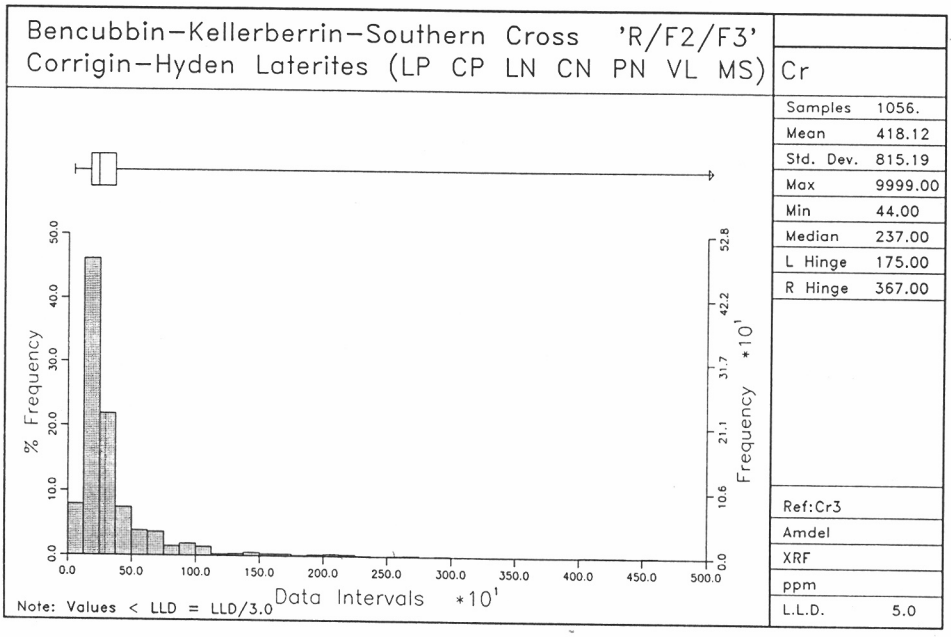

Figure 13b

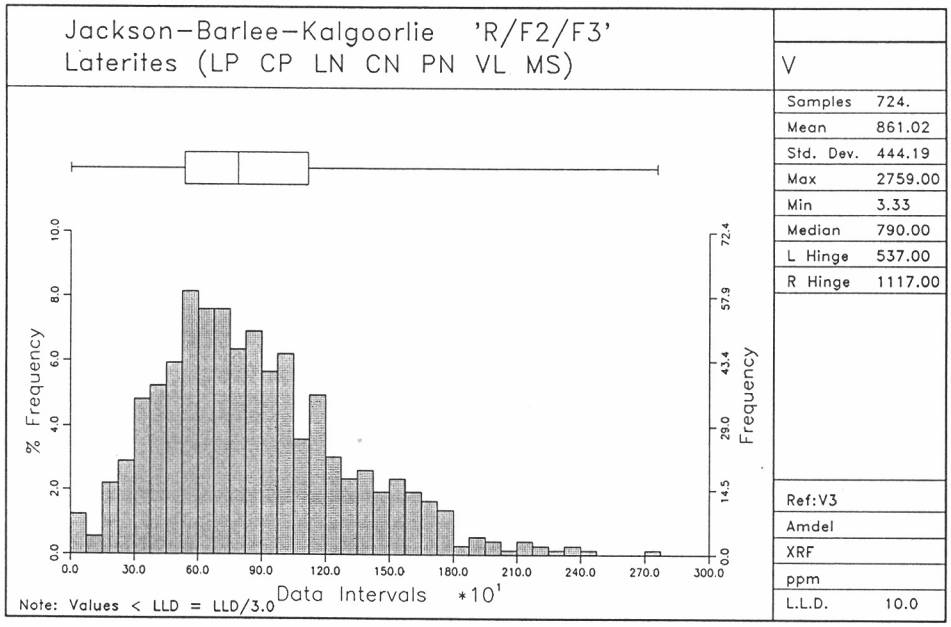

Figure 14a

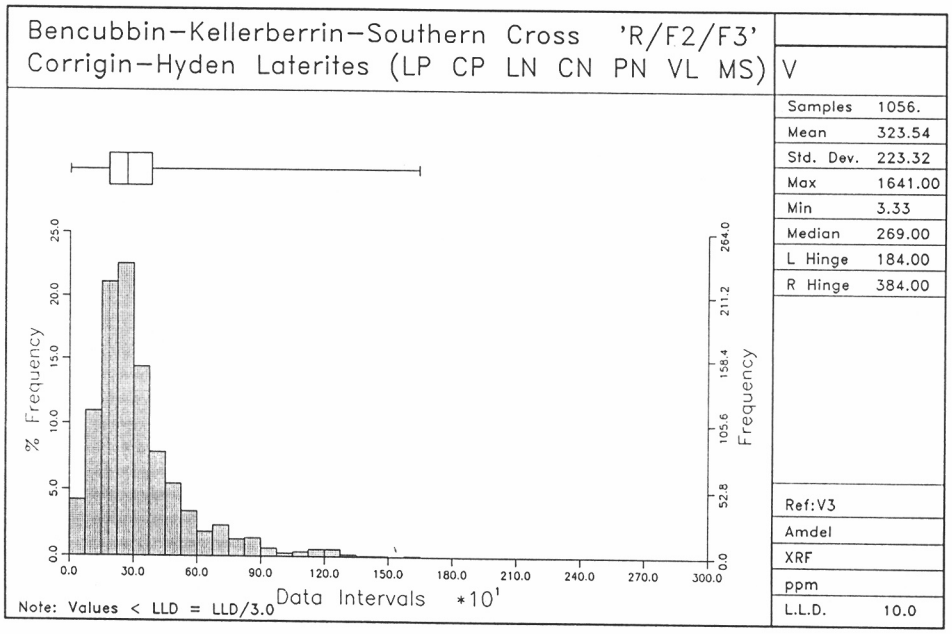

Figure 14b

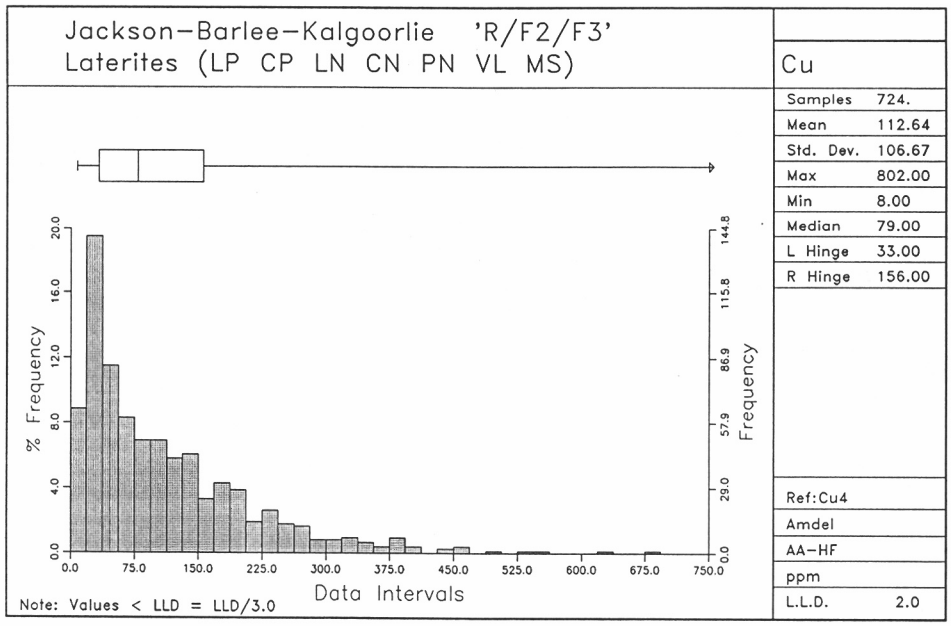

Figure 15a

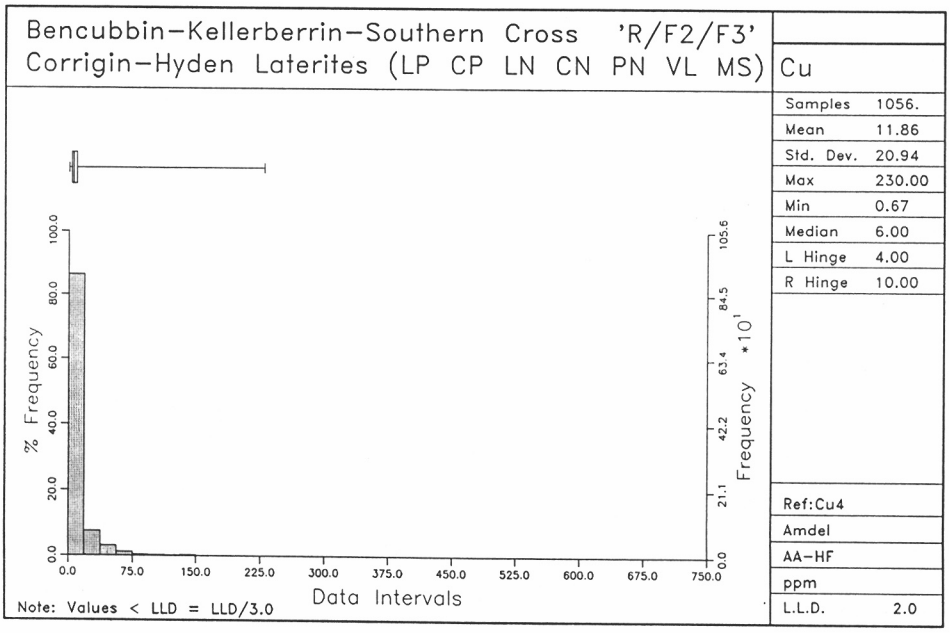

Figure 15b

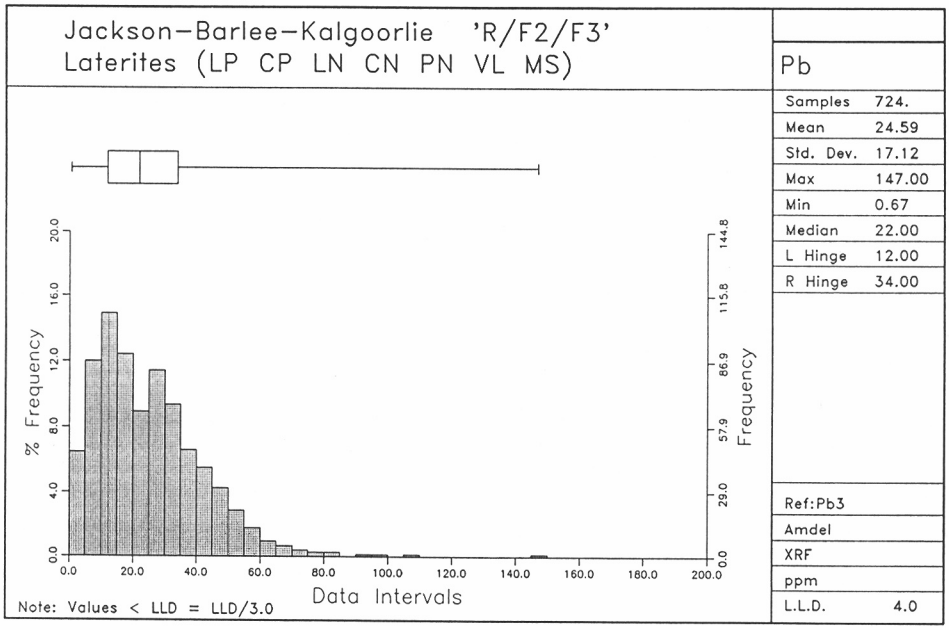

Figure 16a

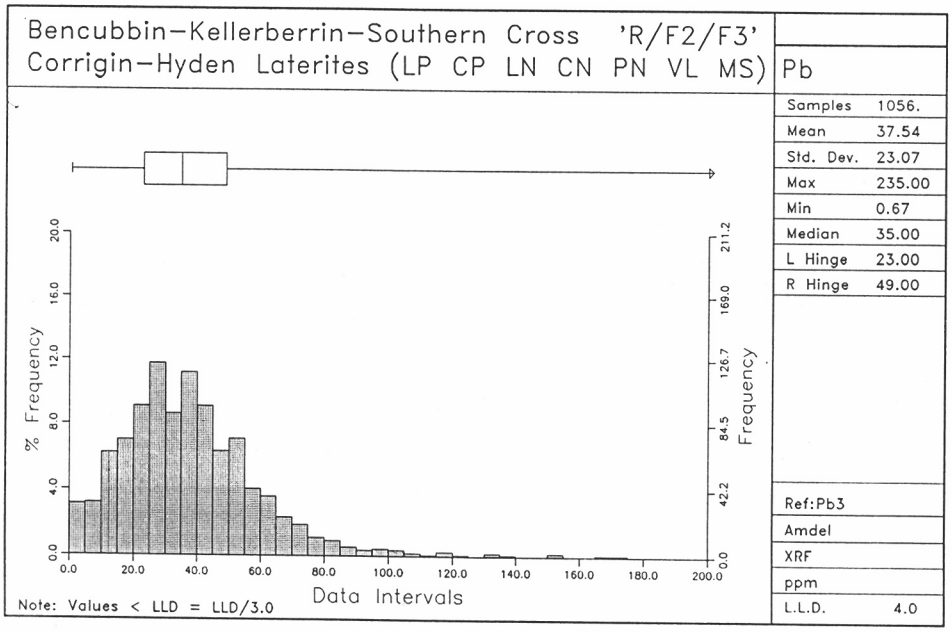

Figure 16b

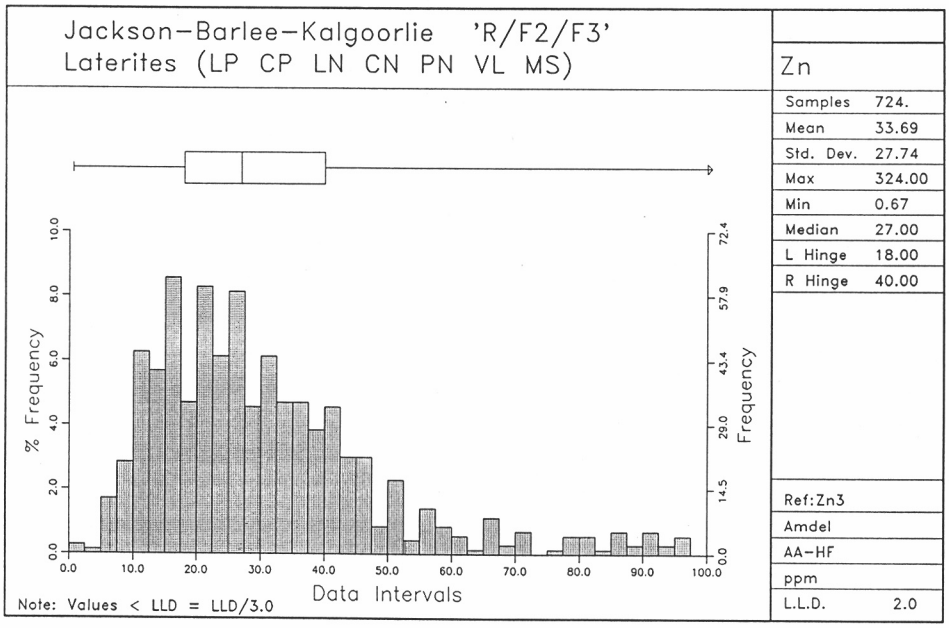

Figure 17a

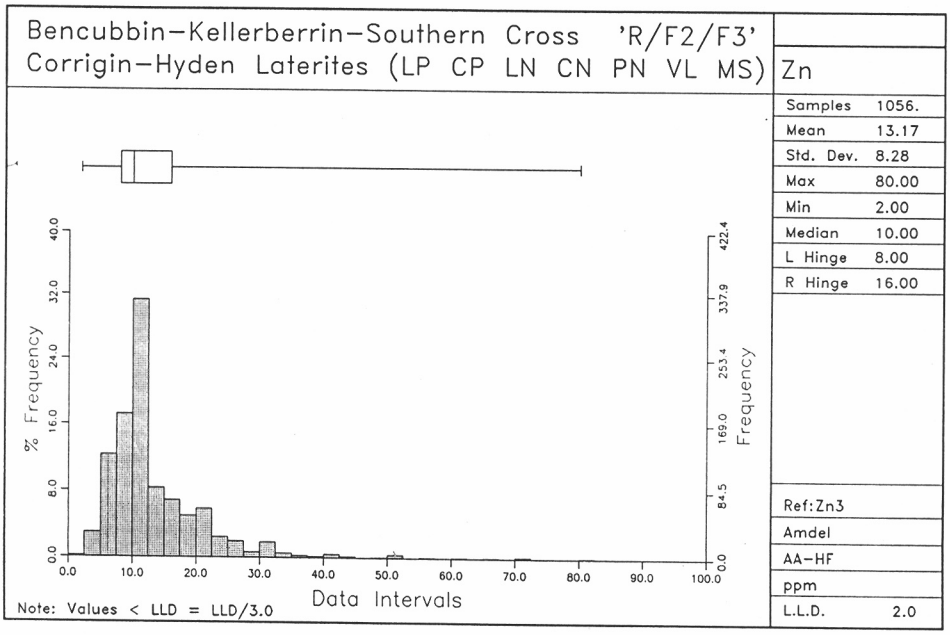

Figure 17b

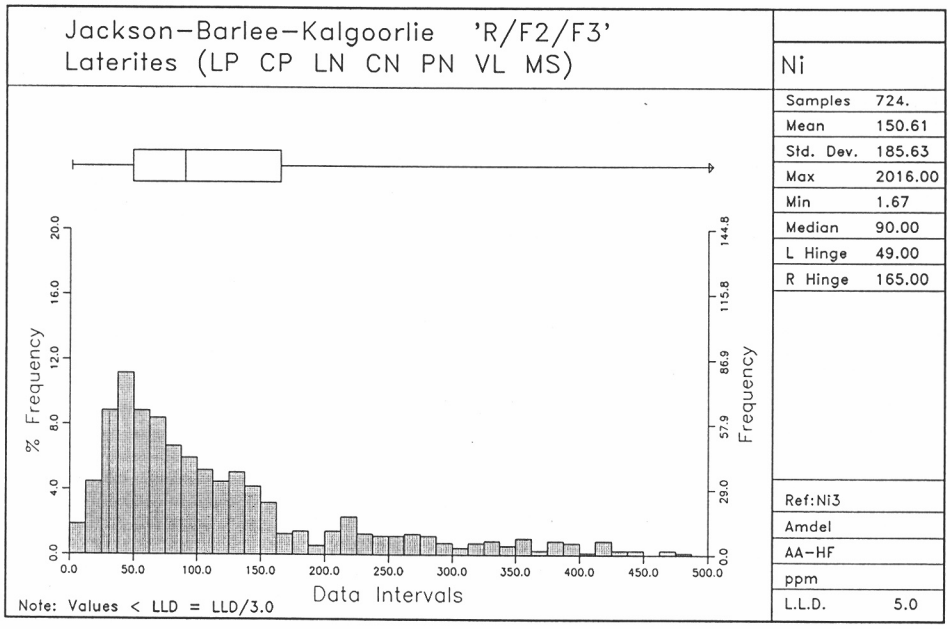

Figure 18a

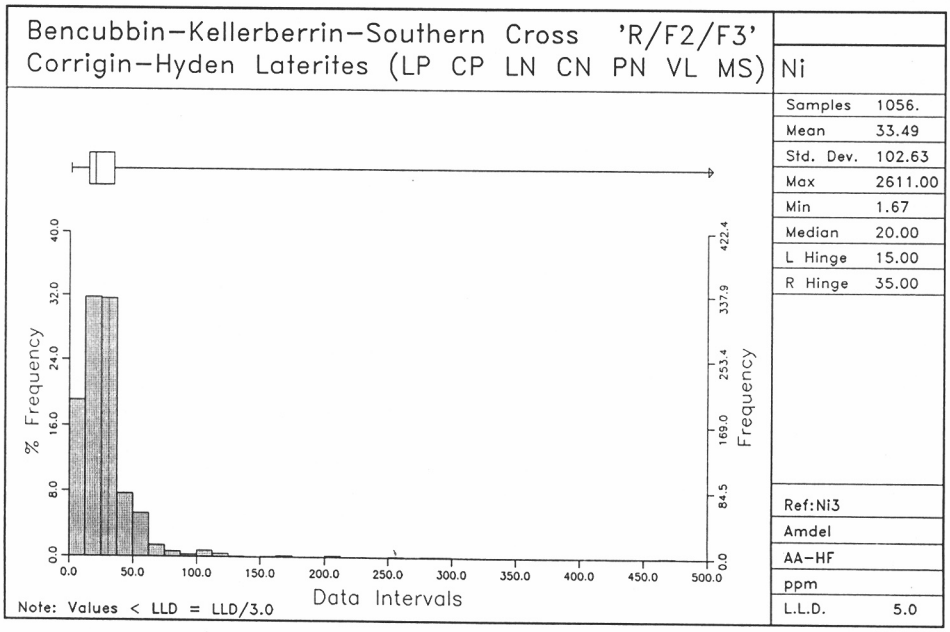

Figure 18b

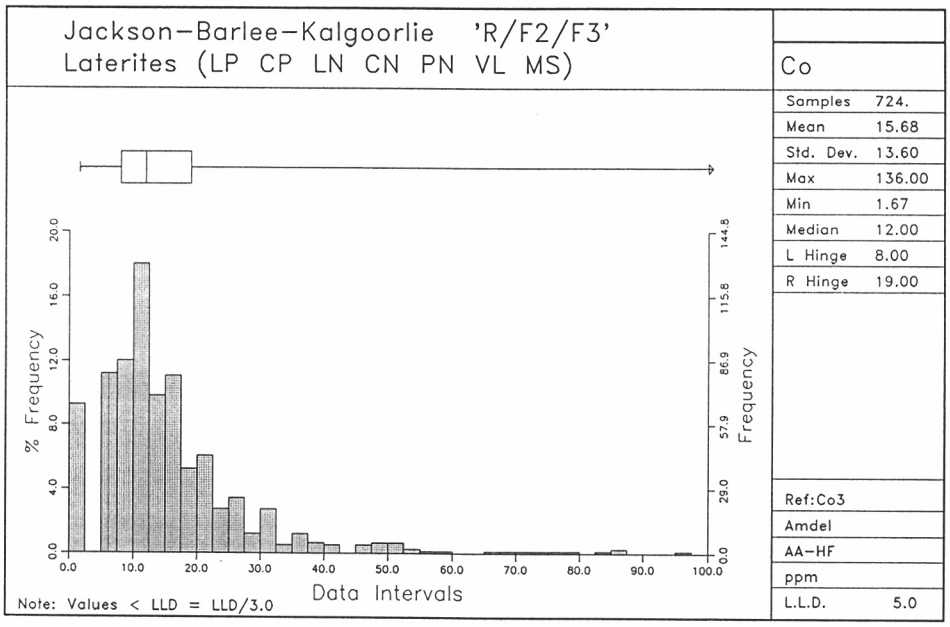

Figure 19a

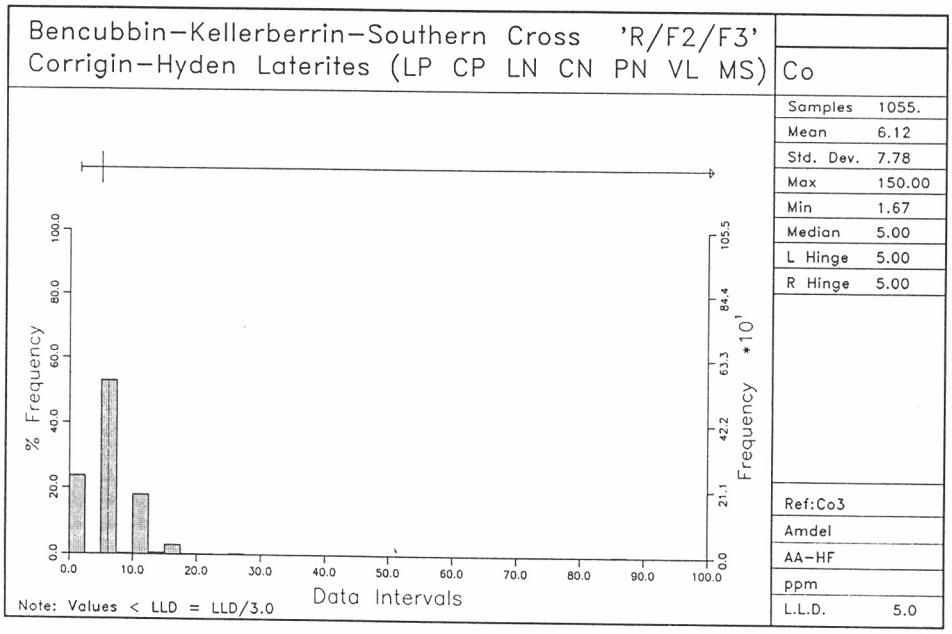

Figure 19b

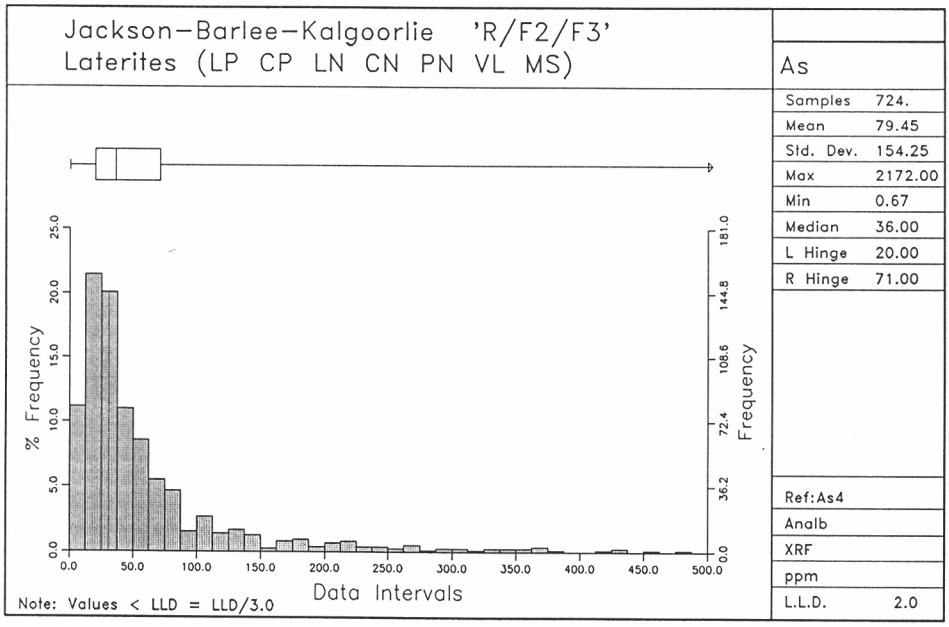

Figure 20a

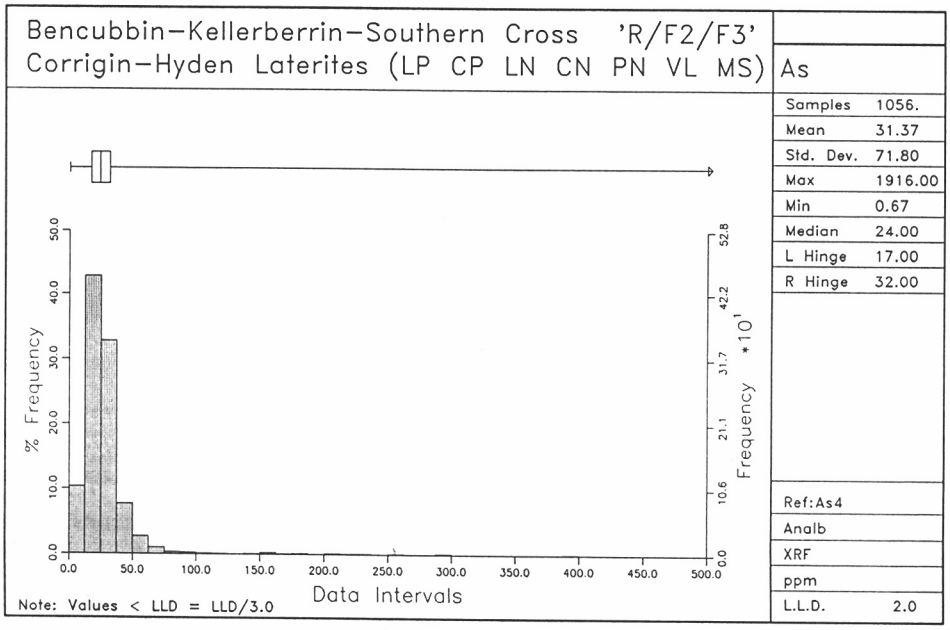

Figure 20b

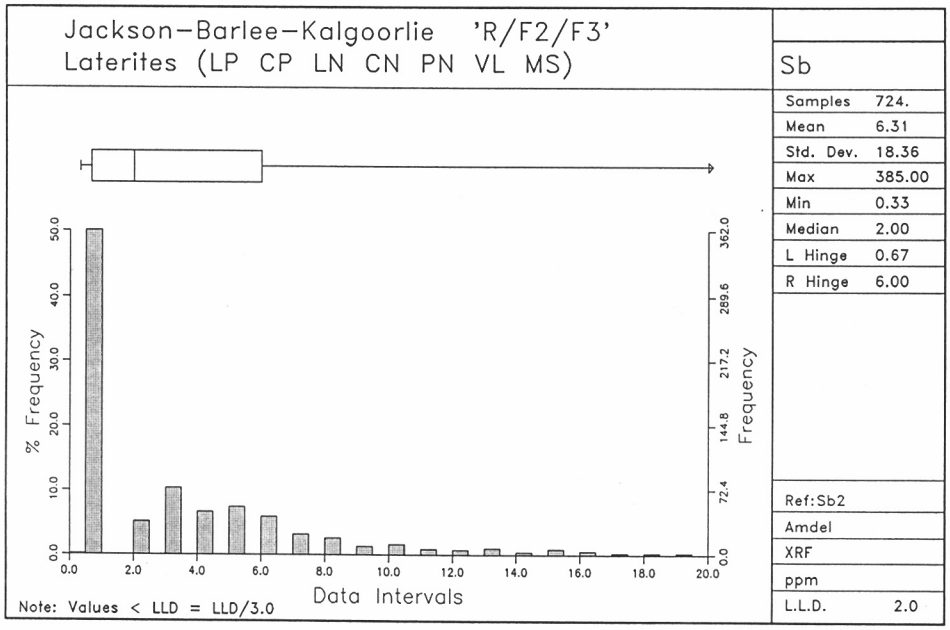

Figure 21a

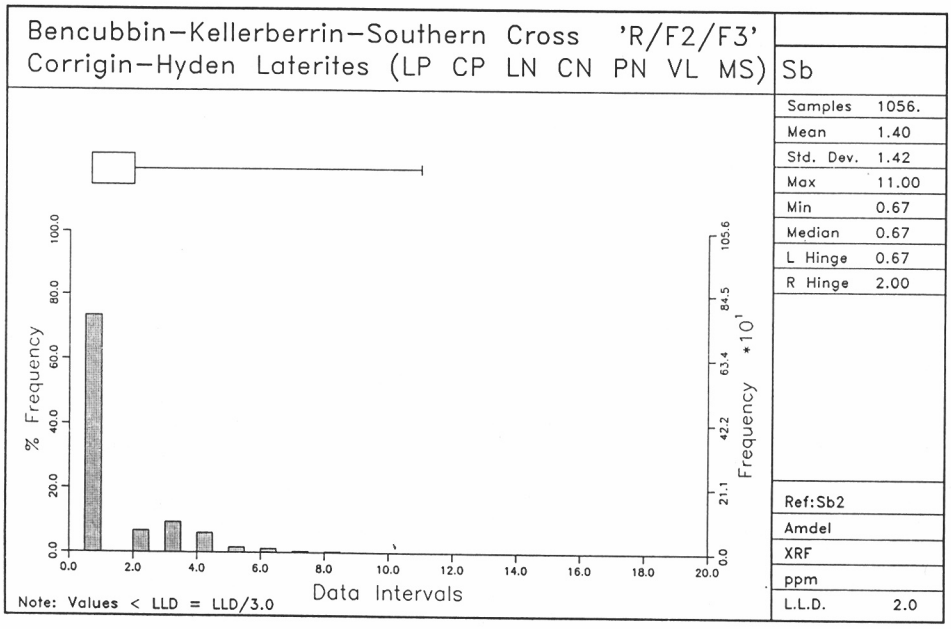

Figure 21b

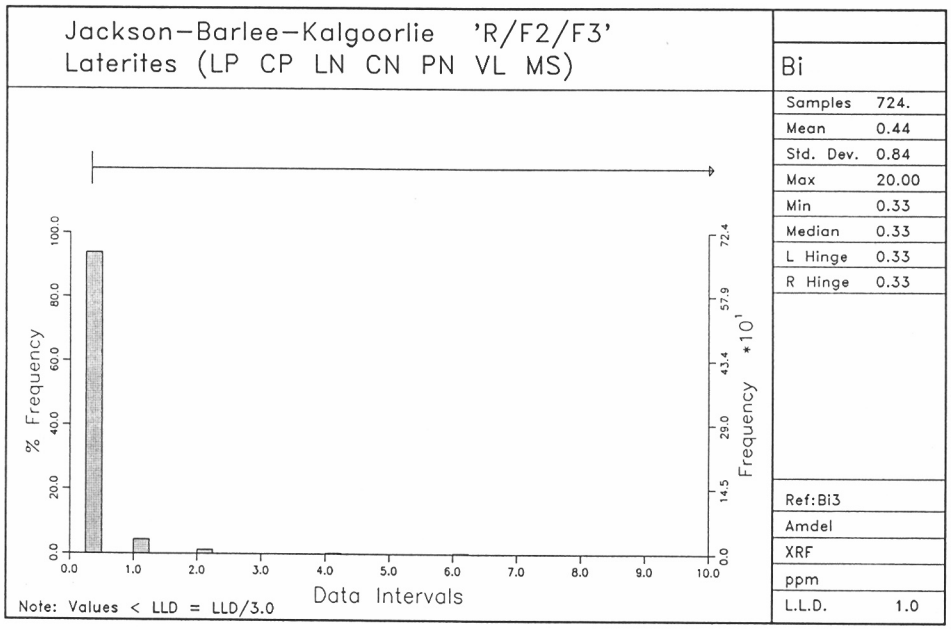

Figure 22a

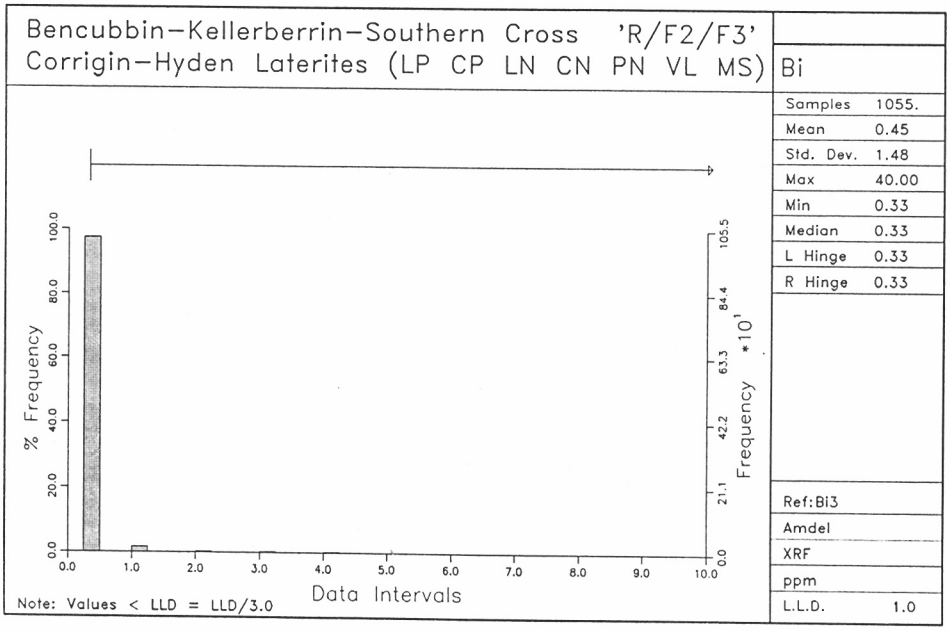

Figure 22b

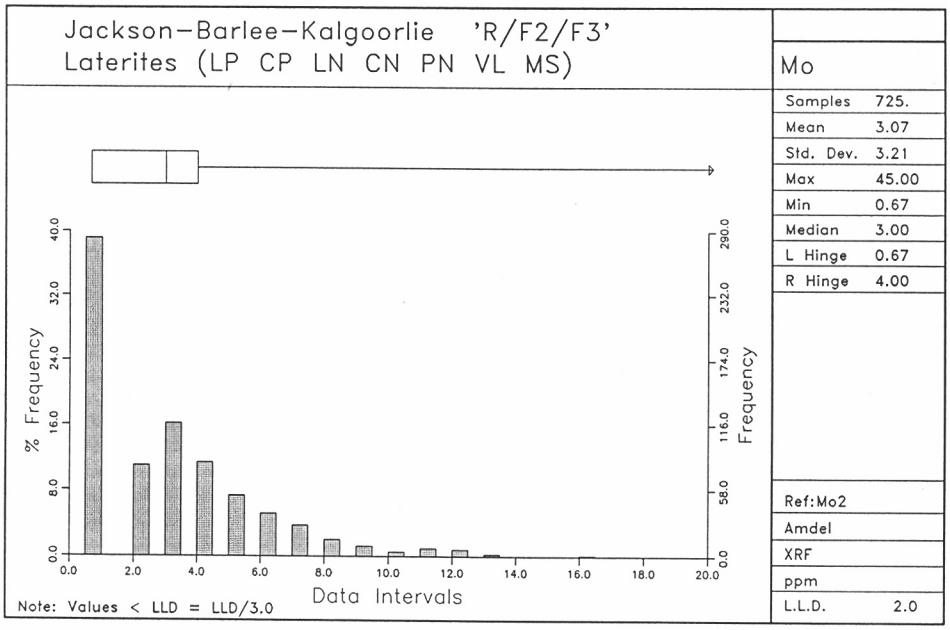

Figure 23a

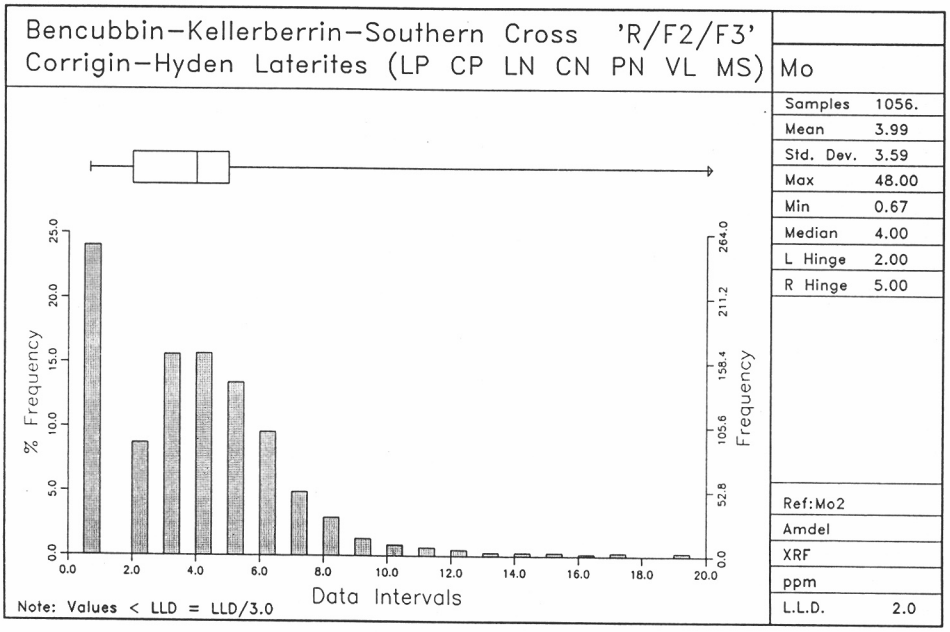

Figure 23b

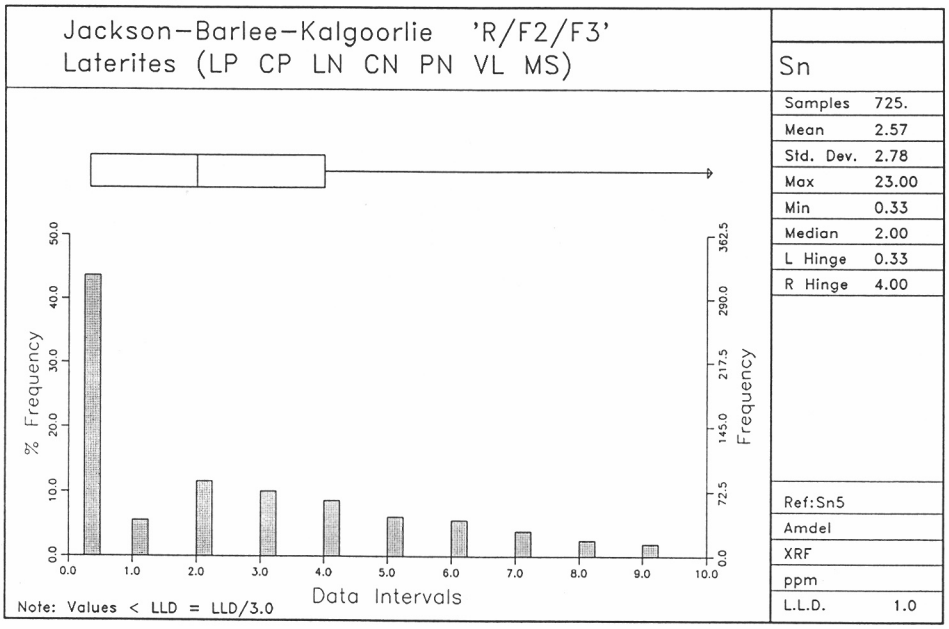

Figure 24a

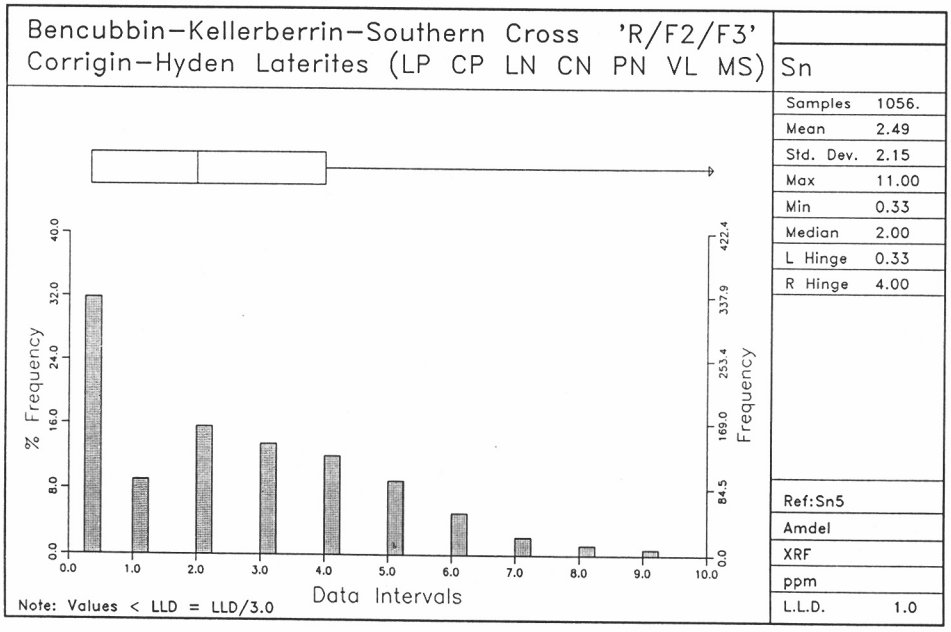

Figure 24b

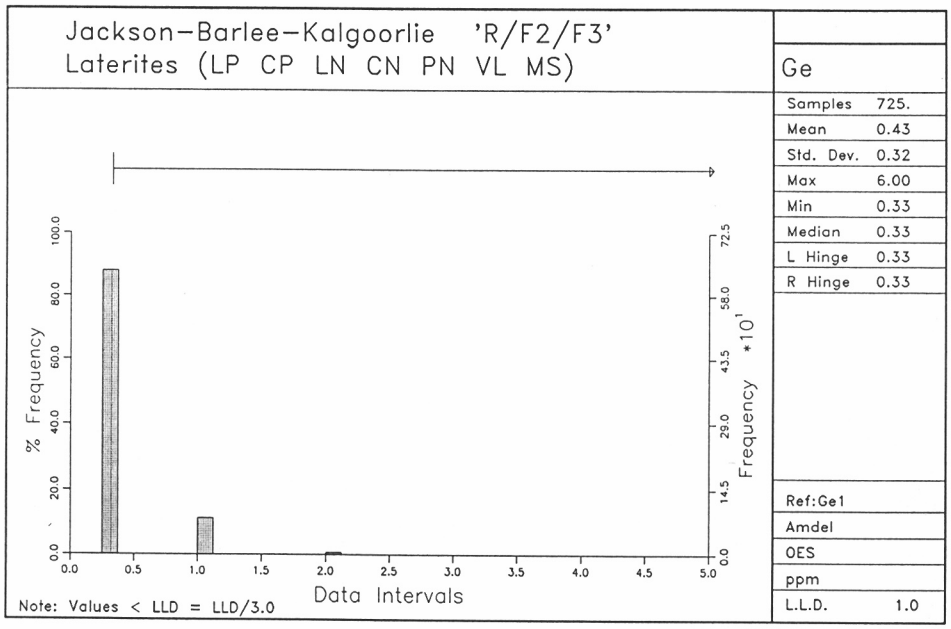

Figure 25a

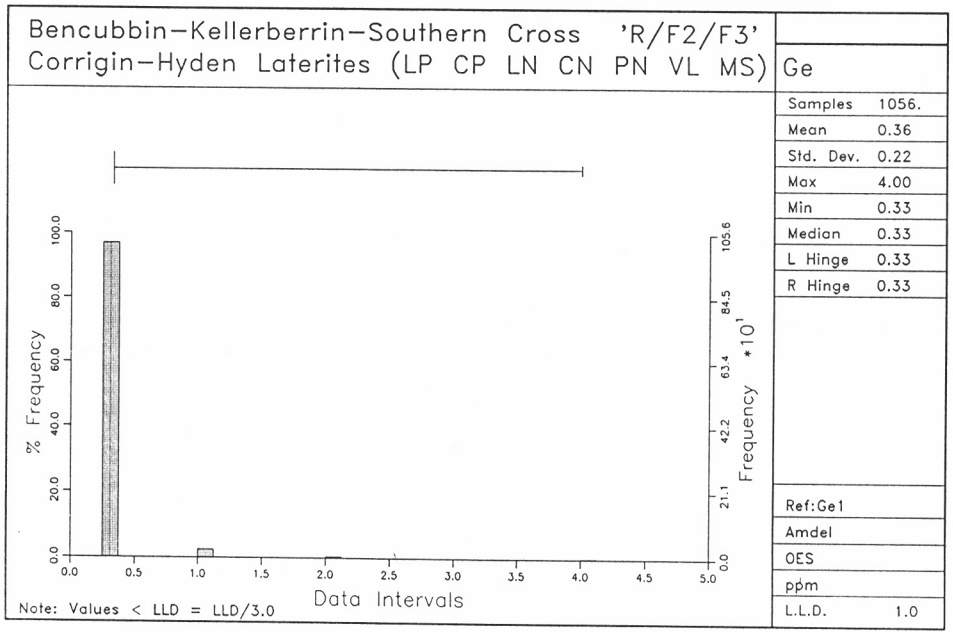

Figure 25b

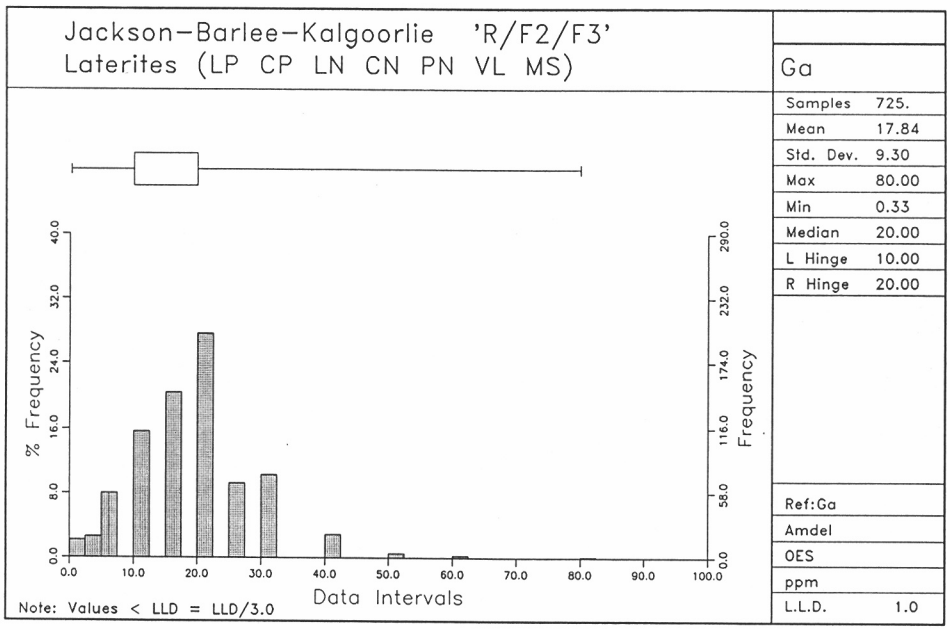

Figure 26a

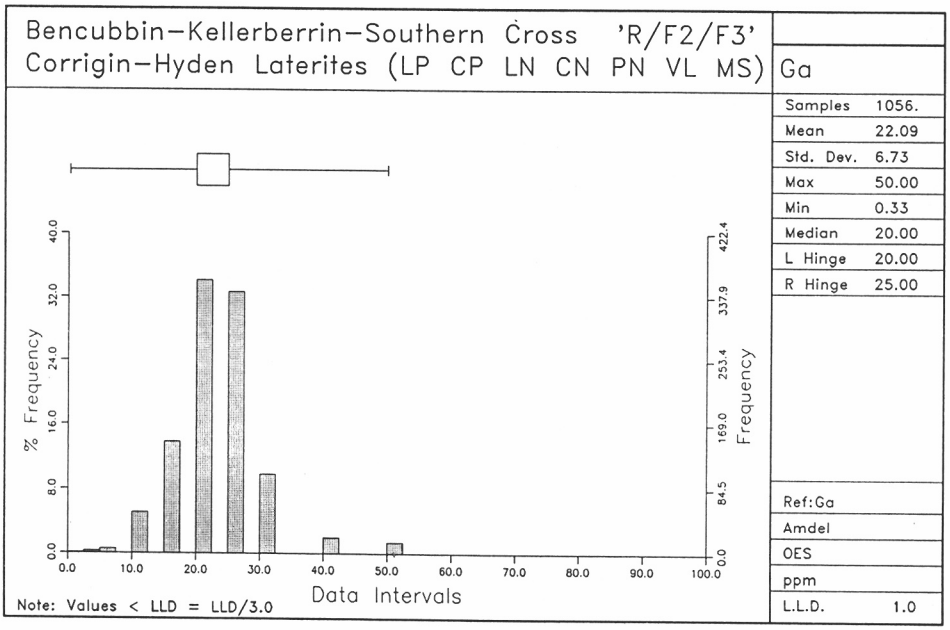

Figure 26b

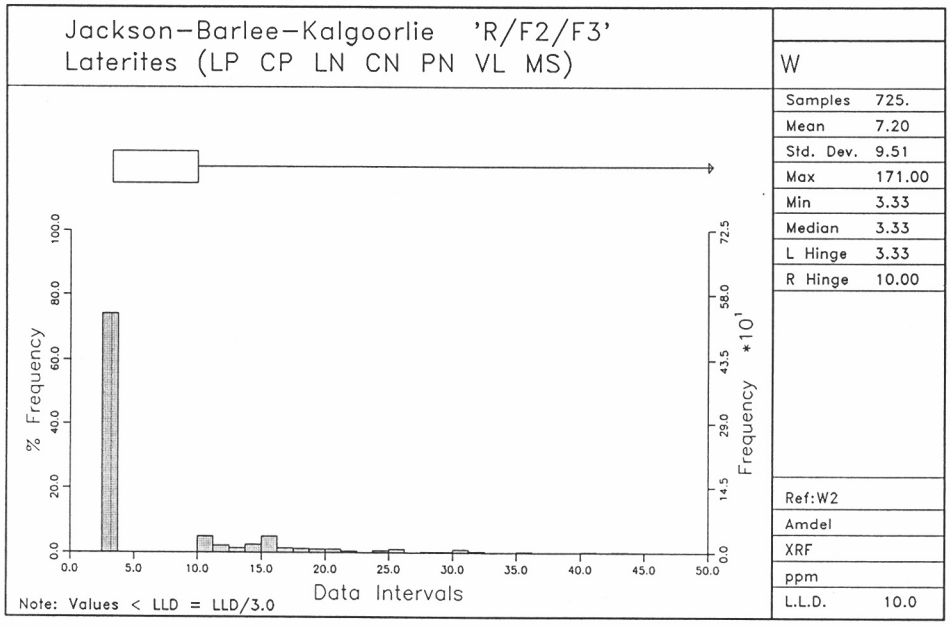

Figure 27a

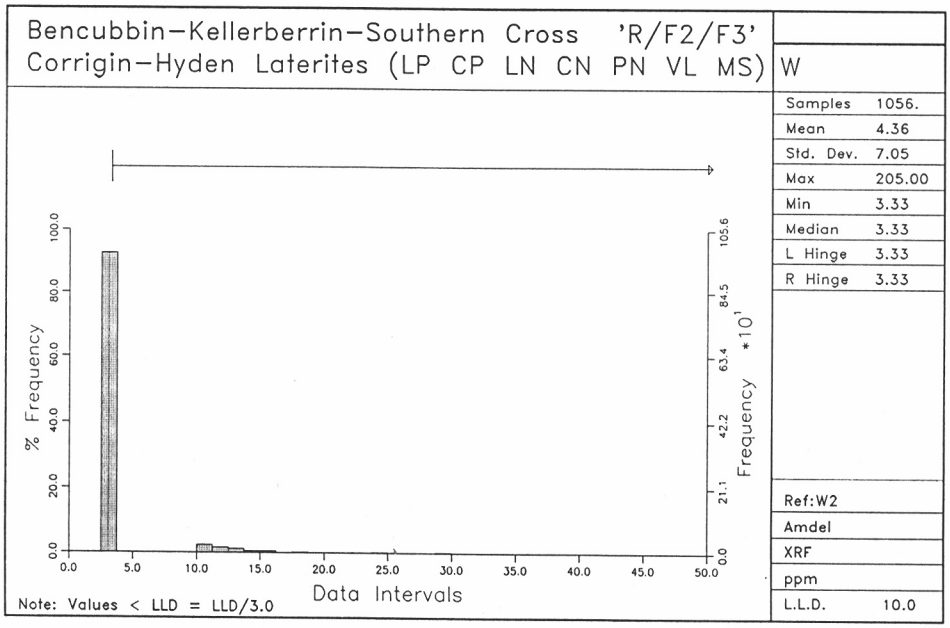

Figure 27b

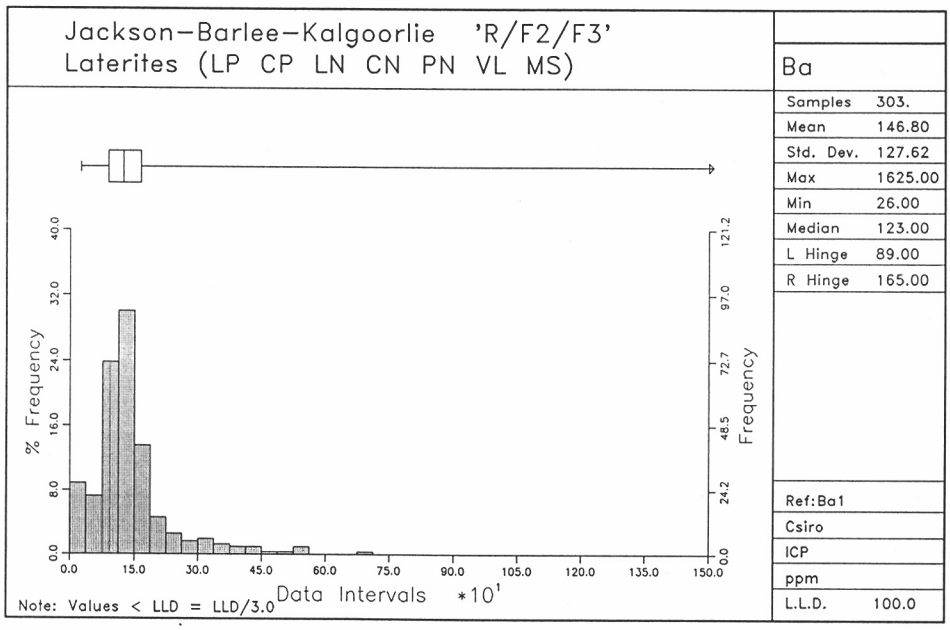

Figure 28a

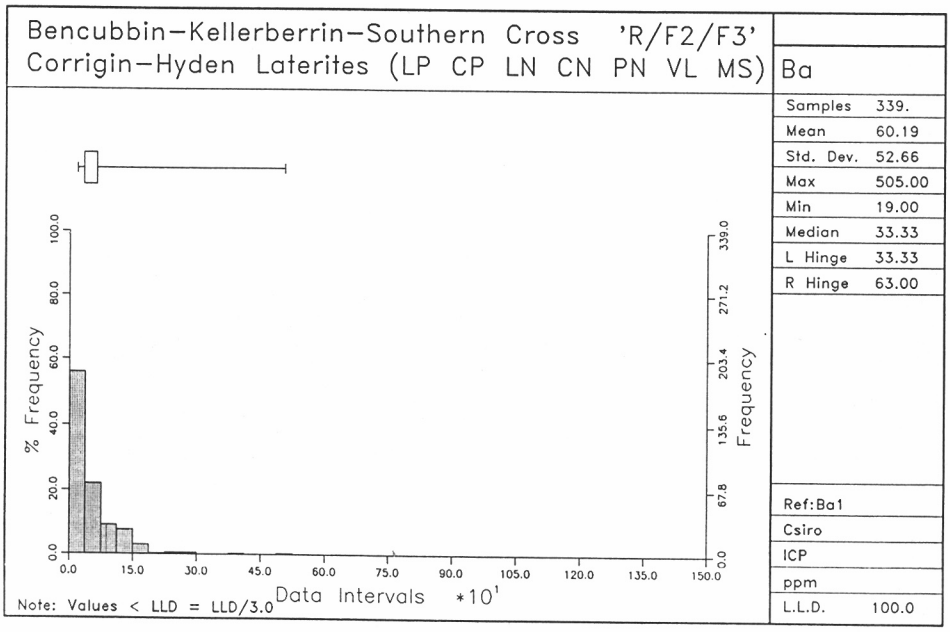

Figure 28b

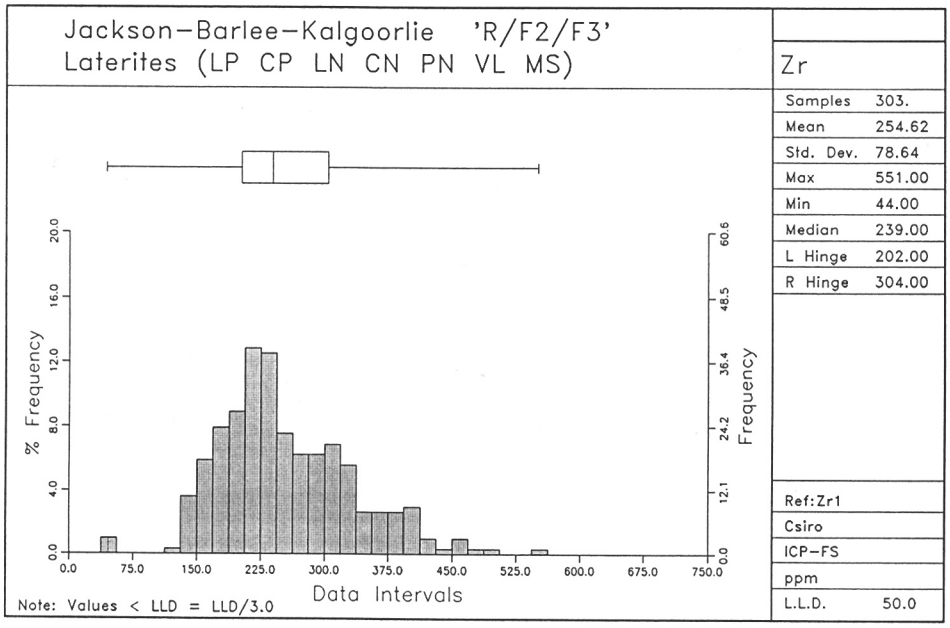

Figure 29a

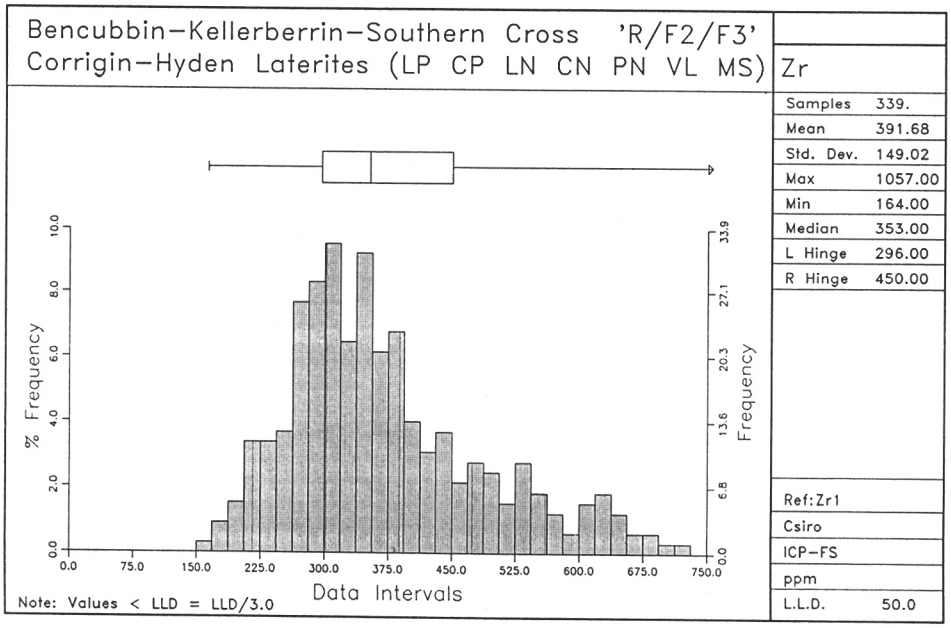

Figure 29b

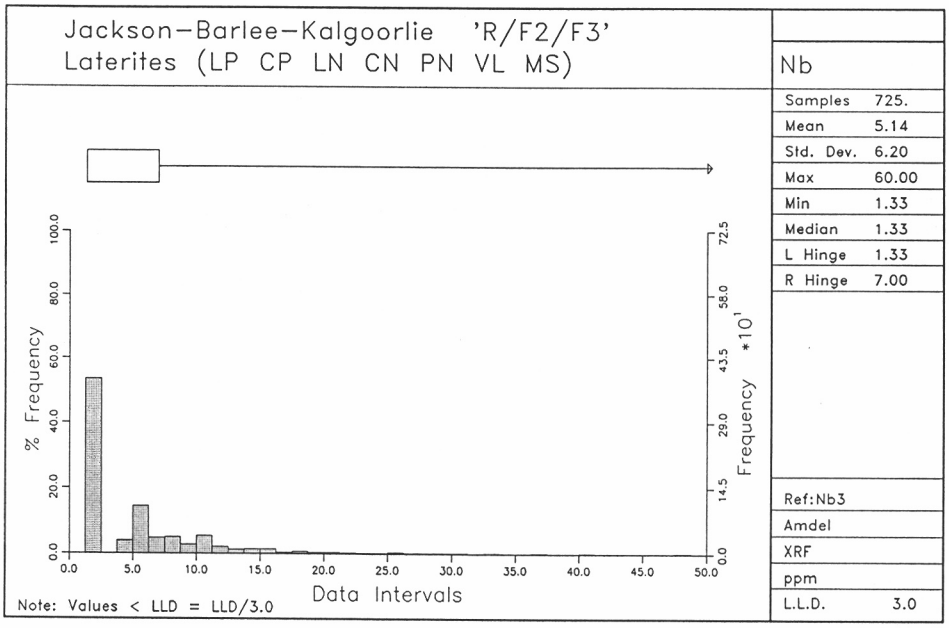

Figure 30a

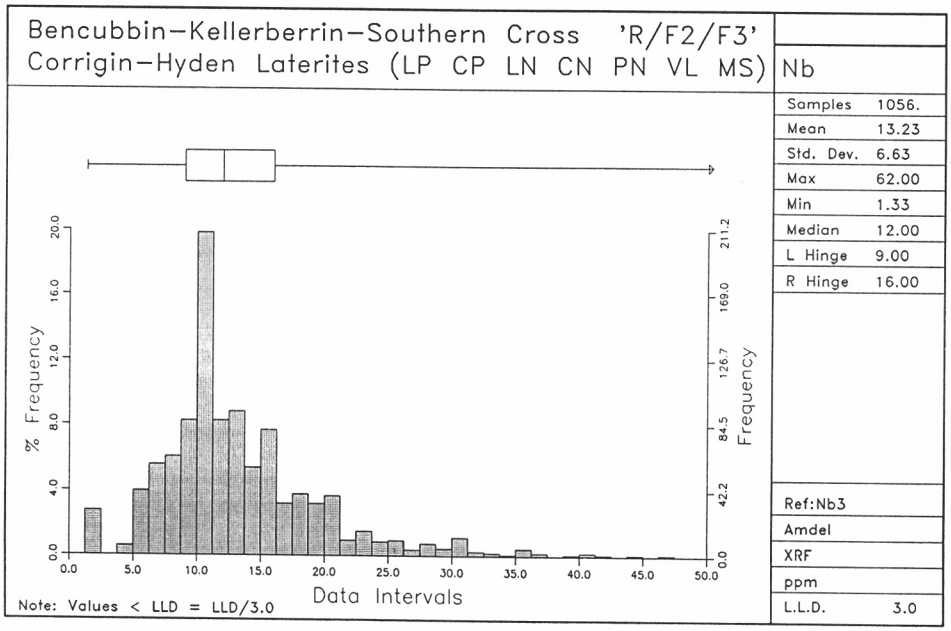

Figure 30b

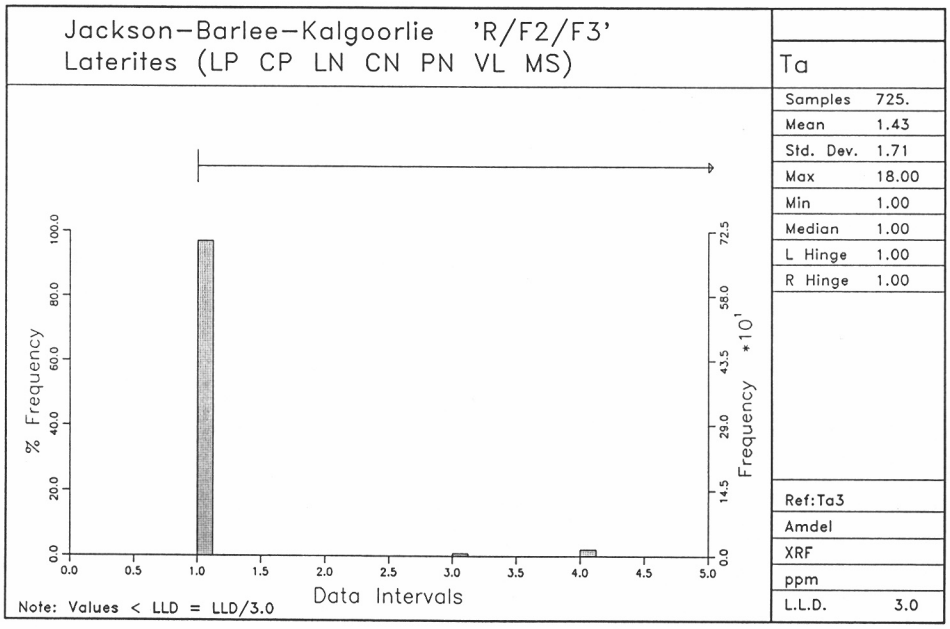

Figure 31a

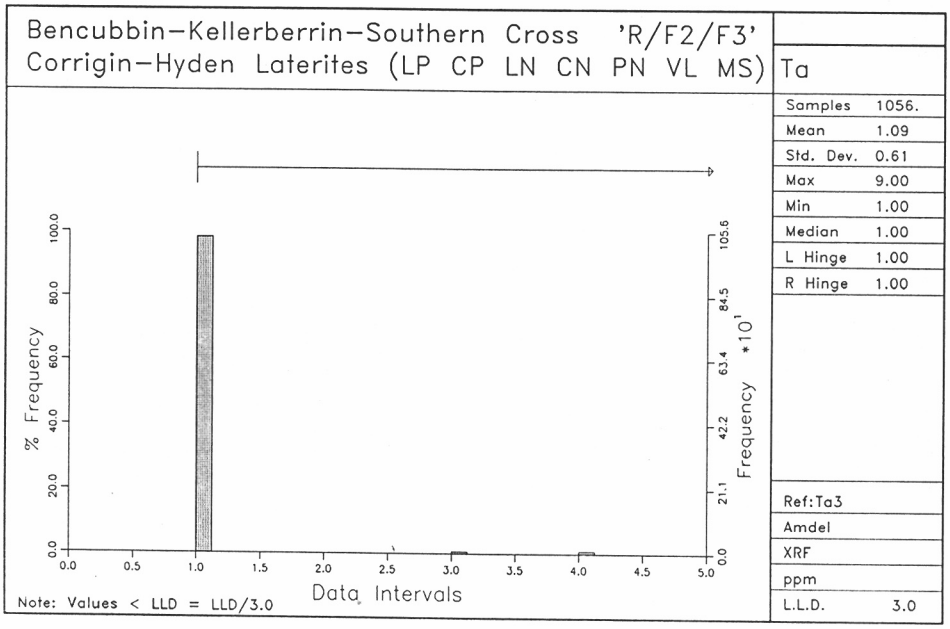

Figure 31b

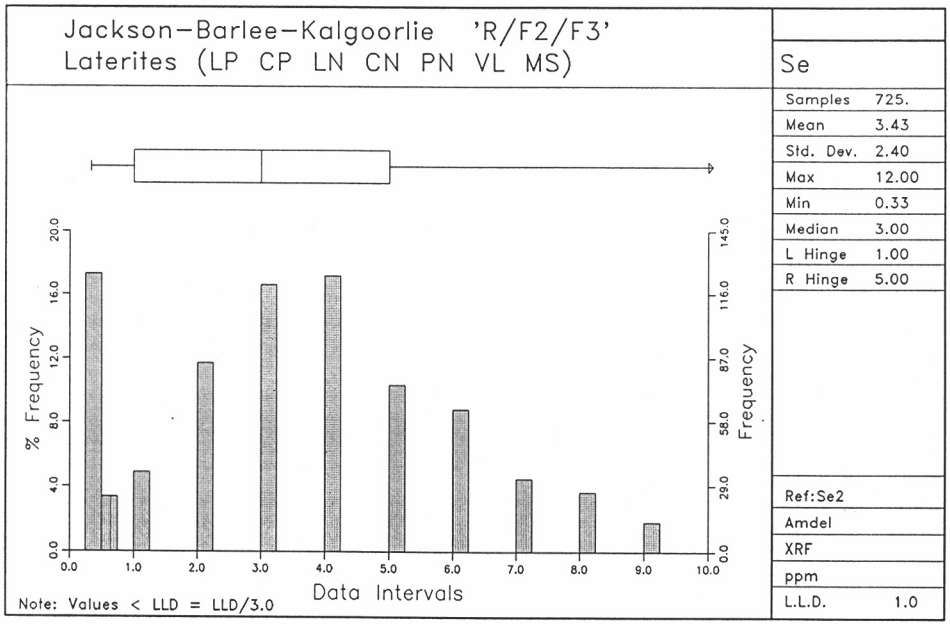

Figure 32a

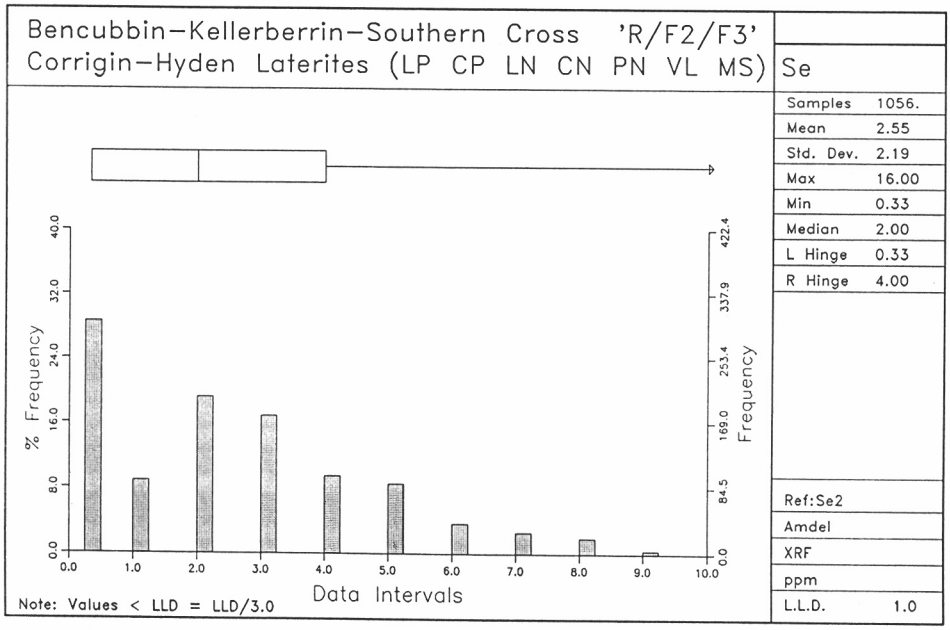

Figure 32b

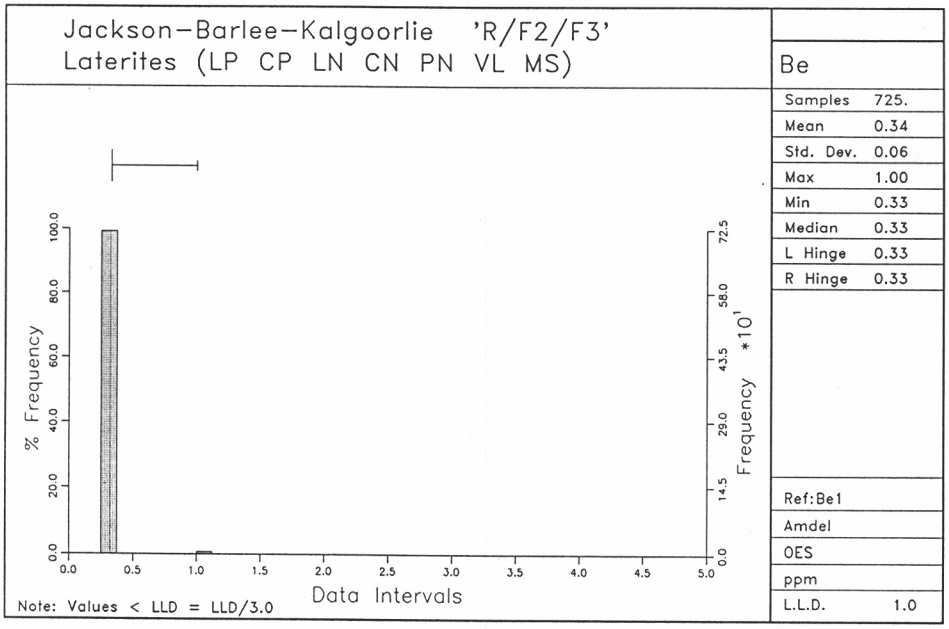

Figure 33a

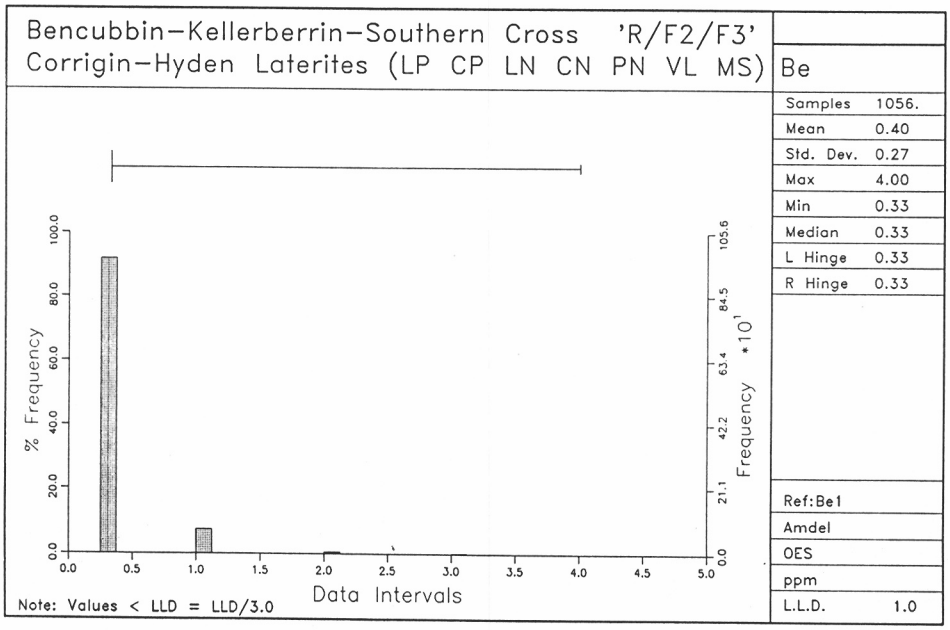

Figure 33b

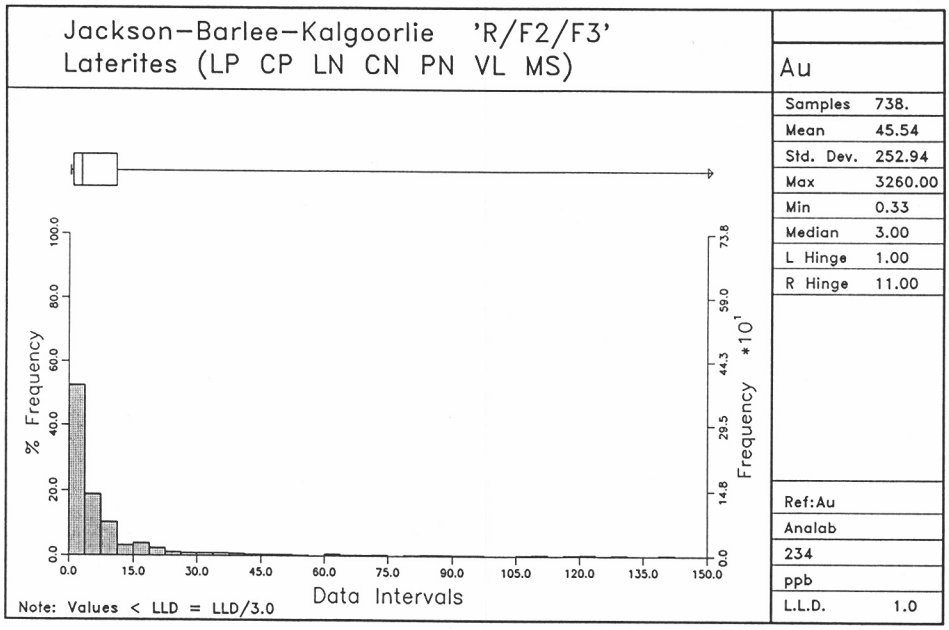

Figure 34a

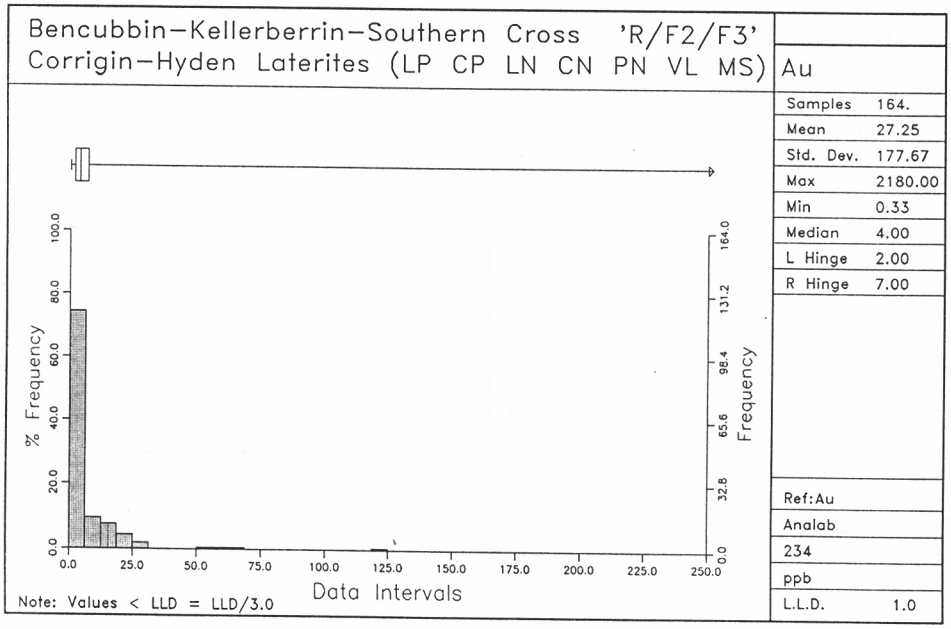

Figure 34b

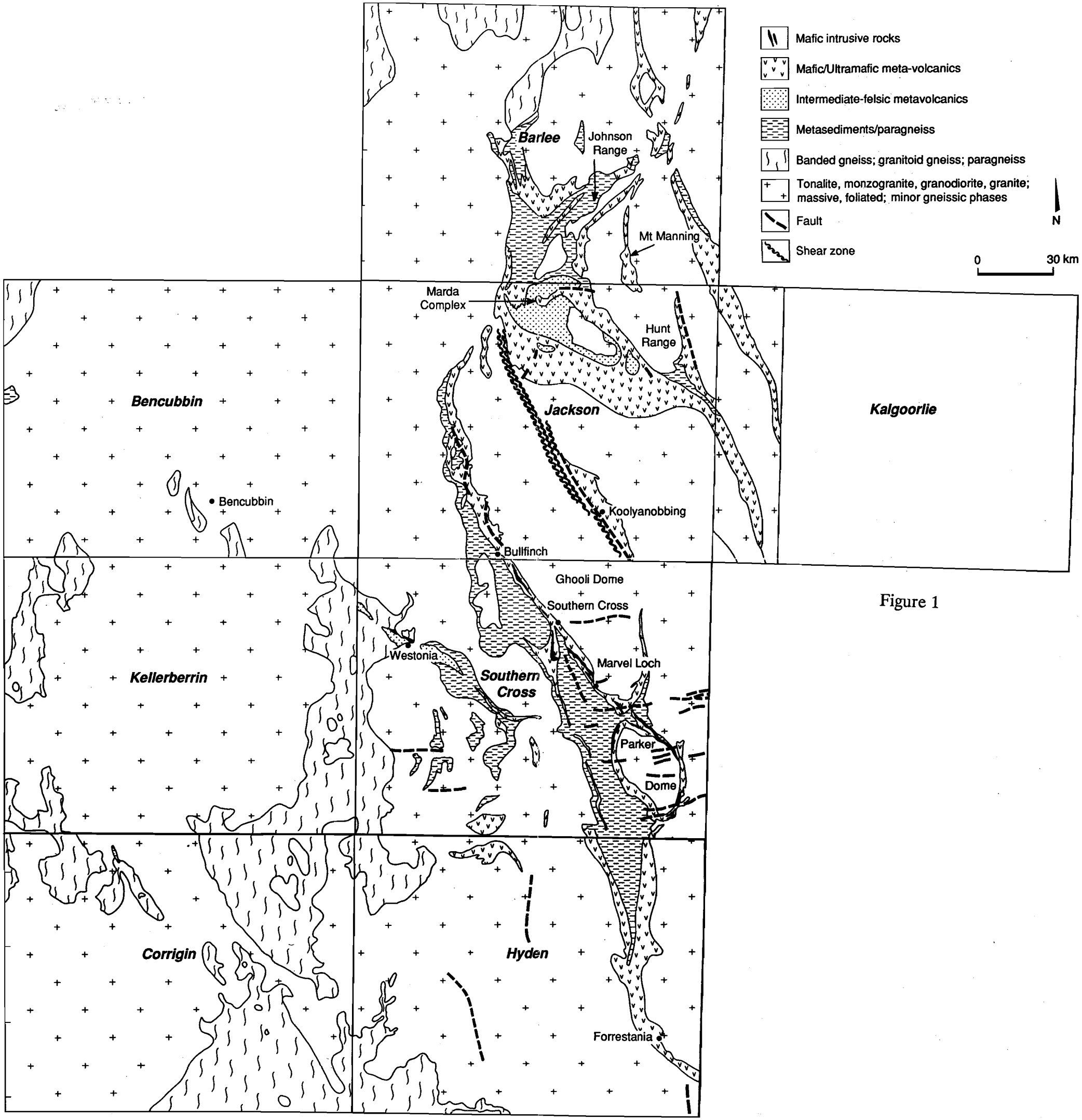
Mafic intrusive rocks
Mafic/Ultramafic meta-volcanics
Intermediate-felsic metavolcanics
Metasediments/paragneiss
Banded gneiss; granitoid gneiss; paragneiss
Tonalite, monzogranite, granodiorite, granite; massive, foliated; minor gneissic phases
Fault
Shear zone
N
0
30 km
Barlee
Johnson Range
Mt Manning
Marda Complex
Hunt Range
Jackson
Kalgoorlie
Bencubbin
Bencubbin
Koolyanobbing
Bullfinch
Ghooli Dome
Southern Cross
Westonia
Marvel Loch
Southern Cross
Parker Dome
Kellerberrin
Corrigin
Hyden
Forrestania

Figure 1